

GUIDEBOOK

*48th. Annual Field Conference
Of Pennsylvania Geologists*

SILURIAN
DEPOSITIONAL HISTORY AND
ALLEGHANIAN DEFORMATION
IN THE
PENNSYLVANIA VALLEY AND RIDGE

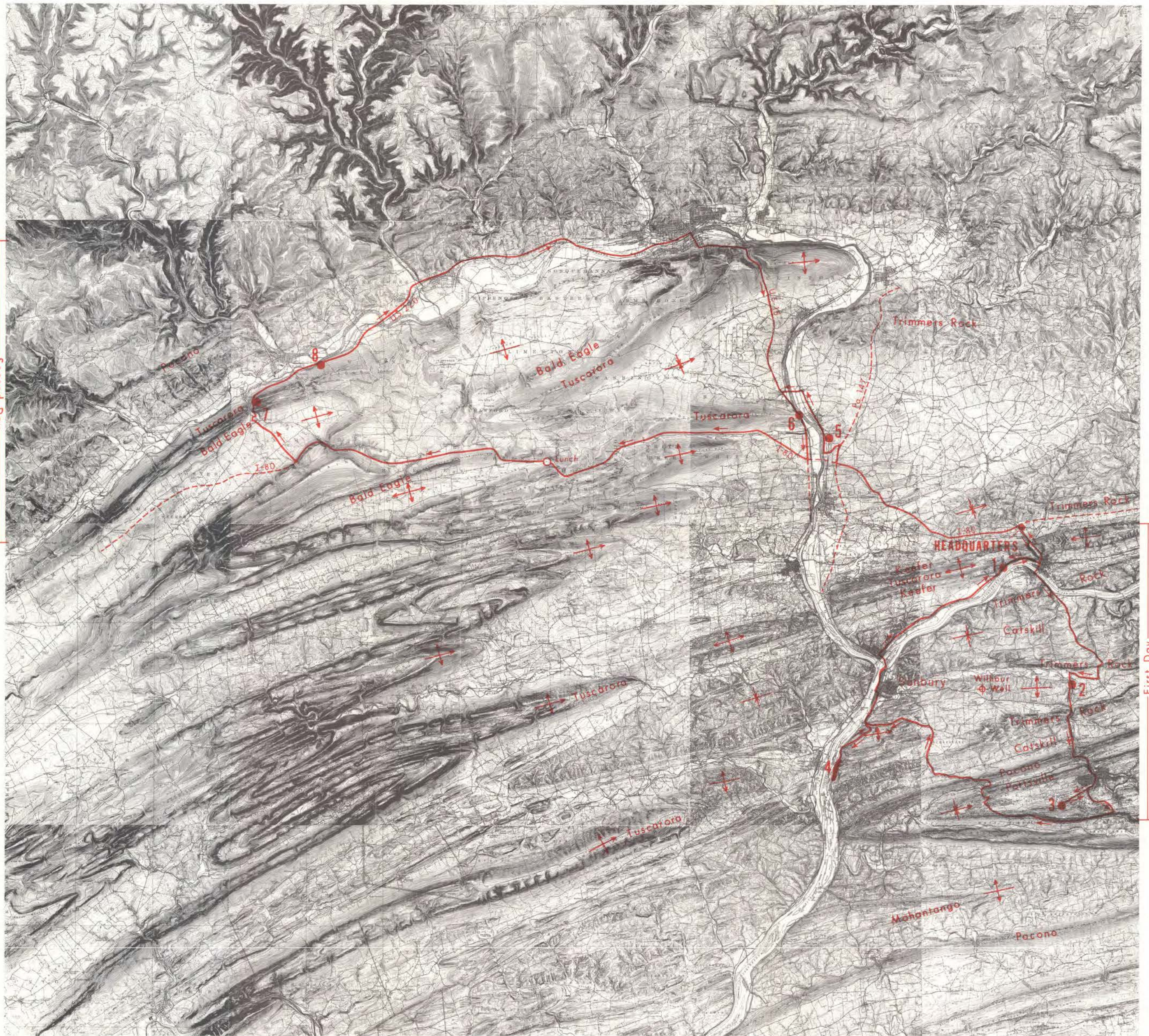
September 30 and

October 1, 1983

Danville, Pa.

Host: Bucknell University

Second Day



First Day

Figure I. Route map.

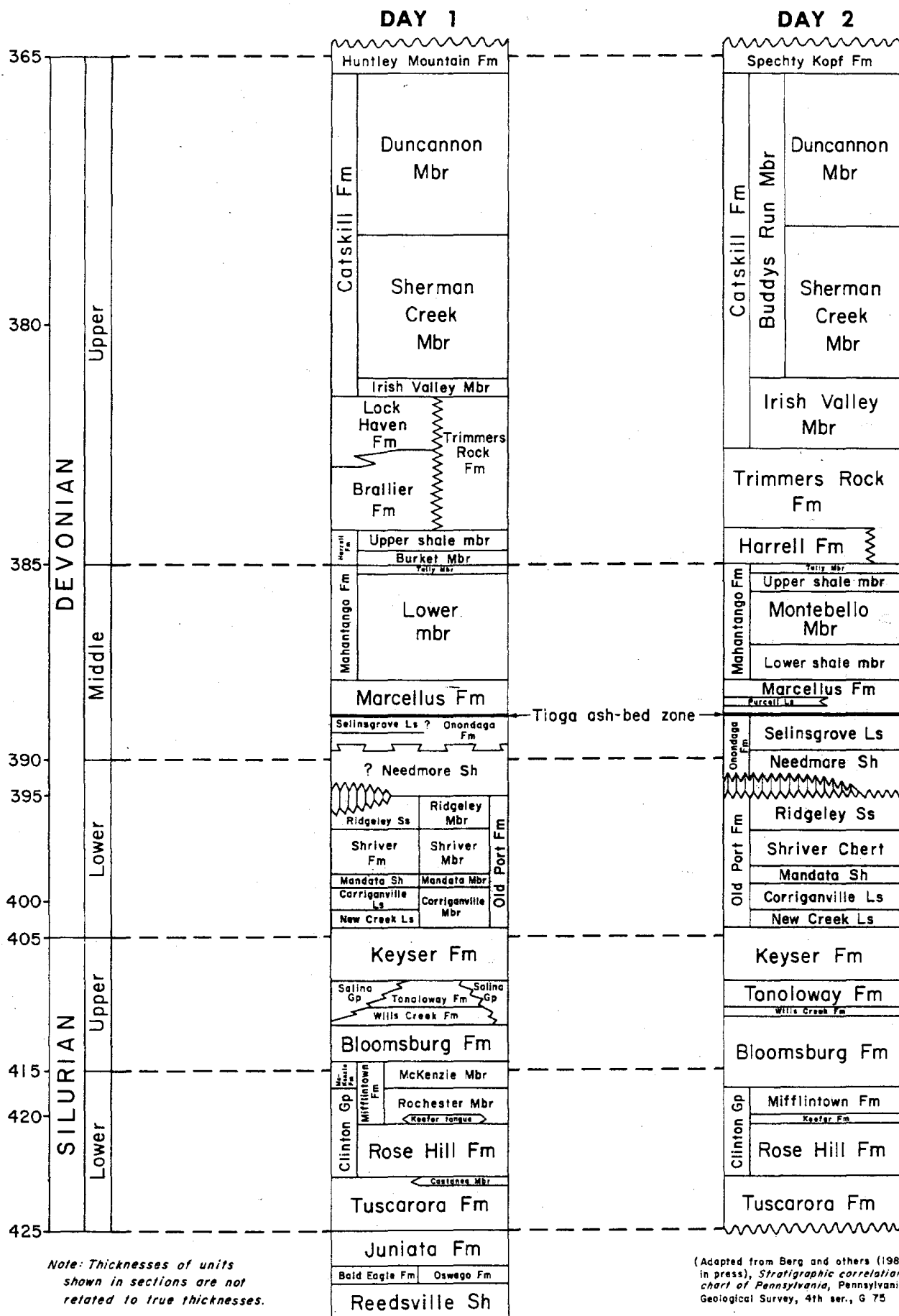


Figure 2. Silurian and Devonian stratigraphic sections.

Guidebook for the
48th ANNUAL FIELD CONFERENCE OF PENNSYLVANIA GEOLOGISTS

**SILURIAN DEPOSITIONAL HISTORY AND ALLEGHANIAN
DEFORMATION IN THE PENNSYLVANIA VALLEY AND RIDGE**

Authors and Leaders: Richard P. Nickelsen, Bucknell University
Edward Cotter, Bucknell University

With Additional Written Contributions From:

Jon D. Inners, Pennsylvania Geological Survey
John H. Williams, U.S. Geological Survey
Jeffrey R. Levine, McGill University
John H. Way, Jr., Pennsylvania Geological Survey
Robert C. Smith, Pennsylvania Geological Survey
Donald M. Hoskins, Pennsylvania Geological Survey
Christopher D. Laughrey, Pennsylvania Geological Survey

September 30 and October 1, 1983

Host: Bucknell University

Headquarters: Sheraton Danville Inn, Danville, Pennsylvania

Cover: Segment of north wall of "whale" at Bear Valley (STOP III).

Frontispiece: Silurian and Devonian stratigraphic units in Field Conference area.

Guidebook Distributed By:

Field Conference of Pennsylvania Geologists
c/o Department of Environmental Resources
Bureau of Topographic and Geologic Survey
P. O. Box 2357
Harrisburg, PA 17120

PLEASE

DO NOT HAMMER

OR SAMPLE INDISCRIMINATELY

ALL THE OUTCROPS VISITED DURING THIS CONFERENCE CONTINUE TO BE SUBJECTS OF OBSERVATION AND RESEARCH BY STAFF AND STUDENTS OF BUCKNELL UNIVERSITY AND BY COLLEAGUES AT OTHER INSTITUTIONS. PLEASE AVOID RANDOM HAMMERING. COLLECT ONLY THOSE SAMPLES THAT ARE DESTINED FOR RESEARCH OR FOR INSTITUTIONAL TEACHING COLLECTIONS. MANY ROCKS ARE FRAGILE AND CAN ONLY BE SAMPLED AFTER A PROCESS OF GLUEING TOGETHER ON THE OUTCROP; ATTEMPTS TO COLLECT THESE WITHOUT THE APPROPRIATE PREPARATION WILL ONLY DESTROY IRREPLACEABLE FEATURES. LEAVE THE ROCKS SO THAT GEOLOGISTS, STUDENTS, AND OTHER VISITORS WILL CONTINUE TO BENEFIT FROM THEM. WHO KNOWS WHICH FEATURES AND WHICH VISITORS WILL CONTRIBUTE TO THE NEXT SUCCESSIVE REFINEMENT AND MODIFICATION OF OUR CONCEPTS.

TABLE OF CONTENTS

	Page
Introduction.	1
Acknowledgements.	1
Silurian Depositional History, by Edward Cotter	3
Preliminary Statement.	3
Tuscarora Formation	3
General Framework	3
Lithofacies.	5
Depositional History of the Tuscarora	10
Rose Hill, Keefer, and Mifflintown Formations	12
Introduction	12
General Orientation	12
Lithologies.	14
Heterolithic Associations	14
Monolithic Associations	22
Iron Mineralization of the Clinton Ores	25
Genesis of the Middle Silurian Succession.	27
Aspects of Alleghanian Deformation, by Richard P. Nickelsen	29
Introduction	29
Sequence of Structural Stages of the Alleghany Orogeny	29
Description of Finite Strain and its Origins	31
Strain Disharmonies	37
Thrust Systems	39
References Cited by Cotter and Nickelsen.	40
Clinton Iron-Ore Mines of the Danville-Bloomsburg Area, Pennsylvania: Their Geology, History, and Present-Day Environmental Effects, by Jon D. Inners and John H. Williams	53
Ambient Temperatures During the Alleghany Orogeny, by Richard P. Nickelsen.	64
Coal Rank Patterns in the Pennsylvania Anthracite Region, by Jeffrey R. Levine	67
The Tioga Ash Beds at Selinsgrove Junction, by Robert C. Smith and John H. Way	74
Lower Silurian Clastics in the Subsurface of Northwestern Pennsylvania, by Christopher D. Laughrey	89

Road Log and Stop Descriptions	99
--	----

Day 1

Stop I. DANVILLE	99
Stop II. JACOB CHURCH - SHAMROCK	120
Stop III. BEAR VALLEY	128
Stop IV. SELINGSGROVE JUNCTION	141

Day 2

Stop V. WATSONTOWN BRICK QUARRY	158
(Paleontology by D. M. Hoskins)	
Stop VI. SOUTH WHITE DEER RIDGE	167
Stop VII. MILL HALL	174
Stop VIII. CASTANEA	187

LIST OF FIGURES

Figure 1	Field Conference regional map, with route and stops (folded map)	
2	Silurian and Devonian stratigraphic sections (inside front cover)	
3	Lower and Middle Silurian succession, central Pennsylvania	4
4	Tuscarora lithofacies profile	8
5	Reconstruction of Tuscarora Paleoenvironments.	9
6	Middle Silurian formations, members, and informal units	13
7	Middle Silurian lithofacies profile, Appalachian Basin	15
8	Middle Silurian paleoenvironments, Appalachian Basin	16
9	Styles of coarser-grained beds, Danville, Pennsylvania (Stop I).	18
10	Idealized composite storm bed, Danville, Pennsylvania (Stop I)	19
11	Hummocky cross stratification: terms, sequence, and genesis. From Dott and Bourgeois (1982).	20
12	Map of finite strain data in field conference region	32
13	Examples of strain partitioning in crinoid ossicles	34
14	Evolution of the reduction-spot deformation ellipsoid	36
15	Typical section, Clinton ore-bearing beds, Bloomsburg-Danville	54
16	Generalized geologic map, Danville-Bloomsburg areas	55
17	Lithograph of Montour Iron Company works at Danville, circa 1855	57
18	Limestone and slag piles of the old Irondale works	57
19	Photomicrograph, ferruginous sandstone of Centre Member	57
20	Adit of the Irondale mine	57
21	Simplified mine maps of same Montour Iron Company workings	60
22	Hypothetical slope mine showing potential environmental problems	61
23	CAI - conodont isograds in field conference region.	65
24	Regional coal rank variations in the Pennsylvania Anthracite Region	68
25	Coal rank contours, Western Middle Anthracite Field	69
26	Coalification gradients from unbroken stratigraphic sequences	70
27	Map and section of high-angle reverse faults	71
28	Measured stratigraphic section of the Tioga ash-bed zone, Selinsgrove Junction.	78
29	Thin section of Tioga ash bed F	81
30	Acicular zircon and apatite crystals separated from Tioga ash beds, Selinsgrove Junction	81
31	Plots of percent Al ₂ O ₃ and percent SiO ₂ within each ash bed, Selinsgrove Junction.	85
32	Regional stratigraphic correlation of the Medina Group	90
33	Regional subsurface cross section of the Medina Group and Tuscarora Formation in the subsurface of western Pennsylvania	91
34	Subsurface distribution of Medina Group clastics in northwestern Pennsylvania	93

Stop Figure I-1.	Middle Silurian stratigraphic column, Danville, PA.	100
I-2.	Bloomsburg Formation column, Danville, PA	101
I-3.	Photographs of features of storm beds, Danville, PA	103
I-4.	Photos of storm bed features and cleavage, Danville, PA	105
I-5.	Photomicrographs, hematite and chamosite, Clinton ores	107
I-6.	Geologic map, Berwick Anticlinorium (after Berg and Dodge, 1981).	111
I-7.	Stereographic projection, structural data at Stop I.	112
I-8.	Schematic drawing, rotated and extended veins	113
I-9.	Hand specimen drawing, interbedded limestone and shale	114
I-10.	Drawing of pre- or syn-tectonic calcite veins	115
I-11.	A. Drawing of folded, rotated, and extended sandstone dikes	116
	B. Stereographic projection of bedding, cleavage, and sandstone dikes (folded and unfolded)	117
I-12.	Drawing of early quartz veins.	118
I-13.	Cartoon summarizing structural features, Stop I.	119
II-1.	A. Polished and etched slab of bioturbated Mahantango Fm.	122
	B. Photomicrograph, Mahantango cleavage zone	122
II-2.	Drawing of Mahantango outcrop near Shamrock	124
II-3.	Summary orientation diagram of rotated structures, Stop II	125
III-1.	Geologic map of the Bear Valley Strip Mine.	129
III-2.	Section of Bear Valley Strip Mine	130
III-3.	Drawing of structures, north limb, Whaleback Anticline	131
III-4.	Structures in southwest corner, Bear Valley Strip Mine	131
III-5.	Wrench faults, cleavage/bedding intersections, gash veins	132
III-6.	Deformed tree trunk, bedding, and cleavage	133
III-7.	Drawing, exposed fault surface; Projection of angular relations	134
III-8.	Interpretation of curved slickenlines on transverse fault	135
III-9.	Relative ages of structural Stages I-VII	136
III-10.	Sequential development of structures, Stages I-VI	137
III-11.	Photomicrographs, cleavage and deformation mechanisms	139
IV-1.	Geologic map of Selinsgrove Junction area	144
IV-2.	Seven geologic selections, Selinsgrove Junction area	145
IV-3.	Composite geologic section showing main structural features	145
IV-4.	Composite stratigraphic sections, with structural features	146
IV-5.	Outcrop drawing showing cleavage duplex	147
IV-6.	Gamma ray log from Wilhour well, Stonington, PA	148
IV-7.	Gamma ray log at Station IV-A, Selinsgrove Junction	149
IV-8.	Drawing, Marcellus Formation structural features	150
IV-9.	Photos of crenulation cleavage and cleavage halos.	151
IV-10.	Structural features above and below basal thrust	152
IV-11.	Drawing of thin cleavage duplex, Station IV-F.	153
IV-12.	Drawing of duplex propagation, after Boyer and Elliott (1982)	154
IV-13.	Inferred sequence of propagation of cleavage duplex	155
V-1.	Flinn diagram to show shape of 54 reduction spots	161
V-2.	Flinn diagram to show possible volume loss, same spots.	162
V-3.	Saucer-shaped slickensided surfaces	163
V-4.	3-D sketch of SSS surfaces viewed normal and parallel to cleavage.	164
V-5.	Fiber-filled wedge faults and other structural features	165
V-6.	Attitude change, Moyer Ridge Member.	166

Figure VI-1	Columnar Section, sandstone/shale units, lower Rose Hill Fm. . . .	168
VI-2	Map of joints and faults in Units A and C of Fig. VI-1	169
VI-3	Circular histogram summarizing structural features	171
VI-4	Drawing showing sequential formation of fracture pattern	172
VI-5	Plot of T_H vs. T_F for aqueous fluid inclusions from veins	172
VII-1	Stratigraphic column of Tuscarora Formation at Mill Hall	176
VII-2	Photos of Tuscarora Formation features at Mill Hall	179
VII-3	Photos, beach unit (C) and shelf shoals unit (D)	181
VII-4	Photos, Castanea Member features at Mill Hall	183
VII-5	Generalized structure section from Faill and Wells, 1977	184
VII-6	Drawing of structural details at three localities	185
VIII-1	Sketch map of outcrop surface, McKenzie Ls. at Castanea	187
VIII-2	Photos of rippled and megarippled surfaces at Castanea	189
VIII-3	Stereographic projection of rotated wrench faults and joints	191

LIST OF TABLES

Table 1	Lithofacies characteristics, Tuscarora Formation, central PA . . .	6-7
2	Summary of thin-section data for Tioga ash beds, Selinsgrove Junction.	80
3	Relative abundance of minerals in Tioga ash beds from Selinsgrove Junction.	82
4	Relative abundance of chlorite-group minerals in Tioga ash beds from Selinsgrove Junction	82
5	Estimates of relative abundance of smectite and mica-group minerals in Tioga ash beds from Selinsgrove Junction	83
6	Quantitative analyses for Tioga ash beds from Selinsgrove Junction.	83
7	Summary of facies and sedimentary characteristics of the Grimbsy Sandstone in northwestern PA.	94
8	Summary of facies and sedimentary characteristics of the Cabot Head Shale in northwestern PA	95
9	Summary of facies and sedimentary characteristics of the Whirlpool Sandstone in northwestern PA	96
III-1	Coal rank measurements near Bear Balley Strip Mine	135

SILURIAN DEPOSITIONAL HISTORY AND ALLEGHANIAN DEFORMATION IN THE PENNSYLVANIA VALLEY AND RIDGE

INTRODUCTION

The central Pennsylvania landscape is dominated by imposing linear ridges and flanking fertile valleys stretching away to the horizon. That this dramatic Valley and Ridge topography is the result of millions of years of differential erosion of a folded Paleozoic stratigraphic succession has been appreciated since the middle of the last century. Yet in the more than 100 years since that initial appreciation, detailed conceptions of the depositional origins of the strata and of the nature and conditions of their tectonic deformation have moved through successive modifications and refinements.

We have been participating in the development of some of these modified and refined conceptions, and the objective of this 48th Annual Field Conference of Pennsylvania Geologists is to demonstrate a number of them. For the Lower and Middle Silurian stratigraphic units we shall show a pattern in the complex paleoenvironmental picture that is related to Appalachian Basin configuration, source area tectonics, and sea-level fluctuations. We shall also show a new appreciation for the role of shallow-marine shelf processes in generating particular lithologies. In terms of the tectonic history, we shall examine a variety of strain features through which the complexity of events known as the Alleghany Orogeny may be better understood as a progression of overlapping stages during which different strain mechanisms and geologic structures dominated. We shall demonstrate the influence of rock types, primary sedimentary structures, position (structural, stratigraphic, and geologic), and history in creating the differences in finite strain in the region.

These two emphases of this field conference - the Silurian depositional history and the Alleghanian deformation - are wedded in the Valley and Ridge landscape through which we will travel. Without these particular sedimentary and tectonic histories there would not be the distribution and dispositions of the variety of lithologies through which this region derives its physiographic character.

Acknowledgements

Many persons have assisted, stimulated, and tolerated us in our investigations of central Pennsylvania geology. We would like to single out the following persons and organizations.

BUCKNELL UNIVERSITY STUDENTS

Among the many students whose undergraduate field projects have assisted in the development of descriptions and ideas, these have contributed to information on stops for this field conference.

STOP I. Susan Hallam Pollman, Lynne Settzo Emerson, William Grennon,
Eric Schmitt

STOP II. Stephanie Davis, Eric Miller

STOP III. Christina Quittman

STOP IV. David Egan, Doris Bajak

STOP V. Paul Knowles, Mary Beth Gray

STOP VI. Amy Lilly, Eric Miller

STOP VIII. Richard Sacks, Eric Miller

COLLEAGUES IN GEOLOGY

While it is not possible to single out each colleague who has contributed to our understanding and who has accompanied us to these localities, we would like to acknowledge the continuing professional and personal cooperation we have received from present and former members of the Pennsylvania Geological Survey.

BUCKNELL UNIVERSITY

We are grateful for the financial assistance, the transportation and the intellectual stimulation we have received over the years.

GRANTING AGENCIES

Nickelsen wishes to acknowledge receipt of funds from the Petroleum Research Fund of the American Chemical Society. Cotter studied these Lower and Middle Silurian units with the assistance of a Cottrell College Science Grant from the Research Corporation.

CONFERENCE AND GUIDEBOOK ASSISTANCE

Donald M. Hoskins and the staff of the Pennsylvania Geological Survey.

Jody Maddox, Secretary, Bucknell University, Department of Geology.

Eugene Williams, for advice on features at STOPS I and V.

Eric Miller, for drafting assistance.

Mr. Charles Fisher, of Watsontown Brick Company, for cooperation and access.

Bucknell University students assisting with traffic control.

John H. Way, Jr., for the diagram on the inside cover (Fig. 2).

SILURIAN DEPOSITIONAL HISTORY

by

Edward Cotter

Preliminary Statement

There are three background factors that controlled the character of the Lower and Middle Silurian stratigraphic succession in central Pennsylvania. First, during this time there was a gradual return to tectonic tranquillity following the crisis of Late Ordovician Taconic events. As a result, both the calibre and composition of accumulating Appalachian Basin sediment changed, first from largely terrigenous sands to terrigenous muds, and then to marine carbonates. The second factor was that sea level experienced a series of fluctuations during this period. The consequent migration of depositional environments and changes of depositional conditions (such as depth) imparted distinctive physical and chemical features to the deposits. Third, even though the depositional environments migrated and changed, in central Pennsylvania conditions persisted as shallow-marine shelf dominated by storm processes.

These three factors are responsible for features at different scales or magnitudes. The first deals with the compositional evolution of the entire Lower and Middle Silurian stratigraphic succession. Through the second factor changes in lithology resulted that permit subdivision of the succession into formations, members, and units. And the third factor was responsible for features of individual beds or groups of beds. Our scale of observation on this field trip will be at the level of beds and groups of beds, and thus you might be more able to evaluate the interpretation of storm-dominated shelf conditions. By examining several extensive sequences at various positions in the succession you will see the major features on which interpretation of the other two factors is based. However, because a more complete understanding of the first two factors is difficult to achieve from a few outcrops, the first part of this guidebook presents the regional picture into which those outcrops fit. Consideration will proceed in two parts, with the Lower Silurian Tuscarora Formation treated first, followed by the Middle Silurian units - Rose Hill, Keefer, and Mifflintown Formations.

Tuscarora Formation

Interpretations of the depositional origin of the Tuscarora go back to the early part of this century, when Grabau (1913) proposed a fluvial origin, and Schuchert (1916) countered with a shallow-marine interpretation. Subsequently, prevailing views fluctuated between these two - the origin was either all fluvial or all marine. For a time the marine origin received support (Woodward, 1941; Folk, 1960), but in the last two decades the fluvial interpretation has become widely accepted, largely as the result of the important contributions by Yeakel (1962) and Smith (1970). It is my contention that the Tuscarora Formation is both marine and fluvial in origin, with eastern parts largely fluvial, and western parts largely marine. The complex relationships between these parts has been described by me earlier (Cotter, 1982, 1983) and they are summarized below.

GENERAL FRAMEWORK

The Tuscarora Formation is distributed through an extensive part of the eastern Appalachian Basin as the uppermost coarse clastic unit of the Queenston (Taconic) Clastic Wedge. It was defined by Darton and Taff (1896), the name being derived from Tuscarora Mountain in south-central Pennsylvania. The name is presently applied to the

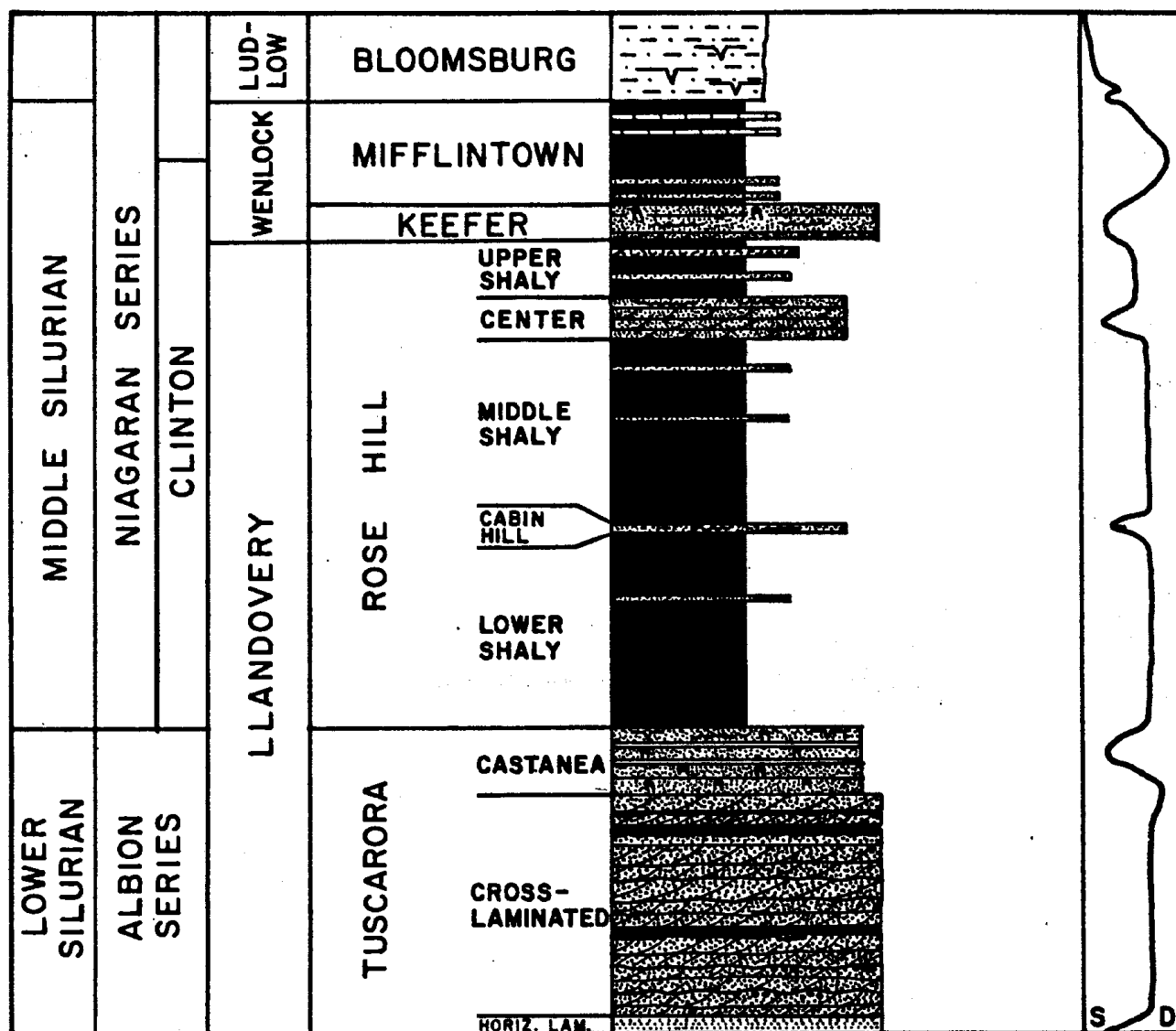


Figure 3. Lower and Middle Silurian stratigraphic column - central Pennsylvania

Lower Silurian coarse clastic deposits in Pennsylvania, Maryland, West Virginia, and the northern part of Virginia. Correlative rock units include the Clinch Sandstone in southern parts of Virginia and in Tennessee, and the Medina Group in western New York and contiguous Ontario (Berry and Boucot, 1970). As the Tuscarora is traced eastward from central Pennsylvania to the Delaware Water Gap and then into New Jersey and New York, it becomes the lower part of the Shawangunk Conglomerate (Epstein and Epstein, 1972).

Age diagnosis of the Tuscarora Formation is inexact and somewhat arbitrary, principally because it lacks body fossils. Over most of the outcrop region the Tuscarora rests conformably on the Juniata Formation, and in turn it is conformably overlain by the Rose Hill Shale (Figs. 2 and 3). The Juniata is assigned a Late Ordovician (Ashgill) age (Dennison, 1976), and the Rose Hill is Middle Silurian (late Llandovery) (Berry and Boucot, 1970, P. 2) (Fig. 3). On these bases the Tuscarora is conventionally assigned an age ranging from the base of the Llandovery to the Llandovery C2-3 stage (Berry and Boucot, 1970).

The Tuscarora in the central Pennsylvania outcrop belt is generally from 150 to 200 meters thick. The pattern, however, is somewhat erratic, and measured thicknesses can be above or below these values (Yeakel, 1962, Fig. 4; Faill and Wells, 1974, Table 6). There is generally a somewhat thicker Tuscarora in the central part of the Valley and Ridge outcrop belt, probably as a result of slightly greater subsidence there.

Not all of the exposed Tuscarora succession is sandstone, and not all of the sandstone is quartz arenite. The Tuscarora can comprise 25 or 30% shale, particularly in the northern part of the outcrop belt (see Stop VII, Mill Hall). The sandstones are both quartz arenites and sublitharenites, with variable and locally significant minor quantities of chert and other rock fragments, derived from the Taconic Highlands to the southeast, and transported down the regional paleoslope to the northwest (Yeakel, 1962).

The Early Silurian paleolatitude for this part of North America was subtropical at about 25 to 30 degrees south latitude (Ziegler and others, 1977, Fig. 2; Khain and others, 1978; Seslavinsky, 1979). At this latitude, not only would there have been marked seasonal variations in rainfall, but also the topography would influence the local climate. One can sense the significance of this location by considering the variations in climate across modern South America 25 to 30 degrees south of the equator - from the Atacama Desert on the west, to the humid forests east of the Andes. Previous interpretations of the Tuscarora paleoclimate generally agree with this postulated paleolatitude in specifying that the region was warm, and with seasonal variations in rainfall (Swartz, 1957, p. 22 Folk, 1960, p. 25; Hunter, 1970; Epstein and Epstein, 1972).

The Taconic Highlands and the eastern part of the Appalachian Basin experienced a slight tectonic "adjustment" just as Ordovician time was coming to a close. Through much of the development of the Juniata Formation there was progressive degradation of the source terrain and decreasing gradient on the marginal alluvial plain. However, the conglomeratic Run Gap Member at the top of the Juniata demonstrates that coarser debris was coming from a source terrain of somewhat different composition (Tuttle, 1940; Swartz, 1957; Diecchio, 1980). At the same time there began a sourceward (southeastward) shift in the fall line such that sediment at the base of the Tuscarora Formation accumulated on an erosion surfaces in the proximal part of the basin east of the Susquehanna (Swartz, 1957; Wood and others, 1969).

At the time of this Latest Ordovician-Earliest Silurian tectonically-generated renewed sediment influx, there was a relatively rapid glacioeustatic rise of sea level (among others, see Berry and Boucot, 1973; McKerrow, 1979; Brenchley, 1980; Leggett and others, 1981). This rapid rise came at a time when seas were still at the generally higher long-period stand that accompanied higher rates of oceanic rifting in the Lower to Middle Paleozoic (first-order cycle of Vail and others, 1977; see Shanmugam and Moiola, 1982). Additional sea level fluctuations occurred later in the Silurian, and these are shown in the reports of McKerrow (1979), Johnson (1980), Johnson and Campbell (1982), Petryk (1981) and Cotter (1983). There is a good general agreement between these changes and the sea level changes interpreted from the Lower and Middle Silurian succession of central Pennsylvania (Fig. 3).

LITHOFACIES

My interpretation of the depositional history of the Tuscarora Formation in central Pennsylvania is based on the identification and interpretation of five lithofacies in the outcrop belt. A detailed outline of the characteristics of these lithofacies may be found in Table 1. More extended descriptions and interpretations are in other reports (Cotter, 1982; 1983). Some summary comments are immediately below. It might prove

Table 1. Lithofacies characteristics, Tuscarora Formation, central PA

LITHOFACIES	DEPOSITIONAL ENVIRONMENT	GEOMETRY AND POSITION	LITHOLOGY AND TEXTURE	SEDIMENTARY STRUCTURES	SEQUENCES
Eastern cross-laminated	Braided, fluvial, organized as medial-distal alluvial fan complex.	Eastern localities; thins to west and northwest. Overlies and, in places, intercalated with horizontally laminated lithofacies.	Medium to thick zones of sandstone and conglomerate; subordinate thin beds and lenses of green to gray shale. Sandstone less mature, sublitharenite; medium to coarse-grained, commonly pebbly, some basal lags; poorly sorted; not well rounded; intraclasts common.	Conglomerates mostly structureless; some scours and troughs. Slight channeling; beds have high width-thickness ratios. Sandstones mostly trough cross laminated; some planar at distal places; current ripple lamination uncommon; few beds graded. <u>Arthropycus</u> on bed soles more common at distal localities.	Little consistent order at most places; some fining-upward thin sequences similar to those of Smith (1970, Fig. 17).
Basal, horizontally laminated	Beach system as regional strandplain complex.	Thin sheet at base of Tuscarora; extends over most of central PA to east of Swatara Gap. Associated with basal pink transition in south-central PA; overlain by eastern or western cross-laminated lithofacies.	All continuous sandstone up to 29 m thick; no shale or gravel as clasts or interbeds; light gray to white. Supermature; >98% quartz; traces of chert and lithic grains; some laminae have concentrated heavies; well sorted and rounded, with bed-to-bed changes; fine- or medium-grained, some inversely graded laminae.	Largely horizontally (even parallel) laminated; symmetrical ripples common; antidune lamination uncommon; medium-scale cross lamination present, some dipping SE. <u>Skolithos</u> and <u>Monocraterion</u> present; no <u>Arthropycus</u> .	Continuously uniform, no sequential changes.
Basal pink transition	Estuarine	South-central to southwestern part of PA outcrop belt. Transitional from Juniata Formation; overlain by western cross-laminated lithofacies, except for some situations of intervening horizontally laminated lithofacies. Thin and sheetlike.	More than 80% sandstone in thin to medium, tabular beds; intercalated with thinner beds of red shale. Fine- to medium-grained quartz arenite; grains rounded and generally well-sorted; some bed-to-bed changes. Red shale clasts in some beds.	Sandstone mostly planar and trough cross-laminated; some horizontal lamination; some upper bed surfaces have symmetrical ripples. Cross laminae inclined generally to NW; rare bipolar.	No systematic pattern.
Western cross-laminated	Shelf sand complexes; shoreface-connected sand ridges.	Laterally extensive sheet above basal lithofacies and below red Castanea Member; seaward of eastern cross-laminated lithofacies the relations with which are indeterminate.	Proximal: Thick units of medium- to coarse-grained sandstone in beds 15-75 cm thick; coarser sand and fine gravel along laminae and as bed-top concentrations; sorting moderate to poor, better in individual laminae; composition mature, quartz arenites; very few, very thin shales.	Proximal: Broadly wavy, nonparallel bed top; apparent channels are filling swales in top of underlying beds. Cross lamination dominates; both planar and trough; transport dominantly unimodally NW, also coast-parallel; bipolar flow rarely recorded. Uncommon <u>Arthropycus</u> on bed soles above thin shales.	Proximal: Apart from beds that coarsen upward to granules, no discernible pattern.

Medial:

Thick units of medium-to coarse-grained sandstone; uncommon granules; grains subround to round, moderately to well-sorted.

Thin intercalations of fine sandstone and coarse siltstone; some few beds with siltstone intraclasts.

Quartz arenitic composition.

Medial:

Beds 15-40 cm thick have wavy, nonparallel bed tops; internally cross-laminated; mostly NW transport, some coast-parallel or bipolar.

Bed tops uncommonly have symmetrical ripples
Arthropycus abundant as intersecting horizontal shafts; rare Skolithos.

Medial:

No systematic pattern.

Distal:

Alternating tabular units (> 2 m thick) or medium-grained sandstone; grains round to subround; sorting moderate to well; rare coarse sand; and

Thinner tabular units (< 1 m thick) of very fine to fine-grained sandstone and siltstone.

Concentrations of siltstone intraclasts in some beds. Most sandstone quartz arenites.

North-central PA sequences have up to 30% gray shale interbedded with medium-to coarse-grained sublitharenites (see text for discussion).

Distal:

Thicker units have beds 10-30 cm thick with planar and minor trough cross lamination.

Thinner units have common symmetrical ripples in thin beds.

Arthropycus common on bed soles overlying siltstone; some beds internally bioturbated.

North-central PA sequence at Mill Hall has greater variety of biogenic structures in shale-rich sequence.

Distal:

Alternating thicker, coarser-grained units and thinner, finer-grained commonly rippled units.

Red,
Skolithos-
burrowed
(Castanea
Member)

Coastal sand/mud
flats

Sheetlike unit at top of Tuscarora; transitional from underlying western cross-laminated lithofacies; more sharply transitional into overlying Rose Hill Shale. Thins eastward and southward from north-central part of outcrop belt.

Alternating tabular beds of maroon-red Skolithos-burrowed wacke sandstone and thinner beds of red shale.

Units several meters thick of tan, cross-laminated sublitharenites.

Toward top, common units of drab, greenish shale.

Red sandstone very fine-to fine-grained, poorly to moderately sorted quartz or lithic wacke with up to 25% argillaceous hematitic matrix.

Red sandstone mostly bioturbated, some scattered remnants of parallel and ripple laminae; uncommon interbeds of thin rippled sandstone and shale.

Symmetrical ripples and dessication marks less common.

Tan sandstone units have internal scour surfaces and cross lamination of trough type showing NW transport.

Characteristic Skolithos very common; vertical to oblique shafts are long or short, unbranched, 1-3 cm. diam; coarser sand fillings.

Lower part has Arthropycus; upper greenish shales contain Chondrites and uncommon Monocraterion in interbedded thin sandstones.

No consistent trends in grain size, bed thickness, or sedimentary structures.

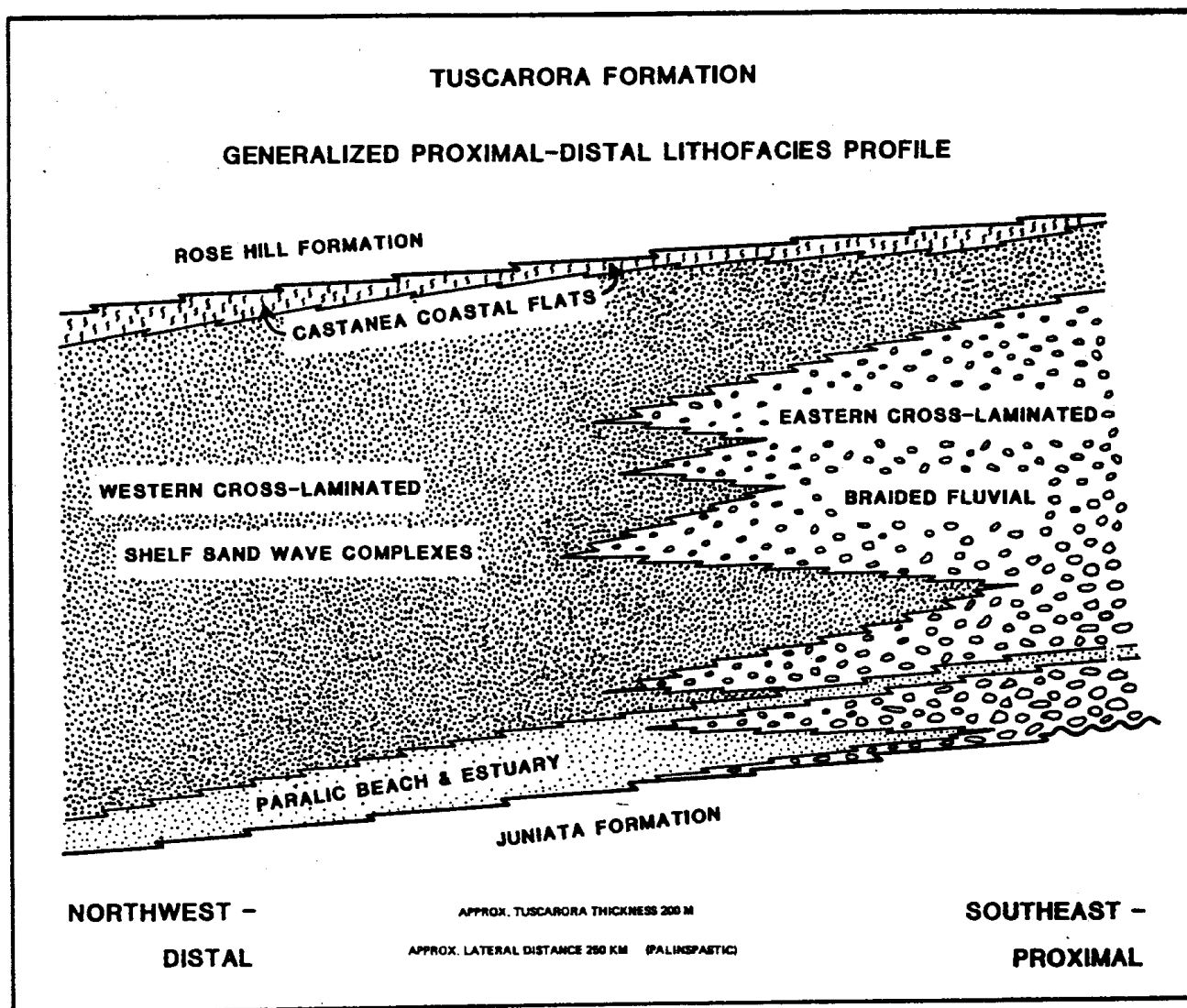


Figure 4. Tuscarora lithofacies profile

useful in considering these to refer to the lithofacies profile (Fig. 4) and the diagrammatic reconstruction of paleoenvironments (Fig. 5).

An important influence on my reinterpretation of the Tuscarora was the identification of the horizontally laminated lithofacies over most of the central Pennsylvania outcrop belt. This thin basal unit is a supermature quartz arenite (Smith and Berkheiser, 1983), with characteristic horizontal lamination and symmetrical, wave-generated ripples. It is not uncommon to find the vertical shafts of *Skolithos* (made by a filter-feeder) associated with this lithofacies, but the *Arthropycus* made by deposit-feeders that are typical of much of the rest of the Tuscarora are not present. This lithofacies was deposited in the foreshore and shoreface zones of a moderate to high energy beach system. There were some variations in the nature of this beach system along the coast. At Mill Hall (Stop VII) there is evidence that the beach system was separated from the adjacent coastal plain by a shallow lagoon (Fig. 5).

Another variation in the nature of the coast can be seen in the presence of pink transitional lithofacies at the base of the Tuscarora toward the southern border of

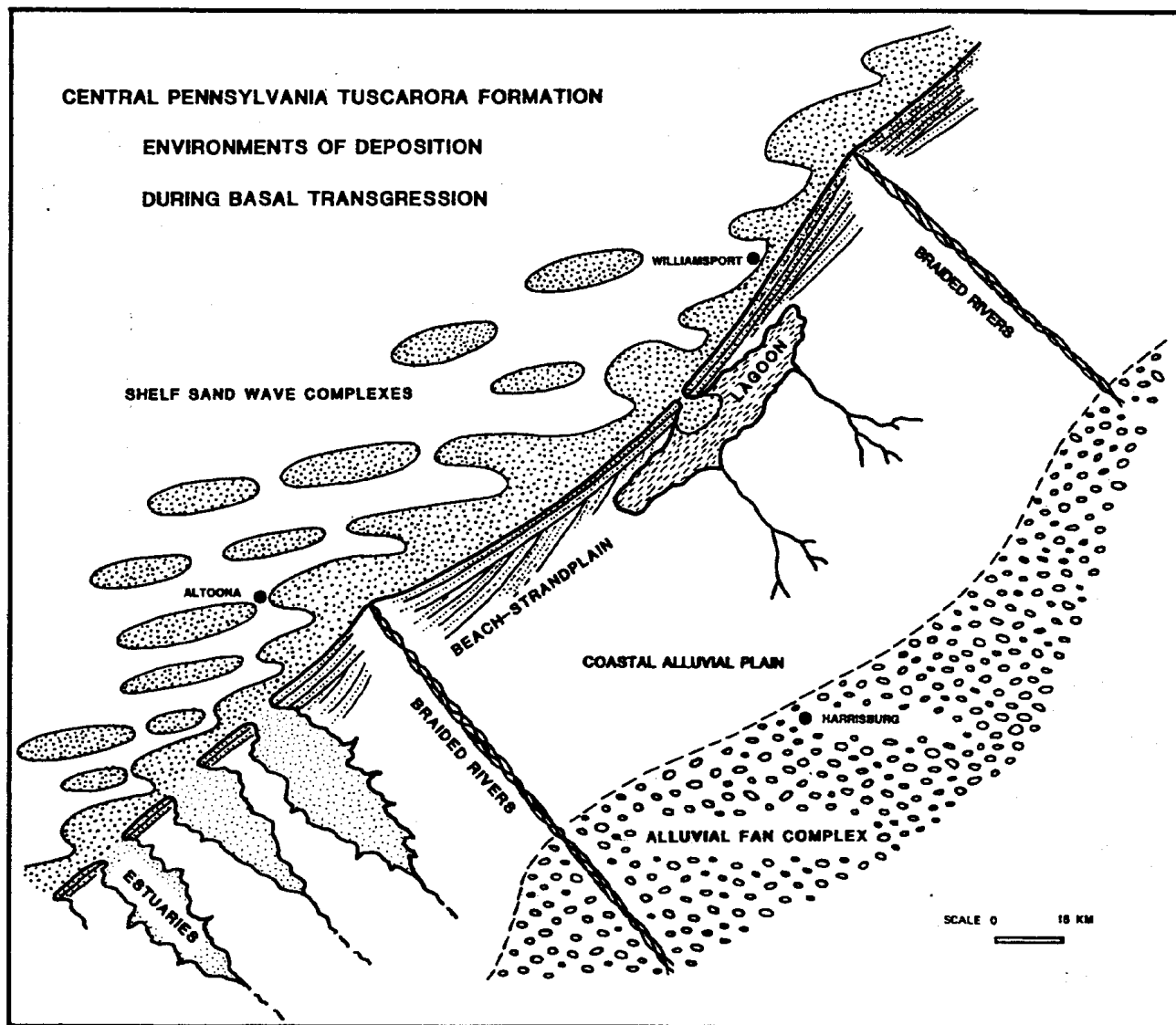


Figure 5. Reconstruction of Tuscarora paleoenvironments

Pennsylvania. This is the unit that was termed the "red Tuscarora" by the Folk (1960) in a study just south of Pennsylvania. The pink sandstones are only slightly less mature than the horizontally laminated lithofacies. Some beds are horizontally laminated and/or symmetrically rippled, but most sandstones are cross laminated. Thin red shales are interbedded with the sandstones. The unit thus has sandstone characteristics approaching those of the Tuscarora but it continues to have the red shales typical of the underlying Juniata. My judgement was that the most likely depositional setting was estuarine, diagrammatically shown in Figure 5.

The base of the Tuscarora, then, is marked across all of central Pennsylvania by thin units that were deposited in coastal environments. For such coastal deposits to accumulate on the top of the fluvial deposits of the Juniata Formation (conglomeratic Run Gap Member) there had to have been a relative rise of sea level. And above these transgressive basal Tuscarora units one would expect to find shallow marine deposits.

That is just what happens. At most localities west of the Susquehanna River the medial part of the Tuscarora consists of the western cross-laminated lithofacies

(Fig. 4). Deposition of this unit occurred on a shallow marine shelf, largely as sand wave complexes that migrated toward deeper water. Many parallels can be found with the features of modern shelves that have been called "shoreface-connected sand ridges" (Swift and Field, 1981). At Stop VII (Mill Hall), we shall examine this lithofacies at one of its more distal exposures. The relative abundance of shale here permits easy recognition of the distinctive bed geometry of the sandstones - flat bases and broadly arched tops. We shall also examine one of the few examples of bipolar (herringbone) transport found in the Tuscarora, as well as a variety of biogenic structures, including Rusophycus, Monocraterion, Diplocraterion, Skolithos, as well as the more common Arthropycus.

Laterally equivalent to this shelf lithofacies, proximal localities contain the eastern cross-laminated lithofacies (Fig. 4). This coarse-grained, pebbly sublitharenite has characteristics of braided river deposits. It conforms best to the Platte River braided model of Miall (1978), which is not too surprising in view of the development of the Platte River model by Norman Smith (1970) partly with reference to the Tuscarora. One difference from Smith's work is that I believe the braided fluvial interpretation applies only to the eastern cross-laminated lithofacies, not to the entire exposed Tuscarora. The braided rivers flowed from the source terrain, through alluvial fan complexes, and then across a coastal alluvial plain to the coast (Fig. 5). Seaward of that coast was the array of sand wave complexes that developed the western cross-laminated lithofacies.

Capping the Tuscarora over much of central Pennsylvania is the red, Skolithos-burrowed lithofacies. This is the Castanea Member that was defined by Swartz (1934) from a locality very close to Stop VIII. This lithofacies is thickest (about 45 m) near this northerly type locality, and it thins southward and eastward from there. It consists largely of very fine grained sandstone that is rich in red, hematitic matrix, and that is thoroughly penetrated by vertical shafts of Skolithos. Additional features are described at Stop VII (Mill Hall). The lithofacies accumulated in coastal sand/mud flats through which drainage channels flowed seaward. Minor fluctuations of sea level produced a number of intercalations of green shales with Chondrites, and periodic exposure led to development of desiccation cracks. This represents a general episode of progradation and coastal exposure just before submergence under the Middle Silurian Rose Hill Sea.

DEPOSITIONAL HISTORY OF THE TUSCARORA

You will recall that in central Pennsylvania at the beginning of Silurian time two significant geologic events were in progress. Sea level was rising rapidly following the waning of Late Ordovician glaciers, and the rejuvenated Taconic Highlands were contributing sediment of greater quantity and coarser size to the eastern margin of the Appalachian Basin. The glacioeustatic rise of sea level was so rapid that, even at a time of increased sedimentation, the shoreline migrated sourceward (southeastward) to a position east of Swatara Gap.

My conception of the paleoenvironmental pattern that existed during this basal Tuscarora transgression is shown in Figure 5. Sublitharenitic detritus coursed northwestward down the regional paleoslope to the coast. A broad alluvial fan complex and a distal coastal alluvial plain were constructed as linear braided belts shifted laterally. At the coast were beaches (and estuaries toward the southwest) on which wave energy was sufficiently intense to remove less durable grains, leaving nearly all monocrystalline quartz. Some localities show evidence of temporary minor progradations of the shoreline, possibly associated with exceptionally large floods, but overall the basal Tuscarora records the sourceward migration of the coast as sea level continued to rise.

Seaward of this beach coastal zone, the shelf contained an array of parallel sand wave complexes (Fig. 5) ("megarippled sand shoals"), analogous to present-day features labelled shore-face-connected sand ridges. Sand (and some gravel) reached the shelf as a result of partial truncation of the beach sediment prism as retrogradation continued. Shoal morphologies were initially inherited from the shoreface, but in the shelf hydraulic system they were modified and translated to preferred configurations and orientations (Swift and Field, 1981; Figueiredo and others, 1982; Parker and others, 1982). The shelf sand is quartz arenitic, largely because it was inherited from the beach system, but also because the dynamic conditions of the shelf can increase compositional maturity (Allen, 1980). Toward north-central Pennsylvania the sand wave complexes were separated from each other by muddy intershoal areas. This is the situation to be examined at Mill Hall (Stop VII), where the sandstone is somewhat more sublitharenitic.

What was the dominant process operating to move the sediment in these shelf sand wave complexes? In the last few years it has become evident that there are few unequivocal criteria for differentiating between tidal processes and storm processes in the generation of stratigraphic successions (Johnson, 1978; Levell, 1980b). My bias is that wind-driven, storm-generated currents operated in the Tuscarora shelf environment. This is suggested (but not proven) by the largely unimodal paleoflow system recorded in the cross stratification (Yeakel, 1962). Symmetrical ripples at distal localities indicate wave action, and gravel lags at the tops of beds demonstrate a storm influence (Levell, 1980b).

There still remains the enigma of the absence of body fossils in deposits judged to be of marine origin. Yet there are other well-documented examples of Phanerozoic marine shelf deposits with essentially no body fossils (e.g., see de Raaf and others, 1977). And there are more biogenic structures in the Tuscarora in Pennsylvania (Cotter, 1982, 1983; see Stop VII description in this guidebook) and in nearby states (Diecchio, 1973) than heretofore recognized. I favor an explanation for the absence of Tuscarora body fossils that involves the chemistry of the sea water, specifically, the possibility that the waters were brackish and/or seasonally changeable (Cotter, 1983, p. 44).

This period of shelf sedimentation in central Pennsylvania went on for something like 10 million years (McKerrow and others, 1980; accepting the assigned age for the Tuscarora from Berry and Boucot, 1970). With only about 150 meters of sediment in 10 million years, there must have been many episodes of reworking of the clastic particles. Over much of the shelf little mud could accumulate, but toward north-central Pennsylvania mud was deposited between sand shoals, either because of greater depth or greater sheltering.

The shelf conditions lasted until about Llandovery C₂₋₃ time (age of top of Tuscarora, Berry and Boucot, 1970). This corresponded with sea level fluctuations, first a eustatic regression in C₂₋₃ time, followed by a continent-wide transgression in C₄ time (McKerrow, 1979; Johnson, 1980; Johnson and Campbell, 1980). With the regression, a coastal sand/mud flat complex prograded to the northwest. The shoreline this time was of much lower energy than that of the beginning of Tuscarora time, possibly because of the greater quantities of mud entering the depositional system from the lowered Taconic Highlands. The muddy sands of these coastal flats were populated by incredible numbers of vertical filter-feeding organisms (*Skolithos*). This terminal unit of the Tuscarora became red because of the abundance of hematite (Folk, 1960). Possible factors in the accumulation of hematite will be considered in the next section of this guidebook, where the "Clinton" ores are discussed.

Subaerial exposure of this low-energy coastal zone lasted only a short time. The Llandovery C₄ transgression reintroduced shelf conditions to central Pennsylvania. This brought what we can call the Rose Hill sea, in which conditions were now compatible with the existence of skeletonized life. The depositional history from this point will be considered in the next section.

Rose Hill, Keefer, and Mifflintown Formations

INTRODUCTION

There are two reasons why this contribution on the origin of the Middle Silurian units appears to be longer and more complex than that on the Tuscarora. First, my views on these units have not previously been published, so there are no other sources to which one might refer for details. And second, the Middle Silurian succession contains a greater variety of lithologies, many of which require additional discussion. To assist you to see the simple pattern in all this apparent complexity, note that this is the order of presentation.

GENERAL ORIENTATION - to the Middle Silurian succession in central Pennsylvania and in contiguous parts of the Appalachian Basin.

LITHOLOGIES AND THEIR ORIGIN. It will take some space to go over the principal lithologies. I will try to show that one can divide them into heterolithic (thinly interbedded mudrock and sandstone or grainstone) and monolithic (dominated by one of these) associations. The major theme in the origin of the heterolithic associations is that storms periodically lashed the Middle Silurian shelf. The composition of the sediment slowly evolved, but the continuity of this storm/interstorm pattern imprinted a recognizable similarity on the lithologies. Monolithic associations developed in central Pennsylvania when fluctuations of sea level changed the process dynamics in the shelf. When sea level was lowered hematite/chamosite-rich sediments or quartz arenite formed, and at a time of higher sea level, black shale blanketed the area.

SUMMARY AND CONCLUSIONS on the genesis of the Middle Silurian succession attempts to pull together the ideas from the consideration of the separate lithologies and to place them in the Appalachian Basin context reviewed in the first part.

GENERAL ORIENTATION

In central Pennsylvania, the Middle Silurian is represented by the Rose Hill, Keefer, and Mifflintown Formations (Figs. 2, 3, 6). Conformably above the Tuscarora, these units typically occur at the margins of the broad valleys, where they commonly are mantled by colluvium from the flanking Tuscarora ridge. Although a number of members have been proposed with different degrees of formality, I have found it convenient to use informal unit members (from 1 through 10) to simplify the presentation. Some of the member names are used in passing in the text and on stratigraphic diagrams (Figs. 3, 6).

By Middle Silurian time, continued northward movement had brought the North American plate closer to the evaporative latitudes of the Southern Hemisphere (Scotese and others, 1979; Ziegler and others, 1979). However, clear signs of climatic aridity would not appear in the strata until the Bloomsburg (see the incipient caliche at Stop I and the vertisol-generated slickensided planes at Stop V) and the Wills Creek-Tonoloway above that (see Tourek, 1970).

There was a change in the general pattern of the Appalachian Basin during the Middle Silurian. Until near the end of the Llandovery Epoch, the basin behaved in a generally uniform manner, and the sedimentary record is relatively similar along much of the basin's southeastern flank (Smosna and Patchen, 1978). However, a pattern emerged during the Middle Silurian, a pattern that would persist into the Devonian Period

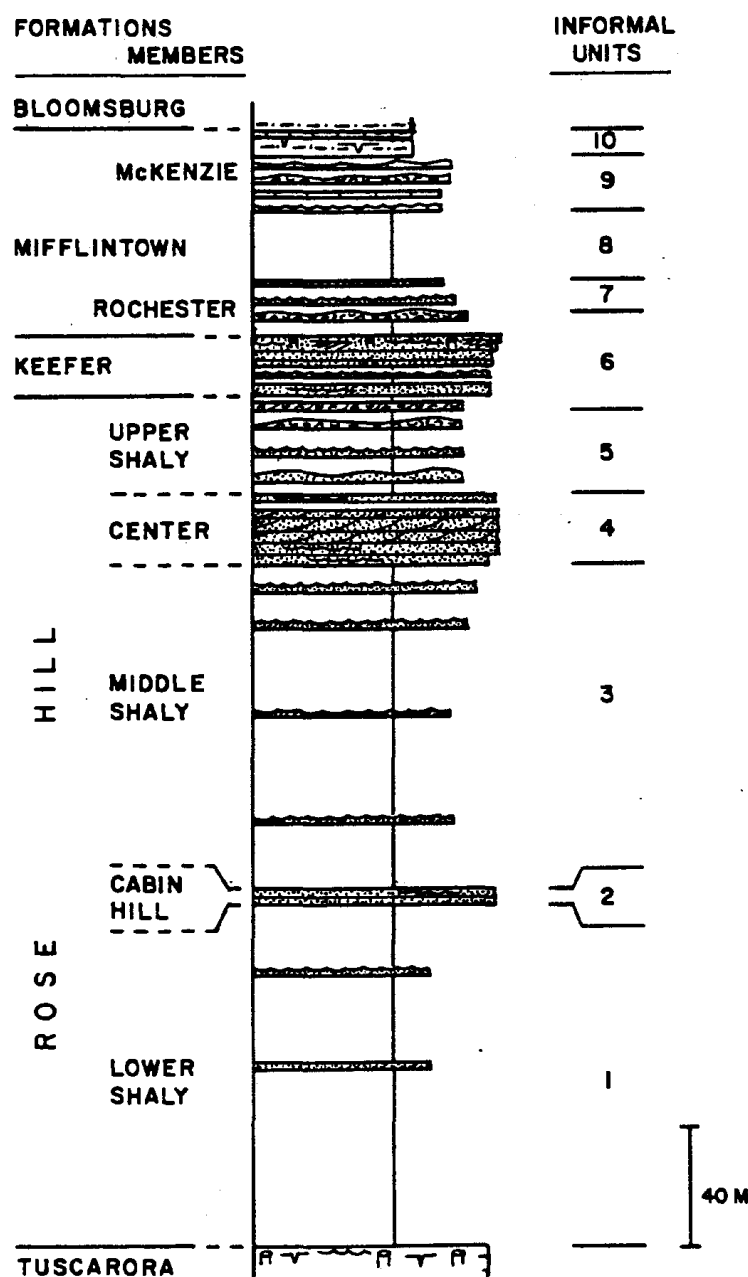


Figure 6. Middle Silurian column, with formations and members, and informal units (Dennison and Head, 1975). An elongate basin axis ran northeast-southwest, much as the keel-line of a rowboat (see comment by Dennison, 1983). Along this axis, slightly greater differential subsidence (Smosna and Patchen, 1978) at a time of limited sediment input kept the central part of the basin deeper than the margins. Then through the Wenlock, some differential subsidence in the central part of the basin created more localized subbasins among shallower platforms (Smosna and Patchen, 1978).

The greater depth along the Appalachian Basin axis means that through the Middle Silurian there persisted the deposition of a lower-energy mud facies in which there are few unconformities. On the other hand, the flanking basin margins, both northwest and southeast of the deeper axial region, were sites of shallower, higher-energy conditions, dominated principally by terrigenous clastic sands on the southeastern margin and by marine carbonates on the northwestern flank (Fig. 8).

The general paleoenvironmental pattern shows up in the composite lithofacies profile (Fig. 7) constructed for the general region from central Pennsylvania to the vicinity of Niagara Falls (transverse to the basin axis). In the center, mudrock dominates the lithofacies. Into the axial part, sandstone-dominated wedges extend from the southeast, and carbonate-dominated wedges extend from the northwest. The Middle Silurian history of this part of the Appalachian Basin, therefore, can be seen as a sequence of axial expansions (when the muddy central facies spread over the shallower marginal shelves) and contractions (when the marginal, higher-energy facies spread toward the basin center). The most important factor controlling the sequence of expansions and contractions was the pattern of sea-level fluctuations. We shall return to these issues in summing up the Middle Silurian history after consideration of the origin of the variety of lithologies to be seen on this field excursion.

The area of the field excursion is represented on that part of the lithofacies profile (Fig. 7) just to the left of the vertical row of unit members. This is a transitional part of the succession, between the sandstone-dominated southeastern margin and the mudrock-dominated central zone. The column here consists of alternating units of heterolithic and monolithic lithologic associations. The heterolithic associations are largely made of basin-center mudrock in which there are numerous thin interbeds of sandstone or grainstone derived from more marginal locations. These heterolithic associations are the basis of designating informal units 1, 3, 5, 7, and 9 on the profile (Fig. 7), on stratigraphic columns (Figs. 3, 6), and in the written part of this guidebook. Monolithic units are dominated by one or the other lithology (mudrock or sandstone/grainstone). Most of the monolithic units (2, 4, 6, and 10) represent deposits of the southeastern basin margin; one monolithic unit (8) is characteristic of the basin center.

LITHOLOGIES AND THEIR ORIGIN

Heterolithic Associations

"Heterolithic" is a trendy term for thinly interbedded mudrock and sandstone (or coarse-grained limestone), with proportions that vary from mud-dominated (10-50% ss.) to mixed (50-75% ss.) to sand-dominated (75-90% ss.) (Johnson, 1978, p. 233).

The Middle Silurian succession in the field-conference area has a high proportion of mudrock. This forms what might be called the "background" lithology of the heterolithic associations. It is nearly all fissile clay shale composed of mixtures of illite and chlorite (Folk, 1960, 1962; Hunter, 1970). There is a progressive upward increase in the degree of mudrock calcareousness that accompanies the increase in the number and proportion of thin interbeds of coarse-grained limestone. Mudrock color, in the lower three-fourths of the succession, is mostly pale grayish olive (10Y 5/2). A change to medium and dark gray begins approximately at the base of Unit 6 (Figs. 6, I-1), within the upper shaly member of the Rose Hill Formation. There is a return to pale green at the top of the Middle Silurian, within Unit 10, the transition to the Bloomsburg Formation. There are some thin bands of purplish-red mudrock, commonly bioturbated and generally associated with the more sandstone-dominated parts of the succession (see Stop I).

Some individual biogenic structures can be recognized, most commonly at interfaces between sandstone and overlying mudrock. Chondrites, of several different sizes, is most common, but Planolites, Rusophycus, and Bifungites are also present. Based largely on collections from Danville (Stop I), Garlock and Isaacson (1977) determined that the biogenic structures are characteristic of Seilacher's shallow-marine Cruziana ichnofacies. The preservation of biogenic structures is roughly related to the proportion of sandstone interbeds in heterolithic associations.

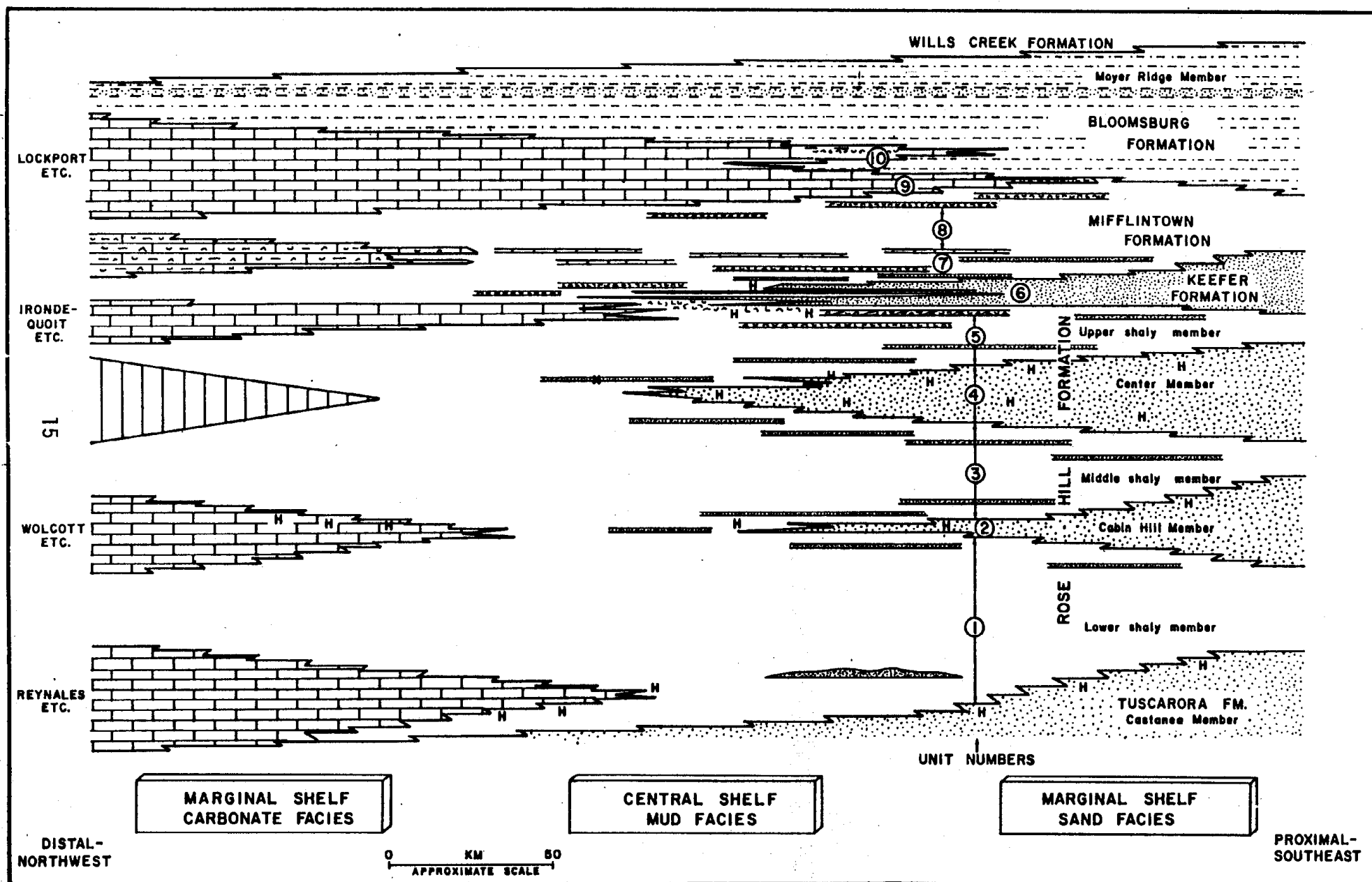


Figure 7. Middle Silurian lithofacies profile normal to Appalachian Basin axis

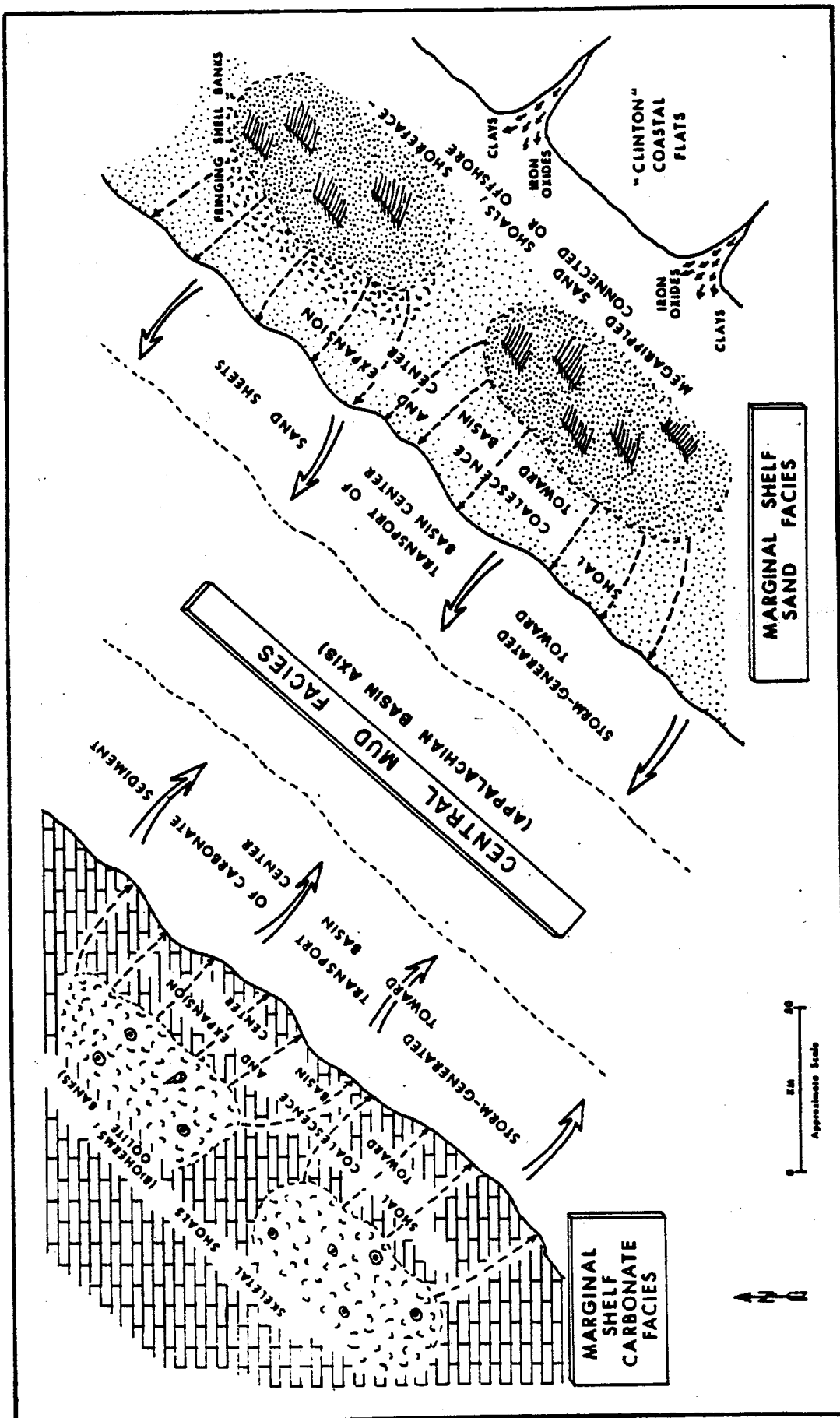


Figure 8. Conceptual model - Appalachian Basin Middle Silurian paleoenvironments

The mudrock contains few body fossils. Most commonly noted are ostracods and Tentaculites, and at most localities one must look carefully even for these. Also present in sparse quantity are trilobites, nautiloids, crinoid ossicles, and small, delicate brachiopods and bivalves. Essentially all forms were epifaunal or nektonic. Sessile forms had shapes adapted to a muddy substrate. You may be familiar with faunal lists from this Middle Silurian succession, such as those by Swartz and Swartz (1931). What such lists do not make clear is that most of the identified taxa came from coarser-grained sandstones or limestones, introduced as storm beds into the depositional environment of the mudrock.

This depositional environment of the mudrock was placid. For prolonged periods, possibly lasting thousands of years (see frequency of storm beds, below), little agitation reached down to these muds from the hydrodynamically active surface waters. Salinities at some times were normal marine (crinoids, brachiopods), but the presence of large numbers of ostracods on bedding planes suggests that waters were at times brackish, especially toward the end of the Middle Silurian (Units 9, 10). Typically, oxygen was in limited supply, inhibiting the presence of both skeletonized and soft-bodied infauna. For much of the later Llandovery (Units 1-5) conditions were mildly reducing (dysaerobic to anaerobic - Byers, 1977), but they became even more anaerobic, culminating in Unit 8, in the Wenlock.

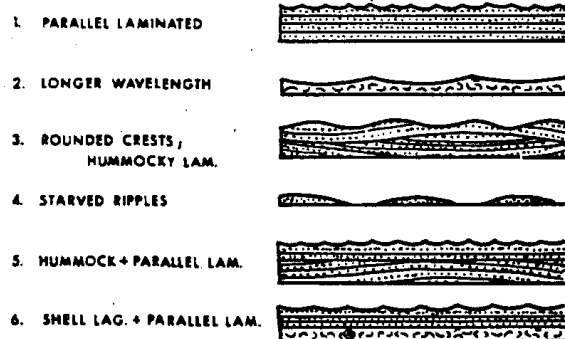
A modern analogue for this environment that still has appeal was suggested by Folk (1960, p. 41). He proposed that the environment might have been similar to the Gulf of Paria (van Andel and Postma, 1954), where a marine shelf of low energy lies offshore from a low coastal plain traversed by turbid, sluggish rivers. For central Pennsylvania, this analogue is more appropriately applied only to the mud-dominated axial part of the basin, not to the higher energy marginal platforms. The second component of the coarser-grained lithologies is the coarser-grained beds. Up through Unit 6 (Rose Hill, Keefer, lower Mifflintown Formations) (Figs. 3, 6, I-1), these are largely beds of terrigenous clastic sandstone (although bioclastic skeletal grainstones are common in Units 5 and 6). Within Unit 7, however, there is a transition to all limestone interbeds. The sandstones are quartz-rich and generally cemented by hematite or chlorite. Carbonates are grainstones, packstones, or wackestones, containing skeletal, pelletal, or intraclastic grains. A general summary of the distribution of lithologies is presented by Hunter (1970), and petrographic details are in the reports by Folk (1960, 1962).

There are two characteristics of these coarser-grained beds that can be used to sort out meaningful categories: (1) bed geometry, and (2) the nature of the internal lamination. Figure 9 contains a scheme showing how the coarser-grained beds at Danville (Stop I) can be systematically organized. This diagram will serve as a reference for the descriptive comments below, but the next paragraph is a brief introduction to the diagram.

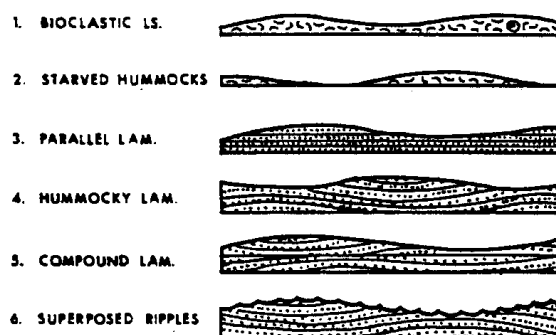
The first observation to note about bed geometry is that basal surfaces are almost always flat. Differences in bed geometry, therefore, result from the character of the upper surfaces. This leads to two major categories (A and B of Fig. 9), based on whether the upper surface is symmetrically rippled, or whether it is broadly wavy and hummocklike. Some beds have neither of these two characteristics, and are categorized largely on the basis of whether they are cross-stratified (C of Fig. 9), or structureless (D of Fig. 9). Two exceptional categories complete the diagram. Category E consists of laterally discontinuous beds that fall under the term "gutter marks." And in category F are those beds showing features of penecontemporaneous erosion and sculpting.

This next section of the guidebook is a consideration of the features and origin of each of these categories.

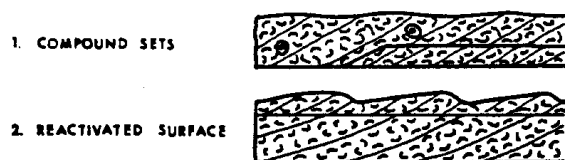
A. SYMMETRICALLY RIPPLED SURFACES



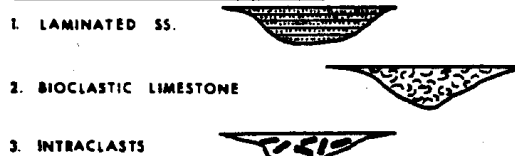
B. HUMMOCKLIKE WAVY SURFACES



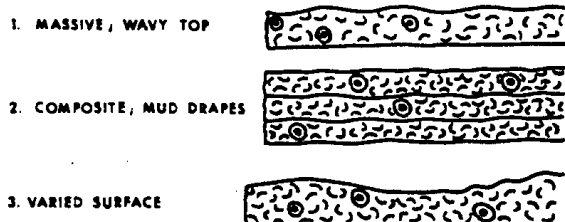
C. CROSS-STRATIFIED BEDS



E. CHANNELFORMS - GUTTERS



D. COMPOSITE AND MASSIVE



F. TERMINATED AND SCULPTED

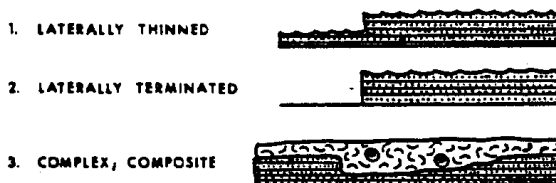


Figure 9. Styles of coarser-grained beds, Middle Silurian, Danville

Category A. Symmetrically rippled surfaces. This is the most common variety of coarser-grained beds. Aside from the ripples, the beds are flat-based and parallel-sided. Thicknesses are typically between 1 and 20 cm. Ripple patterns can be parallel and rectilinear, or they can be curvilinear (Figs. I-3, VIII-2). Interference patterns are common (Figs. I-3, VIII-2). Ripple wavelengths are generally between 10 and 20 cm, but others can be as large as 50 cm (Fig. VIII-2).

Even though symmetrical ripples form such prominent external features, the internal structures seldom show ripple lamination, and even that is in the uppermost fraction of the bed. Of the chief types of internal lamination, parallel (horizontal) lamination is most common (Fig. 9, types A1, A6; Fig. I-3). In other beds, there are very narrow acute angles between several internal sets of parallel laminae; the laminae of the overlying set are parallel to the internal discontinuity (Fig. 9, types A3, A5; Fig. I-3). When traced laterally, these are seen to be parts of hummocky cross-stratified (HCS) beds (defined by Harms and others, 1975; analysis by Dott and Bourgeois, 1982), and the internal laminae have hummock dimensions similar to those of the broadly wavy upper surfaces (see Category B). The beds with symmetrically rippled surfaces are more commonly sandstone than carbonate grainstone, for most bioclastic limestones are too coarse for development of the smaller-scale features. In some beds, there is a basal shell lag, commonly in the form of broad, hummock-like lenses, overlain by parallel-laminated sandstone, and capped by a symmetrically rippled surface (type A6 of Fig. 9).

Category B. Hummocklike, wavy surfaces. Most typically, these are associated with skeletal grainstones (bioclastic limestones). Basal surfaces are flat, and upper surfaces are broadly wavy, with slight domes. There is such a distinct pinch-and-swell character to some beds that when the beds are thin, the "pinch" parts in the troughs are missing, and the "swell" parts of the crests are isolated like "starved hummocks" (Fig. 9, type B2). Internally, beds can be structureless or have the parallel or hummocky lamination seen in beds of Category A (see types in Category B of Fig. 9). As might be expected, the most common internal structure is hummocky lamination.

Origin of Categories A and B - rippled and hummocklike surfaces.

These are storm beds. Ideas on the generation of such thin interbeds of sandstone within mudrock have come into vogue in the last decade, possibly beginning with the influential paper by Goldring and Bridges (1973) on "sublittoral sheet sands." Good summaries are presented by Johnson (1978), Brenner (1980), Reineck and Singh (1980). A recurring idea about the conditions of formation is the "storm-surge-ebb" concept (Hayes, 1967, as modified by Morton, 1981). This involves the storm-wind-forced buildup of seawater in the nearshore zone, leading to development of an intense, seaward-directed return flow near the bottom. The coarser sediment is entrained in such currents from the shoreface or from offshore bars. It then spreads as a density current out over the normally muddy substrate of the lower-energy, deeper-water shelf.

We can judge better whether such storm-bed concepts apply to the Middle Silurian succession if we consider an idealized, composite coarse-grained bed, based on the section at Danville (Stop I) (Fig. 10). This idealized bed contains all the essential elements of the major types of beds, with the features in the order in which they are found in the beds. Above a flat base, a basal shell lag has wavy, lenticular form. The next overlying laminae are broadly undulated, with sets above discontinuities having laminae parallel to the discontinuity. There follows a set of horizontal (flat) laminae, and finally a capping surface of symmetrical ripples.

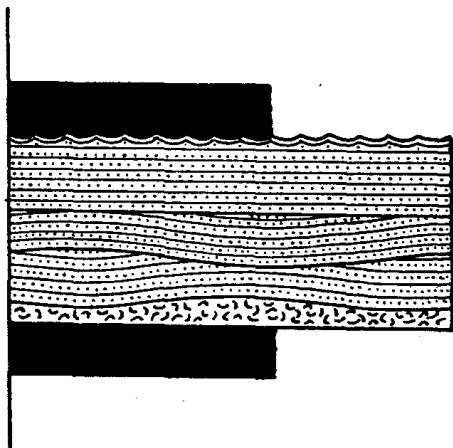


Figure 10. Idealized composite storm bed, Middle Silurian, Danville. Bed thickness varies from 3 cm to 20 cm

This idealized composite bed (Fig. 10) is similar to the "idealized hummocky sequence" proposed by Dott and Bourgeois (1982) (reproduced as Fig. 11) as a conceptual model for the recognition and interpretation of such ancient storm deposits. A similar sequence and conceptual framework have been presented by Hunter and Clifton (1982), and this also is interpreted in the context of storms. There are presently a number of other proposals for idealized storm beds, and some of these show horizontal lamination below, rather than above the hummocky lamination (see Brenchley and others, 1979;

Allen, 1981; Kreisa, 1981; and Mount, 1982). Because of the greater experience of Dott and Bourgeois (1982) and Hunter and Clifton (1982) with appropriate shallow-marine deposits, their analysis is followed here.

With the storm-generated transport of shells and sand to deeper water, a sequence of bedforms is generated as the flow intensity wanes (Fig. 11). The initially aggrading sediment (shells, if any, and sand) will have an undulatory surface of hummocks and swales. The origin of this surface form still is poorly understood, but it involves fallout of fine sand from suspension and lateral traction related to oscillatory flow at the bed (Dott and Bourgeois, 1982, p. 675; Hunter and Clifton, 1982). If the flow intensity and sediment aggradation were to cease abruptly at this stage, the bed surface would have the broadly wavy, hummocklike form of the Middle Silurian beds in Category B (Fig. 9B).

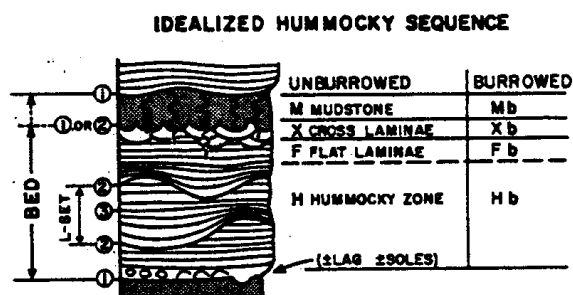


Figure 3. The idealized hummocky sequence showing suggested notation for its component zones. Note distinction of hummocky beds from lamina sets and a hierarchical order of surfaces (numbers) explained in text. Burrowing may overprint the top or even the entire sequence. (After Dott and Bourgeois, 1979, 1980.)

Figure 20. Maximum orbital velocity thresholds for initiation of grain movement for four different wave periods as well as change from rippled to flat bed for quartz sand in oscillatory water flow (after Clifton, 1976, and Dingle, 1974). We have added inferred position of hummocky stratification.

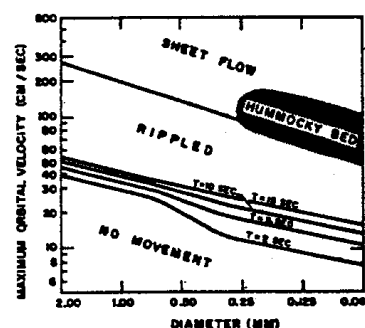


Figure 11. Hummocky cross stratification; terms, idealized sequence, and genesis. From Dott and Bourgeois (1982)

On the other hand, sedimentation could continue while oscillatory flow intensity decreased more gradually. The bed forms change to lower-amplitude hummocks, and then to a flat surface. Sedimentation appears to flatten the depositional surface by filling in the swales (Dott and Bourgeois, 1982, p. 667). With still further reduction of oscillatory flow, bed forms enter the field of ripples (Dott and Bourgeois, 1982, Fig. 20; reproduced here as Fig. 11). This is the situation demonstrated by the idealized composite bed from the Middle Silurian of Danville (Fig. 10). Sand aggradation was nearly complete as the field of symmetrical ripples was reached, and for most beds ripples are only a surface molding of the underlying laminated sediment. Beds of Category A (Fig. 9) are very similar in origin to the broadly wavy beds of Category B, differing principally in the exact nature of the relation between the rate of aggradation and the rate of decrease of flow intensity.

The range in values of the ripple wavelength (Fig. VIII-2) on these beds is rather broad, even on beds close to each other in the section. This situation might result from the mixing of orbital ripples and anorbital ripples in the same succession. Orbital ripples form at lower intensities of oscillatory flow during which there is little, if any, exchange of material between adjacent crests (Allen, 1981, p. 371). In such cases the

wavelength of the ripples is related to the orbital diameter of the waves at the bottom (Hunter and Clifton, 1982, p. 138), and the ripple spacing is a function of water depth. If the oscillatory flow is more intense, the ripples can be anorbital (also called rolling-grain ripples), for which the spacing is dependent on the sediment grain size (Hunter and Clifton, 1982). For many Middle Silurian storm beds, there is a general correlation between ripple spacing and grain size (see sequences at Danville, Stop I, and Castanea, Stop VIII). This suggests that these ripples are anorbital, and thus they are dependent on grain size. Further comments about analysis of conditions in which these ripples formed are presented in material dealing with Stop VIII.

Hunter and Clifton (1982, p. 141) present three kinds of evidence by which a bed may be identified as of storm origin. The ripple-topped and wavy-topped beds (Categories A and B of Fig. 9) of the Middle Silurian succession in central Pennsylvania fit all three diagnostic criteria. These are storm beds. Are the other categories of coarser-grained beds also storm beds?

Category D. Composite and massive beds. These have the gross features consistent with a storm bed origin, but they lack internal structures and rippled surfaces. Such beds nearly always are composed of skeletal grainstone, and, therefore, the sequence of internal structures and surface structures appropriate to finer grain sizes (Figs. 11A, 11B) from Dott and Bourgeois (1982) would not form. An important note is that the fauna of these beds is different in composition and type from the fauna in the interbedded mudrock. The coarse, skeletal grainstones have heavier, more robust forms more adapted to higher-energy conditions (shallower water) than the delicate forms found in the mudrock (deeper water).

Category E. Channelforms - Gutters. Laterally discontinuous, channelforms within the succession are the principal exception to the dominance of beds with flat bases and wavy or rippled tops. These have flat tops and concave-upward bases, up to a maximum of a few tens of centimeters thick. These are composed of the same sandstone (Units 1-6) and shell fragments or intraclasts (Units 5-9) as the storm beds in the part of the section in which they are found (Figs. I-1, I-4). In those made of sandstone, horizontal laminae fill the channel (Fig. I-4).

These are the same as features that have been called "gutter marks" (Whitaker, 1973; Greensmith and others, 1980). Their origin involves scouring of the muddy substrate by the storm-generated flow. Normally, the mud is too cohesive to be scoured (leading to the flat bases seen on most storm beds), but where the scour is begun, a relatively deep, narrow channel is incised parallel to the direction of flow. Scouring was done early in the storm-related event, and as flow intensity waned, the gutter was filled by the sediment entrained by the flow earlier (shallower water) (Greensmith and others, 1980; Kreisa, 1981). Those with intraclasts (Fig. I-1, Units 7 and 8) are similar to those reported from subtidal marine carbonates in the Devonian of Poland (Kazmierczak and Goldring, 1978).

Category F. Terminated and sculpted. Many of the storm beds show abrupt thickness changes and even complete terminations against the enclosing fissile shale (Figs. I-1, I-4). When these abruptly terminated margins can be examined, they show delicately fluted erosional forms. The bed was partly eroded and sculpted while still unconsolidated, before deposition of the overlying mudrock. This soft-sediment erosion is likely to have been done when a later storm-generated current that was underloaded re-entrained part of the deposit of an earlier storm. A similar interpretation for similar features in Cambrian storm deposits of Newfoundland has been offered by Hiscott (1982).

Comments about storm beds in the heterolithic associations. Thus, starting with the more common types of beds (rippled and wavy surfaces) and including the less common varieties (gutters, sculpted, massive) it can be shown that most the coarse-grained beds can be explained most readily as the products of storms. The basic types of beds and their contained structures change little through the succession, even though the composition of those beds changed from terrigenous sand to marine skeletal fragments. The storm-related processes remained the same as the composition of the shallow-marine sediment those processes worked on evolved from siliciclastic to bioclastic.

How frequent were the storms that generated these Middle Silurian storm beds in the Appalachian Basin? One approach to this would be to count the total number of storm beds and then divide by the number of elapsed years for that part of the succession. I have chosen not to do this because of the many questionable assumptions and potential sources of error. However, there is an important, consistent message coming from the handful of investigations in which this has been done. They indicate that the events generating shallow-marine storm beds were relatively rare and infrequent, with estimated frequencies ranging between 1000 and 15,000 years (Goldring and Langenstrassen, 1979; Brenchley and others, 1979; Hamblin and Walker, 1980; Kreisa, 1981; Mount, 1982). I believe a similar frequency would apply to the Middle Silurian succession under consideration here. Most of the time (thousands of years) the region received a blanket of very slowly accumulating mud, but every few thousand years there was "terror" as an exceptional storm caused coarse-grained material (sand, shells, oolites, clasts) to flood across the muddy sea floor.

Category C. Cross-stratified beds. These beds are the only ones in the coarse-grained component of the heterolithic associations that do not have the features of storm beds. Two compositions predominate. Close to monolithic units of hematitic sandstone (Units 2 and 4), they are made of similar hematitic sandstone and are interbedded with fissile grayish-olive shale. Within Unit 6, they are made of skeletal grainstone. In fact, the boundaries of Unit 6 are defined so as to include cross-stratified beds within it. These beds are typically 25 to 50 cm thick, and largely parallel-sided, although upper surfaces may be irregularly wavy. The cross stratification is commonly planar, with cross laminae extending through the entire bed. Some beds show compound stratification and/or late-stage reactivation surfaces (Fig. 9C). One mode usually dominates the paleoflow pattern, and that direction tends to be parallel to the ancient shoreline (about NE-SW), although other directions can be found. Bipolar transport is also commonly noted.

The cross stratification demonstrates that these beds formed as persistent traction currents moved bed-load material into bedforms shaped as two-dimensional bars or megaripples. These currents could be coast-parallel, and at times they reversed direction. We shall discuss subsequently the origin of the monolithic units (Units 2, 4, 6) with which these cross-stratified beds are associated, and we shall note that they represent deposition on higher-energy, megarippled sand, shell, or oolite shoals. These cross-stratified beds within the adjacent heterolithic units form at the transitional margins of these shoals. As such, they record the migration of a megaripple over the adjacent off-shoal mud bottom. In the paleoenvironmental summary diagram of Figure 8 the appropriate depositional environment has been labelled as "fringing shell banks."

Monolithic Associations

There are three lithologies that form more than 90% of a significant part of the Middle Silurian succession: hematitic sandstone, quartz arenite, and black shale. A description and interpretation are presented for each of these below. A separate section following these will consider some ideas on the origin of the iron mineralization in these, the "Clinton ores."

Hematitic sandstone occurs monolithically in units thick enough in most places to warrant member status (Cabin Hill, Unit 2; Center, Unit 4). Regionally, these units thin and become finer-grained basinward (Fig. 7). The grayish-maroon, quartz-rich sandstone has immature texture, with subangular grains and poor sorting. Grain size ranges from coarse to fine, and quartz granules can be scattered throughout (as in Unit 4 at Stop I, Danville). The "matrix" is earthy hematite, whose complex origin is in a later section. Interbedded with the thin to medium, commonly lenticular, beds of sandstone are very thin, discontinuous beds of red (rarely grayish-olive) mudrock. This is the same mudrock as that seen as intraclasts in the sandstone at bed boundaries and lining foreset laminae.

The sedimentary structures of the sandstone are cross stratification (mostly planar tangential) and symmetrical ripples, with the proportions of these varying from locality to locality. Flaser structures are found in places. Regional analysis of these structures by Hunter (1970, p. 110) showed that transport was mainly to the west and northwest (seaward). Some monolithic sandstone units have no apparent vertical trends, but others show a "thinning-upward" pattern in which, above a sharp base, there is gradual decrease in the thickness and proportion of sandstone beds until a transition is complete into the overlying heterolithic association. Within some monolithic zones some beds have the flat bases, parallel lamination, and rippled tops much like the storm beds described above. A small amount of biogenic activity is recorded, but body fossils are rare. Hunter (1970, p. 110) reports some possible Lingula.

These hematitic sandstones were formed in the setting of shallow-marine, megarippled and rippled sand shoals (Fig. 8) a somewhat lower-energy equivalent of those suggested for part of the Tuscarora Formation. There were prolonged periods of moderate to high energy, when currents cause the seaward migration of megaripples. Periods of slack water (possibly seasonal) allowed mud to settle out. Storm events ripped up mud as intraclasts, and caused the generation of storm beds, both on the shoals themselves and from the shoals to deeper water. There is little evidence of the tidal conditions indicated for the contemporary shoreline at Schuylkill Gap (Smith, 1968; Smith and Saunders, 1970). These megarippled and rippled sand shoals were located between that low-lying tidal-flat-fringed coastal plain and the deeper-water, muddy axial facies of the Appalachian Basin (Hunter, 1970, Figs. 7, 8) (Fig. 8).

Quartz arenite, the second of the monolithic lithologies, is specifically associated with the Keefer Formation (Figs. 6, 7, I-1; Units 6B, 6D). Although of relatively uniform character over a broad region, the Keefer nevertheless has a number of proximal (SE) to distal (NW) trends that assist in assessing the origin of the unit and its quartz arenite. The following is a list of those proximal-distal trends based on my own observations and those of Folk (1960), Luttrell (1968), and Hunter (1970).

- The monolithic sandstone gives way to more heterolithic associations, with interbedded bioturbated mudrock and skeletal limestones.
- Sandstone composition changes from greater than 99% quartz to large admixtures of carbonate and clay.
- Sandstone texture changes from well-sorted, well-rounded, and finer-grained to only moderately sorted and very fine grained.
- The silica cement of proximal sandstones becomes carbonate cement, including ankerite, distally.
- In proximal parts fossils are rare, and generally only Skolithos burrows are found, whereas distally there are increasing abundances and diversities of body fossils, particularly brachiopods and crinoids.
- Sedimentary structures change from medium-scale cross lamination to large proportions of symmetrical ripples with a variety of wavelengths.

-Sediment transport at proximal locations was dominantly seaward, but it was polymodal at distal places.

The features of the Keefer Formation, including these trends, indicate that its origin was in a shallow-marine setting, with depositional conditions largely shoreface at proximal locations, trending to shallow shelf distally. The quartz arenite was deposited as megarippled and rippled sand shoals in the lower shoreface and/or the inner shelf (Fig. 8). The distal, and possibly also the lateral, fringes of these shoals contained such a diversity and abundance of fauna that they could be called fringing shell banks (Fig. 8). An interpretation such as this has previously been applied to the Keefer in central Pennsylvania by Luttrell (1968) and Faill and Wells (1974). And similar features, trends, and interpretations have been reported for the contemporaneous Herkimer Formation in New York (Zenger, 1971; Osgood and Drennen, 1975).

There is no evidence that any part of the Keefer depositional system ever acted as a barrier beach, separating a dysaerobic Rose Hill Sea from an anaerobic Rochester lagoon, as suggested by Folk (1960, 1962). In addition to the fact that the Rose Hill and Rochester were not contemporaries (Berry and Boucot, 1970), the Rochester lithofacies was seaward (NW) of contemporaneous Keefer lithofacies (Hunter, 1970, Figs. 2, 4, 9; Smosna and Patchen, 1978). A seaward progradation was needed to spread the higher-energy, nearer-shore quartz arenite over such a broad region, a seaward progradation possibly related to a brief eustatic lowering of sea level (Dennison and Head, 1975). What appears likely is that the Rochester lithofacies began as a westward, deeper-water equivalent to the Keefer, possibly situated in an axially located subbasin northwest of the Keefer shelf (Smosna and Patchen, 1978). After the progradation distributed the Keefer quartz arenite widely, subsequent sea-level rise (Dennison and Head, 1975) spread the Rochester lithofacies radially from the basin axis over the marginal quartz arenite (see monolithic black shale, below).

Black shale, is very abundant in the Mifflintown Formation, but most of it is in heterolithic association with thin interbeds of terrigenous sandstone or marine carbonates. However, the middle part of the Mifflintown contains a relatively thick zone of monolithic black shale (Figs. 6, 7, I-1; Unit 8). This is entirely fissile black shale, containing no biogenic structures, but with much finely disseminated pyrite. This represents a long period of slow, low-energy deposition during which the water was totally anaerobic (Byers, 1977), and there were no storm beds. The previous section has stated how these anaerobic conditions spread from the relatively isolated axial subbasins out over the marginal higher-energy shelves (in other words, the Rochester lithofacies spread southeastward over the Keefer sand shoals). This monolithic black shale represents the acme of the transgressive event. Much of central Pennsylvania was covered by anoxic waters, and storm beds were restricted because the marginal sources of coarse sediment were too distant, or because that coarse sediment was trapped in coastal estuaries as sea level rose. It was just this sort of transgression that Hallam and Bradshaw (1979) linked with the development of black, bituminous shales in the Jurassic of Europe.

The black Middle Silurian shale of central Pennsylvania (Units 7, 8, 9, with the acme in Unit 8) is part of a worldwide black-shale-depositing event (Berry and Wilde, 1978, p. 270). Therefore, its widespread development in the Appalachian Basin (Colton, 1970; Hunter, 1970; Smosna and Patchen, 1978) should be considered in a context greater than that of local or regional topographic differences alone. An attractive hypothesis is that this Middle Silurian black shale resulted from an "oceanic anoxic event" (Berry and Wilde, 1978). The basic elements of such events have been presented by Fischer and Arthur (1977), Heckel (1977), and Arthur (1979). At times of little world-wide glaciation, not only would the sea stand higher, but the oceans would be poorly mixed, and the top of

the anoxic layer (oxygen-minimum zone) could rise and extend well into the epeiric seas of continental interiors. These concepts have been used by Leggett and others (1981) to explain the widespread development of black shale at regularly spaced intervals in the Early Paleozoic of the British Isles.

No matter how attractive this hypothesis, a degree of caution is advised before you accept it straightaway. There appear to be conflicting signals about whether there was a world-wide sea-level rise at the time of origin of the Mifflintown Formation (middle and upper Wenlock, Fig. 3). A rise of sea level at that time is certainly suggested for the Appalachian Basin (Dennison and Head, 1975, p. 1097). However, both Leggett and others (1981) and Lenz (1982) show that in the middle of the Wenlock there was a general fall in sea level after an early Wenlock rise. The results shown by McKerrow (1979) for the Wenlock of North America are not very conclusive. Therefore, the assertion of Berry and Wilde (1978) of a world-wide sea-level rise in the middle of the Silurian as an explanation of the origin of the Rochester-type black shale of Unit 8 and related units ought to be treated cautiously until the picture is less murky.

IRON MINERALIZATION OF THE CLINTON ORES

The sedimentary history of the iron mineralization in both the "block ore" and the "fossil ore" (see paper in this guidebook by Inners and Williams, 1983) is related both to the depositional conditions on the marginal shelf sand (and shell) shoals, and to more regional conditions associated with the broader Appalachian Basin. After a brief description of the nature of this mineralization in both the hematitic sandstone ("block ore") and the skeletal grainstone ("fossil ore"), the connection with the local depositional conditions and the regional basin conditions will be made.

Hematite can be quite abundant in the hematitic sandstones of Units 2 and 4 (Cabin Hill and Center Members) and in the individual hematitic sandstones interbedded in heterolithic associations of Units 3, 5, and 6. Amounts commonly comprise 10%, and in places can be more than 20%, of the total rock (Hunter, 1970, p. 111; Faill and Wells, 1974, p. 30; Inners, 1981, p. 131). At first glance the hematite appears to be featureless matrix, but Hunter (1970) has given the evidence and reasoning for the initial accretion of iron compounds as oolitic coatings on the sand grains, and the subsequent remobilization and reprecipitation of the iron oxide.

The skeletal grainstones that have undergone iron mineralization are both the storm beds (Categories B1, B2, D of Fig. 9) and the cross-stratified beds from the fringing shell banks of marginal shoals (Fig. 9, Categories C1, C2; Fig. 8). There are two different forms of iron minerals in these grainstones. The first might be called primary in that the iron minerals (hematite and/or chamosite) occur as concentric oolitic coatings on shell-fragment nuclei (chiefly crinoid ossicles and brachiopod fragments, but also including gastropods, bryozoans, and other forms) (Fig. I-5A, B, C). The primary iron also fills the pores of crinoids and the chambers of gastropods, and it occurs in the shape of fecal pellets. Variations in the distribution of hematite versus chamosite can be quite complex, and the two minerals are interrelated at a variety of scales. As shown in the photos of Figure I-5, the same bed can have hematite coatings in one part, chamosite coatings in another, and even alternating delicate laminae of chamosite and hematite in a third part. In addition to these primary forms, hematite can be secondary, occurring as metallic acicular clusters transecting primary features, such as shell fragments (Fig. I-5D).

A significant summary of the nature and origin of Phanerozoic oolitic ironstone has recently been presented by Van Houten and Bhattacharyya (1982), and further concepts of the generation of "ferriferous ooids" have come from Bhattacharyya

and Kakimoto (1982). If we add to these the ideas on the relation of oolitic ironstones to sea-level fluctuations by Hallam and Bradshaw (1979), we have the essential elements for a satisfactory interpretation of the iron mineralization of the Clinton ores. Although the next several paragraphs have few citations, the works mentioned in this paragraph are the basis of the following ideas.

As Middle Silurian time progressed, terrigenous detritus was reaching the Appalachian Basin in diminishing amounts. The transition to shelf carbonates was imminent. With the Taconic Highlands topography reduced, and the subtropical latitude providing for intense weathering at least seasonally (Folk, 1960, p. 56; Hunter, 1970, p. 116), what reached the sea was probably largely clay minerals (kaolinite?) and hydrated iron oxides. Stretching seaward from the nearshore zone was a complex of megarippled sand shoals and, at times and places, fringing shell banks (Fig. 8). There was sufficient energy on these marginal shoals and banks to agitate sand grains and shell fragments as the bedforms migrated generally seaward. In the moderately agitated, normal salinity, aerobic setting, suspended particulate matter (both hydrated iron oxides and clay minerals) could mechanically accrete to grains (sand, shells, fecal pellets) generating concentric rims that could vary in specific composition. The exact proportion of clays to iron oxides suspended in sea water (and consequently accreted to host grains) could vary seasonally or on a longer-term, climatically related basis.

Hematite and chamosite developed from the accreted rims of suspended particulate matter. Hematite formed from the hydrated iron oxides, and chamosite formed from the kaolinitic clays. Metallic, acicular hematite formed by remobilization and reprecipitation of these iron minerals, or their precursors, in later diagenesis.

The cross-stratified sandstones and skeletal grainstones represent deposits directly associated with the megarippled shoals. At the times of Units 2 (Cabin Hill) and 4 (Center), detrital sand grains formed the host nuclei. At the time of Unit 6, the sites of fringing shell banks had the appropriate combination of agitation and suspended sediment concentration and composition to lead to the accretion of the oolitic coatings on skeletal fragments.

Storm beds, both sandstone and skeletal grainstone, were eroded penecontemporaneously from the marginal shoals and transported to the deeper-water, anaerobic conditions more typical of the central mud facies. The iron-rich oolitic coatings that had been generated in the agitated, shallower environment of the marginal shoals were already on the host grains (either sand or shells) when they were flushed to deeper water. One cannot determine if the transformation of the hydrated iron oxides and kaolinite to hematite and chamosite were complete at this time, but it is possible that the transformations could take place in the deeper-water setting.

Why did the Clinton iron mineralization take place at this time in the Appalachian Basin? During the Middle Silurian, the input of the terrigenous clastics to the basin had lessened, and the appropriate conditions of composition/concentration of suspended particulate matter and the proper degree of agitation could come together. If too great a concentration of clays reached the sea, they would flocculate into larger particles and settle as cohesive mud. The climate had to be appropriate to the production of the hydrated iron oxides and kaolinite. And the proper degree of agitation was necessary to form well-developed oolitic coatings, but not to break the oolitic rims.

The three major periods of iron mineralization in the Middle Silurian of central Pennsylvania are associated with three monolithic zones: Unit 2 (Cabin Hill)-hematitic sandstone; Unit 4 (Center)-hematitic sandstone; Unit 6 (uppermost Rose Hill and

Keefer)-hematitic and chamositic skeletal grainstones (Figs. 6, 7, I-1). In this general period of little influx of particulate matter to the basin, each of these three zones represents a time of lowered sea level, when the agitated marginal shoals expanded their extent considerably toward the basin center (Figs. 7, 8). More, the marginal shelf had the appropriate degree of physical agitation. The suspended particulate matter (hydrated iron oxides and kaolinite) would accrete onto host nuclei (and some would bypass the shoals completely). Those parts of the shelf where we now find the Clinton ore had at that time the appropriate mix of suspended particulate matter and degree of agitation. When sea level rose following each of these periods, there was insufficient agitation in the deeper water, and sedimentation returned to the slow accumulation of muds (from clays that bypassed the shoals that were now farther to the southeast), interrupted every few thousand years or so by the torrential influx of a storm bed, carrying sediment that had been in temporary residence on the marginal shoals and fringing shell banks.

GENESIS OF THE MIDDLE SILURIAN SUCCESSION

Deposition of the Middle Silurian stratigraphic succession in central Pennsylvania (Rose Hill, Keefer, and Mifflintown Formations) took place entirely within the context of a shallow marine shelf. The shallower, proximal margin of this shelf comprised megarippled sand shoals (sandwave complexes), the fringes of which at times contained shell banks (Fig. 8). These marginal shoals and banks commonly had the appropriate conditions of agitation and iron oxide/clay abundance that led to formation of oolitic hematite and chamosite. Closer to the axis of the Appalachian Basin, the distal shelf was normally low-energy and anaerobic to dysaerobic and mud blanketed the bottom (Fig. 8). Into this muddy region, storm-generated currents flushed coarser sediment (sand, shells, clasts) at infrequent intervals from the marginal shoals. Sediment that had been oolitically coated with iron minerals when on the marginal shoals was also flushed in to the distal muddy environment. Storm beds and the background mudrock both evolved in composition from siliciclastic to carbonate as the terrigenous sediment from the Taconic Highlands diminished. The great similarity in character of the siliciclastic storm beds in the lower and middle part of the succession and the carbonate storm beds in the middle and upper part indicates that the hydraulic climate of the shelf persisted unchanged, probably as a storm-surge ebb-dominated variety.

In the region of this field conference, the Middle Silurian succession is organized into alternating units of heterolithic (thinly interbedded mudrock and coarser sediment) associations (Units 1, 3, 5, 7, and 9) and units of monolithic (dominated by mudrock or by coarser sediment) associations (Units 2, 4, 6, 8) (Fig. 6). The basin-wide facies geometry (Fig. 7) shows a mudrock-dominated axial facies into which sandstone-dominated wedges extend from the southeast, and carbonate-dominated wedges contemporaneously extend from the northwest. These opposed wedges dominated by sandstone and carbonate represent deposits of shallow-water marginal shoals (sand and shells on the southeast, and shells and oolites on the northwest) (Fig. 8). With a lowering of sea level, the marginal shoals coalesced and expanded toward the basin axis, contracting the area of the central mud facies (Figs. 7, 8). Subsequent sea-level rise returned the deeper, lower-energy, mud-dominated conditions over each of the marginal areas. These sea-level changes are shown at the right-hand edge of the stratigraphic column of Figure 3.

The first two of these axially directed wedges in the central Pennsylvania Middle Silurian (Fig. 7) are seen in the monolithic Cabin Hill and Center hematitic sandstone member (Units 2 and 4), thinning distally into the heterolithic shaly Rose Hill Formation (Units 1, 3, 5). A more complex pattern emerged with the third such Middle Silurian regression couplet (Keefer; Unit 6). Facies patterns then were more complicated

because the sea-level changes took place at a time of increased basin disruption and differential subsidence, and at a time of increased abundance of fringing shell banks. Iron mineralization at this time was less related to the high-energy sand shoals (now quartz arenites) themselves, and more connected with the fringing shell banks. The sea-level rise that followed caused the extension of anoxic mud conditions farther sourceward than earlier rises, and introduced monolithic pyritic black shale (Unit 8) over much of Pennsylvania.

A long period of quiescence of the Taconic Highlands ended toward the end of Middle Silurian time, and a low-energy, muddy shoreline prograded northwestward. This was probably accompanied by another period of lowered sea level (Dennison and Head, 1975) (Fig. 3). The resulting Bloomsburg Formation has features consistent with the increased aridity shown by the accumulation of halite in the Appalachian Basin sea west of the shoreline (Rickard, 1969).

ASPECTS OF ALLEGHANIAN DEFORMATION

by

Richard P. Nickelsen

Introduction

The structural part of this field conference could deal with a number of timely aspects of the Alleghany Orogeny in central Pennsylvania: fold geometry and fold mechanics, thrust-fault tectonics, description of finite strain and its origins, the sequence of structural stages, strain mechanisms, and environmental conditions during the Alleghany Orogeny. We will limit the scope because of time, suitability of outcrops of certain features, and our current level of interest and understanding, to 2 major topics: the sequence of stages of the Alleghany Orogeny, and the description of finite strain and its origins. These topics impinge on many of the others. A minor topic to be discussed in two other introductory sections by Levine and by Nickelsen and mentioned at several field-trip stops is the growing evidence about environmental conditions (primarily temperature) that may have existed during the Alleghany Orogeny.

Sequence of Structural Stages of the Alleghany Orogeny

Underlying other structural considerations is the relative sequence of structural stages that has been established at the Bear Valley Strip Mine and extended to the rest of the Valley and Ridge Province in Pennsylvania (Faill and Nickelsen, 1973; Nickelsen, 1979). Others have recognized a similar sequence farther south (Perry, 1978; Burger, Perry, and Wheeler, 1979). The overlapping sequence of different structures was established and corroborated by many observations of structural overprinting, but is also indicated by the spatial distribution of different structures (Means, 1976). Early structures in the sequence occur alone farthest northwest and are successively overprinted by later structures as one proceeds southeast (Nickelsen, 1980). A few places such as the Bear Valley Strip Mine have almost all stages of the presently known sequence superimposed and are important museums of structural relationships and mechanisms for future restudy, evaluation, and debate. What is equally important about Bear Valley is its stratigraphic position near the top of the sedimentary prism that was deformed by the Alleghany Orogeny. It can't be claimed that the Bear Valley structural sequence and mechanisms, which are identical with those down to the Cambrian within the geographic area of the Pennsylvania salient, are Taconian or Acadian features. The Alleghany Orogeny apparently deformed, for the first time, a thick pile of Paleozoic sediments in a miogeocline that had already achieved temperatures and pressures sufficient for coalification and sedimentary compaction. This fact is perhaps significant in the creation of the particular array of structures in overlapping sequential stages that we call the Alleghany Orogeny.

Stage I, Alleghany Orogeny. The seven stages of the Alleghany Orogeny listed in Figure III-9 and illustrated in Figure III-10 include Stage I, joints in coal, which have no known connection with the Alleghany Orogeny and were overprinted by Stage II joints in coal and joints in shale and sandstone that are of Alleghanian age. Stage I joints in coal are across the northern Appalachian Plateau trending NE, E-W and NW (Nickelsen and Hough, 1967) and can be found with NE strikes in the Anthracite Region. They are obscure due to overprinting by all later stages.

Stage II, Alleghany Orogeny. Stage II joints of several regional sets (A,B,C,D,E, of Nickelsen and Hough, 1967) are also best observed in the Appalachian Plateau (Parker, 1942; Engelder and Geiser, 1980) but can be identified at most Valley and Ridge Province exposures by careful measurement and rotation of data. Intersecting Stage II extensional joint sets are not conjugate but rather make up a cumulative pattern (Nickelsen, 1974) requiring different orientations of the least strain axis at different times during Stage II. For example, Engelder and Geiser (1980) have proven the different relative ages of two acutely intersecting Stage II joints of the Appalachian Plateau in New York State. Our field trip will demonstrate the creation of a cumulative joint pattern at Stop VI that is interpreted to include fractures of Stages II, IV, and VI. Joints at this stop include Stage II and IV syntectonic, quartz-filled hydraulic joints related to fluid pressure (Secor, 1960) and different, Stage VI, extensional joints due to late tectonic buckling or relaxation during unloading (Price, 1966). The same differences in joint characteristics are illustrated by the Stage II and Stage VI joints at the Bear Valley Strip Mine, Stop III.

Stage III, Alleghany Orogeny. The Bear Valley Strip Mine is the best place to view overprinting and overlapping relationships between Stage II joints and Stage III rock cleavage. Some Stage II joints are perpendicular to rock cleavage and the same age as the cleavage, while others of the joint array are intersected by cleavage at angles less than 90° . In places, these have been offset by pressure solution and can be proven to be pre-cleavage in age.

Stage IV, Alleghany Orogeny. Cleavage at Bear Valley has been dragged against Stage IV wrench faults and cut by the gash veins that commonly form along these faults. Small thrust faults have tip lines consisting of strongly cleaved rock that rides on the brow of the fault and is dragged against the fault. The relations of Stage III cleavage to Stage IV thrusting is particularly well demonstrated by the cleavage halos, strain gradients, and drag of cleavage against thrust faults at Stop IV. Small-scale examples of the relation of cleavage to wedge and wrench faults in a low-strain environment are at Stop VIII. Cleavage is either rotated or created anew during simple shear against faults, but the most dramatic examples of rotational deformation are on fold limbs such as Stop I.

As shown schematically in Figure III-9, the time of cleavage formation overlaps Stage II jointing but continues through Stage IV faulting into Stage V folding and beyond. Evidence of pure shear in certain beds at Station H, Stop I, may manifest Stage VI inhomogeneous bulk flattening and layer-parallel extension.

Stage V, Alleghany Orogeny. Stage V folding has rotated previous structures as demonstrated at Stops I, III, VII, and VIII. The best evidence of rotation is provided by pre-folding Stage IV wrench faults which can be described by two structural elements - a slickensided fault plane perpendicular to bedding and slickenlines (Fleuty, 1975) parallel to the bedding-fault intersection. During Stage V folding these slickenlines are bent with bedding as is demonstrated throughout Bear Valley (Stop III) and at Stop VII. When Stage IV and V overlap, curving slickenlines such as at Station G, Stop III, are formed, but they are relatively rare. Slickenlines on wrench-fault surfaces throughout the region most commonly parallel fault-bedding intersections, whatever the bedding dip angle, thus proving that most wrench faulting precedes Stage V folding. Acute bisectors of conjugate wrench faults commonly trend obliquely to the strike of strata or fold hinges as shown at Stop III, Station A, and Stop VI and VIII. This suggests a change in orientation of the principal stress axis between wrench faulting and folding (Figure III-7B). The evidence for relative timing of wedge (thrust) faults is less certain. They seem to be slightly later than associated wrench faults as at Stop II and Stop VI and prior to Stage V folding as at Stop III (Figure III-7). Generally, wrench faults and wedge faults are placed together in Stage IV, preceding Stage V folding but perhaps continuing into the period of folding.

Finally, some wedge faults seem to form as a consequence of folding as demonstrated at Stop VII in stratigraphic Unit C.

Stage VI, Alleghany Orogeny. Late in the history of the Alleghany Orogeny all rocks were subjected to flattening and vertical extension, predominantly by brittle mechanisms. Where beds had been rotated to dips of greater than 45° by Stage V, this resulted in layer-parallel extension. At Bear Valley, Stop III, this flattening and extension is primarily manifested in local fault "grabens" on the north limb of the Whaleback Anticline (Figure III-3, Stations B and F) but may also form faults like the Bear Valley fault under the North Anticline. To explain higher coal ranks at the surface in coals of the center of western Middle Field Synclinorium, Levine (see accompanying article) invokes significant uplift of the center of the basin along such high-angle reverse faults. Where bedding had remained nearly horizontal as at Stop V the late extension appears as quartz-filled extension joints in sandstone dikes and fiber-filled wedge faults.

Stage VII, Alleghany Orogeny. The evidence for Stage VII is graphically shown in Figure III-10 but will not be seen at any stop on the field trip. Late wrench faults that are restricted to major gaps on lineaments have horizontal slickenlines cutting the fault-bedding intersection at angles approaching 90° . These wrench faults cut all previous structures including the extensional faults of Stage VI. In some gaps there is evidence of wrench faulting initiated during Stage IV, prior to folding, that has remained continuously active until Stage VII. This wrench faulting has segmented the fold belt into blocks, deforming independently, that may reflect pre-existing sedimentation patterns, basement fractures, or major changes in trend. The lineaments paralleling these long active wrench faults have been identified by Kowalik and Gold (1975) as likely spots for mineralization.

In summary, the stages of the Alleghany Orogeny that are now widely recognized and will be demonstrated on the field trip include Pre-Alleghany joints (Stage I) of uncertain basinal origin and Stage II joints related to the gradual increase of horizontal stress difference that lead to the orogeny. Before major folding, layer-parallel shortening was accomplished by formation of Stage III spaced cleavage and Stage IV conjugate wrench and wedge faulting. Stage V folding was followed by Stage VI layer-parallel extension or general flattening and vertical extension by wedging, extension faulting, high-angle reverse faulting, and inhomogeneous bulk flattening in ductile beds. Stage VII wrench faulting is found in a few places cutting all previous structures.

This structural sequence has served as a framework for identifying the time of origin of potentially economically important structural features (eg., the fracture porosity of Stop VI) and as a help in separating the strain increments of the heterogeneous, finite strain pattern in the region (see below). We hope that continuing study of the mechanisms and environmental parameters associated with the various stages will lead us to a better understanding of how rocks deform.

Description of Finite Strain and its Origins

The history of work on the finite strains of this region has included two phases: first, description and tracing of highly deformed horizons, and second, analysis to discover why some horizons are penetratively deformed while others are apparently not. We are currently interested in what characteristics of rock composition and facies change, sedimentary textures, sedimentary structures, position (stratigraphic, structural, or geographic), tectonic heredity, or environmental conditions (T , P_p , P_c) may be most important in controlling the structures we see at a particular outcrop. Though our current concern is to find, map, and interpret the strain disharmonies and their abrupt (strain

discontinuities) or gradual (strain gradients) contacts with penetratively unstrained rocks, we first need to describe the finite strains that have been observed.

An imperfect picture of the two-dimensional finite strain in the Pennsylvania portion of the Appalachian Foreland has emerged since the first report of deformed fossils on the Plateau (Nickelsen, 1966). Strain markers, oriented parallel to bedding, that have been used by various authors are inarticulate and articulate brachiopods, crinoid ossicles, mud-crack polygons, partially dissolved calcareous fossils, stigmata (plant roots), insoluble residues, trains of parasitic folds, and crenulation cleavages. Such a variety of strain markers of different validity, located in different rock types and stratigraphic horizons, has yielded some real or apparent discrepancies in the strains recorded in the region. These generally minor strain discrepancies have been overprinted in certain geographic and structural positions by large strains of uncertain origin that have created local strain disharmonies such as we will see on the field trip at Stop I, IV and V.

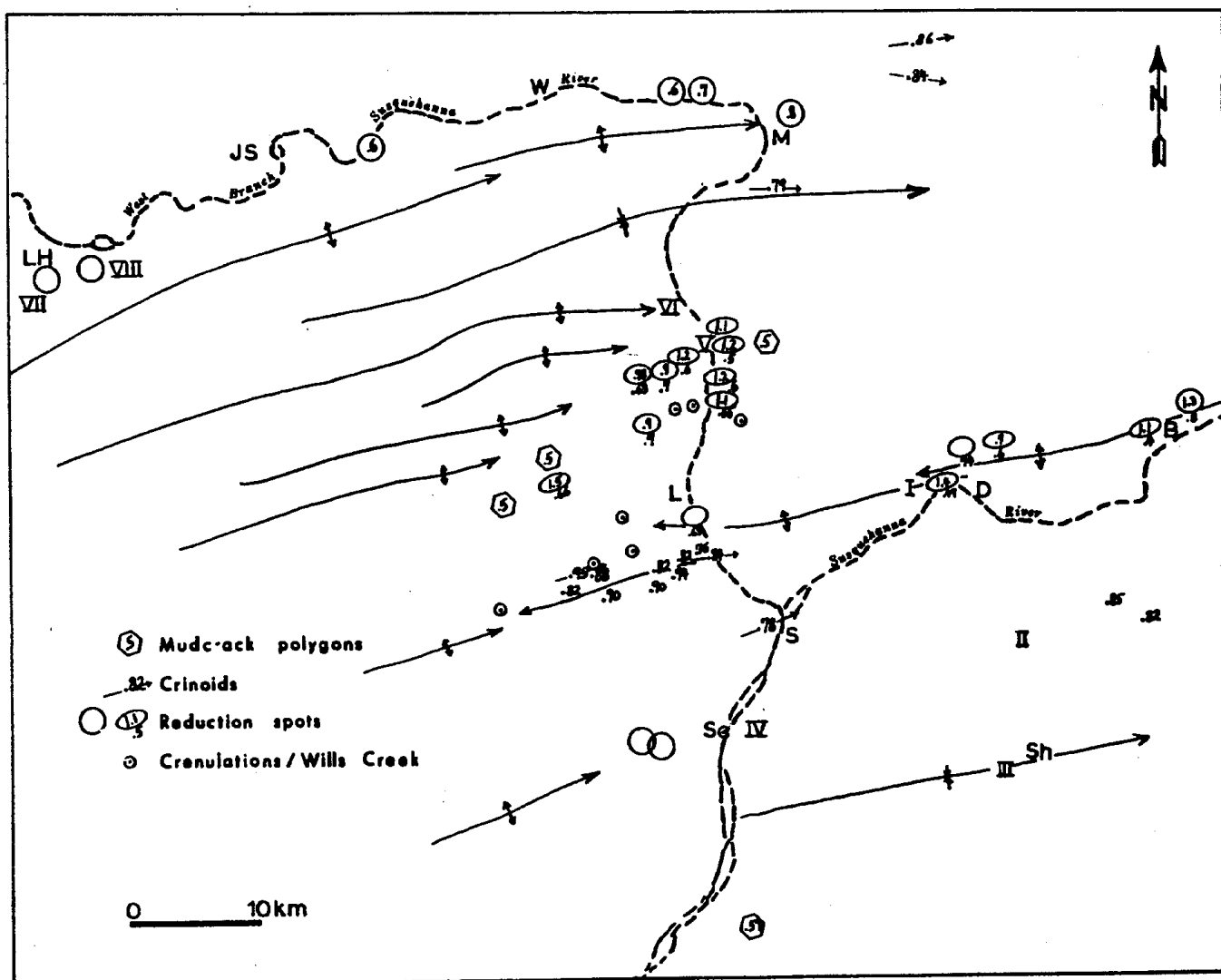


Figure 12 Map of finite strain data in field conference region

I - VIII = Field Trip Stops; LH = Lock Haven; JS = Jersey Shore;
W = Williamsport; M = Muncy; L = Lewisburg; D = Danville;; S = Sunbury;
Se = Selinsgrove; Sh = Shamokin; B = Bloomsburg

Crinoids. The least complicated two-dimensional strain picture is provided by crinoid ossicles lying on bedding planes of shales and sandstones, particularly the Reedsville Shale (Upper Ordovician), the Keefer Sandstone (Lower Silurian) and the Trimmers Rock-Lock Haven Formation (Upper Devonian). Crinoids have been deformed into ellipses with a width to length ratio ($W : L$) of approximately .8 (range is .63 to .97). The short dimension (W) is oriented NW - SE perpendicular to the strike of fold axes and rock cleavage, and the long dimension (L) is oriented NE -SW or E-W approximately parallel to the strike of fold axes and rock cleavage. Mean $W : L$ ratios of distorted crinoids from the Keefer Sandstone on the Berwick Anticlinorium south of Lewisburg (Vernon, 1974), from localities of Trimmers Rock Sandstone on the Shade Mountain Anticlinorium near STOP II (Vaskov, 1974), and from the Muncy-Hughesville area on the Nittany Anticlinorium in the Lock Haven Formation (Ricci, 1970) have been plotted on Figure 12. The $W : L$ ratios are very similar to ratios of .95 to .80 reported by Engelder and Engelder* (1977) and Engelder (1979) in the Upper Devonian rocks of the Appalachian Plateau of New York State, 200 km northwest of the south border of the field-trip area. The penetrative strain recorded in crinoids over this 200 km section is essentially constant and occurred during layer-parallel shortening before folding (Engelder, 1979). We know this because deformed crinoids were rotated by folding without receiving additional deformation (Faill and Nickelsen, 1973; Faill, 1979, p. 53) and because the deformed Appalachian Plateau crinoids in unfolded rocks are an excellent example of the northwestern spatial equivalent of prefolding, Stage III strains in the Valley and Ridge Province. This is a regional example of Sherwin and Chapple's (1968) observation that layer-parallel shortening occurs during the early stages of the formation of buckle folds.

The strain recorded in the crinoids is partitioned between volume-constant calcite twinning and pressure-solution volume loss (Groshong, 1972, 1975; Engelder, 1979, fig. 3). Using Groshong's Calcite Twin Strain Gauge (1972) both of them found layer-parallel shortening of 1 - 5% due to calcite twinning plus larger pressure-solution strains sufficient to explain shape change in crinoids or strains calculated for theoretical models of folding. Figure 13 shows a local example of strain partitioning in crinoid ossicles on bedding planes in the Keefer Sandstone. The observed $W : L$ ratio in these examples ranges from .73 to .86, implying layer-parallel shortening of 27 to 14%. When effects of diffusion (pressure solution and overgrowth) are removed graphically, $W : L$ ratios become .91 to .98 implying layer-parallel shortening by twinning of 9 to 2%. Thus, during tectonic strain the L axis of crinoid columns remained constant in length while twinning thickened ossicles perpendicular to bedding, and volume loss by pressure solution reduced W . $W : L$ ratios of .8 to .9 represent 10 to 20% layer-parallel shortening, similar to the 10-15% suggested for the Appalachian Plateau by Engelder and Engelder (1977) and Engelder (1977). Lingulas of the Appalachian Plateau were deformed by volume-constant flow that resulted in crinkles oriented NE. Jointing in a few specimens resulted in extension of up to 4.4% parallel to crinkle axes but the deformation was largely plane strain, NW-oriented negative elongation of 7-10.5%. If the rare jointing of Lingula shells is ignored, layer-parallel shortening up to 15% is present, in agreement with Engelder's estimate.

In summary, volume-constant strain and volume loss by pressure solution caused penetrative layer-parallel shortening of 10 to 20% over a 200 km section of the Valley and Ridge and Appalachian Plateau without appreciable extension in the NE strike direction. Crinoid specimens with mean axial ratios less than .8, and therefore more layer-parallel shortening, must be explained as extension in L by jointing as occurred in some Lingulas, by calcite overgrowths parallel to L , or by more pressure solution volume loss in the W direction (Fig. 13).

*Engelder actually reported $L : W$ ratios of 1.05 to 1.26

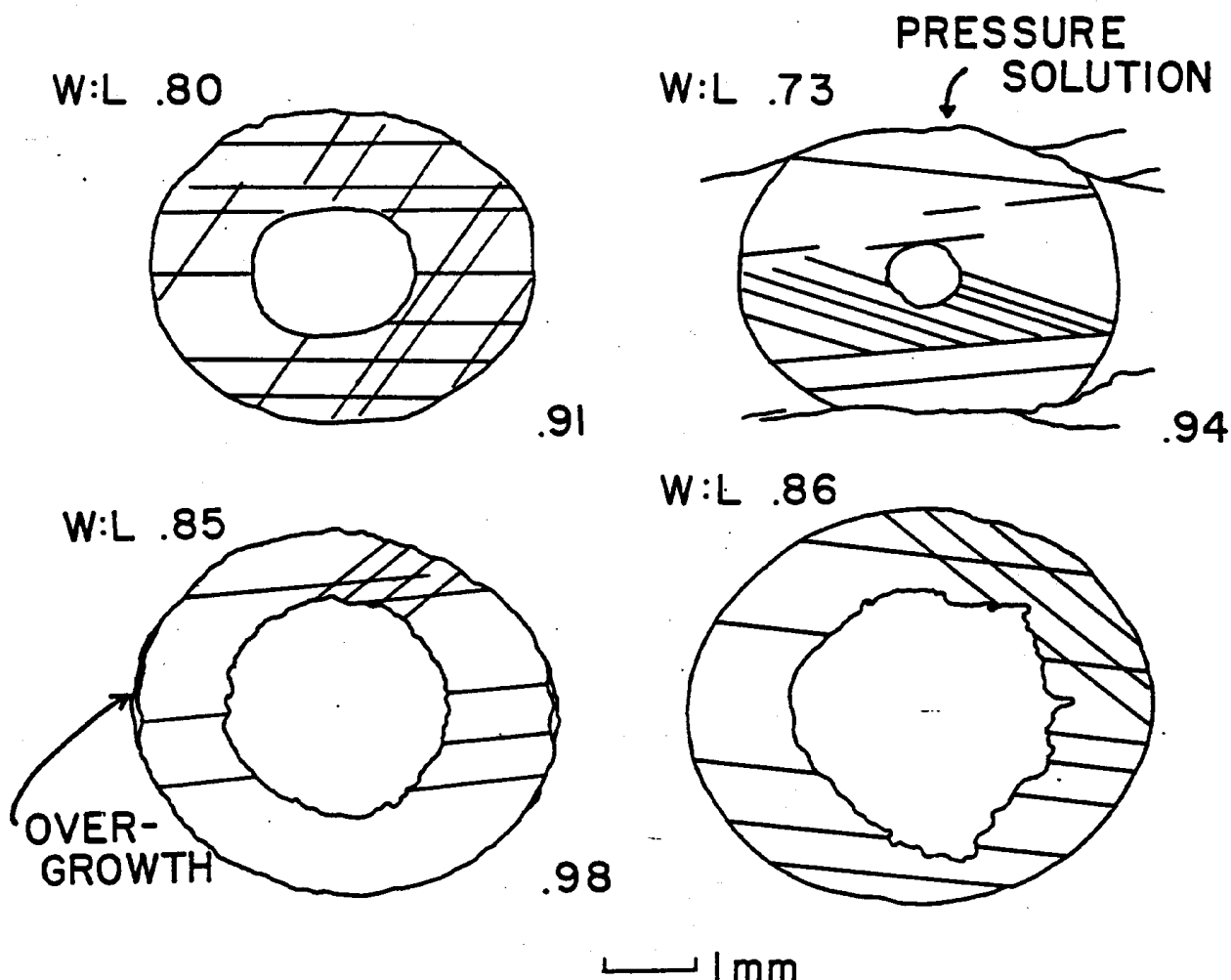


Figure 13 Examples of strain partitioning in crinoid ossicles

W : L Width : Length ratio ; upper left is ratio measured;
lower right - pressure solution strain has been subtracted

Crenulation Cleavages. This "background" of 10 - 20% layer-parallel shortening has been detected as a crenulation cleavage recording 6% LPS in the Wills Creek Shales of the Lackawanna Synclinorium near Lewisburg by Pringle (1980). Superimposed Stage III small-scale folding and pressure solution may cause additional layer-parallel shortening in the shales, mudstones, and limestones of the Wills Creek to reach total amounts of 14 - 36%, somewhat higher than recorded by crinoids. Lower strains in crinoids may result from strain inhomogeneities between matrix and stiff crinoid ossicles.

Mud-Crack Polygons. Mud-crack polygons at a few localities (Fig. 12) of the same region in the Bloomsburg Formation, Wills Creek Formation and Keyser Limestone have yielded W : L ratios of approximately .5, as exemplified by STOP V, Station C. Other outcrops of the same stratigraphic units in adjacent areas show little or no distortion of mud-crack polygons (STOP I). Mud-crack polygons may be better strain markers because they are large and similar in composition to the enclosing rock, but can't be used to map regional strain because of their rarity and apparent inconsistency in recording strain. Where seen together mud cracks may either record the same strain as reduction spots (STOP V) or fail to record strains which are locally present in reduction spots (STOP I).

Reduction Spots. When reduction spots were discovered in the region in 1973 (Faill and Nickelsen, 1973) they seemed to offer the perfect solution to mapping local and regional strains. They are large, three-dimensional markers, mechanically similar to enclosing rock, available in the structurally interesting Bloomsburg Formation, and of proven usefulness as strain markers in other regions (Wood, 1973; Wood and Oertel, 1980; Graham, 1978). Our study of one locality (STOP V) has been very rewarding and we have learned much about Bloomsburg deformation from a regional study still being pursued. The quality of exposure has precluded R_f/ϕ analysis of the effect of initial shape upon the deformed reduction spots (Dunnet and Siddens, 1971) and made it difficult to assess the role of rock type and local structural disturbances upon the strain recorded by reduction spots. Thus, our preliminary results plotted on Figure 12 should be viewed with caution. On Figure 12 the ellipses drawn represent the orientation and ratio of the $y : z$ section of the reduction spots (or, rarely, the $x : z$ section) where $x > y > z$. y (or rarely x) is oriented NE parallel to strike and has been taken arbitrarily as 1 because this dimension has been relatively constant during tectonic strain. The ratio of the short axis (z) and vertical axis (x) are plotted respectively below and inside the ellipse for each station.

The generalized pattern that can be seen on on Figure 12 is reduction spots deformed into oblate ellipsoids flattened in bedding by sedimentary compaction in the northern, low-strain area paralleling the Alleghany Front between Lock Haven and Muncy. To the south the deformed shape of reduction spots changes to either oblate ellipsoids flattened in the cleavage or prolate ellipsoids elongated parallel to the strike or to the dip of cleavage. This transition in shape results from superposition of a vertically elongated prolate deformation ellipsoid upon the pre-existing oblate ellipsoid that had resulted from sedimentary compaction. Graham (1978) has described such a transition in the Alpes Maritimes. We are fortunate to see the compaction strain in the north before the Bloomsburg disappears beneath the Appalachian Plateau but it would be desirable to find exposures to demonstrate the transition from compaction to deformation strains in the 18 kilometer gap between Muncy and Watsontown.

The inferred sequence of shape changes in ellipsoidal reduction spots is shown in Figure 14. Figure 14-1 represents sedimentary compaction with ratios of the axis of compaction to the long axis of .6 to .8. Ellipsoids similar to Figure 14-2, with the x axis parallel to the NE strike of cleavage, are rare in the region but appear west of Watsontown and on the north limb of the Berwick Anticlinorium near the Field Conference Motel. Figures 14-3 and 14-4 represent the reduction-spot shapes in the vicinity of Watsontown (STOP V), deformed by pure shear to some of the largest reduction spot strains recorded in the region. Elongation parallel to the dip of cleavage (x direction) is slight but mimicked by brittle extension and shear fractures.

The most deformed reduction spots of the region at STOP I on the south limb of the Berwick Anticlinorium owe their shape to concentrated simple shear in one part of the Bloomsburg section, perhaps related to rock type or to structural position (Figure 14-5). A few other exposures along the south limb of the Berwick Anticlinorium corroborate that this is an environment of high strain through simple shear which is unique in the region. There is a strong contrast between the cleavage-bedding angles and orientations of the reduction-spot ellipsoids on the south and the north limbs of the Berwick Anticlinorium (Figure 1-6). Thus in this region the strain path may have been 1 to 2 to 5 on Figure 14 because 3 may never have been attained before simple shear was activated on the fold limb.

An unexpected observation was the lack of tectonic strain at the two southernmost Bloomsburg localities on the Shade Mountain Anticlinorium west of Selinsgrove. Crinoid W : L ratios of .82 and .85 are present to the east of these outcrops in the Trimmers Rock Formation and at many localities, reduction-spot strain exceeds

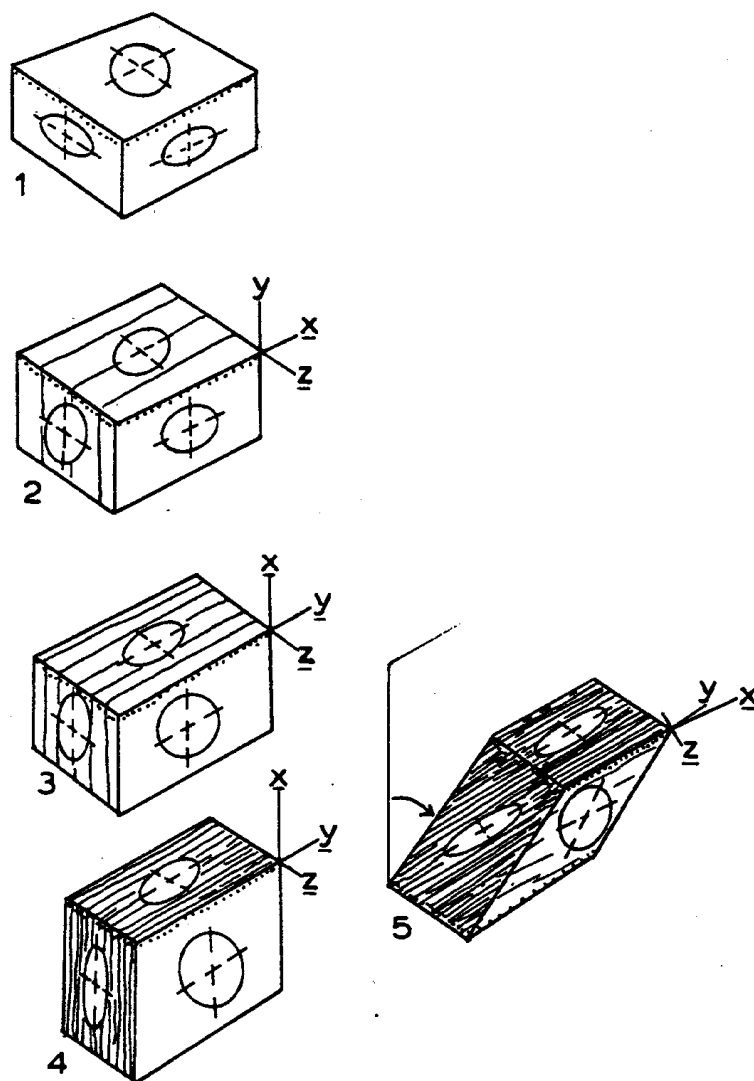


Figure 14 Evolution of the reduction spot deformation ellipsoid

- 1.-sedimentary compaction in bedding
- 2.-tectonic strain to produce a prolate ellipsoid, \underline{x} axis parallel to strike
- 3.-more tectonic strain to produce an oblate ellipsoid flattened in cleavage, $\underline{x} = \underline{y}$
- 4.-tectonic elongation vertically in cleavage plane to produce a prolate ellipsoid, \underline{x} axis down dip of cleavage plane
- 5.-superimposed simple shear to produce prolate ellipsoid with extreme flattening in $\underline{x} \underline{y}$ plane and elongation in \underline{x}

crinoid strain. A similar discrepancy between strains recorded by two different strain markers in the same region is in the Muncy - Williamsport area. Here Faill (1979, fig. 13, Table 1) has measured crinoid distortion in the Reedsville Shale and Trimmers Rock -Lock Haven Formations occurring either below or above the Bloomsburg Formation in the stratigraphic column. The Bloomsburg Formation reduction spots record only compaction. Intuitively, we would expect more deformation in suitable beds in the Bloomsburg Formation, but here, this is not the case.

Strain Disharmonies

From what has preceded, it is already evident that marked differences in finite strain occur and demand explanation. Some strain disharmonies, referred to as disturbed zones, have been identified as fault (detachment?) zones (Pohn and Purdy, 1982) and others are too enigmatic to classify. The following features or attributes may cause a rock to appear more deformed than surrounding rock, creating an apparent or real strain disharmony.

Rock Composition or Texture
Sedimentary Structures
Stratigraphic Position
Structural Position
Tectonic Heredity
Environmental Conditions

This discussion is keyed to features that will be seen on the field trip.

Rock Composition or Texture - STOP I - Station H - The green shale at this station shows higher strain, and deformation by pure shear in a simple shear environment, perhaps because it is different rock from its surroundings. STOP II - Two different styles of deformation and groups of structures are present, related solely to rock type. Argillaceous sandstone is broadly folded and cleaved along close-spaced planes of extensive pressure solution. Quartz arenite in the same environment displays spaced pressure-solution cleavage, conjugate, orthogonal pressure-solution slip surfaces, and wedging that is beginning to develop into small-scale, flat-ramp-flat thrusts, and fault complexes. The quartz arenite may seem to be more deformed? STOP III and IV - The contrast between surrounding rocks and the concretions produces sharp discontinuities in strain, marked by slickensided surfaces and cleavage halos. Could these be small-scale models of how clastic wedges may influence adjacent basinal facies during layer-parallel shortening? The first cleavage to form in true clay shales (i.e., phyllosilicates with fabric parallel to bedding) is a primary crenulation cleavage (Fig. III-11A), whereas mudstones, sandy mudstones, sandstones, and argillaceous limestones deform by dissolution or combinations of mechanisms (Fig. III-11B,C; Fig. IV-9; Fig. 11-1.)

Sedimentary Structures - Striking examples are at STOP V, Watsontown, where diffusion and pressure solution have been greatly influenced by perpendicular-to-bedding structures such as burrows and sandstone dikes. Is the high strain at Watsontown a result of sedimentary structures, or perhaps structural position at the tip line of a blind thrust or. . . .? Saucer-shaped slickensided surfaces that formed during wetting and drying of muds or soils and have persisted through 50% layer-parallel shortening and cleavage formation are important boundaries between packets of shale being deformed independently. Do SSS surfaces enhance cleavage formation by facilitating pressure solution or grain-boundary sliding? Are fiber-filled wedge faults present only because the SSS surfaces were available in approximately correct shear orientations when the Stage VI vertical extension began? Preferred orientation of phyllosilicates parallel to cleavage in some Bloomsburg Formation rock types may be relict soil structures enhanced by pressure solution. Fractures along cleavage planes reveal blocky soil (?) structures or peds (?) with clay-film coatings. If these speculations are valid, this may be another process for initiating foliation.

Stratigraphic Position - Relative stratigraphic position, considered in conjunction with rock composition and sedimentary structures, plays a major role in establishing the basic conditions for the development of thrust systems. The thin cleavage duplex at STOP IV is a detachment horizon because of its position between stiffer units of limestone and sandstone and because of its composition and texture. This carbon-rich shale with clay

content influenced by the Tioga ash bed may have been overpressured. It is typical of shales at a number of Appalachian localities that have served as detachment horizons.

Structural Position - The most highly strained reduction spots of the region at STOP I are deformed in simple shear on one limb of an anticlinorium. Does the south limb of the Berwick Anticlinorium show higher shear strains because of unequal kinking on the two limbs of the structure or is STOP I merely the zone where a ramp on a major thrust system is passing through the Lower Silurian section?

At STOP IV a thin and a thick cleavage duplex cut up-section in the direction of transport through either shales of the Marcellus Formation or argillaceous sandstones of the Mahantango Formation. The "channels" of high strain (>30% LPS) that pass through the section as cleavage duplexes may have originated at the Tioga ash bed or large-scale equivalents of the cleavage halos, but, once initiated, now cut up through the Marcellus Formation into the Mahantango Formation (Figure IV-4). Thus, in this case, a strain disharmony (the cleavage duplex with sharp fault boundaries at top and bottom) can be unequivocally related to a thrust zone passing through the section. At STOP VI the position of the zone of fracture porosity is apparently unrelated to the most obvious large structural feature, the South White Deer Anticline. The structural feature that may be important in establishing the position of the fracture porosity is apparently a transversely oriented zone of extensional jointing and/or wrench faulting.

Tectonic Heredity - The concept of tectonic heredity and its influence on later structures is usually applied to basement-cover relations and the effect of structures of a previous tectonic cycle upon those that develop during a later tectonic cycle in cover rocks. If one accepts the multistage model for development of the Alleghany Orogeny, the effect of earlier stages (incremental or infinitesimal strains) upon the finite strain must be considered. Fractures formed in earlier stages are possibly important in directing pressure-solution slip as at STOP II or may effect the frequency and the orientation of conjugate wrench-fault systems as at STOP II, STOP III and, particularly, STOP VI. Marshak et. al. (1982) and Geiser and Sansone (1981) have explored the possible influence of earlier fractures upon later jointing, pressure-solution cleavage or wrench faults.

Environmental Conditions - Insufficient data is available on ambient environmental parameters during Alleghanian deformation to assess the role of changing environmental conditions during the history of structural development of an outcrop. Another section of the guidebook will describe our present information and sources of information on this issue.

Thrust Systems

Though no discussion of the major thrust tectonics of the field trip area was promised, some clarification of terminology for STOP IV is essential. The general configuration of thrust systems in foreland thrust belts such as the Pennsylvania Valley and Ridge and Appalachian Plateau is now understood to consist of thrust faults that cut up-section in the direction of transport following a staircase trajectory consisting of ramps through stiff rocks (limestone, sandstone) and flats in more ductile rocks (shales, salts) (Butler, 1982). Above the basal thrust an imbricate zone or schuppen may develop, consisting of many smaller thrusts fanning upward from the basal thrust (Boyer and Elliott, 1982, fig. 12). It is now well documented that an imbricate zone or schuppen zone that fans upward from a basal thrust may converge at a roof thrust at the top of the zone. This creates an intensely deformed imbricate zone between two major thrusts - a sole or floor thrust and a roof thrust - which has been called a duplex (Dahlstrom, 1970, p. 352; Boyer and Elliott, 1982, p. 1199, fig. 12). It is important to note that the duplex is a zone of intense deformation sandwiched between underlying and overlying little-deformed rocks. The duplex may cut up-section following the sole thrust but generally is thought to

stay within one part of the section bounded by sole and roof flats at decollement or detachment horizons in ductile rocks. Several models for propagation of duplexes exist but the sequence illustrated in Boyer and Elliott (1982, fig. 19) and copied for use in this guidebook as Figure IV-12 is widely accepted. Propagation proceeds from back to front in the thrust belt by successive extensions of the sole thrust and ramp thrusts to the stratigraphic horizon of the roof thrust. We propose that the zones of intense cleavage in the Marcellus Formation at STOP IV are cleavage duplexes, formed as shown in Figure IV-13, bounded at top and bottom by roof and floor thrusts, and displaying marked disharmony in strain with respect to overlying and underlying rocks.

REFERENCES CITED BY COTTER AND NICKELSEN

Allen, J.R.L., 1979, A model for the interpretation of wave ripplemarks using their wavelength, textural composition and shape: *Journal of the Geological Society of London*, v. 136, p. 673-680.

_____, 1980, Sand-wave mobility and the internal master bedding of sand-wave deposits: *Geol. Mag.*, v. 117, p. 437-446.

Allen, P.A., 1981, Wave-generated structures in the Devonian lacustrine sediments of south-east Shetland and ancient wave conditions: *Sedimentology*, v. 28, p. 369-379.

Andel, Tj.H., van, and Postma, H., 1954, *Recent sediments of the Gulf of Paria*: North Holland Publ. Co., Amsterdam, 245 p.

Arthur, M.A., 1979, Paleooceanographic events - recognition, resolution, and reconsideration: *Rev. Geophys. Space Physics*, v. 17, p. 1474-1494.

Bajak, D.M., 1981, Pressure solution cleavage and calcite-filled extension joints in the Upper Silurian Tonoloway and Siluro-Devonian Keyser Formations, central Pennsylvania: unpub. Senior Thesis, Lewisburg, Bucknell University, 67 p.

Bell, T.H., 1978, Progressive deformation and reorientation of fold axes in a ductile mylonite zone, the Woodroffe Thrust: *Tectonophysics*, v. 44, p. 285-320.

Berg, T.M. and Dodge, C.M., eds., 1981, *Atlas of preliminary geologic quadrangle maps of Pennsylvania*: Pennsylvania Geologic Survey, 4th ser., Map 61.

Berger, P.S. and Wheeler, R.L., 1979, Late Tectonic extension faulting in the central Appalachians: *Proceedings - Third Eastern Gas Shales Symposium*, Oct. 13, 1979, Morgantown, W. Virginia, p. 51-61.

Berger, P.S., Perry, W.J., and Wheeler, R.L., 1979, Three-stage model of brittle deformation in the central Appalachians: *Southeastern Geology*, v. 20, p. 59-67.

Berry, W.B.N., and Boucot, A.J., 1970, Correlation of the North American Silurian rocks: *Geol. Soc. America*, Spec. Paper 102, 289 p.

_____, 1973, Glacio-eustatic control of Late Ordovician-Early Silurian platform sedimentation and faunal changes: *Geol. Soc. America Bull.*, v. 84, p. 275-284.

Berry, W.B.N., and Wilke, Pat, 1978, Progressive ventilation of the oceans - an explanation for the distribution of the Lower Paleozoic black shales: *Am. Jour. Science*, v. 278, p. 257-275.

Bhattacharyya, D.P., and Kakimoto, P.K., 1982, Origin of ferriferous ooids: an SEM study of ironstone ooids and bauxite pisoids: *Jour. Sedimentary Petrology*, v. 52, p. 849-857.

Boyer, S.E., 1972, Jointing in the Mifflinburg area: unpub. Senior Thesis, Lewisburg, Bucknell University, 68 p.

Boyer, S.E. and Elliott, D., 1982, Thrust Systems: *Am. Assoc. Petroleum Geol. Bull.*, v. 66, p. 1196-1230.

Brenchley, P.J., and Newall, G., 1980, A facies analysis of Upper Ordovician regressive sequences in the Oslo region, Norway - a record of glacio-eustatic changes: *Palaeogeog., Palaeoclimatol., Palaeoecol.*, v. 31, p. 1-38.

Brenchley, P.J., Newall, G., and Stanistreet, I.G., 1979, A storm surge origin for sandstone beds in an epicontinental platform sequence, Ordovician, Norway: *Sedimentary Geology*, v. 22, p. 185-217.

Brenner, R.L., 1980, Construction of process-response models for ancient epicontinental seaway depositional systems using partial analogs: *Am. Assoc. Petroleum Geol. Bull.*, v. 64, p. 1223-1224.

Buol, S.W., Hole, F.D., and McCracken, R.J., 1980, Soil genesis and classification: 2nd ed., Iowa State Univ. Press, Ames.

Butler, R.W.H., 1982. The terminology of structures in thrust belts: *Jour. Struct. Geol.*, v. 4, No. 3, p. 239-245.

Byers, C.W., 1977, Biofacies patterns in euxinic basins: a general model: *in* Cook, H.E., and Enos, P., eds., *Deep Water Carbonate Environments*, S.E.P.M. Spec. Publ. No. 25, p. 5-17.

Carroll, E., 1958, Role of clay minerals in the transportation of iron: *Geochim. et Cosmochim. Acta*, v. 14, p. 1-28.

Clifton, H.E., 1976, Wave-formed sedimentary structures - a conceptual model: *in* Davis, R.A., Jr., and Ethington, R.L., eds., *Beach and Nearshore Sedimentation*: S.E.P.M. Spec. Publ., No. 24, p. 126-148.

Cotter, E., 1982, Tuscarora Formation of Pennsylvania: S.E.P.M. Eastern Section 1982 Field Trip Guidebook, 105 p.

_____, 1983, Shelf, paralic, and fluvial environments and eustatic sea-level fluctuations in the origin of the Tuscarora Formation (Lower Silurian) of central Pennsylvania: *Jour. Sedimentary Petrology*, v. 53, p. 25-49.

Crawford, M.L., 1981, Fluid inclusions in metamorphic rocks - low and medium grade, p. 157-181, *in* Hollister, L.S. and Crawford, M.L. eds. *Short Course in fluid inclusions: Applications to Petrology*; Min. Assoc. of Canada, v. 6, 304 p.

Crowley, D.J., 1973, Middle Silurian patch reefs in Gasport Member (Lockport Formation), New York: *Am. Assoc. Petroleum Geol. Bull.*, v. 57, p. 283-300,

Currie, J.B., Patnode, H.W., and Trump, R.P., 1962, Development of folds in sedimentary strata: *Geol. Soc. America Bull.*, v. 73, p. 655-674.

Dahlstrom, C.D.A., 1970, Structural geology in the eastern margin of the Canadian Rocky Mountains: *Bull. Canadian Petroleum Geology*, v. 18, no. 3, p. 332-406.

Davis, S., 1981, Structural history of a third order anticline at Shamrock, Pennsylvania: unpub. Senior Thesis, Lewisburg, Bucknell University, 82 p.

Darton, N.H., and Taff, J.A., 1896, Description of the Piedmont Quadrangle, West Virginia and Maryland: U.S. Geol. Survey Atlas, Folio 28.

Dennison, J.M., 1976, Appalachian Queenston delta related to eustatic sea-level drop accompanying Late Ordovician glaciation centered in Africa: *in* Basett, M.G., editor, *The Ordovician System*; Univ. Wales Press, Cardiff, p. 107-120.

_____, 1983, Comment on "Tectonic model for Kimberlite emplacement in the Appalachian Plateau of Pennsylvania": *Geology*, v. 11, p. 252-254.

Dennison, J.M., and Head, J.W., 1975, Sealevel variations interpreted from the Appalachian Basin Silurian and Devonian: *American Journal of Science*, v. 275, p. 1089-1120.

DeWindt, J.T., 1973, The Landisburg Tongue of central Pennsylvania: A Late Silurian delta: *Proc. Pa. Acad. Sci.*, v. 47, p. 25-29.

Diecchio, R.J., 1973, Lower and Middle Silurian ichnofacies and their paleoenvironmental significance, central Appalachian Basin of the Virginias: unpub. M.S. thesis, Durham, Duke University.

_____, 1980, Stratigraphic and petrologic evidence for partial closure of the Proto-Atlantic during the Taconic Orogeny: *Geol. Soc. America, Abstracts with Programs*, v. 12, n. 7, p. 413 (abstract).

Dott, R.H., Jr. and Bourgeois, Joanne, 1982, Hummocky stratification: significance of its variable bedding sequences: *Geol. Soc. America Bull.*, v. 93, p. 663-680.

Dunnet, D. and Siddans, A.W.B., 1971, Non-random sedimentary fabrics and their modification by strain: *Tectonophysics*, v. 12, p. 307-325.

Egan, D.E., 1980, Structural observations in the tectonically thickened Marcellus Formation at Selinsgrove Junction, central Pennsylvania: unpub. Senior Thesis, Lewisburg, Bucknell University, 34 p.

Elliott, Trevor, 1978, Clastic shorelines: *in* Reading, H.G., editor, *Sedimentary Environments and Facies*; Elsevier, New York, p. 143-177.

Engelder, T., 1979, Mechanisms for strain within the Upper Devonian clastic sequence of the Appalachian Plateau, western New York: *Am. Jour. Science*, v. 279, p. 527-542.

Engelder, T. and Engelder, R., 1977, Fossil distortion and decollement tectonics of the Appalachian Plateau: *Geology*, v. 5, p. 457-460.

Engelder, T. and Geiser, P., 1980, On the use of regional joint sets as trajectories of paleostress fields during the development of the Appalachian Plateau, N.Y.: *Jour. Geophysical Research*, v. 85, p. 6319-6341.

Epstein, J.B., and Epstein, A.G., 1972, The Shawangunk Formation (Upper Ordovician (?) to Middle Silurian) in eastern Pennsylvania: *U.S. Geol. Survey Prof. Paper* 744, 45 p.

Epstein, A.G., Epstein, J.B., and Harris, L.D., 1977, Conodont color alteration - an index to organic metamorphism: *U.S. Geol. Survey Prof. Paper* 995, 27 p.

Faill, R.T., 1979, Montoursville south and Muncy quadrangle and part of the Hughesville quadrangle, Pennsylvania: *Pennsylvania Geological Survey, 4th ser., Atlas* 144ab.

Faill, R.T., and Nichelsen, R.P., 1973, Structural geology in Faill, R.T., and others, eds. Structure and Silurian and Devonian stratigraphy of the Valley and Ridge province in central Pennsylvania, in Guidebook for the 38th Annual Field Conference of Pennsylvania Geologists, October 5-6, 1973: p. 9-38.

Faill, R.T., and Wells, R.B., 1974, Geology and mineral resources of the Millerstown Quadrangle, Perry, Juniata, and Snyder Counties, Pennsylvania: Penn. Geol. Survey, 4th ser., Atlas 136, 276 p.

Figueiredo, A.G., Jr., Sanders, J.E., and Swift, D.J.P., 1982, Storm-graded layers on inner continental shelves: examples from southern Brazil and the Atlantic coast of the United States: Sedimentary Geology, v. 31, p. 171-190.

Fischer, A.G., and Arthur, M.A., 1977, Secular variations in the pelagic realm: in Cook, H.E., and Enos, P., eds., Deep Water Carbonate Environments, S.E.P.M. Spec. Publ., No. 25, p. 19-50.

Fleuty, M.J., 1975, Slickensides and slickenlines: Geological Mag., v. 112, p. 319-322.

Folk, R.L., 1960, Petrography and origin of the Tuscarora, Rose Hill, and Keefer Formations, Lower and Middle Silurian of eastern West Virginia: Jour. Sedimentary Petrology, v. 30, p. 1-58.

_____, 1962, Petrography and origin of the Silurian Rochester and McKenzie shales, Morgan County, West Virginia: Jour. Sedimentary Petrology, v. 32, p. 539-578.

Foth, H.D. and Schafer, J.W., 1980, Soil geography and land use: John Wiley and Sons, Inc., New York, 484 p.

Friedman, G.M., and Sanders, J.C., 1978, Principles of sedimentology: John Wiley and Sons, New York, 792 p.

Garlock, T.L., and Isaacson, P.E., 1977, Trace fossil ichnocoenoses from the Rose Hill Formation (Early Silurian), north-central Pennsylvania: Geol. Soc. America, Abstracts with Programs, v. 9, n. 3, p. 267 (abstract).

Geiser, P.A., 1974, Cleavage in some sedimentary rocks of the central Valley and Ridge Province, Maryland: Geol. Soc. America Bull., v. 85, p. 1399-1412.

Geiser, P.A. and Sansone, S., 1981, Joints, microfractures and the formation of solution cleavage in limestone: Geology, v. 9, p. 280-285.

Goldring, R., and Bridges, P., 1973, Sublittoral sheet sandstones: Jour. Sedimentary Petrology, v. 43, p. 736-747.

Goldring, R., and Langenstrassen, F., 1979, Open shelf and near-shore clastic facies in the Devonian: in House, M.R., et al, eds., The Devonian System. Spec. Papers Palaeontol., No. 23, p. 81-97.

Grabau, A.W., 1913, Early Paleozoic delta deposits of North America: Geol. Soc. America Bull., v. 24, p. 399-528.

Graham, R.H., 1978, Quantitative deformation studies in the Permian rocks of Alpes Maritimes: Mem. BRG-M 91, p. 219-239.

Greensmith, J.T., and others, 1980, An association of minor fining-upward cycles and aligned gutter marks in the Middle Lias (Lower Jurassic) of the Yorkshire coast: Yorkshire Geol. Soc. Proc., v. 42, p. 525-538.

Greer, S.A., 1975, Sandbody geometry and sedimentary facies at the estuary-marine transition zone, Ossabaw Sound, Georgia: a stratigraphic model: Senckenberg. Mar., v. 7, p. 105-135.

Grennon, B., 1982, Strain analysis of the Montour Anticline at Dannville, PA: unpub. Senior Thesis, Lewisburg, Bucknell University, 55 p.

Groshong, R.H., 1967, Systematic joints across a syncline in the Valley and Ridge Province. unpub. Senior Thesis, Lewisburg, Bucknell University.

_____, 1972, Strain calculated from twinning in calcite: Geol. Soc. America Bull., v. 83, p. 2025-2038.

_____, 1975, Strain, fractures, and pressure solution in natural single-layer folds: Geol. Soc. America Bull., v. 86, p. 1363-1376.

Hallam, A., and Bradshaw, M.J., 1979, Bituminous shales and oolitic ironstones as indicators of transgressions and regressions: Jour. Geol. Soc. London, v. 136, p. 157-164.

Hamblin, A.P., and Walker, R.G., 1979, Storm-dominated shallow-marine deposits -- the Fernie-Kootenay (Jurassic) transition, southern Rocky Mountains: Canadian Jour. Earth Sci., v. 16, p. 1673-1690.

Hanor, J.S., 1979, The sedimentary genesis of hydrothermal fluids, p. 137-172 in Barnes, H.L. (ed.): Geochemistry of Hydrothermal Ore Deposits: Wiley-Interscience, 798 p.

Harms, C., 1969, Hydraulic significance of some sand ripples: Geological Society of America Bull., v. 80, p. 363-396.

Harms, J.C., and others, 1975, Depositional environments as interpreted from primary sedimentary structures and stratification sequences: S.E.P.M. Short Course Notes No. 2, 161 p.

Harper, J.A., and Piotrowski, R.G., 1979, Stratigraphic correlation of surface and subsurface Middle and Upper Devonian, southwestern Pennsylvania: in Guidebook for the 44th Annual Field Conference of Pennsylvania Geologists, p. 18-37.

Harris, L.D. and Milici, R.C., 1977, Characteristics of thin-skinned style of deformation in the southern Appalachians, and potential hydrocarbon traps: U.S. Geol. Survey Prof. Paper 1018.

Harris, A.G., Harris, L.D., and Epstein, J.B., 1978, Oil and gas data from Paleozoic rocks in the Appalachian Basin: Maps for assessing hydrocarbon potential and thermal maturity (conodont color alteration isograds and overburden isopachs): U.S. Geological Survey Map I-917-E.

Hayes, M.O., 1967, Hurricanes as geological agents, south Texas coast: Am. Assoc. Petroleum Geol. Bull., v. 51, p. 937-942.

_____, 1980, General morphology and sediment patterns in tidal inlets: *Sedimentary Geology*, v. 26, p. 139-156.

Hayes, M.O., and Kana, T.W., editors, 1976, Terrigenous clastic depositional environments, some modern examples: Coastal Research Div., Dept. Geol., Univ. South Carolina, Tech. Rept. No. 11-CRD, variously paged.

Heckel, P.H., 1977, Origin of phosphatic black shale facies in Pennsylvanian cyclothems of Mid-Continent North America: *Am. Assoc. Petroleum Geol. Bull.*, v. 61, p. 1045-1068.

Hiscott, R.N., 1982, Tidal deposits of the Lower Cambrian Random Formation, eastern Newfoundland: facies and paleoenvironments: *Canadian Jour. Earth Sci.*, v. 19, p. 2028-2042.

Hoskins, D.M., 1961, Stratigraphy and paleontology of the Bloomsburg Formation of Pennsylvania and adjacent states: *Pennsylvania Geological Survey*, 4th ser., General Geology Report 36, 125 p.

Hosterman, J.W., Wood, G.H., and Bergin, M.J., 1970, Mineralogy of underclays in the Pennsylvania Anthracite Region: *U.S. Geol. Survey Prof. Paper* 700-C, p. C89-97.

Hoyt, J.H., and Henry, V.J., 1967, Influence of island migration on barrier island sedimentation: *Geol. Soc. America Bull.*, v. 78, p. 77-86.

Hunter, R.E., 1970, Facies of iron sedimentation in the Clinton Group in Fisher, G.W., and others, editors, *Studies of Appalachian geology, central and southern*: Interscience Publishers John Wiley and Sons, Inc., New York, p. 101-121.

Hunter, R.E., and Clifton, H.E., 1982, Cyclic deposits and hummocky cross-stratification of probable storm origin in Upper Cretaceous rocks of the Cape Sebastian area, southwestern Oregon: *Jour. Sedimentary Petrology*, v. 52, p. 127-143.

Inners, J.D., 1981, Geology and mineral resources of the Bloomsburg and Mifflinville Quadrangles and part of the Catawissa Quadrangle, Columbia County, Pennsylvania: *Pennsylvania Geological Survey*, 4th ser., Atlas 164 cd., 152 p.

Inners, J.D., and Williams, J.H., 1983, Clinton iron-ore mines of the Danville-Bloomsburg area: their geology, history, and present-day environmental effects: in Nickelsen, R.P., and Cotter, E., eds., *Silurian depositional history and Alleghanian deformation in the Pennsylvania Valley and Ridge*; Guidebook for the 48th Annual Field Conference of Pennsylvania Geologists.

Johnson, H.D., 1978, Shallow siliciclastic seas: in Reading, H.G., editor, *Sedimentary Environments and Facies*: Elsevier, New York, p. 207-258.

Johnson, M.E., 1980, Paleoecological structure in Early Silurian platform seas of the North American midcontinent: *Palaeogeog., Palaeoclimatol., Palaeoecol.*, v. 30, p. 191-216.

Johnson, M.E., and Campbell, G.T., 1980, Recurrent carbonate environments in the Lower Silurian of northern Michigan and their inter-regional correlation: *Jour. Paleontol.*, v. 54, p. 1041-1057.

Kaiser, W.R., 1972, Delta cycles in the Middle Devonian of central Pennsylvania: unpubl. Ph.D. dissertation, Baltimore, The Johns Hopkins University, 183 p.

Kazmierczak, J., and Goldring, R., 1978, Subtidal flat-pebble conglomerate from the Upper Devonian of Poland: a multiprovenant high-energy product: *Geol. Mag.*, v. 115, p. 359-366.

Kepferle, R.C., Potter, P.E., and Pryor, W.A., 1981, Stratigraphy of the Chattanooga shale (U. Dev. and L. Miss.) in vicinity of Big Stone Gap, Wise Co., VA: *U.S. Geol. Survey Bull.* 1499, p. 1-20.

Khain, V.Y., Ronov, A.B., and Seslavinsky, K.B., 1978, Silurian lithologic associations of the world: *International Geology Review*, v. 20, p. 249-268.

Knowles, P.A., 1978, Strain in the Bloomsburg Formation in the Milton 7 1/2' quadrangle: unpub. Senior Thesis, Lewisburg, Bucknell University, 60 p.

Komer, P.D., 1974, Oscillatory ripple marks and the evolution of ancient wave conditions and environments: *Journal of Sedimentary Petrology*, v. 44, n. 1, p. 169-180.

Kowalik, W.S., and Gold, D.P., 1975, Lineaments and mineral occurrences in Pennsylvania: NASA Technical Rept., ORSER/SSEL Rept. 14-75, The Pennsylvania State University, University Park, Pennsylvania.

Kraft, J.C., and John, C.J., 1979, Lateral and vertical facies relations of transgressive barrier: *Am. Assoc. Petroleum Geol. Bull.*, v. 63, p. 2145-2163.

Kreisa, R.D., 1981, Storm-generated structure in sub-tidal marine facies with examples from the Middle and Upper Ordovician of southwestern Virginia: *Jour. Sedimentary Petrology*, v. 51, p. 823-848.

Leggett, J.K., and others, 1981, Periodicity in the Early Paleozoic marine realm: *Jour. Geol. Soc. London*, v. 138, p. 167-176.

Lenz, A.C., 1982, Ordovician to Silurian sea-level changes in western and northern Canada: *Canadian Jour. Earth Sci.*, v. 19, p. 1919-1932.

Levell, B.K., 1980a, Evidence for currents associated with waves in Late Precambrian shelf deposits from Finnmark, North Norway: *Sedimentology*, v. 27, p. 153-166.

_____, 1980b, A late Precambrian tidal shelf deposit, the lower Sandfjord Formation, Finnmark, North Norway: *Sedimentology*, v. 27, p. 539-557.

Lilly, A.M., 1982, A study of fluid inclusions in quartz-filled veins of the Allegheny Orogeny at White Deer, Pennsylvania: unpub. Senior Thesis, Lewisburg, Bucknell University, 46 p.

Luttrell, E.M., 1968, An analysis of the Silurian Keefer Sandstone of Pennsylvania: unpubl. Ph.D. dissertation, Princeton Univ., 111 p.

Mack, G.H., 1978, The survivability of labile light-mineral grains in fluvial, aeolian and littoral marine environments: the Permian Cutler and Cedar Mesa Formations, Moab, Utah: *Sedimentology*, v. 25, p. 587-604.

Marshak, S., Geiser, P.A., Alvarez, W., Engelder, T., 1982, Mesoscopic fault array of the northern Umbrian Apennine fold belt, Italy: geometry of conjugate shear by pressure-solution slip: *Geol. Soc. America Bull.*, v. 93, p. 1013-1022.

Matsumoto, R., and Iijima, A., 1981, Origin and diagenetic evolution of Ca-Mg-Fe carbonates in some coalfields of Japan: *Sedimentology*, v. 28, p. 239-259.

McKerrow, W.S., 1979, Ordovician and Silurian changes in sea level: *Jour. Geol. Soc. London*, v. 136, p. 137-145.

McKerrow, W.S., and others, 1980, The Ordovician, Silurian, and Devonian time-scale: *Earth and Planetary Sci. Letters*, v. 51, p. 1-8.

Means, W.D., 1976, Stress and strain: Basic concepts of continuum mechanics for geologists: Springer-Verlag, 333 p.

Miall, A.D., 1978, Lithofacies types and vertical profile models in braided river deposits: a summary: in Miall, A.D., editor, *Fluvial Sedimentology*; Canadian Society Petroleum Geologists, Memoir 5, p. 597-604.

Mitra, G., 1979, Ductile deformation zones in Blue Ridge basement rocks and estimation of finite strains: *Geol. Soc. America Bull.* v. 90, p. 935-951.

Morton, R.A., 1981, Formation of storm deposits by wind-forced currents in the Gulf of Mexico and the North Sea: in Nio, S.-D. et al, eds., *Holocene Marine sedimentation in the North Sea Basin*. Spec. Publ. Int. Assoc. Sedimentol., No. 5, p. 385-396.

Moslow, T.F., and Heron, J.D., Jr., 1978, Relict inlets: preservation and occurrences in the Holocene stratigraphy of southern Core Banks, North Carolina: *Jour. Sedimentary Petrology*, v. 48, p. 1275-1286.

Mount, J.F., 1982, Storm-surge-ebb origin of hummocky cross-stratified units of the Andrews Mountain Member, Campito Formation (Lower Cambrian), White-Inyo Mountains, eastern California: *Jour. Sedimentary Petrology*, v. 52, p. 941-958.

Mullis, Josef, 1979, The system methane-water as a geologic thermometer and barometer from the external part of the Central Alps: *Bull. Mineral.*, v. 102, p. 526-536.

Myer, G.H., DeSantis, J., Grandstaff, B.E. and Grandstaff, D.E., 1977, A multistage model of preservation in some fossil plants: *Geol. Soc. America Abstracts with Programs*, v. 9, n. 3, p. 304.

Nickelsen, R.P., 1966, Fossil distortion and penetrative rock deformation in the Appalachian Plateau, PA: *Journal of Geology*, v. 74, no. 6, p. 924-931.

_____, 1972, Attributes of rock cleavage in some mudstones and limestones of the Valley and Ridge Province, Pennsylvania: *Proceedings, Pennsylvania Acad. Science*, v. 46, p. 107-112.

_____, 1974, Early jointing and cumulative fracture patterns: *Proc. 1st International Conf. on the New Basement Tectonics*, Utah Geological Assoc. Pub. No. 5, p. 193-199

_____, 1974, Origin of cleavage and distorted mudcrack polygons: Geol. Soc. America, Abstracts with Programs, v. 5, p. 59.

_____, 1979, Sequence of structural stages of the Allegheny orogeny, at the Bear Valley Strip Mine, Shamokin, Pennsylvania: Am. Jour. Science, v. 279, p. 225-271.

_____, 1980, Sequential and spatial development of the Allegheny Orogeny in the Middle Appalachians: Geol. Soc. America, Abstracts with Programs (Northeastern Section), v. 12, p. 75.

Nickelsen, R.P. and Hough, Van Ness D., 1967, Jointing in the Appalachian Plateau of Pennsylvania: Geol. Soc. America Bull., v. 78, p. 609-630.

Onasch, C.M., 1983, Dynamic analysis of rough cleavage in the Martinsburg Formation, Maryland: Jour. Structural Geology, v. 5, p. 73-81.

Osgood, R.G., Jr., and Drennen, W.T., 1975, Trilobite trace fossils from the Clinton Group (Middle Silurian) of east-central New York State: Bull. American Paleontology, v. 67, n. 287, p. 299-348.

Parker, G., Lanfredi, N.W., and Swift, D.J.P., 1982, Sea floor response to flow in a southern hemisphere sand-ridge field: Argentine inner shelf: Sedimentary Geology, v. 33, p. 195-216.

Parker, J.M., 1942, Regional systematic jointing in slightly deformed sedimentary rocks: Geol. Soc. America Bull., v. 53, p. 381-408.

Patchen, D.G., and Smosna, R.A., 1975, Stratigraphy and petrology of the Middle Silurian McKenzie Formation in West Virginia: The Am. Assoc. Petroleum Geol. Bull., v. 59, n. 12, p. 2266-2287.

Perry, W.J., Jr., 1978, Sequential deformation in the central Appalachians: Am. Jour. Science, v. 278, p. 518-542.

Petryk, A.A., 1981, Stratigraphy, sedimentology, and paleogeography of the Upper Ordovician-Lower Silurian of Anticosti Island, Quebec: p. 11-39 in Lesperance, P.J., ed., Subcomm. on Silurian Stratig., Ord.-Sil. Bndry. Working Group Field Meeting, Anticosti-Gaspe, Quebec, Vol. II. Stratigraphy and Paleontology.

Pierce, K.L., 1966, Bedrock and surficial geology of the McConnellsburg quadrangle, Pennsylvania: Pennsylvania Geological Survey, 4th ser., Atlas 109a.

Pohn, H.A. and Purdy, T.L., 1982, Disturbed zones: indicators of deep-seated subsurface faults in the Valley and Ridge and Appalachian structural front of Pennsylvania: U.S. Geol. Survey Open-File Rept. 82-967.

Price, N.J., 1966, Fault and joint development in brittle and semi-brittle rock: Pergamon Press, 176 p.

Pringle, L.R., 1980, Strain mechanisms in the Upper Silurian Wills Creek Formation, central Pennsylvania: unpub. Senior Thesis, Lewisburg, Bucknell University, 87 p.

Raaf, J.F.M. de, Boersma, J.R., and van Gelder, A., 1977, Wave-generated structures and sequences from a shallow marine succession, Lower Carboniferous, Co. Cork, Ireland, Sedimentology, v. 24, 451-483.

Raiswell, R., and White, N.J.M., 1978, Spatial aspects of concretionary growth in the Upper Lias of northeast England: *Sedimentary Geology*, v. 20, p. 291-300.

Ramsay, J.G., 1967, *Folding and fracturing of rocks*: McGraw-Hill, New York, 568 p.

_____, 1980a, The crack-seal mechanism of rock deformation: *Nature*, v. 284, p. 135-139.

_____, 1980b, Shear zone geometry: a review: *Jour. Struct. Geol.* v. 2, p. 83-99.

Ramsay, J.G. and Allison, I., 1979, Structural analysis of shear zones in an Alpinised Hercynian Granite: *Schweizer. Mineralog. u. Petrog. Mitt.*, v. 59, p. 251-279.

Ramsay, J.G. and Graham, R.H., 1970, Strain variation in shear belts: *Can. Jour. Earth Sci.*, v. 7, p. 786-813.

Reineck, H.E., and Singh, I.B., 1980, *Depositional sedimentary environments with reference to terrigenous clastics*: Springer-Verlag, 2nd ed., 549 p.

Reinson, G.E., 1979, Facies models 6. barrier island systems: in Walker, R.G., editor, *Facies Models*, Geoscience Canada Reprint Series 1, Toronto, Ontario, p. 57-74.

Reks, I.J., and Gray, D.R., 1982, Pencil structure and strain in weakly deformed mudstone and siltstone: *Jour. Struct. Geol.*, v. 4, n. 2, p. 161-176.

Ricci, M.P., 1979, Regional joint patterns in the Valley and Ridge and Appalachian Plateau Province of central Pennsylvania: unpub. Senior Thesis, Lewisburg, Bucknell University, 42 p.

Rickard, L.V., 1969, *Stratigraphy of the Upper Silurian Salina Group*, New York, Pennsylvania, Ohio, Ontario: New York State Museum Science Service, Map and Chart Series No. 12.

Sacks, R.E., 1981, Interpretation of the depositional environment of the Middle Silurian Upper McKenzie Formation in central Pennsylvania with the aid of ripple analysis: unpub. Senior Thesis, Lewisburg, Bucknell University, 71 p.

Schmitt, E., 1983, Penetrative strain measured in reduction spots of the Bloomsburg Formation at the Berwick Anticlinorium between Bloomsburg and Berwick, PA: unpub. Senior Thesis, Lewisburg, Bucknell University, 49 p.

Schuchert, Charles, 1916, *Silurian formations of southeastern New York, New Jersey, and Pennsylvania*: *Geol. Soc. America Bull.*, v. 27, p. 531-554.

Scotese, C.R., and others, 1979, Paleozoic base maps: *Journal of Geology*, v. 87, p. 217-277.

Secor, D.T., Jr., 1960, Role of fluid pressure in jointing: *Am. Jour. Science*, v. 263, p. 633-646.

Seslavinsky, K.B., 1979, Ordovician and Silurian climates and global climatic belts: *International Geology Review*, v. 21, p. 140-152.

Shanmugam, G., and Moiola, R.J., 1982, Eustatic control of turbidites and winnowed turbidites: *Geology*, v. 10, p. 231-235.

Sherwin, J. and Chapple, W.M., 1968, Wavelength of single layer folds: a comparison between theory and observation. *Am. Jour. Science* v. 266, p. 167-179.

Simpson, C., 1983, Strain and shape-fabric variations associated with ductile shear zones: *Jour. Struct. Geol.*, v. 5, n. 1, p. 61-72.

Smith, N.D., 1968, Cyclic sedimentation in a Silurian intertidal sequence in eastern Pennsylvania: *Jour. Sedimentary Petrology*, v. 38, no. 4, p. 1301-1304.

_____, 1970, The braided stream depositional environment: comparison of the Platte River with some Silurian clastic rocks, north-central Appalachians: *Geol. Soc. America Bull.*, v. 81, p. 2993-3014.

Smith, N.D., and Saunders, R.S., 1970, Paleoenvironments and their control of acritarch distribution: Silurian of eastern and central Pennsylvania: *Jour. Sedimentary Petrology*, v. 40, p. 324-333.

Smith, R.C., II, and Berkheiser, S.W., Jr., 1983, Silica as pure as the driven snow? Not yet, but we're getting closer: *Pennsylvania Geology*, v. 14, n. 1, p. 13-16.

Smosna, R.A., and Patchen, D.E., 1978, Silurian evolution of central Appalachian Basin: *Am. Assoc. Petroleum Geol. Bull.*, v. 62, p. 2308-2328.

_____, 1980, Niagaran bioherms and interbioherm deposits of western West Virginia: *The Am. Assoc. Petroleum Geol. Bull.*, v. 64, n. 5, p. 629-637.

Stahl, L., Koczan, J., and Swift, D.J.P., 1974, Anatomy of a shoreface-connected sand ridge on the New Jersey shelf: implications for the genesis of a surficial sand sheet: *Geology*, v. 2, p. 117-120.

Swartz, C.K., and Swartz, F.M., 1931, Early Silurian formations of southeast Pennsylvania: *Geol. Soc. America Bull.*, v. 42, p. 621-662.

Swartz, F.M., 1934, Silurian sections near Mount Union, central Pennsylvania: *Geol. Soc. America Bull.*, v. 45, p. 18-134.

_____, 1957, Silurian sediments and relationships at Susquehanna Gap in Blue or Kittatinny Mountain, five miles north of Harrisburg, Pennsylvania: Contribution No. 3, Dept. Geology, College Min. Industries, Penna. State Univ., University Park, PA, 58 p.

Swift, D.J.P., 1976, Continental shelf sedimentation: in Stanley, D.J., and Swift, D.J.P., editors, *Marine Sediment Transport and Environmental Management*; John Wiley and Sons, Inc., New York, p. 311-350.

Swift, D.J.P., and Field, M.E., 1981, Evolution of a classic sand ridge field: Maryland sector, North American inner shelf: *Sedimentology*, v. 28, p. 461-482.

Swift, D.J.P., and others, 1978, Shoreface-connected sand ridges on American and European shelves: a comparison: *Estuarine Coastal Mar. Sci.*, v. 7, p. 257-273.

Tanner, W.F., 1967, Ripple mark indices and their uses: *Sedimentology*, v. 9, p. 89-104.

_____, 1971, Numerical estimates of ancient waves, water depth and fetch: *Sedimentology*, v. 16, p. 71-88.

Tourek, T.J., 1970, The depositional environments and sediment accumulation models for the Upper Silurian Wills Creek Shale and Tonoloway Limestone, central Appalachians: unpubl. Ph.D. dissertation, Baltimore, The Johns Hopkins Univ., 282 p.

Tuttle, O.F., 1940, Heavy minerals of the Ordovician-Silurian boundary in central Pennsylvania: *Pennsylvania Acad. Sci., Proceedings*, v. 14, p. 55-59.

Vail, P.R., and others, 1977, Seismic stratigraphy and global changes of sea level, Part 3: relative changes of sea level from coastal onlap: *Am. Assoc. Petroleum Geol. Spec. Pub.* 26, p. 63-98.

Van Houten, E.B., and Bhattacharyya, D.P., 1982, Phanerozoic oolitic ironstones-geologic record and facies model: *Ann. Rev. Earth Planet. Sci.*, v. 10, p. 441-457.

Vaskov, E., 1974, Fossil deformation in the Devonian Trimmers Rock Formation of central Pennsylvania: unpub. Senior Thesis, Lewisburg, Bucknell University, 43 p.

Vernon, J.H., 1974, Crinoid deformation, Shamokin Mountain: unpub. Senior Thesis, Lewisburg, Bucknell University, 61 p.

Wescott, W.A., 1982, Nature of porosity in Tuscarora Sandstone (Lower Silurian) in the Appalachian Basin: *Oil and Gas Journal*, Aug. 23, 1982, p. 159-173.

Wheeler, R.L., 1978, Slip planes from Devonian Millboro shale, Appalachian Plateau Province: Statistical extensions of disclod analysis: *Am. Jour. Science*, v. 278, p. 497-517.

Whitaker, J.H.M., 1973, "Gutter casts," a new name for scour-and-fill structures: with examples from the Llandoveryan of Ringerike and Malmoya, southern Norway: *Norsk Geog. Tidsskr.*, v. 53, p. 403-417.

Wood, D.S., 1973, Patterns and magnitude of natural strain in rocks: *Royal Soc. London Philos. Trans., Series, A.*, v. 274, p. 373-382.

Wood, D.S. and Oertel, G., 1980, Deformation in the Cambrian Slate Belt of Wales: *Journal of Geology*, v. 88, p. 285-308.

Wood, G.H., and Bergin, M.J., 1970, Structural controls of the anthracite region, Pennsylvania, in Fisher, G.W., Pettijohn, F.J. Reed, J.C., Jr., and Weaver, K.N., eds. *Studies of Appalachian geology central and southern*: New York Intersci. Publishers, p. 147-160.

Wood, G.H., Jr., Trexler, J.P., and Kehn, T.M., 1969, Geology of the west-central part of the southern anthracite field and adjoining areas, Pennsylvania: *U.S. Geol. Survey Prof. Paper* 602, 150 p.

Woodward, H.P., 1941, Silurian system of West Virginia: *West Virginia Geol. Survey*, v. 14, 326 p.

Yeakel, L.S., Jr., 1962, Tuscarora, Juniata, and Bald Eagle paleocurrents and paleogeography in the central Appalachians: *Geol. Soc. America Bull.*, v. 73, p. 1515-1540.

Zenger, D.H., 1971, Uppermost Clinton (Middle Silurian) stratigraphy and petrology, east-central New York: New York Museum Bull. 417, 58 p.

Ziegler, A.M., and others, 1977, Silurian continental distributions, paleogeography, climatology, and biogeography: Tectonophysics, v. 40, p. 13-51.

Ziegler, A.M., and others, 1979, Paleozoic paleogeography: Ann. Rev. Earth Planet Sci., v. 7, p. 473-502.

CLINTON IRON-ORE MINES OF THE DANVILLE-BLOOMSBURG AREA, PENNSYLVANIA: THEIR GEOLOGY, HISTORY, AND PRESENT-DAY ENVIRONMENTAL EFFECTS

by

Jon D. Inners, Pennsylvania Geological Survey, and
John H. Williams, U.S. Geological Survey

Introduction

The mining of sedimentary iron ore from the Middle Silurian Clinton beds was one of the major extractive industries in the central Appalachian region during the middle years of the nineteenth century. In Pennsylvania, the ore region extended from Bedford County, northeastward through the Valley and Ridge Province to Columbia County, an arcuate distance of about 125 miles. The large-scale mining of these ores, together with the ready availability of limestone for flux and anthracite for fuel, permitted the central and northeastern Pennsylvania iron industry to be self-sufficient for several decades (Wright and others, 1968). A rapid decline set in during the closing quarter of the century, however, and by 1900 the Clinton ore industry in Pennsylvania was dead.

This report presents an overview of some of the geological, historical, technological, and environmental aspects of the iron industry in the northeastern Pennsylvania, Clinton ore region near Danville and Bloomsburg, Montour and Columbia Counties.

Geology

The two main Clinton ores mined in the Dannville-Bloomsburg area were the "fossil ore" in the upper member of the Rose Hill Formation and the "block ore" in the Centre Member of the same formation (Figure 15). A third—"the lower block ore"—was prospected at several localities between Danville and Bloomsburg, but it apparently was mined only on a small scale. The ore beds occur on the flanks and crest of the prominent elongate ridge formed by the several en echelon folds of the Berwick anticlinorium (Figure 16). Both the fossil ore and block ore were mined on the sides of Mahoning Creek gap at Danville. Only the fossil ore was extensively mined between Danville and Bloomsburg.

The fossil ore consists of thin to medium beds of reddish-brown, highly ferruginous bioskeletal limestone that lie 10 to 33 feet below the Keefer sandstone. Iron occurs as hematite coatings and partial replacements of fragmental fossils, particularly crinoids, brachiopods, and bryozoans. The ore is highly variable. In the Danville mines, it typically consisted of two and sometimes three beds within a four-foot-thick interval. The middle bed, or "buncombe"—15 to 20 inches thick, was the main ore body (Stoek, 1892). In mines near Bloomsburg, the fossil ore most often consisted of two beds—an upper "big bed," 10 to 12 inches thick, and a lower "little bed," 2 to 4 inches thick, separated by 2 to 3 feet of barren rock (White, 1883). Good exposures of this ore horizon can be seen in the long road cut along U.S. Route 11 about 2 miles west of Danville and in an old quarry along an abandoned railroad grade on the south side of Fishing Creek, 1.3 miles north of Bloomsburg.

The fossil ore occurs in two varieties. Most valuable to the nineteenth century miners was the "soft ore," a spongy, thoroughly weathered, near-surface deposit formed

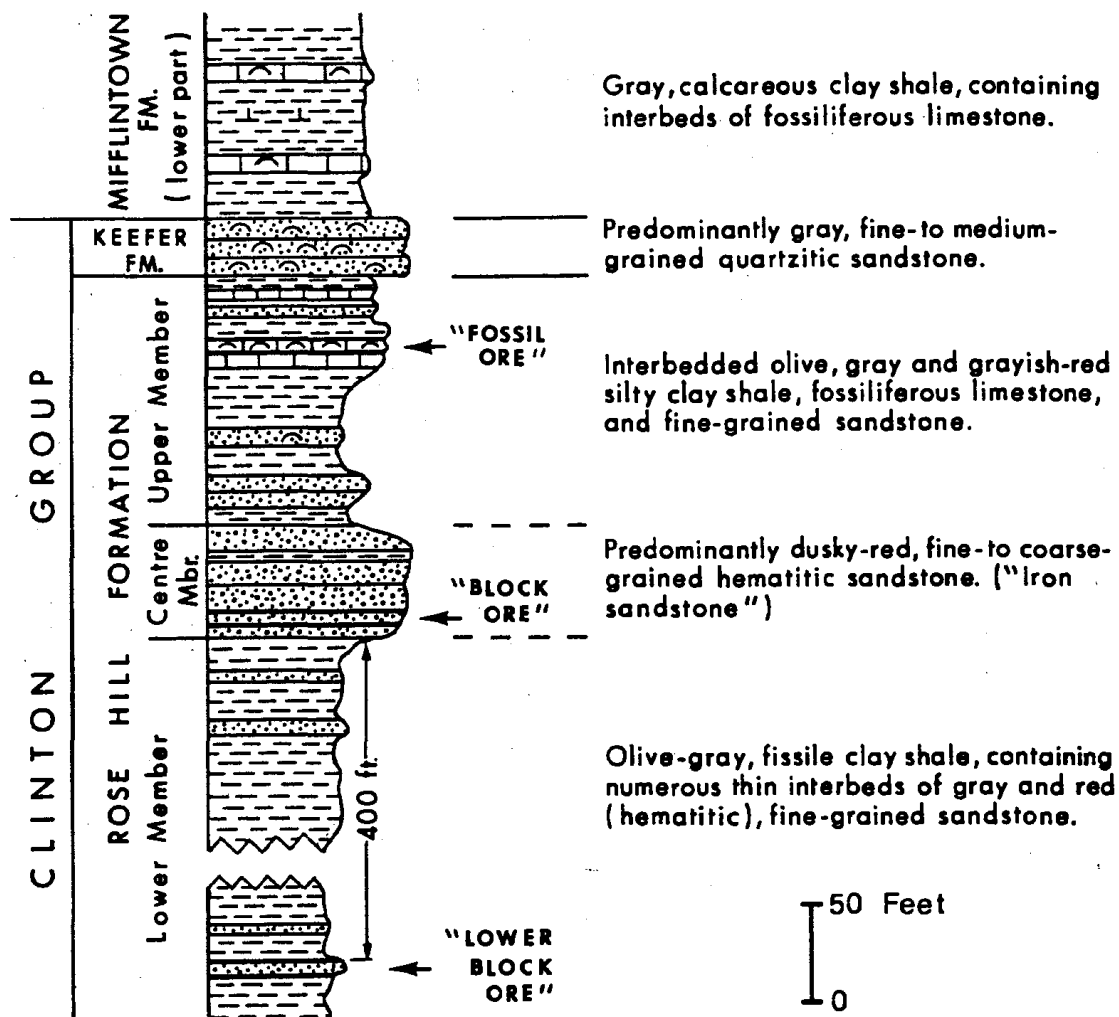


Figure 15 Typical stratigraphic section of Clinton iron-ore bearing beds in the Danville-Bloomsburg area.

by the removal of calcium carbonate from the original, hard hematitic limestone, or "hard ore." The latter typically contained 20 to 40 percent ferric oxide, whereas the soft ore was commonly enriched to 60 to 70 percent ferric oxide. As mining progressed along the strike and down the dip of beds, the hard and soft types of fossil ore were found to be extremely variable in occurrence, the soft ore at some places changing gradually and at other places abruptly into hard ore. Generally the top rock of the hard ore was solid, but that of the soft ore was cracked and broken (Stoek, 1892). The variable nature of the ores, largely caused by the nonhomogeneous distribution of bedrock fractures along which the weathering process occurred, must have confused as well as frustrated the early miners. Along the flanks of the anticlinal ridge, the transition between the soft and hard ores usually occurred 90 to 120 feet down dip from the outcrop (Rogers, 1858), about 50 feet below land surface. Particularly large quantities of soft ore were developed by surficial weathering on the noses of gently-plunging anticlines in the vicinity of Bloomsburg (Rogers, 1858; Figure 16).

The block ore occurs in the lower part of the Centre Member ("iron sandstone") in the Danville area and consists of 18 to 24 inches of highly ferruginous sandstone. The ore is typically about 50 percent ferric oxide (Stoek, 1892). Although the block ore was a valuable horizon at Danville, it apparently thins and becomes inseparable from the main mass of the "iron sandstone" to the east. The block ore is exposed along Pa. Route 54 near the Danville Borough line.

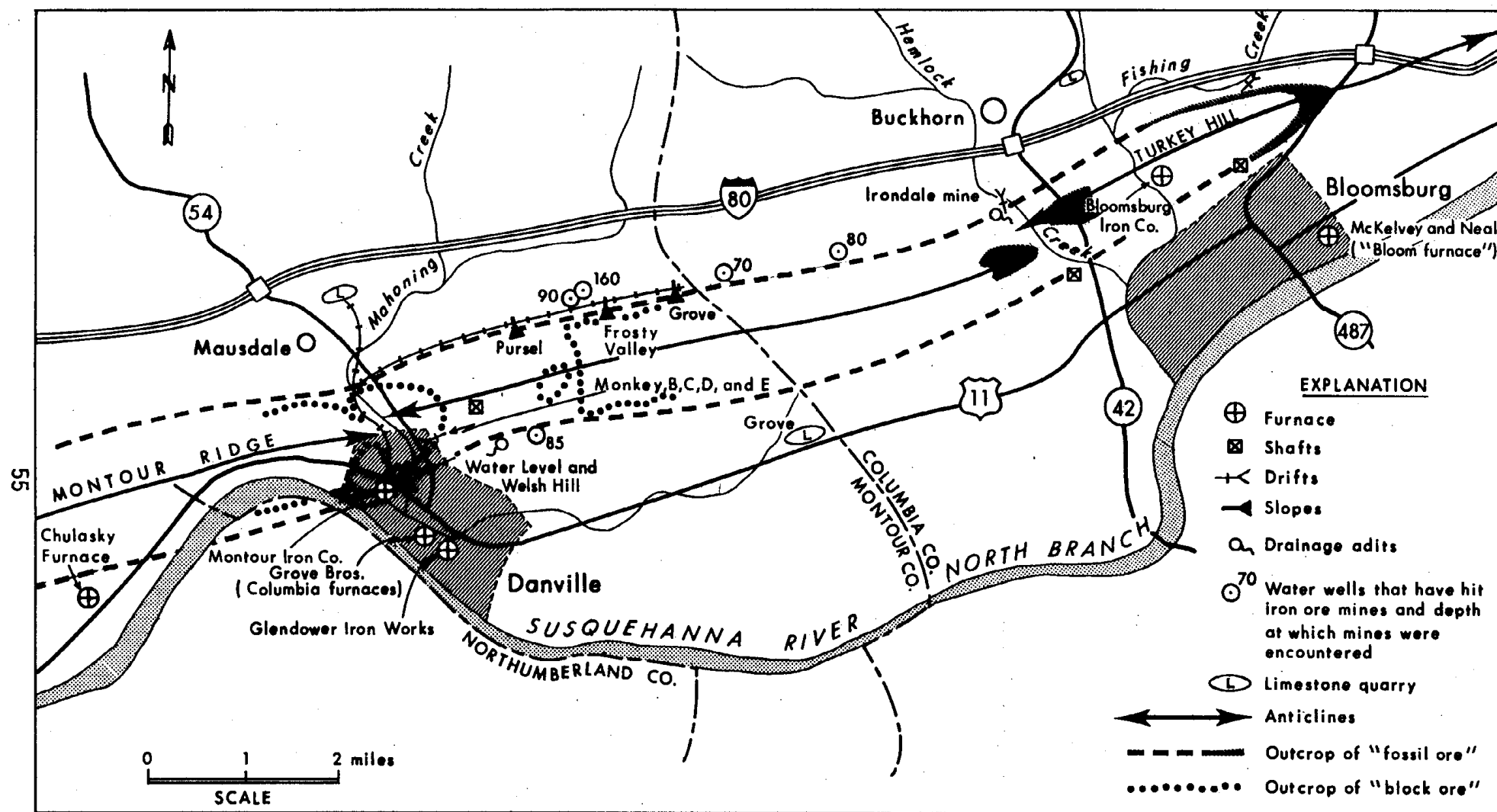


Figure 16 Generalized geologic map of the Danville-Bloomsburg area, showing outcrop of ore beds, *en echelon* pattern of anticlinal axes along Berwick anticlinorium, and location of blast furnaces, mine workings, fluxstone quarries, and selected present-day water wells.

Historical Development

The initial discovery of iron ore in the Danville-Bloomsburg area took place about 1822 somewhere west of Hemlock Creek in Columbia County. Drift mining was initiated soon after samples were assayed and the ore was transported across the North Branch of the Susquehanna River to charcoal furnaces near Catawissa. Additional discoveries followed, and in 1837 Eli Trego of Danville put into full-blast the first charcoal furnace build specifically to smelt locally mined ore (Diehl, 1969). The fate of the local charcoal furnaces was sealed, however, when technological innovations, especially introduction of the hot air blast (Binder, 1974), made possible the use of anthracite for smelting iron.

After the charcoal furnaces were abandoned and the process of smelting by anthracite was instituted on a large scale, the North Branch iron industry developed apace (Beers and Co., 1915). These halcyon days began in the early 1840's with the building of large iron works in Danville and Bloomsburg and lasted into the 1870's.

Danville was clearly the most important of the two North Branch iron mining towns. In 1840, the Montour Iron Company works was constructed south of what is now U.S. Route 11 at the present site of the Danville Senior High School (Figures 16 and 17). The "twin furnaces" of these works, among the first in the United States to use anthracite as fuel, became the nucleus of what was to become known locally as "the Big Mill." The first iron T-rail was manufactured at the rolling mill here in 1845. Although its ownership and name changed several times, the Montour Iron works prospered for the next three decades and Danville became a "company town." In 1870, the works produced 36,000 tons of rails and consumed 80,000 tons of iron ore (half of which was mined on company property nearby), 20,000 tons of limestone, and 125,000 tons of anthracite (Diehl, 1969).

Numerous other furnaces were built in the Danville area during the heyday of the iron industry. Among the most important of these were the Grove Brother's Columbia furnace (1839-1840), the Chulasky furnace (1846), and the National Iron works (1871), later to become the Glendower Iron works (1877) (Figure 16; Brower, 1881). In 1881, the

Figure 17 *Montour Iron Company works at Danville, circa 1855. Lithograph by James Queen. Reproduced from O'Connor and Yeager (1980), with the permission of the authors and Salina Press, Syracuse, New York.*

Figure 18 *Limestone and slag piles of the old Irondale works (Bloomsburg Iron Company) in Fishing Creek gap, town of Bloomsburg. Centre Member of Rose Hill Formation caps gently curved ridge crest to west of waste piles.*

Figure 19 *Photomicrograph of thin section of fine-grained, ferruginous sandstone of Centre Member (plane-polarized light). Specimen collected from abandoned dimension stone quarry on northwest side of Fishing Creek gap, Hemlock Township. (Q= quartz; H= hematite).*

Figure 20 *An adit of the Irondale mine, located on the south side of L.R. 19027, about 100 feet west of the bridge over Hemlock Creek, 1.5 miles northwest of Bloomsburg.*



18



17



0.5 mm

19



20

Reading Railroad acquired many local furnaces and consolidated them into the Montour Iron and Steel works, or "the Big Mill" (Diehl, 1969). At full capacity, this mill employed more than 1100 workers.

Although not as dominant in the Clinton iron industry as its neighbor, Bloomsburg could also boast of several large iron works (Figure 16). The first big anthracite furnace in the town, that of the Bloomsburg Iron Company (originally the Bloomsburg Railroad and Iron Company) was "blown-in" in 1844 at Irondale in the gap of Fishing Creek north of Bloomsburg. In 1854, McKelvey, Neal and Company (after 1873, William Neal and Sons) put into full-blast Bloom furnace, the second large works in the Bloomsburg area. The Bloom furnace was located along the Pennsylvania Canal, North Branch Division, in the southeastern part of Bloomsburg (near the present airport). The site of the Irondale works is today marked only by heaps of slag and limestone on the flat, glacial outwash terrace east of Fishing Creek (Figure 18) and by the row of "company houses" (formerly Morgantown) on the west side of Iron street a few hundred yards away. Modern construction has apparently obliterated all evidence of the Bloom furnace (Inners, 1981).

Production of one ton of pig iron in the anthracite furnaces of the Danville-Bloomsburg area typically required 3 tons of iron ore, 2 tons of coal, and 1.6 tons of limestone (Beers, 1915). The Montour Iron works obtained ore locally from drift mines in the gap of Mahoning Creek at Danville and from slope mines on the north side of the anticlinal ridge about 2 miles to the northeast. Most of the ore for the Bloomsburg Iron Company works came from mines west of Fishing Creek, particularly on the north side of the anticlinal ridge. The Bloom furnace was supplied mainly from McKelvey and Neal holdings on Turkey Hill. Much of the coal came from the Northern Anthracite field, the Montour Iron Company using coal from its own mines near Kingston. The limestone for flux was obtained from many local quarries in the Upper Silurian to Lower Devonian Tonoloway-Keyser carbonate sequence that outcrops parallel to the ore beds but farther out on the flanks of the anticlinal ridge. Three of the largest intact examples of these old fluxstone quarries are located (1) 2000 feet northeast of Pa. Route 54, 0.6 mile north-northeast of Mausdale, Montour County (Montour Iron Company); (2) on the west bank of Fishing Creek, just south of Pa. Route 42, 1.1 miles northeast of Buckhorn, Columbia County (Bloomsburg Iron Company); and (3) on the north side of old U.S. Route 11 on the Montour-Columbia County line (Grove Brothers) (Figure 16). (Until quite recently, the Lycoming Silica Sand Company used the latter quarry as a source of crushed stone.) Numerous quarries along U.S. Route 11 east of Bloomsburg probably supplied limestone to the Bloom Furnace.

As a result of the success of the iron furnaces, many ancillary iron manufacturing companies were established in the Danville-Bloomsburg area. In addition to the "T-rails," on which much of the prosperity of Danville was based, manufactured iron products included nails, stoves, plow shares, railroad and mine cars, car wheels, and cannons and mortars used in the Mexican and Civil Wars.

After 1880, the local iron industry entered a steady decline brought about by the discovery of much larger and richer ore deposits in the Great Lakes region, by the increasing use of coke as blast furnace fuel, and by rapid advances in steel-manufacturing technology which lowered the price of steel to the point that recovery of the lower grade Clinton ores was not longer profitable (Lesley, 1892; Mensch, 1977). In 1886, the Glendower Iron works was closed down by a strike and never reopened. By 1890, all mining of the Danville-Bloomsburg iron ores had ceased (Stoek, 1892), and the remaining furnaces were supplied solely by imported ore. The Bloom furnace was abandoned in 1892, and its competitor at Irondale in 1893. The "Big Mill" at Danville produced steel rails

until 1935, at which time it was completely shut down. Three years later the plant was dismantled.

Prospects for renewed mining of the Clinton hematite ores of the Danville-Bloomsburg area depend to a large extent on improvements in the technology of iron-ore beneficiation. As early as 1847, Rogers (1858) foresaw that the most valuable ore of the area, the soft fossil ore, would be exhausted within about 25 years. Surely enough, by the mid-1870's most of the ore being mined was of the hard fossil-ore and block-ore varieties. All of these thin ore zones are today of historical interest only. The most likely target for future commercial development is the low-grade "iron sandstone" of the Centre Member. Point counts of two thin sections from visually iron-rich beds at this horizon suggest a hematite content of 28 to 38 percent, of an elemental iron content of approximately 20 to 26 percent (Figure 19). Since the lower economic limit for iron ores is now about 25 percent iron (Wright and others, 1968), such ore is clearly subeconomic to very marginally economic. With improvements in the technology of iron-ore beneficiation, however, and under the proper economic and environmental conditions, many millions of tons of low-grade iron ore could be recovered by surface mining methods from the 35 to 40 feet of highly ferruginous sandstone in the Centre Member.

Mines and Mining Methods

The mining of iron ore in the Danville-Bloomsburg area was done by open-pit workings, shallow underground mines, and deep drifts and slopes (Figure 16). The fossil-ore outcrop along both sides of the Berwick anticlinal ridge between Danville and Bloomsburg was exploited for the removal of soft fossil ore by open-pit and shallow underground workings. Good examples of open-pit mines, including shallow surface depression and spoil piles, are still evident 0.5 mile north of Ridgeville, Montour County, and on the north side of the anticlinal ridge between Fishing and Hemlock Creeks in Columbia County. Large quantities of soft ore were mined by shallow underground drifts on the noses of gently plunging anticlines northwest and northeast of Bloomsburg. A good example of a shallow underground drift can be seen at the site of the old Irondale mine of the Bloomsburg Iron Company on the west side of Hemlock Creek, 1.5 miles northwest of Bloomsburg (Figure 20).

Deep mining of iron ore occurred in the gap of Mahoning Creek at Danville, on the north side of the anticlinal ridge between Danville and Bloomsburg, and on the south side of the ridge east of Danville. The most extensive and only well-documented deep mines were owned by the Montour Iron Company. The company mined the block and fossil ores at Danville by driving a series of drifts into the hillsides on both sides of Mahoning Creek gap (Figure 16). The first mining was done in the block ore on the west side of the creek. In 1853, drift A was driven into the fossil ore. This mine eventually reached a depth of nearly 500 feet, but it was finally abandoned because of "the constantly increasing cost of pumping, the difficulty of ventilation, and the large amount of ore above water level owned by the company" (Stoek, 1892). On the east side of Mahoning Creek, about 2,500 yards of gangways, the Water Level and Welsh Hill drifts, were driven into the fossil ore (Figures 16 and 21). Five drifts, Monkey, B, C, D, and E, were driven higher up on the hillside into the block ore. An air shaft was sunk at the top of the ridge to provide ventilation. By 1889, when mining ceased at Danville, most of the ore had been worked out between the gangways of these drifts (Stoek, 1892). The cemented mine opening that can be seen in the roadcut along Pa. Route 54 at the Danville Borough line is possibly drift E.

The fossil ore was also mined by the Montour Iron Company at the Pursel and Frosty Valley slopes on the north side of the anticlinal ridge northeast of Danville

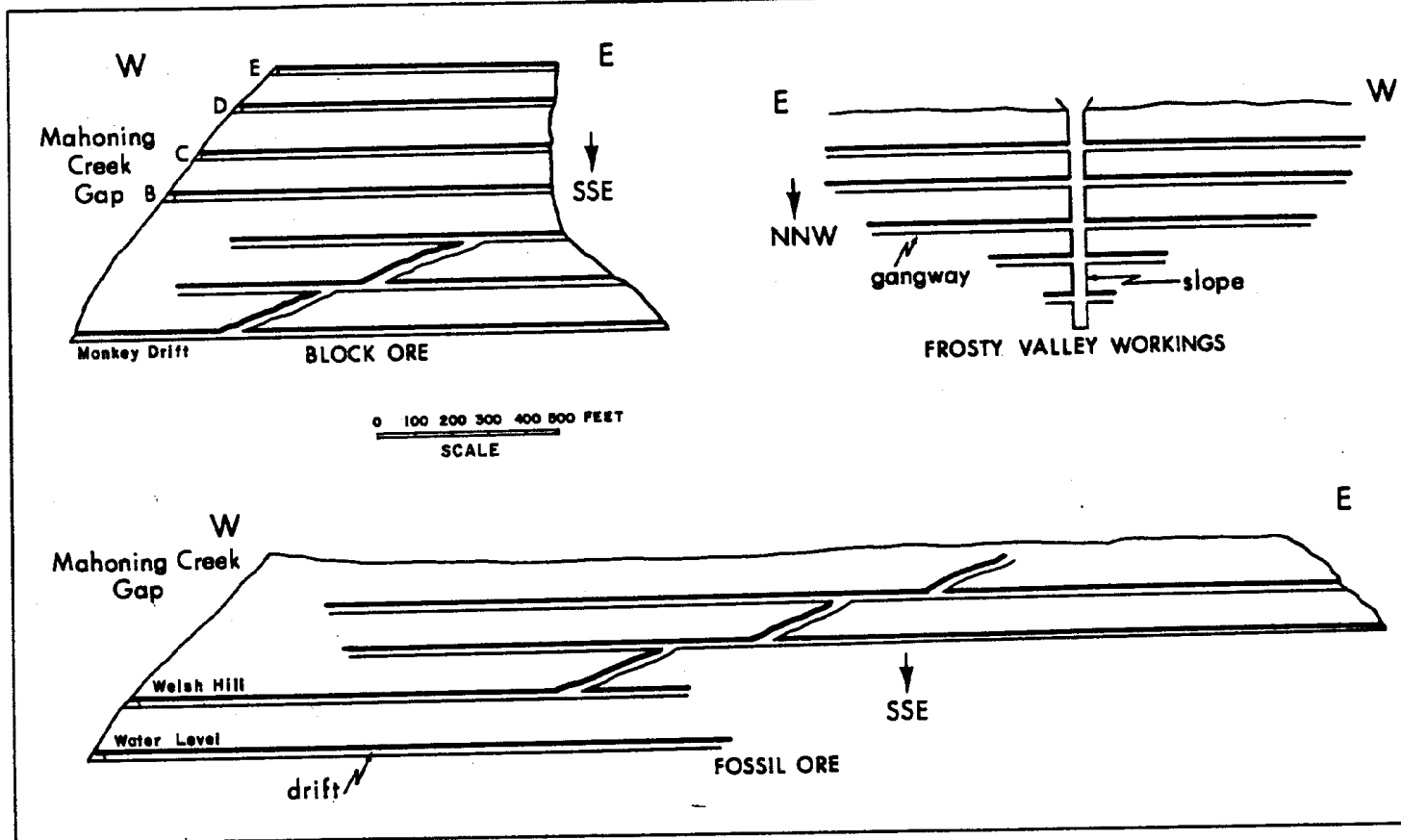


Figure 21 Simplified mine maps of some Montour Iron Company workings. (Slightly modified from Stoek, 1892).

(Figure 16). Both of these workings were started about 1860. The Frosty Valley slope was sunk along the dip of the ore bed, (40 degrees north-northwest) for a length of 400 feet, reaching a maximum depth of about 200 feet below land surface (Figure 21). Three-fourths of a mile away, the Pursel slope was sunk 600 feet upon a northwest dip of 30 degrees, attaining a depth of about 250 feet below land surface. Gangways were driven east and west 75 feet apart in the Frosty Valley workings and 90 feet apart in the Pursel slope. The top two gangways of the Frosty Valley slope were driven to connect with the Pursel gangways to the west. The water intercepted by the Pursel slope was pumped from a sump at the bottom of the mine to the uppermost gangway, which had been driven to the surface and was used as a drainage adit. The amount of water to be lifted through the Pursel and Frosty Valley slopes was greatly increased when the Grove slope, located 0.75 mile to the east, was abandoned in 1882. When the Frosty Valley and Pursel slopes ceased operation in 1889, the upper two levels had been worked out and the remaining lower levels only partly worked (Stoek, 1892). Large piles of waste rock, now overgrown with vegetation, can be seen near the site of the old Pursel slope.

The long-wall method was used in the underground mines of the Montour Iron Company. Gangways were dug 7 to 10 feet wide and 5.5 to 7 feet high, or just high enough for a man or mule to pass through. The gangways on the soft ore were timbered, but in the hard ore and block ore, this was not usually necessary. The area between the gangways was worked out by a series of breasts. The hard ore and block ore had to be blasted, while the soft ore could be scraped out. The breasts were 2 to 5 feet high depending on the characteristics of the ore. Waste rock was carefully piled, or stowed, at

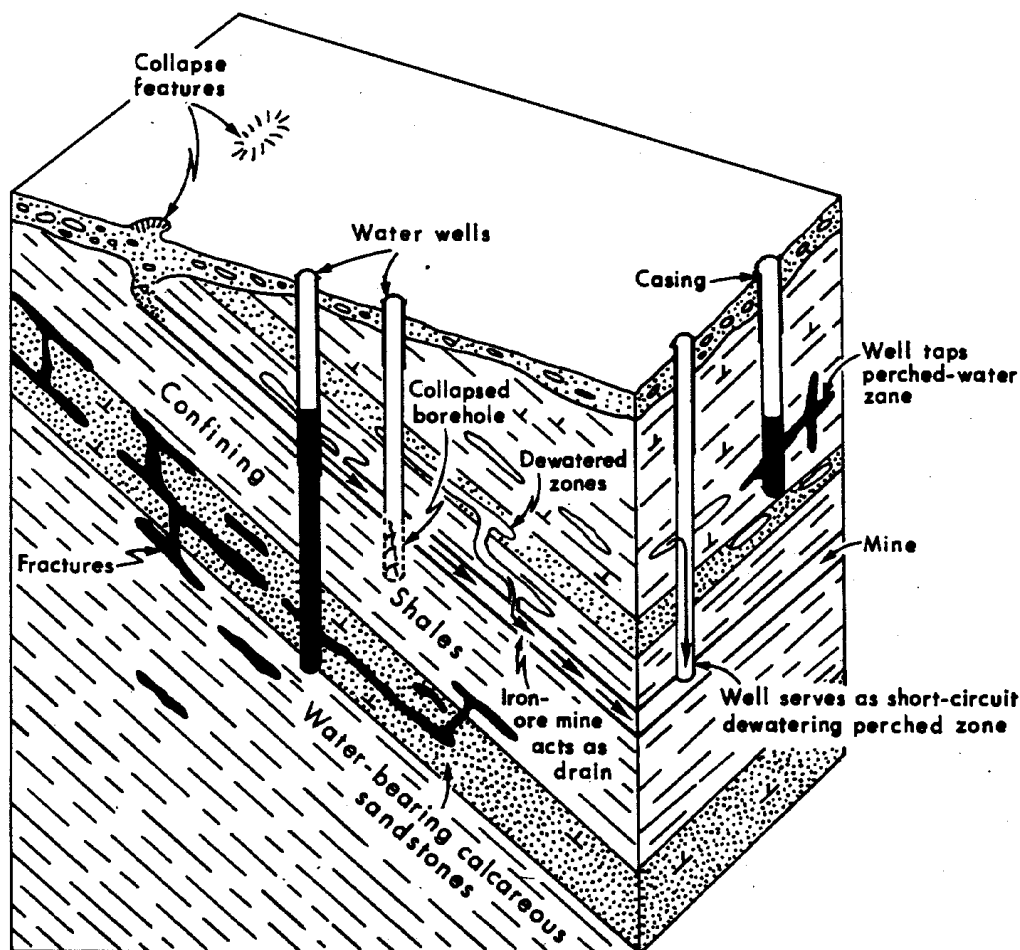


Figure 22 Block diagram of hypothetical slope mine showing potential environmental problems

spaced intervals to support the roof and protect chutes which the ore was thrown down to the gangway below. To minimize the amount of water that needed to be pumped from a mine, the face of each gangway should have been kept in advance of higher gangways. However, as seen in Figure 21, this was not done because it necessitated the outlay of a large amount of capital before any return could be realized (Stoek, 1892). By mining as they did, the miners created an up-dip, high-permeability drain which greatly aggravated their flooding problems.

The average rate of advance for gangways was 15 feet per month for those open on one side to stowing and 7 feet for those driven into solid rock. One ton per day for a miner and his laborer was considered average output for a shift of 10 hours (Stoek, 1892).

Present-Day Environmental Effects

The abandoned iron-ore workings pose several potential problems and a possible opportunity for present-day developers and residents of the Danville-Bloomsburg area. Potential problems include foundation instability, ground-water contamination, collapsed water wells, and dewatered aquifers (Figure 22). On the other hand, considerable benefit could be derived if the flooded iron workings were tapped as a water-supply source.

Although no serious foundation problems related to the old mines have been reported, the probability of structural damage to buildings caused by subsidence above abandoned mines increases as residential development proceeds along the anticlinal ridge between Danville and Bloomsburg. Construction in such areas is safe only after underground mines have been located and backfilled. Most of the minor subsidence problems that have been reported involve small sinkhole-like collapses in open fields brought about by heavy rains or the weight of farm machinery. Several small roadway construction projects also encountered mine voids that had to be backfilled.

Underground mines can act as zones of conduit flow for septic effluent and other contaminated surface waters, thereby increasing the potential for ground-water contamination in a mined area. In addition, open-pit workings and mine breakthroughs are commonly used as local waste-disposal sites (Williams, 1980).

Wells that penetrate the deep mines should be cased through the mined void in order to prevent well-bore collapse. The added expense of casing through the mine generally makes cost of a well excessive. Five domestic wells are believed to have encountered slope workings at depths of 70 to 160 feet below land surface (Figure 16). One of the wells penetrated the underground workings of the Frosty Valley slope at a depth of 160 feet. The driller reported that the drill stem dropped about 8 feet. Loss of air circulation made drilling difficult, and the hole was stopped at 180 feet, with no water encountered. The mine void was not cased off, and the well collapsed at 160 feet. A decision was made to drill a new well up dip of the previous site in order to minimize the amount of casing that would be needed if the mine was penetrated again. The new well was subsequently drilled 90 feet up dip. A void was hit at a depth of 110 feet *; it was cased off and drilling was continued. Water-bearing calcareous sandstone was encountered at 235 feet and drilling was stopped at 250 feet. The well required 120 feet of casing instead of the normal 50 feet of casing typically required in the area.

Abandoned iron-ore mines can act as effective ground-water drains that dewater the overlying aquifer. Evidence for this capability is given by the fact that keeping the underground iron workings dry was constant problem for the nineteenth-century miners. Drainage adits, in some cases combined with pumps, were used to dewater the mines. Small streams still originate at two such adits, one located near Geisinger Medical Center east of Danville, and the other at the old Irondale mine northwest of Bloomsburg.

Due to the presence of unfractured shale, perched-water zones may be encountered above deep mines. If a well is drilled through a perched zone and is then extended down into a mine void, it can serve as a short circuit past the perching shales and dewater the zone (Figure 22). Such conditions were possibly encountered during the drilling of a well on the south flank of the anticlinal ridge about one mile east of Danville.

On the positive side, good supplies of water may be obtained if test drilling can locate saturated zones of the old iron workings. The previously mentioned drainage adit, or "spring" east of Danville is currently being tapped as a water-supply source for the Geisinger Medical Center. Wells completed with slotted casing in mine-void intervals could potentially produce large quantities of good quality water. Probably the most promising areas for water-supply development would be located north of Danville in the A and Water-Level drifts and the Pursel and Frosty Valley slope workings.

* Inclination of the old slope workings between the mine voids penetrated by the two wells was calculated to be 43 degrees, which is in close agreement with the dip of the Frosty Valley slope as reported by Stoek (1892).

References Cited

- Beers, J. H., and Co. (1915), Historical and biographical annals of Columbia and Montour Counties, Chicago, J. H. Beers and Co., 1260 p.
- Binder, F. M. (1974), Coal age empire, Harrisburg, Pennsylvania Historical and Museum Commission, 184 p.
- Brower, D. H. B. (1881), Danville, Montour County, Pennsylvania, Harrisburg, Lane S. Hart, Printer, 288 p.
- Diehl, F. W. (1969), A history of Montour County, Pennsylvania, Berwick, Keystone Publishing Co., 450 p.
- Inners, J. D. (1981), Geology and mineral resources of the Bloomsburg and Mifflinville quadrangles and part of the Catawissa quadrangle, Columbia County, Pennsylvania, Pennsylvania Geological Survey, 4th ser., Atlas 164cd, 152 p.
- Lesley, J. P. (1892), Upper Silurian and Devonian, Pennsylvania Geological Survey, 2nd ser., Summary Final Report, v. 2, p. 721-1628.
- Mensch, L. F. (1977), Danville: 1887-1891, Columbia County Historical Society, Historical Leaflet Series, v. 4, no. 3, 20 p.
- O'Connor, J. C., and Yeager, R. M. (1980), Pennsylvania prints, University Park, Pa., Museum of Art, The Pennsylvania State University.
- Rogers, H. D. (1858), The geology of Pennsylvania, a government survey, Pennsylvania Geological Survey, 1st. ser., v. 1, 586 p.
- Stoek, H. H. (1892), Notes on the iron-ores of Danville, Pennsylvania, with a description of the long-wall method of mining used in working them, Transaction of the American Institute of Mining Engineers, v. 20, p. 369-385.
- White, I. C. (1883), Geology of the Susquehanna River region in the six counties of Wyoming, Lackawanna, Luzerne, Columbia, Montour, and Northumberland, Pennsylvania Geological Survey, 2nd ser., Report G7, 464 p.
- Williams, J. H. (1980), The hydrogeology of the Danville area, Pennsylvania, unpublished MS thesis, The Pennsylvania State University, 251 p.
- Wright, W. B., Guild, P. W., Fish, G. E., Jr., and Sweeney, J. W. (1968), Iron and steel, in Mineral resources of the Appalachian region, U.S. Geological Survey Professional Paper 580, p. 396-416.

AMBIENT TEMPERATURES DURING THE ALLEGHANY OROGENY

by

Richard P. Nickelsen

Introduction

Data from several sources indicate that the Anthracite Region experienced temperatures during diagenesis and Alleghanian Deformation that were higher than those for the same structural position along strike to the southwest. At the southwestern border of the Anthracite Region along the Susquehanna River near STOP IV the paleo-isotherms trend NW - SE across the strike of Valley and Ridge folds. There are implications for structural geology in this observation. Should a gradual change in structural features, particularly those related to recrystallization and growth of new fabrics, appear northeastward from the Susquehanna River? Was the apparently higher temperature to the northeast a consequence of a greater paleo-geothermal gradient or a deeper burial? If geothermal gradients were normal, thus requiring a thick section and deeper burial of the Anthracite Region, was that section of sedimentary or tectonic origin? Is it possible to relatively date the higher temperature by careful application of techniques of paleo-temperature analysis in conjunction with the sequence of structural stages of the Alleghany Orogeny? These and other questions may be addressed more thoroughly when the evidence for Alleghanian paleo-temperatures has been assembled.

Sources of Paleo-Temperature Data

The trend of paleo-isotherms is best documented regionally by CAI data on the color alteration of conodonts (Harris, Harris, and Epstein, 1978) but is also suggested by coal rank contours and a few preliminary data from Temperatures of Homogenization (T_h) of fluid inclusions. Correlation of paleo-temperature data from the various sources requires comparison between different geographic areas and stratigraphic horizons that were buried to different depths. For example, CAI data is available only from conodonts collected in Silurian and Devonian limestones around the periphery of the Anthracite Region, whereas coal-rank data is restricted to Pennsylvanian rocks. Fluid-inclusion data is available at most outcrops containing veins but in most cases must be corrected for ambient pressures at the time of filling of fluid inclusions. Pressure corrections are based upon the inferred overlying stratigraphic column at the time of the Alleghany Orogeny but either hydrostatic (increasing at 100 bars/km), lithostatic (increasing at 250 bars/km) or some intermediate pressure may be assumed. At depths greater than 3 km hydrostatic pressure (P_p) begins to approach lithostatic pressure (P_c) (Hanor, 1979, p. 145) so our pressure corrections have ranged from the mean of $P_c + P_p$ to $.9 \times P_c$. Despite these geographic and stratigraphic gaps and the assumptions necessary, there is reasonably good agreement between temperatures estimated by different techniques.

COAL RANK

The accompanying article by Jeffrey R. Levine summarizes the evidence from coal-rank and vitrinite reflectance regarding the former heating temperature of anthracite coals. His evidence suggests a temperature of 185°C in the Western Middle Field near STOP III.

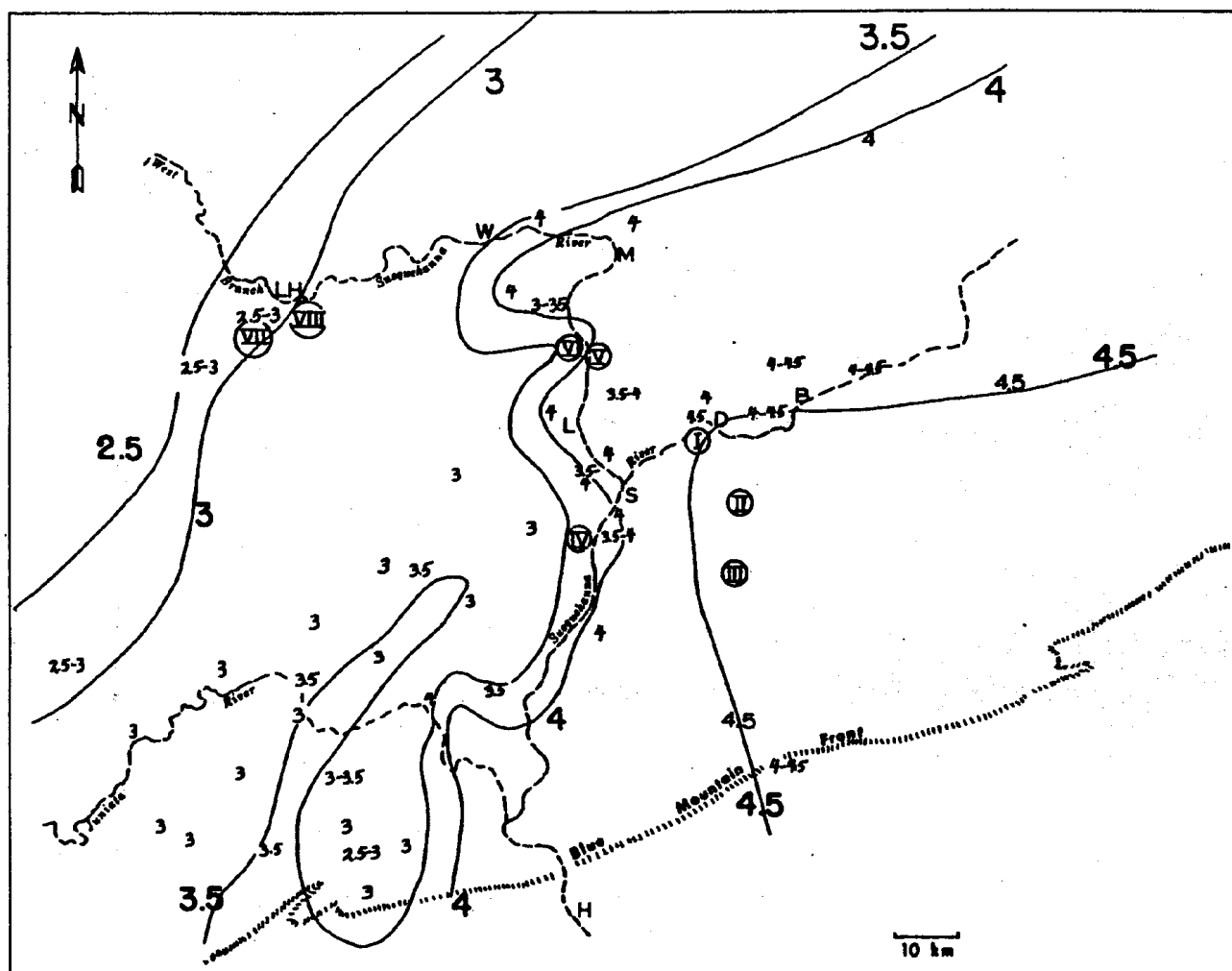


Figure 23 CAI - conodont isograds in field conference region.
 Source: Harris, et al 1978, CAI Isograd map for Silurian through Middle Devonian and personal communication, A. Harris, 1981

I - VIII = Field trip stops; D = Danville; B = Bloomsburg; L = Lewisburg;
 LH = Lock Haven; W = Williamsport; M = Muncy; S = Sunbury; H = Harrisburg

CAI - CONODONTS

Color alterations of conodonts due to heating during geologic intervals of time have been shown to correlate well with experimental color alterations and other field data (Epstein, Epstein, and Harris, 1977). A portion of the CAI isograd map for Silurian through Middle Devonian carbonates has been enlarged and reproduced in Figure 23 to show the temperature anomaly in the Anthracite Region (Harris, Harris, and Epstein, 1978). CAI observations from localities in the field-trip area were provided by A. Harris (personal communication, 1981) and were plotted on Figure 23. Color alteration of conodonts is affected by depth (temperature) and duration of burial so CAI index values can only indicate a range of possible paleo-temperatures which might have produced the color alteration. The CAI isograd of 4 which runs NW - SE along the Susquehanna River through the field-trip area is interpreted to indicate a paleo-temperature of 190 to 300°C. Temperatures were higher to the east and northeast, lower to the west and southwest. The estimated temperature ranges of other CAI isograds in the region are given in the following table:

CAI Estimated Temperature

2 60-140°C
3 110-200°C

CAI Estimated Temperature

4 190-300°C
5 300-400°C

Because of long heating times temperatures below the middle of the range for each CAI index are most likely.

FLUID-INCLUSION TEMPERATURES OF HOMOGENIZATION

Fluid inclusions provide an opportunity to estimate the temperatures of emplacement and sample the compositions of precipitating fluids in veins of the region. On many of the field-trip stops, we can demonstrate proof that veins were emplaced during one or more stages of the Alleghany Orogeny, thus making it feasible to estimate ambient temperatures during the orogeny. Recently techniques for estimating ambient pressures have been developed, using fluid inclusions filled with methane or mixtures of methane, carbon dioxide and other hydrocarbons (personal communication, Orkan and Voight, 1983). Their method is an extension of the work of Mullis (1979) in Switzerland, evaluated by Crawford (1981, p. 170).

The results of fluid-inclusion studies by students at Bucknell have been described for STOP I, STOP II and STOP VI and compared with CAI conodont information. Fluid-inclusion data from Orkan and Voight and coal-rank data from Levine have been described and compared in the description of STOP III.

The most consistent and complete fluid-inclusion information was collected by Bajak (1981, and unpublished manuscript) from fluorite in calcite-dolomite veins of three quarries in the Lower Devonian Keyser Limestone at the southwestern border of the Anthracite Region. Her T_h measurements were from veins formed during structural stages II through V of the Alleghany Orogeny. No trend of changing T_h was noted. The CAI conodont color index has been determined from all three quarries (A. Harris, personal communication, 1981). Briefly, T_h for 285 aqueous inclusions ranged from 67° to 109°C and Freezing Temperatures (T_f) ranged between -23.8°C and -17.7°C. Assuming an overlying stratigraphic column 7.7 km and pressure correction ranging from 1.3 kb to 1.7 kb the Temperature of Filling (T_{ff}) of these fluid inclusions was estimated to range from 192°C to 260°C. The CAI index for the three quarries was 3 to 4 suggesting temperatures of heating of 110 to 300°C, in fairly good agreement with the fluid-inclusion data.

Conclusions

There is general agreement between estimates of Alleghanian paleo-temperatures from three different sources: coal rank, conodont-alteration colors, and fluid-inclusion Temperatures of Homogenization. Some of the preliminary results have been described under STOPS I, II, III, and VI. Fluid-inclusion temperatures can be determined for minerals that filled veins during different stages of the Alleghany Orogeny. Our information to date from the best documented studies (Bajak, 1981 and Lilly, 1982, STOP VI) does not show a pattern of changing temperatures throughout the stages of the Alleghany Orogeny. Orkan and Voight (personal communication, 1983), on the other hand, have detected a progressive increase of temperature with stage of the Alleghany deformation at STOP III.

The coal-rank temperature estimate for the western part of the Western Middle Anthracite Field was approximately 185°C, close to the fluid-inclusion estimate of 205°C at the same locality. Despite the inferred increase in temperature northeastward from the Susquehanna River, these temperatures are lower than fluid-inclusion and CAI - conodont temperatures in Siluro-Devonian rocks to the southwest. This is because they were determined from Pennsylvanian-age surface rocks, approximately 6 km higher in the stratigraphic column. The higher temperatures that we should expect in Devonian rocks under the Anthracite Region are perhaps suggested by the preliminary data of Temperatures of Homogenization from STOP II.

COAL RANK PATTERNS IN THE PENNSYLVANIA ANTHRACITE REGION

by

Jeffrey R. Levine

Organic sediments are sensitive indicators of the diagenetic conditions which existed during their burial and deformation history. For this reason organic maturation studies are being used with increasing frequency to study the tectonic and thermal histories of sedimentary basins. Coal "rank" is determined empirically on the basis of a variety of physical properties. Of particular concern to the present discussion are fixed carbon,¹ volatile matter¹, and vitrinite reflectance² (Ro, average).

Coal rank increases primarily as a function of temperature and time during organic metamorphism [Linear increases in temperature produce an exponential increase in rank whereas increasing exposure time has an approximately linear effect]. Thus, the final rank attained by a coal represents a summation of the thermal history of the coal-bearing rocks. In flat-lying sedimentary rocks, coal rank increases with depth (Hilt's Rule), on account of the increasing temperatures with depth. In the Pennsylvania Anthracite fields, however, any such simple relationships have been disrupted by structural deformation. It has been suggested that "tectonic pressure" may also have been an important influence on the coal rank in the Anthracite region (White, 1925, Turner, 1934; Wood, et al., 1969) but all available evidence indicates that if pressure had any effect at all, it would be very slight (see M. & R. Teichmuller, 1981; Damberger, 1974). Therefore, assuming that all the coals in the region were subjected to elevated temperatures for approximately the same period of time (i.e., the "burial histories" are similar) then any variation in rank must be attributed solely to differences in their former maximum temperatures of heating.

Coal rank variations are observable on several different scales in the Pennsylvania Anthracite region, including the following: 1. Regionally, the outcropping coals indicate a west to east increase in rank. The isorank lines (Figure 24) intersect the structural trend of the basin transversely. 2. A more detailed appraisal of the coal rank patterns indicates that in the Western Middle Anthracite and Southern Anthracite fields, the outcropping coals exhibit higher ranks along the centers of the basins than along the adjacent limbs (Figure 25 a&b) (Wood et al., 1969, Arndt, unpublished; and Levine, 1983). This trend is the opposite of what one would expect in synclinal basins such as these. 3. At localities where it is possible to measure rank variations in an uninterrupted stratigraphic sequence, the stratigraphically lower coals always exhibit the higher ranks (Figures 26 a,b). In the following discussions these coal rank patterns will be evaluated regarding their implications for the tectonic and structural evolution of the Anthracite region.

¹ As determined in "proximate analysis", the total weight of any coal is comprised of four components, fixed carbon, volatile matter, ash, and moisture, each expressed as a weight percent. On a "dry, ash-free" basis (d.a.f.), fixed carbon and volatile matter comprise 100% of the total weight. Thus, volatile matter (d.a.f.) = 100%-fixed carbon (d.a.f.). Fixed carbon increases with rank; volatile matter decreases.

² Reflectance (Ro%) pertains to the percentage of vertically incident light reflected from a highly polished surface of coal in an oil immersion medium. This ranges from less than 0.5% to 2.0% in bituminous coals and can exceed 6% in anthracite.

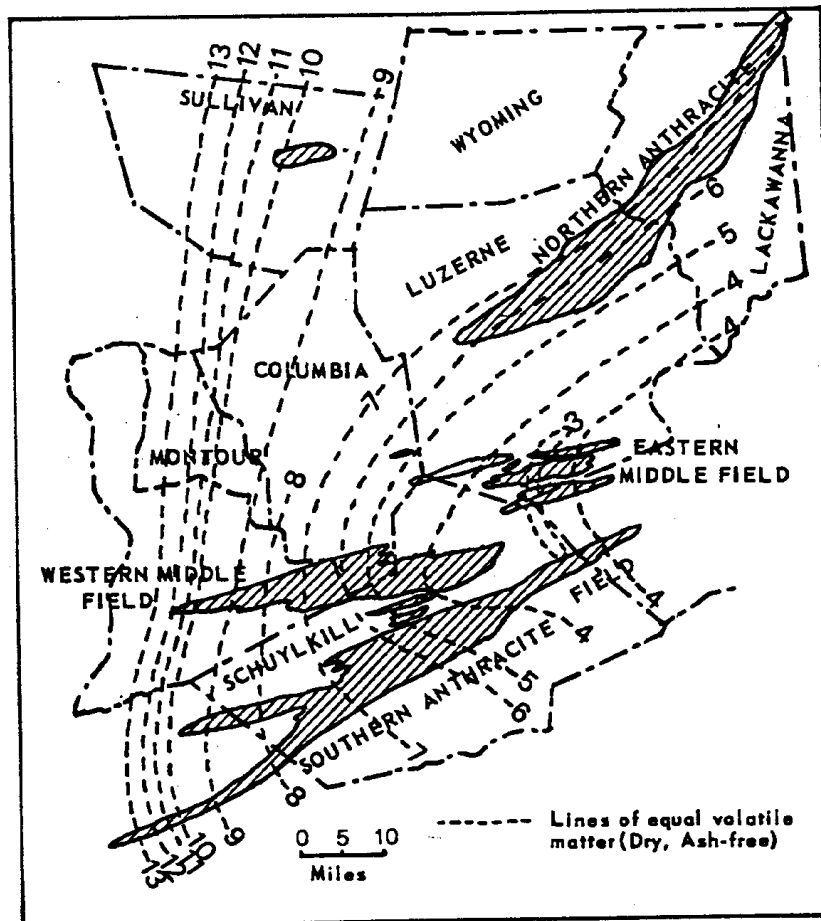
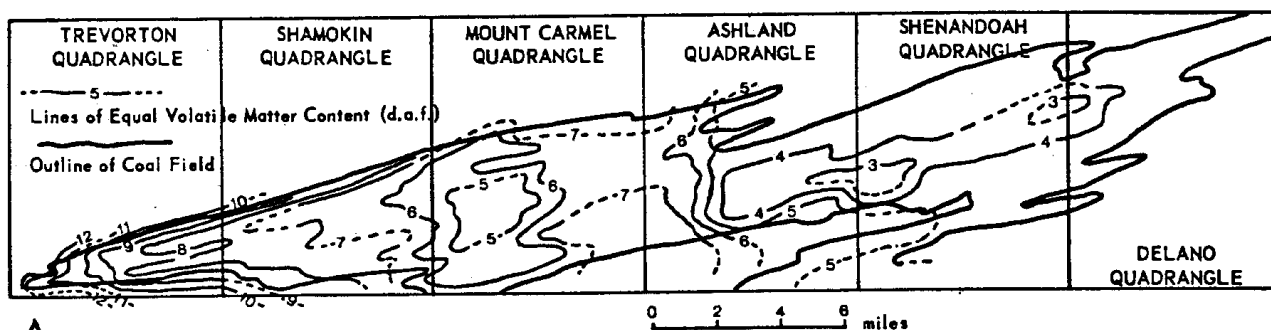
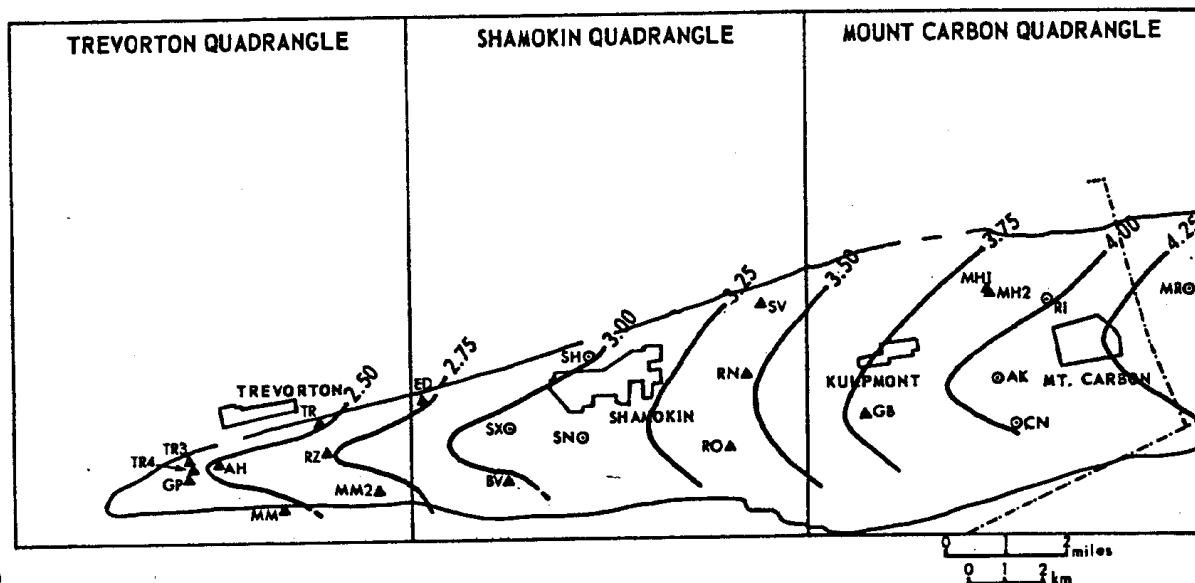


Figure 24 Regional coal rank variations in the Pennsylvania anthracite region. The dashed lines (volatile matter, d.a.f.) depict the west-to-east increase in coal rank. This is interpreted as being a consequence of increasing overburden toward the east.

Let us first consider the regional west-to-east increase in coal rank (Figure 24). By employing empirical and theoretical models of coalification it is possible to estimate the former maximum heating temperatures of these coals (see Hood, et al., 1975; Waples, 1980). These procedures entail a number of assumptions, but they suggest that temperatures in the western end of the Western Middle field approached 185°C (based on R_o avg. 2.5%; Figure 25b). In the eastern end of the Southern field, the temperatures probably exceeded 240°C (based on volatile matter (d.a.f.) <4%). This suggests a minimum temperature difference of 55°C. Inasmuch as the coals are currently exposed at the same erosional level, there are potentially two ways to explain this difference: 1. the coals were formerly buried at the same depth below the surface and the higher temperatures in the east were a consequence of a higher geothermal gradient, or 2. the geothermal gradient was constant across the area and the higher temperatures in the east were a consequence of greater depth of burial. Most of the available evidence indicates that the latter is the correct explanation. For example, Paxton (1983) has shown that the northwest to southeast increase in bulk density and decrease in porosity of Carboniferous sandstones in eastern Pennsylvania are best explained by increasing depths of burial toward the southeast. The depth estimates proposed by Paxton (3 to 4 km on the eastern Allegheny Plateau, increasing to over 8 km in the Anthracite region) are sufficient to explain the coal rank variations, assuming a constant, normal geothermal gradient. Several lines of evidence do, in fact, suggest that the geothermal gradient was normal in this region. For example, in the Parker bore holes, a pair of vertical drill holes



A.



B.

Figure 25 Coal rank contours from the Western Middle Anthracite field. a) the volatile matter content of the coals (d.a.f.) is lower at the center of the basin than along the basin margins indicating higher ranks (H. Arndt, unpublished), b) the mean vitrinite reflectance of coals also indicates higher ranks at the center of the western end of the basin. In detail, the rank patterns would be much more complex, showing the influence of local structural features. There is insufficient data available, however, for any greater accuracy (Levine, 1983).

situated near Minersville, Pa., in the Southern Anthracite field, the coal rank gradient with depth has been used to estimate the paleogeothermal gradient (see Figure 26). This result ($33^{\circ}\text{C}/\text{km}$) is "normal" for this type of tectonic setting and is similar to estimates of paleogeothermal gradients from the bituminous coal fields of the Allegheny Plateau (Hower and Davis, 1981). Using the gradient, along with the previous temperature estimates, the estimated former depth of burial are close to those derived by Paxton. The fluid inclusion data discussed elsewhere in this guide will also corroborate these estimates.

Superimposed on the regional west-to-east increase in rank are a number of complexities, which developed in consequence of the Alleghanian structural deformation. One such complexity is exemplified at the Pioneer Mine, a 1200 foot long horizontal tunnel which intersects an unbroken sequence of steeply-dipping and coal-bearing strata along the southern margin of the Western Middle field. The coals exposed along the length of the tunnel were formerly vertically disposed to one another but are now at the

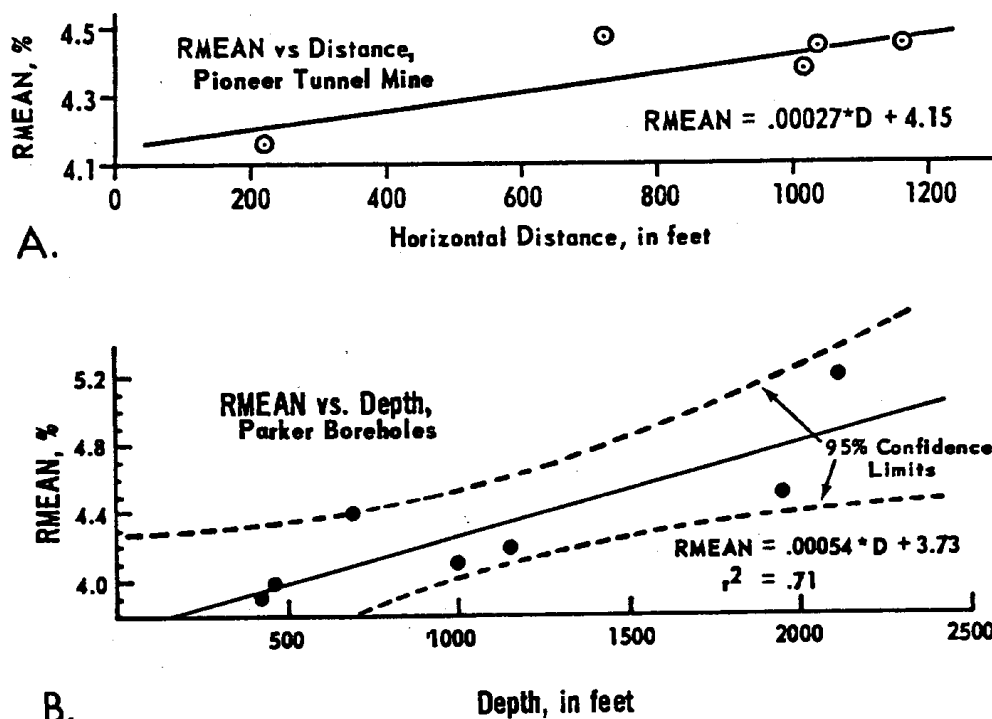


Figure 26 Local coalification gradients from unbroken stratigraphic sequences. (a) with increasing distance into the Pioneer Mine, stratigraphically lower coal seams are intersected. These indicate increasing rank with "stratigraphic depth." b) the mean reflectance increases with depth in coal seams intersected by the Parker bore holes.

same level. Nevertheless, they exhibit a slight increase in rank with "stratigraphic depth", presumably a relict of the prefolding rank gradient with depth. Hower (1978, p. 182) has reported two additional localities which indicate that the stratigraphically lower coals have higher ranks in unbroken sections. Thus, these data all show coal rank decreasing toward the center of the basin, as would be expected in a synclinal fold. In contrast, the coalification trends expressed on Figure 24 indicate that the coals exposed in the center of the Western Middle field synclinorium have higher ranks than those along the adjacent margins (comparing coals from approximately the same stratigraphic interval). Thus, some discontinuities or reversals must exist in the rank patterns of the Western Middle ifield. It is possible to resolve this apparent inconsistency by invoking two structural mechanisms: 1. relative uplift of strata in the center of the basin along "high-angle reverse faults", and 2. flexural upwarping of strata in the center of the basin along the axes of 2nd-order anticlines. Both of these mechanisms have served to uplift "hotter", more deeply-buried coals in the center of the basin with respect to the margins. This, coupled with the pre-existing increase in coal rank with depth has produced a discontinuous, disrupted rank pattern which is, in reality, much more complex than those depicted in Figure 25.

High-angle reverse faults are ubiquitous throughout the Anthracite basin (Figure 27), excluding, perhaps, the northeastern end of the Northern field. Based upon mapping by U.S.G.S. geologists, the following features characterize these faults: 1. they dip toward the center of the basin at about 15-20° steeper than bedding, 2. for the most part, they appear to be confined to the coal-bearing Llewellyn Fm., being rooted in bedding plane faults at depth, 3. they are frequently associated with thick ductile coal horizons, especially the Mammoth Zone, 4. they occur with roughly equal frequency on the northwestern limb of the basin (i.e. SE-dipping; "synthetic" direction) and on the

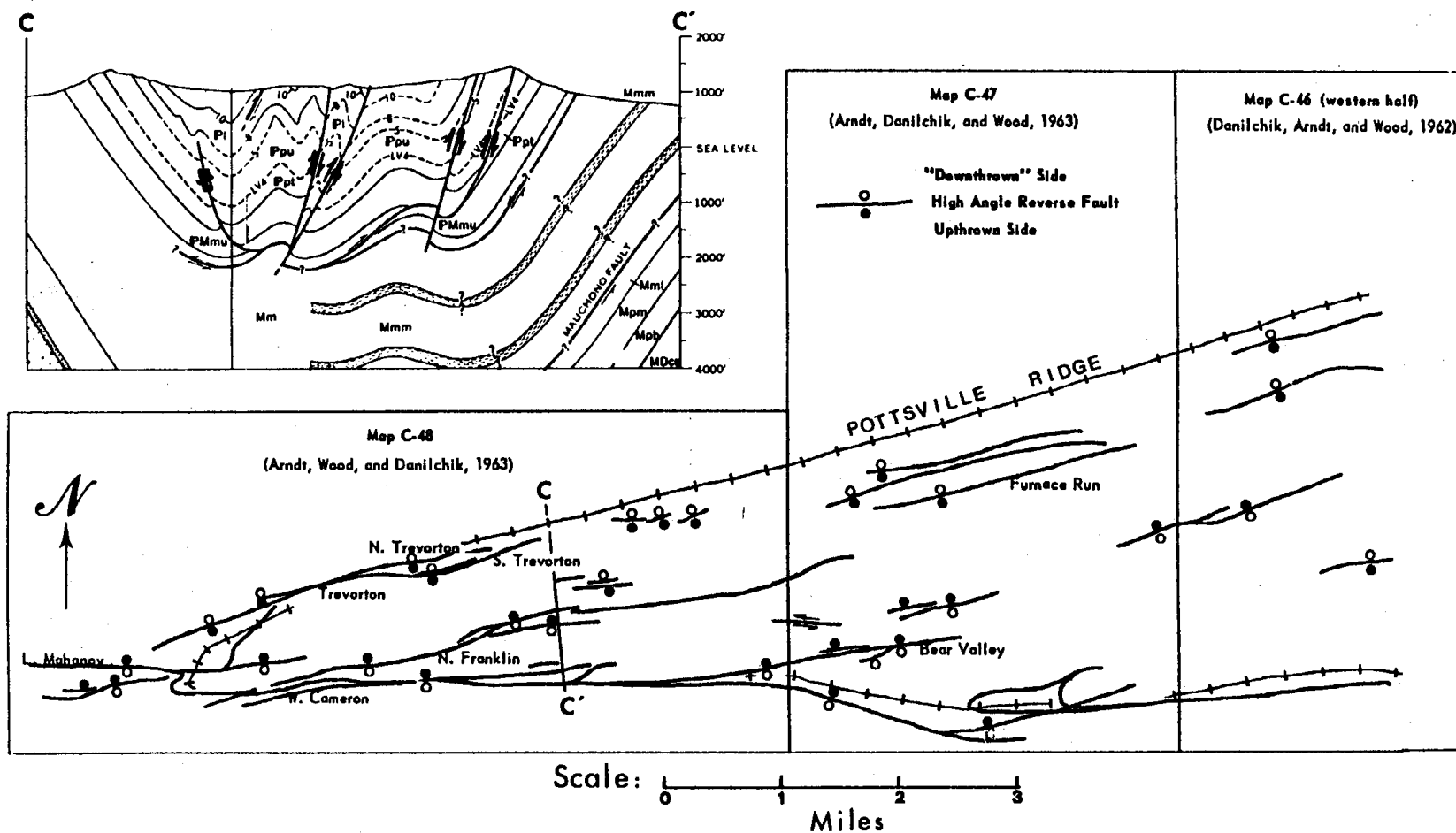


Figure 27 High angle reverse faults in the western end of the Western Middle Field. In plan view, the fault traces lie parallel to the structural grain of the basin. In most cases the upthrown side is the one toward the center of the basin. Relative uplift of strata along the basin axis is illustrated in the cross section from Arndt et al (1973).

southeastern limb (i.e. NW-dipping; "antithetic" direction) (see Figure 27), 5. the fault planes are often associated with "shear-type" folds which indicate the same sense of motion as the faults themselves.

The fault planes of these high-angle reverse faults initially develop early in the progressive structural evolution of these basins as indicated by cross sections through the Northern Anthracite field (Darton, 1940; Bergin, 1976). They continue to grow and evolve, however, during subsequent closure of the basins, partially to satisfy the "space problems" in the core zones of the chevron-shaped Anthracite-basin folds. During the development of a chevron fold, there is considerable thickening of material of the hinge zone (Ramsay, 1974; Levine, 1983). In a layered sequence, such as the Carboniferous section in the Anthracite region, much of the concomitant deformation is concentrated in the incompetent layers (i.e., the coal-bearing Llewellyn Fm. rather than the underlying rigid Pottsville Group sandstones). Once the dip angle on the basin limbs exceeds 45° , this effectively produces a net uplift of the "core zone" of the folds with respect to the margins (Levine and Davis, 1982; Levine, 1983). In the Western Middle fields, where the limb dips typically range from 50° to 75° , much of this uplift is hypothesized to have occurred along the high-angle reverse faults.

An excellent example of a high-angle reverse fault is provided by the Bear Valley fault (Figure 27) which extends for several kilometers westward from the Bear Valley mine (Stop III). Within the mine itself, the fault disappears into a complex of 3rd-order folds but to the west, the northern side of the fault has been uplifted 300-400 ft. (90-120 m) relative to the southern side (Arndt et al., 1963). In the area of the Bear Valley mine, the coals exposed at the center of the basin have reflectances approximately 15% higher than those along the margins. An offset of 90-120 m is conceivably sufficient to produce the observed "inversion" of the coalification gradient, depending on the timing of uplift with respect to coalification. Certainly, if accompanied by motion along other high-angle reverse faults, as well as by upward flexure of 2nd-order anticlines, the observed increase in coal rank at the center of the basin could easily be produced.

References Cited

- Arndt, H.H., Danilchik, W. and Wood, G.H., Jr., 1963, Geology of anthracite in the western part of the Shamokin quadrangle, Northumberland County, Pennsylvania: U.S. Geol. Survey Coal Inv. Map C-47.
- Arndt, H.H., Wood, G.H., Jr., and Danilchik, W., 1963, Geology of anthracite in the southern part of the Trevorton quadrangle, Northumberland County, Pennsylvania: U.S. Geol. Survey Coal Inv. Map C-48.
- Bergin, M.J., 1976, Bedrock geologic map of the anthracite-bearing rocks in the Wilkes-Barre West Quadrangle, Luzerne County, Pennsylvania: U.S. Geological Survey Misc. Inv. Map I-838.
- Damberger, H.H., 1974, Coalification patterns of Pennsylvania coal basins of the eastern United States: Geological Society of America Special Publication 153, p. 53-74.
- Danilchik, W., Arndt, H.H. and Wood, G.H., Jr., 1962, Geology of the anthracite in the eastern part of the Shamokin quadrangle, Northumberland County, Pennsylvania: U.S. Geol. Survey Coal Inv. Map C-46.
- Darton, N.H., 1940, Some structural features of the Northern Anthracite coal basin, Pennsylvania: U.S. Geol. Survey Prof. Paper 193-D, p. 69-81.

Hood, A., Gutjahr, C.C.M. and Heacock, R.L., 1975, Organic metamorphisms and the generation of petroleum: American Association of Petroleum Geologists Bulletin, v. 59, n. 6, p. 986-996.

Hower, J.C., 1978, Anisotropy of vitrinite reflectance in relation to coal metamorphism for selected United States coals [Ph.D. Thesis]: The Pennsylvania State University, University Park, PA, 339 p.

Hower, J.C. and Davis, A., 1981, Application of vitrinite reflectance anisotropy in the evaluation of coal metamorphism: Geological Society of America Bulletin, pt. I, v. 92, p. 350-366.

Levine, J.R., 1983, Tectonic history of coal-bearing sediments in eastern Pennsylvania using coal reflectance anisotropy (Ph.D. Thesis): The Pennsylvania State University, University Park, PA, 314 p.

Levine, J.R. and Davis, A., 1982, Structural evolution of the Western Middle Field Synclinorium, Pennsylvania, using coal reflectance: Geological Society of America Abstracts with Programs, v. 14, p. 546.

Paxton, S.T., 1983, Relationships between Pennsylvania age lithic sandstone and mudrock diagenesis and coal rank in the Central Appalachians [Ph.D. Thesis]: The Pennsylvania State University, University Park, PA, 503 p.

Ramsay, J.G., 1974, Development of chevron folds: Geological Society of America Bulletin, v. 85, p. 1741-1754.

Teichmüller, M. and Teichmüller, R., 1981, The significance of coalification studies to geology - a review, in *La Géologie des charbons, des schistes bitumineux et des kérogènes*: Bull. Centres Rech. Explor.-Prod. Elf-Aquitaine, F-64018, Parc, p. 491-534.

Turner, H.G., 1934, Anthracites and semi-anthracites of Pennsylvania: American Institute of Mining and Metallurgical Engineers Transactions, v. 108, p. 330-343.

Waples, D., 1980, Time and temperature in petroleum formation: application of Lopatin's method to petroleum exploration: American Association of Petroleum Geologists Bulletin, v. 64, n. 6, p. 916-926.

White, D., 1925, Progressive regional carbonization of coals: Transactions of the American Institute of Mining and Metallurgical Engineers, v. 71, p. 253-281.

Wood, G.H., Arndt, H.H. and Carter, M.D., 1969, Systematic jointing in the western part of the Anthracite region of eastern Pennsylvania; U.S. Geological Survey Bulletin 1271-D, 17 p.

Wood, G.H., Jr., Trexler, J.P. Kehn, T.M., 1969, Geology of the west-central part of the Southern Anthracite field and adjoining areas, Pennsylvania: U.S. Geol. Survey Prof. Paper 602, 150 p.

The Tioga Ash Beds at Selinsgrove Junction

by

Robert C. Smith and John H. Way

Pennsylvania Geological Survey

INTRODUCTION

Homogeneous and distinct lithic material deposited over a large geographic area in a brief period of geologic time may produce a stratigraphic unit that becomes a useful key bed for interpreting and correlating sequences within that area. One such time-rock, or chronostratigraphic, unit is the ash bed or tuff consisting of fine, pyroclastic debris ejected from an erupting volcano. Altered and compacted volcanic ash layers within the stratigraphic record came to be known as bentonites, a name proposed by Knight (1898) for soap-like clays found in the Benton Shale, a Cretaceous deposit in eastern Wyoming. True bentonites have several unique physical and chemical properties, among which are their unusual absorbent and swelling capacity, up to 8 times their original size, and their ability to behave thixotropically. Because of these characteristics, ascribed to the expandable-lattice, clay-mineral group smectite, bentonites have become important industrial minerals, primarily used to thicken oil-well-drilling muds.

Several ash-bed horizons occur within the Paleozoic strata of the eastern United States and Canada and there remains the possibility of identifying even more. The altered ash beds consist largely of mica and chlorite, with only minor smectite, and as such, do not possess the properties of a bentonite (Roen and Hosterman, 1982, p. 922). They do, nevertheless, serve as important stratigraphic marker beds. The oldest ash beds have been reported in Ordovician formations from Alabama to Ontario. At least 16 stratigraphically separate beds have been identified from the Middle Ordovician Black River and Trenton Stages, from central Pennsylvania (Kay, 1944, p. 2; Weaver, 1953; Thompson, 1963). Three ash beds are documented from the Devonian. The lowest, the Tioga, is Middle Devonian, post-Onondaga. The Belpre of eastern Ohio (Collins, 1979) and the Center Hill of Tennessee (Conant and Swanson, 1961), considered correlative with each other by Collins (1979, p. 656), are Upper Devonian, post-Tully, in age. A bed of kaolinitic mudstone, referred to as a tonstein and thought to be an ash bed by Spears (1970), was reported from the Carboniferous British coal measures. In Pennsylvania, at least two extensive and pervasive, thin clay partings exist within the Pittsburgh coal (Ashley, 1928, p. 103) from the western portion of the state. These seem to be possible candidates for Pennsylvanian ash beds in North America. No diagnostic heavy minerals were found in the sample collected from one of these partings; however it does contain well-crystallized kaolinite (Pa. Survey X-ray diffraction scan D83-7) which, according to Bruce Bohor (1982), is a characteristic of ash in coal. Thus, it is likely that several partings within the Mississippian and Pennsylvanian sequences in the Appalachian Basin could be derived from pyroclastic ash falls.

Of particular interest in connection with this year's field conference are the Tioga ash beds which are so well-exposed at Stop 4, Selinsgrove Junction. These beds have been found throughout an area stretching from central New York to western Virginia and from eastern Pennsylvania to central Ohio. In addition, the Tioga has been correlated with ash beds in the Michigan and Illinois basins (Baltrusaitis, 1974; Meents and Swann, 1965) and with beds in southern Ontario (Sanford, 1967, p. 987) giving it broad regional significance and suggesting that it represents a major volcanic episode during the Middle Devonian.

PREVIOUS WORK

In 1931, C. R. Fettke published his interpretations of cuttings from deep wells drilled within the Tioga Gas Field beneath the Sabinsville anticline, Tioga County, north-central Pennsylvania. He noted the presence of "particles of brown shale which . . . are easily recognized if the cuttings are examined under water in a watchglass" in association with the Onondaga Formation (Fettke, 1931, p. 8). Later, he reported observing a "thin but persistent seam of brown micaceous shale with abundant pyrite" in drill cuttings from the Summit Gas Pool, Fayette County, in the southwestern part of the state (Fettke, 1940, p. 17). By the late 1940's, the Tioga "bentonite"* had been recognized in drill-cutting samples from the Oriskany Sand gas fields from south-central New York to northern West Virginia and was considered an "excellent marker in the Middle Devonian series" (Ebright, Fettke, and Ingram, 1949, p. 10).

A thin "meta-bentonite" bed, not more than a few inches thick, described by Flowers (1952, p. 2036) from the subsurface of West Virginia was considered by Fettke (1952) to be equivalent to his Tioga "bentonite," in that samples from both areas had a greasy luster and commonly contained euhedral biotite mica and exceptionally large amounts of finely disseminated pyrite. He further agreed with Flowers that only one layer was present and that it occurred at or near the boundary between the Hamilton Group and the Onondaga Formation (Fettke, 1952, p. 2039).

Citing Fettke's work in Pennsylvania, Oliver (1954, p. 629) correlated the Tioga with a "remarkably uniform bed of clay 6 inches thick" which occurs at the base of the Seneca Limestone, the upper member of the Onondaga Formation in New York. He also noted that this clay bed was recognized by James Hall (1843, p. 163) in the Waterloo area of central New York and that a volcanic origin was proposed for a "soft layer" at approximately the same horizon by Luther (1894, p. 240) working in salt-mine shafts farther to the west. Oliver also suggested that the Tioga "bentonite" represented an important paleontological break (1954, p. 621), and that the ash fall hastened a westward shift in fauna assemblages (1956, p. 1473).

The usefulness of the Tioga horizon in interpreting stratigraphic sequences at the surface was successfully demonstrated by J. M. Dennison who has identified and mapped this unit throughout the Appalachian basin. He first reported the Tioga "metabentonite" in outcrop in his comprehensive work on the Onesquethaw stage in West Virginia (Dennison, 1961). Included within this report, and of great interest to this discussion, is an isopachous map based on thickness of outcrop and subsurface data for the Tioga (Dennison, 1961, p. 37). Dennison's conclusion was "that the source volcano probably was located several miles southeast of the position of Lexington or Staunton [in the Piedmont of central] Virginia" (1961, p. 39) or about 400 km (250 mi) south-southwest of Selinsgrove Junction. (In the 37th Pa. Field Conference Guidebook (Dennison, deWitt, Jr., Hasson, and others, 1972, p. 56) he moved the source northeast, about 50 km, closer to Charlottesville, and more recently Dennison and Textoris (1978, p. 171), located the volcanic center in northeastern Virginia in the latitude of Fredericksburg). Several papers by Dennison and Textoris (1967, 1970, 1971, 1978; Textoris and Dennison, 1970) contain more details of the Tioga "Bentonite" stratigraphy and present data on its petrology.

* quotes placed around term used by cited author

In a recent paper by Roen and Hosterman (1982), the problem of nomenclature is addressed. They present X-ray data of the clay mineralogy for the three recognized Devonian ash units, the Tioga, Belpre, and Center Hill, and compare them with a bentonite sample from Wyoming. It is their contention that "the name 'bentonite' has been incorrectly applied [to the Devonian units] because smectite is not the major component (1982, p. 922). Instead, they propose the term "ash" in the names of these "and all other beds formed from volcanic ash that are not principally smectite" (1982, p. 922). Huff (1983) challenges this proposed terminology and presumably this duel will continue for some time to come.

STRATIGRAPHIC INTERVAL

Regional Generalizations

Debris from the Middle Devonian volcanic eruptions responsible for the Tioga ash beds probably spread over much of the northeastern United States, portions of the northern midwest, and, to some degree, southeastern Canada. The Tioga ash beds are best known from exposed sequences in Virginia, West Virginia, and Pennsylvania, and to a lesser degree in New York, Ohio, and Kentucky. Ash beds have been identified in the subsurface in those states as well as Indiana and Illinois. Correlation with similar horizons in Michigan and southern Ontario suggest the broad extent of this volcanic influence.

In northern Virginia, near the source, Dennison (1982, p. 130) reports that beds of pyroclastic material are found deposited throughout a 62-m-(103-ft.-) thick section of strata, his maximum thickness figure. Thicknesses rapidly decrease to the north and west. Along the Virginia - West Virginia border the interval is between 3.0 and 9.1 m (10 and 30 ft), and in central West Virginia, it is 0.9 m (3 ft) or less (Dennison, 1978, p. 174). For Pennsylvania, he has recorded tuffaceous beds in 9.1 m (30 ft.) of the upper Needmore and lower Marcellus Formations (Dennison, 1982, p. 130). At Bellefonte, in Center County, the zone thins to a fine-grained single horizon 0.09 m (0.3 ft.) thick at the contact of the Selinsgrove and Marcellus Formations (Dennison and Textoris, 1978, p. 168).

Throughout the Valley and Ridge province of the state, one or more ash beds can usually be found near the base of the Marcellus Formation. In the north-central region, the Tioga was reported at the Onondaga-Marcellus contact in the subsurface. Farther to the west, however, near the McKean-Warren county line, the ash was found to be 9 m (30 ft.) below the top of the Onondaga Limestone (Fettke, 1952, p. 2040) indicating that the Onondaga-Marcellus contact is time transgressive, becoming younger to the west. A similar situation was recognized by Oliver (1954, 1956) in New York, again using the Tioga "bentonite" as a time plane. Still farther to the west, the Tioga "bentonite" has been identified in quarries in the Columbus area of central Ohio; however, it seldom is present in outcrop (Dennison, 1982, p. 130). Here the Tioga is at the contact of the Columbus and Delaware Limestones, some 14 m (45 ft.) below the base of the [Marcellus-equivalent] Devonian shales (Dennison, 1978, p. 168).

The Tioga and the Onesquethawan Stage

Based on his work in the late 1950's, Dennison recognized the importance of the Tioga as a time surface, and, in 1961, proposed that the top of the Tioga "metabentonite," or its equivalent stratigraphic position, be used to define the top of the Onesquethawan Stage (1961, p. 10). Later, this upper boundary was further refined to use "the top of the middle coarse zone" of the Tioga "Bentonite" (Dennison and Head, 1975, p. 1106). (The middle coarse zone, which consists of three or four tuff beds within an interval of approximately 0.6 m (2 ft.), is the principal marker horizon of the Tioga (Dennison and Textoris, 1978, p. 167).)

Overlying the Onesquethawan is the Cazenovian Stage. Rickard (1964) modified the base of the Cazenovian and defined the lower boundary as the top of the Tioga. Thus, in New York and northwestern Pennsylvania, the Seneca Member of the Onondaga Limestone, as well as the Marcellus Formation, are included within the Cazenovian Stage.

The Onesquethawan Stage includes the strata between the top of the Tioga and the top of the Oriskany Sandstone, or its correlatives, which marks the top of the underlying Deerparkian Stage. The Onesquethawan interval consists of a complex intertonguing of marine lithofacies, including limestones, cherts, mudstones, and siltstones. The Tioga ash beds are on top of, or interbedded with, the Onondaga Limestone, Needmore Formation, Selinsgrove Limestone, Moorehouse Limestone, and Buttermilk Falls Limestone in Pennsylvania (Inners, 1979; Epstein, Sevon, and Glaeser, 1974). The contact of the Onesquethawan Stage with the overlying Marcellus Formation is always conformable (Inners, 1979, p. 41) and ash beds are found interbedded with these dark-gray to black pyritic mudstones of the Marcellus as well. Exposures at Grazierville and Hollidaysburg, Blair County; West Bowmans, Carbon County; and Selinsgrove Junction, Northumberland County, among other places, demonstrate this interbedding very well.

Six Tioga Ash Beds at Selinsgrove Junction

Dennison recognized the Tioga "Metabentonite" a few feet below the top of the Selinsgrove Limestone, here at Selinsgrove Junction, early in his work on the Tioga (1963, p. 220). The Selinsgrove Limestone, considered a member of the Needmore Formation by Inners (1975, 1979), but included here as a member of the Onondaga Formation, consists of interbedded, fine-grained fossiliferous limestones and calcareous shales, with limestones constituting about 60% here in the Susquehanna Valley (Inners, 1975) (see Figs. 28, IV-5). Often the shales are fossiliferous and Inners (1975, Figure 110) includes a photomicrograph of crinoid stems and juvenile brachiopods within a "metabentonite" bed from this locality.

Here at Selinsgrove Junction, six individual ash beds occur within the Selinsgrove Limestone and the Marcellus Formations (Fig. 28). Because of the excellence of this exposure, the thinner ash beds could be measured and sampled. Unfortunately, most outcrops of this horizon exhibit faulting, folding, slumping, or an overgrowth of crown vetch. As discussed below, these thinner ash beds are distinctly different, chemically and mineralogically, from the enclosing mudstones and vary in several ways from the thicker ash beds as well. The number, thickness, and composition of the ash beds at each locality is therefore of significance and the thinner beds should be sought if exposures permit.

LABORATORY INVESTIGATIONS

Thin-Section Data

One thin section cut perpendicular to bedding was obtained for each of the six observed Tioga ash beds at Selinsgrove Junction. For the thin beds, A, C, and E, the entire thickness was examined. For the thicker beds, B, D, and F, only one coherent piece was examined per bed.

The observed ash beds consist of quartz shards, partly altered feldspar, and mica phenocrysts in a murky, mica-clay matrix. Pyrite is ubiquitous in beds A through E, whereas in bed F it is rare in some areas and has replaced the matrix in others. Trace

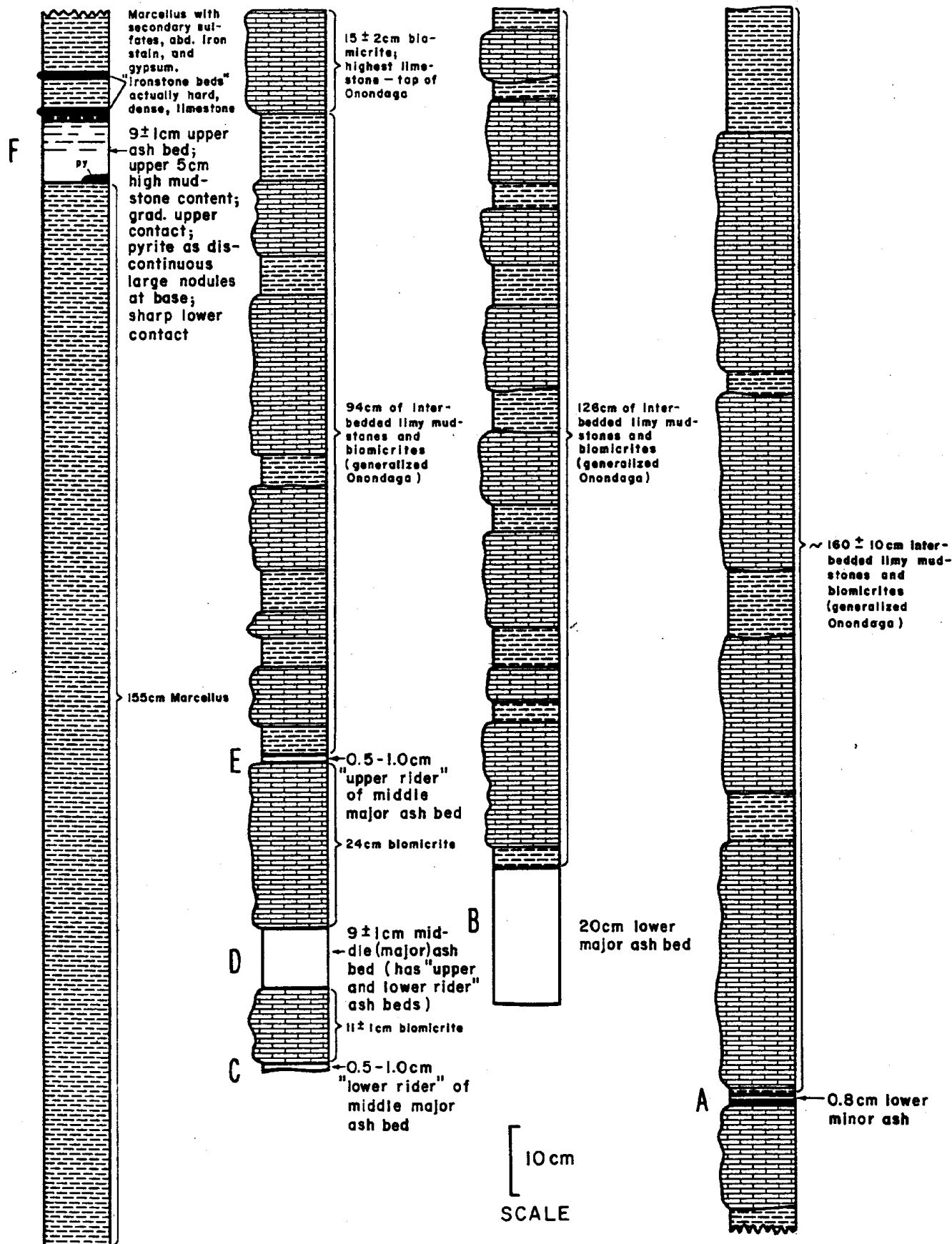


Figure 28 Measured stratigraphic section of the Tioga ash-bed zone within the Upper Onondaga and Lower Marcellus Formations, Selinsgrove Junction, Lower Augusta Township, Northumberland County, Pennsylvania (40°47'48"N, 76°50'34"W)

amounts of zircon with radiation halos and apatite occur in the thicker beds (B, D, and F). The sampled portions of the thicker beds tend to be medium-grained, whereas the thinner beds are fine-grained and tend to lack obvious zircon and apatite. Data for the individual beds are summarized in Table 2.

Most beds appear to be graded within one thin section with respect to size and abundance of phenocrysts. Such graded bedding likely reflects more rapid wetting of the phenocrysts. Further study is needed to determine if the thicker beds contain more than one graded cycle, i.e., volcanic event.

In addition to its bimodal pyrite abundance, bed F is distinct because it is very rich in euhedral phenocrysts and lacks a sharp upper contact. Above the 9 cm of sampled ash, at least another 5 cm of ash-rich rock appears to be present. Samples of bed F with the matrix replaced by pyrite contain less-altered biotite and feldspar phenocrysts. This tends to suggest that the pyrite "armor" was introduced early.

X-ray Diffractometer Data

Splits of the channel samples collected for chemical analyses were also examined by X-ray diffractometer scans. Relative amounts of the major and minor minerals were estimated from the diffraction intensity, using either peak heights or areas. Three scans of each sample were obtained using packed holders. One scan was of "raw" sample material, another was heated at 300°C for 1 hr., and the third was placed in an atmosphere of ethylene glycol for about 2½ days.

Major minerals observed include the smectite (= montmorillonite = "bentonite") group, chlorite group, mica group, and plagioclase-feldspar group. Pyrite is consistently present in minor but variable amounts. Quartz varies from not detected (ash bed C) to minor amounts and "kaolinite" from not detected to trace amounts. Minor amounts of a regular mixed-layer clay mineral may be present.

Minerals formed by secondary alteration include gypsum (trace to major), calcite (mostly trace) and aragonite (one sample).

Data for the individual ash beds are summarized in Tables 3, 4, and 5. Notable observations include the large amounts of "plagioclase" in ash beds B and F and the presence of minor quartz in beds B, D, and F. Unlike the thicker ash beds or normal shaly partings, the thin ash beds (A, C, and E) are nearly quartz free.

The relative abundance of chlorite was estimated from the 14Å peak height of samples heated to 300°C for 1 hr. to collapse any smectite which might interfere (Table 4, column 2). No systematic variation in chlorite was observed.

Mica peaks are relatively sharp. The relative abundance of mica was estimated from the 10.1Å peak of samples glycolated for 2½ days to expand any smectite which might interfere (Table 5, column 8). No systematic variation in chlorite or mica was observed.

Attempts to estimate the relative abundance of smectite were largely unsuccessful. The first and second consisted of estimates of the area between the 10Å mica and 14Å chlorite peaks for untreated and glycolated samples (Table 5, columns 5 and 6, respectively). The third consisted of a subtraction of a mica peak from a mica plus smectite peak (Table 5, column 10). From these conflicting data it is possible to conclude only that the six observed Tioga ash samples each contain minor to major amounts of smectite.

<u>Sample</u>	<u>Relative Grain Size</u>	<u>Bedding</u>	<u>Quartz</u>	<u>Feldspar</u>	<u>Mica</u>	<u>Accessory</u>
F	Coarse, with amount pheno. > matrix	----	Shards & euhedral β (?)	Partly alt., few plagioclase. Possible zoning.	?. Biotite in sample with pyrite matrix.	Rare euhedral zircon. Common subhedral apatite.
E	Fine	Graded	?, sheared	?, altered to mica	"Muscovite"	Anhedral pyrite
D	Med.	Graded	Shards	Partly alt., few plagioclase.	"Muscovite"	Subhedral pyrite. Rare subhedral zircon. Common subhedral apatite.
C	Fine	Graded?	Rare	?, altered to mica	"Muscovite"	Trace anhedral pyrite.
B	Med. pheno. in fine matrix. pheno. < matrix	----	Shards	Partly alt., subhedral; some plagioclase.	Bent biotite pheno.	Common euhedral pyrite. Radioactive euhedral to subhedral zircon. Common subhedral apatite.
A	Fine	Graded?	Sparse shards	?, altered to mica	"Muscovite"	Common anhedral pyrite. Rare subhedral zircon.

Table 2. Summary of thin-section data for six observed Tioga ash beds, Selinsgrove

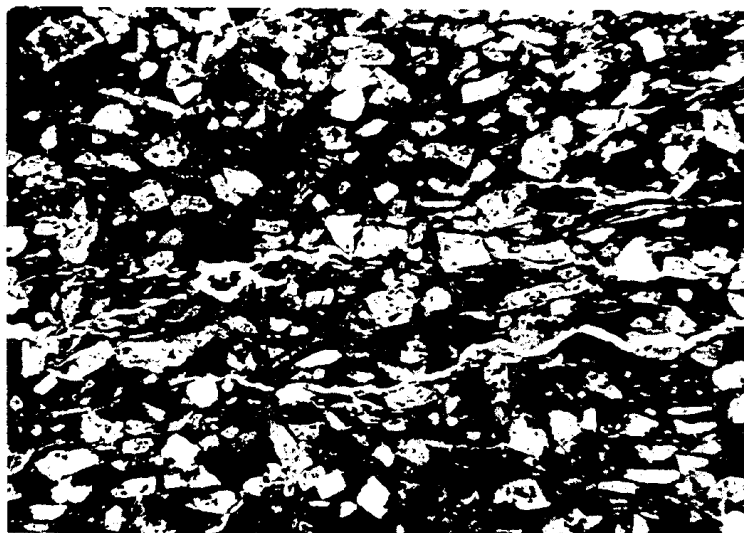


Figure 29 Thin section of Tioga ash bed F showing quartz shards with concave surfaces. (25 X; 100 X)

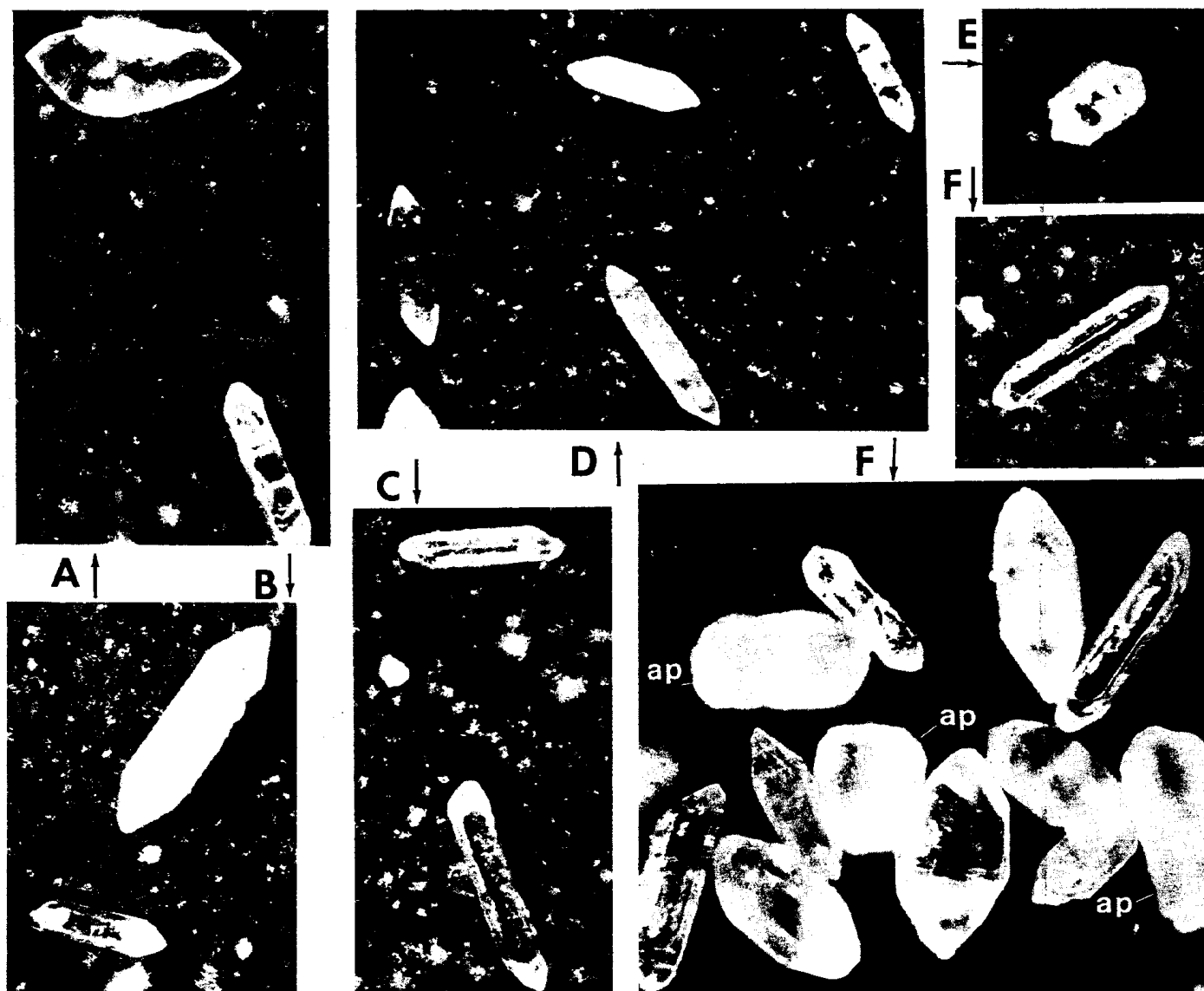


Figure 30

Acicular zircon and apatite crystals separated from Tioga ash beds, A - F, Selinsgrove Junction. (100 X)

Definitive evidence of mixed-layer minerals with smectite, chlorite, or mica was not obtained with the methods used. Based on possible weak peaks in the 25Å region, trace to minor amounts of a regular mixed layer cannot be ruled out.

Amphiboles were not verified. Except for possible microcline in ash bed D, potash feldspars are also unverified. Further study of the feldspar group is recommended.

Table 3. Relative abundance of minerals in six Tioga ash beds from Selinsgrove Junction as estimated from X-ray diffraction peak heights

Ash Bed	I@ 3.20 ±0.01Å ^a "Plagioclase"	I@ 4.26Å ^b Quartz	I@ 1.633Å ^c Pyrite	I@ 2.34Å "Kaolinite"	I@ 7.5Å Gypsum	I@ 3.03Å Calcite	I@ 3.39Å Aragonite
F	~138	≤27	10	-	27	1	0
E	2	≤ 5	3	3	30	~ 24	1?
D	20	34	6	1	4	1	0
C	25	≤14	3	1	42	2	21
B	~125	28	2	-	5	1	0
A	2	≤ 5	3	1	30	2	1?

a Includes slight interference from mica.

b Bed C is quartz-free based on the absence of the 3.34Å, I=100 spacing. Beds B and F contain relatively slight interferences from the 4.27Å, I=50 spacing of gypsum. Beds A, C, and E contain more significant interferences from gypsum... A possible interference from potash feldspar cannot be ruled out for Bed D, but no diagnostic K-spar peak at 3.24Å is present. Further study is recommended.

c Includes slight interference from mica.

Table 4. Relative abundance of chlorite-group minerals in six Tioga ash beds from Selinsgrove Junction as estimated from X-ray diffraction peak heights

Ash Bed	(1) Untreated I@ 14Å Chlorite	(2) Heated 300°C 1 hr. I@ 14Å Chlorite	(3) Untreated I@ 7.0Å Chlorite	(4) Heated 300°C 1 hr. I@ 7.0Å Chlorite
F	4	4	15	15
E	7	6	22	25
D	7	7	35	32
C	7	6	18	17
B	8	7	44	41
A	8	7	40	38

Table 5. Estimates of relative abundance of smectite and mica-group minerals in six Tioga ash beds from Selinsgrove Junction

Ash Bed	(5) Untreated Area between 10.5 and 13.6 Å "Smectite"	(6) Glycolated Area between mica & chlorite peaks "Smectite"	(7) Untreated I@ 10.1 Å "Mica"	(8) Glycolated I@ 10.1 Å "Mica"	(9) Heated 300°C 1 hr. I@ 10.1 Å Mica & Smectite	(10) (9) Minus (8) = "Smectite"
F	.38	.14	15	11	22	11
E	.40	.17	9	8	14	6
D	.34	.20	8	7	18	9
C	.11	.10	13	10	17	7
B	.33	.13	10 ^a	11	22	11
A	.15	.11	18	15	24	9

a A peak at 9.93 Å with I=11 suggests the possibility of a second mica.

Major and Minor Element Analyses

Splits of the channel samples were quantitatively analyzed for 9 major and minor elements and 3 trace elements by flame emission and atomic absorption spectrometer methods. The results are summarized in Table 6.

Table 6. Quantitative analyses for six observed Tioga ash beds from Selinsgrove Junction

Ash Bed	% SiO ₂	% Al ₂ O ₃	% ΣFe ₂ O ₃ ^a	% MgO	% CaO	% Na ₂ O	% K ₂ O	% TiO ₂	% MnO	ppm Ba	Rb	Sr
F	58.2	20.55	5.25	1.33	2.17	2.86	1.35	0.94	0.004	1,600	~20	170
E	42.5	28.35	3.61	4.08	4.03	1.02	1.78	0.76	0.010	2,800	810	190
D	54.6	21.50	4.37	2.33	0.92	1.77	1.60	0.58	0.008	2,600	50	85
C	43.0	27.75	6.06	1.71	5.39	1.86	2.00	~1.21	0.019	3,900	110	255
B	55.8	23.05	3.71	2.51	0.92	1.79	3.17	0.56	0.010	2,700	110	65
A	43.0	28.50	3.51	2.88	1.55	0.48	5.10	0.94	0.015	3,900	260	85

^a total iron reported as ferric iron

As a group, the six ash samples are chemically distinct from typical Marcellus Formation shale which, except for the mica flakes, they grossly resemble in outcrop. For example, data from O'Neill and Barnes (1981) yield a median Marcellus composition of 62.1% SiO_2 , 17.05 Al_2O_3 , 5.88 ΣFe as Fe_2O_3 , 0.92 MgO , 0.21 CaO , 0.15 Na_2O , 4.04 K_2O , 0.91 TiO_2 , and 0.012 MnO . Based on a median CaO content of only 1.86% for the six ash beds, they are also chemically distinct from limestone. (Physical dilution by the host marine sediments thus appears to have been slight, supporting use of volcanic terminology, such as "ash," for fine-grained pyroclastic material or "tephra" where no grain size is implied.)

The thinner ash beds (A, C, and E) are chemically distinct from the intervening thicker beds. Thin beds are richer in Al_2O_3 , CaO , MnO , and Ba, whereas the thicker beds are higher in SiO_2 . This correlation of chemistry with thickness and alteration of thin and thick beds suggests 3 pairs of volcanic events.

The amount of silica is surprisingly low and alumina is surprisingly abundant in all the ash beds. Also, these somewhat immobile elements vary antithetically with one another (Fig. 31). Variations in quantities of relatively high-alumina and low-silica minerals, such as micas, is indicated. Relative accumulation of micas, such as muscovite and biotite, in beds A, C, and E seems more likely than simple dilution by quartz in beds B, D, and F. The overall low quantity of silica is also no doubt due in part to the presence of sulfides, sulfates, and carbonates, as noted below. Unfortunately, anions were not determined and the data cannot now be "corrected" to a strict silicate basis. Taken with the thin-section and X-ray data, however, a low silica-low quartz preserved composition is still indicated.

The apparent total iron content of the original ash beds has probably been modified by the formation of diagenetic pyrite by reduction of sulfate of marine origin. Except for ash bed C, there seems to be a rough correlation between total iron and intensity of the pyrite peak.

The CaO content may also have been partly modified by later processes. In this case, the correlation of high CaO with the minerals gypsum, calcite, and aragonite suggests alteration of CaO -bearing minerals during recent weathering. Cations such as Ca^{2+} might, however, have remained nearly constant as sulfides oxidized and carbonate-bearing groundwater was introduced.

Soda, like CaO , at first appears to vary randomly with time. Taken together, however, a pattern appears in which first CaO then Na_2O are alternately higher in successively younger beds (Table 6). Involvement of a mineral containing both Na_2O and CaO , such as plagioclase, is immediately suspected.

With the exception of slightly anomalous ash bed E, potash decreases substantially with time. Concentration of a mineral or material rich in potash and low in soda, such as mica, is again suspected.

Overall, the chemical changes with time suggest that the volcanic source may have accumulated a potash and alumina-rich hydrous magma in the upper portions of a crystal magma chamber while plagioclase phenocrysts accumulated at slightly lower levels. The initial eruption that resulted in ash bed A would have tapped the top of such a magma chamber and therefore been enriched in potash and depleted in plagioclase. After a relatively dormant period, the second, more voluminous eruption completed the first cycle with a slightly denser, crystal-rich magma from lower in the chamber where plagioclase phenocrysts had concentrated by settling. Thereafter, two similar cycles may have followed, each consisting of an early, mica-bearing vitric tuff and a later,

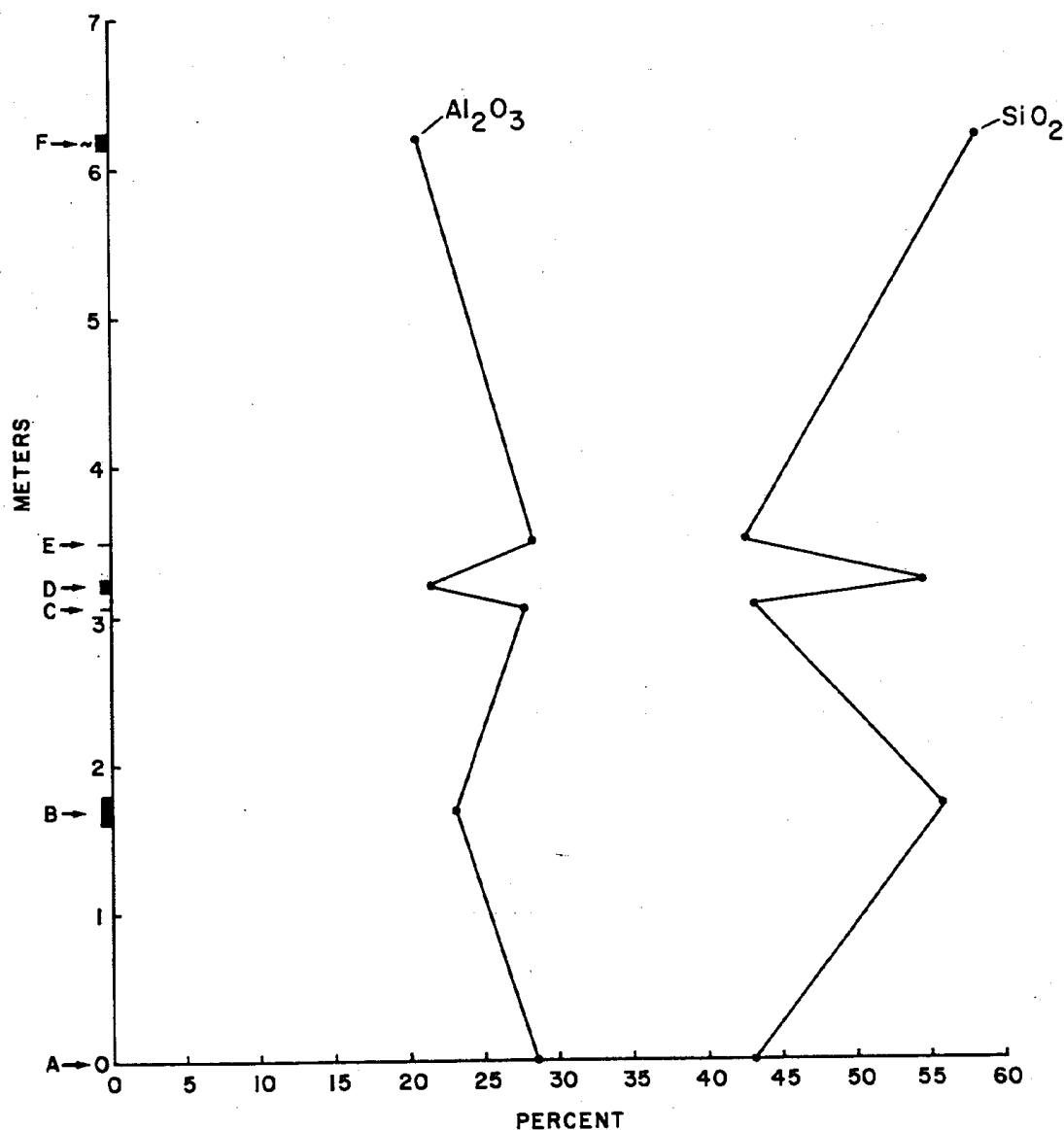


Figure 31 Plots of percent Al_2O_3 and percent SiO_2 within each ash bed versus stratigraphic position of the ash beds, Selinsgrove Junction.

plagioclase-bearing, crystal-vitric tuff. Based on the potash trend, however, differentiation in a crystal magma chamber between cycles was not adequate to reproduce the corresponding magma composition of the previous cycle. It is, perhaps, significant that the youngest observed ash at Selinsgrove Junction is the most plagioclase-rich. Such a phenocryst-rich magma was probably tapped from relatively low in the magma chamber.

If a general mechanism such as the one above is accepted, then one can assume that there were three cycles of volcanic activity, each beginning with a short-lived violent eruption caused by an accumulation of volatiles and ending with a longer, less violent eruption following an intervening "dormant" period during which differentiation was proceeding in a crystal magma chamber.

Obviously such a mechanism is speculative because of possible mineral fractionation by air elutriation and wind direction, current and wave action in the water

in which the ash was deposited, chemical reactions with marine water, diagenesis including devitrification, subtle Alleghanian metamorphism, and recent weathering. Fractionation during transport related to grain size and density (eolian differentiation) might not have been very extensive for vitric tephra but must have been significant for crystal phases. Such effects probably account for the observed graded bedding and certainly for the decrease in grain size with distance from a probable source. Careful chemical analyses of "pairs" of ash beds from additional localities are needed to properly interpret differentiation trends and detect transport and local effects. Also, until a parent magma composition is determined and its density calculated, the float/sink relations in the magma chamber are speculative.

In addition to permitting refinement of magma differentiation, additional ash beds at other localities would permit extremely precise stratigraphic correlations within the Onondaga-Marcellus transition. With the hyperfine resolution added by additional ash beds, it should be possible to define a classic example of lithofacies vs chronostratigraphic units in the folded Valley and Ridge of Pennsylvania.

The authors wish to acknowledge John H. Barnes, Pennsylvania Geological Survey, for his assistance with the atomic absorption analyses, X-ray diffraction interpretation, photomicrographs, and in manuscript review.

REFERENCES CITED

- Ashley, G. H., (1928), Bituminous coalfields of Pennsylvania, Part I, General information on coal: Pennsylvania Geological Survey, 4th ser., Mineral Resource Report 6.
- Bohor, Bruce, (1982), Occurrence of volcanic ash in coal: Paper read at the Third Conference on Inorganic Constituents in Coal, Allenberry, Boiling Springs, PA.
- Baltrusaitis, E. J., (1974), Middle Devonian bentonite in Michigan basin: American Association of Petroleum Geologists Bulletin, v. 58, p. 1323-1330.
- Collins, H. R., (1979), Devonian bentonites in eastern Ohio: American Association of Petroleum Geologists Bulletin, v. 63, p. 655-660.
- Conant, L. C. and Swanson, V.E., (1961), Chattanooga Shale and related rocks of central Tennessee and nearby areas: U.S. Geological Survey Professional Paper 357.
- Dennison, J. M., (1961), Stratigraphy of Onesquethaw Stage of Devonian in West Virginia and bordering states: West Virginia Geological and Economic Survey Bulletin 22.
- _____, (1963), Stratigraphy between Tioga metabentonite and Pocono Formation along Allegheny Front in Maryland and West Virginia, in Shepps, V.C. ed., Symposium on Middle and Upper Devonian stratigraphy of Pennsylvania and adjacent states: Pennsylvania Geological Survey, 4th ser., General Geology Report 39, p. 213-227.
- _____, (1982), Uranium favorability of nonmarine and marginal marine strata of Late Precambrian and Paleozoic age in Ohio, Pennsylvania, New Jersey, and New York: U.S. Department of Energy, National Uranium Resource Evaluation Report, GJBX-50 (82).
- Dennison, J. M., deWitt, Wallace, Jr., Hasson, K. O., and others, (1972), Stratigraphy, sedimentology, and structure of Silurian and Devonian rocks along the Allegheny Front in Bedford County, Pennsylvania, Allegany County, Maryland, and Mineral and Grant

Counties, West Virginia: Guidebook for the 37th Annual Field Conference of Pennsylvania Geologists.

Dennison, J.M., and Head, J.W., (1975), Sea level variations interpreted from the Appalachian basin: *American Journal of Science*, v. 275, p. 1089-1120.

Dennison, J. M., and Textoris, D.A., (1967), Stratigraphy and petrology of Devonian Tioga Ash Fall in Northeastern U.S.: (abs.), *Geological Society of America Special Paper* 101, p.52.

_____, (1970), Devonian Tioga Tuff in northeastern United States: *Bulletin Volcanologique*, v. 4, p.289-294.

_____, (1971), Devonian Tioga Tuff: Virginia Division of Mineral Resources, *Information Circular* 16, p. 64-68.

_____, (1978), Tioga bentonite time-marker associated with Devonian shales in Appalachian basin, in Schott, G.L., Overbey, W.K., Jr., Hunt, A.E., and Komar, C.A., eds., *Proceedings of the First Eastern Gas Shales Symposium*, October 17-19, 1977, Morgantown, West Virginia: U.S. Department of Energy, Morgantown Energy Research Center, Publication MERC/SP-77-5, p. 166-182.

Ebright, J. R., Fettke, C. R., and Ingham, A. I., (1949), East Fork - Wharton gas field, Potter County, Pennsylvania: *Pennsylvania Geological Survey*, 4th ser., Mineral Resource Report 30.

Epstein, J. B., Sevon, W. D., and Glaeser, J. D., (1974), Geology and mineral resources of the Lehigh and Palmerton Quadrangles, Carbon and Northampton Counties, Pennsylvania: *Pennsylvania Geological Survey*, 4th ser., Atlas 195cd.

Fettke, C. R., (1931), Physical characteristics of the Oriskany Sandstone and subsurface studies in the Tioga gas field, Pennsylvania: *Pennsylvania Geological Survey*, 4th ser., Bulletin 102-B, p. 8.

_____, (1940), Summit gas pool, Fayette County, Pennsylvania: *Pennsylvania Geological Survey*, 4th ser., Progress Report 124.

_____, (1952), Tioga Bentonite in Pennsylvania and adjacent states: *American Association of Petroleum Geologists Bulletin*, v. 36, p.2038-2040.

Flowers, R. R., (1952), Lower Middle Devonian Meta-bentonite in West Virginia: *American Association of Petroleum Geologists Bulletin*, v. 36, p.2036-2038.

Hall, James, (1843), *Geology of New York. Part 4, Comprising the Survey of the Fourth Geological District*, Albany, 683 p.

Huff, W. D., (1983), Misuse of the term "bentonite" for ash beds of Devonian age in the Appalachian basin: Discussion and Reply: *Geological Society of America Bulletin*, v. 94, p.681-683.

Inners, J. D., (1975), The stratigraphy and paleontology of the Onesquethaw Stage in Pennsylvania and adjacent states: unpub. Ph.D. dissertation, University of Massachusetts.

_____, (1979), The Onesquethaw Stage in south-central Pennsylvania and nearby areas, in Dennison, J. M., Hasson, K. O., Hoskins, D. M., and others, leaders, Devonian shales in south-central Pennsylvania and Maryland: Guidebook for the 44th Annual Field Conference of Pennsylvania Geologists, p. 38-55.

Kay, G. M., (1944), Middle Devonian in central Pennsylvania: *Journal of Geology*, v. 52, p.1-23, 97-116.

Knight, W. C., (1898), Bentonite: *Engineering and Mining Journal*, v. 66, p.491.

Luther, G. G., (1894), Report on the geology of the Livonia salt shaft: *New York State Museum Annual Report* 47, p.219-324.

Meents, W. F. and Swann, D. H., (1965), Grand Tower Limestone (Devonian) of southern Illinois: *Illinois State Geological Survey, Circular* 389.

Oliver, W. A., (1954), Stratigraphy of the Onondaga Limestone (Devonian) in central New York: *Geological Society of America Bulletin*, v. 65, p.621-652.

_____, (1956), Stratigraphy of the Onondaga Limestone in eastern New York: *Geological Society of America Bulletin*, v. 67, p.1441-1474.

O'Neill, B. J., Jr., and Barnes, J. H., (1981), Properties and use of shales and clays, south-central Pennsylvania: *Pennsylvania Geological Survey, 4th ser., Mineral Resource Report* 79.

Rickard, L. V., (1964), Correlation of the Devonian rocks in New York State: *New York Museum and Science Service, Map and Chart Series* n. 4.

Roen, J. B., and Hosterman, J. W., (1982), Misuse of the term "Bentonite" for ash beds of Devonian age in the Appalachian basin: *Geological Society of America Bulletin*, v. 93, p.921-925.

Sanford, B. V., (1967), Devonian of Ontario and Michigan in *International Symposium on the Devonian System: v.1, Alberta Society of Petroleum Geologists*, p.973-999.

Spears, D. A., (1970), A kaolinitic mudstone (Tonstein) in the British Coal Measures: *Journal of Sedimentary Petrology*, v. 40, p.386-394.

Textoris, D. A., and Dennison, J. M., (1970), Petrology of Devonian Tioga Bentonite: *Geological Society of America, Abstracts with Program, SE Section*, v.2, No. 3, p.243-244.

Thompson, R. R., (1963), Lithostratigraphy of the Middle Ordovician Salona and Coburn Formations in central Pennsylvania: *Pennsylvania Geological Survey, 4th ser., General Geology Report* 38.

Weaver, C. E., (1953), Mineralogy and petrology of some Ordovician K-bentonites and related Limestones: *Geological Society of America Bulletin*, v.64, p.921-944.

LOWER SILURIAN CLASTICS IN THE SUBSURFACE OF NORTHWESTERN PENNSYLVANIA

by

Christopher D. Laughrey

Pennsylvania Geological Survey

Introduction

Several recent investigations into the sedimentology of the Tuscarora Formation of central Pennsylvania have concluded that the Lower Silurian clastics of this unit were deposited in a variety of shallow shelf, littoral, and fluvial environments (Cotter, 1982; Cotter, 1983; Parks et. al, 1982). These studies describe vertical and lateral depositional facies which generally progress from braided fluvial deposits to the southeast through estuarine and littoral facies to a shallow marine shelf sand wave complex in the northwest. The entire sequence is capped by a relatively thin, regressive red bed sequence, the Castanea Member, which is interpreted as a progradational coastal sand/mud flat complex (Cotter, 1983, p. 39).

The basic geologic character of this southeast to northwest, onshore-offshore complex in the Lower Silurian of the central Appalachian Basin has been recognized for some time (Smosna and Patchen, 1978, p. 2310). Most of the recent regional paleogeographic summaries, however, show the Tuscarora Formation as a broad alluvial coastal plain, with deltas and offshore marine bars developed within the equivalent stratigraphic units in the subsurface of the basin's northwest flank (Smosna and Patchen, 1978, p. 231; Berry and Boucot, 1970, p. 54; Piotrowski, 1981, p. 19). The popular acceptance of a fluvial interpretation for the Tuscarora is largely the result of Yeakel's (1962) paleocurrent studies and Smith's (1970) comparisons of the Lower Silurian clastics in Pennsylvania with the braided fluvial deposits of the modern Platte River in Colorado and Nebraska (Cotter, 1982, p. 25).

Thompson and Sevon (1982, p. 23) have pointed out that proposed models of the Silurian depositional record in the central Appalachian Basin depend on how the various Tuscarora paleoenvironments are interpreted:

If marine or coastal, then the transgression initiated during Juniata fluvial deposition continued, bringing high energy shoreline environments eastward over the fluvial facies

If the Tuscarora is continental and fluvial, then a regressive phase followed the Juniata shale deposition, as either source-area uplift was renewed or sea level dropped eustatically (or glacially).

These two possible interpretations are of more than academic importance. Lower Silurian sandstones of the Tuscarora Formation and the Medina Group (Figures 33 and 32) have produced a number of significant hydrocarbon reservoirs in the Appalachian Basin. Most of the proposed depositional models for exploration in these rocks are based on continental and fluvial interpretations of the Tuscarora (Piotrowski, 1981; Knight, 1969; Pees, 1983). Subsurface interpretations of Medina paleoenvironments in northwestern Pennsylvania have been largely based on interpretations of geophysical logs (Piotrowski, 1981; Kelley and McGlade, 1969; Kelley, 1966).

Two whole-diameter cores of the Lower Silurian clastic interval in northwestern Pennsylvania were obtained by the Oil and Gas Geology Division of the

STRATIGRAPHIC NAMES USED IN WESTERN NEW YORK (Fisher, 1954)	
MIDDLE SILURIAN	<p>GUELPH- LOCKPORT DOL.</p> <p>DeCEW DOL. MBR.</p> <p>ROCHESTER SH.</p> <p>IRONDEQUOIT DOL.</p> <p>REYNALDES DOL.</p> <p>NEAHAHA SH.</p> <p>THOROLD SS.</p>
LOWER SILURIAN	<p>GRIMSBY SS.</p> <p>CABOT HEAD SH.</p> <p>MANITOULIN DOL.</p> <p>WHIRLPOOL SS.</p>
U. ORDOVICIAN	<p>QUEENSTON SHALE</p>

STRATIGRAPHIC NAMES USED IN OHIO		
(Knight, 1969)		
MIDDLE SILURIAN	NIAGARA GP.	LOCKPORT DOL.
		CLINTON FM.
LOWER SILURIAN	ALTIUM GP.	BRASSFIELD LS.
	CATARAUGU FM.	THOROLD SS.
		GRIMSBY SS.
		CABOT HEAD SS.
		CABOT HEAD SH.
		MANITOWLIN DOL.
		WHIRLPOOL SS.
U. ORDOVICIAN		QUEENSTON SHALE

STRATIGRAPHIC NAMES USED IN N.W. PENNSYLVANIA (Cato, 1965)	
MIDDLE SILURIAN	CLINTON GP. NIAGARA GP. GUELPH- LOCKPORT DOL.
	ROCHESTER SH.
	IRONDEQUOIT DOL.
	REYNOLDS DOL. THOROLD SS.
LOWER SILURIAN	MEDINA GP. GRIMSBY SS.
	POWER GLEN OR TRACY SS.
	POWER GLEN SH.
	WHIRLPOOL SS.
U. ORDOVICIAN	QUEENSTON SHALE

DRILLERS' TERMINOLOGY
NIAGARAN LIME
GRAY SHALE
PACKER SHELL
PACKER SHELL
STRAY CLINTON SS.
BED CLINTON SS.
WHITE CLINTON SS.
SHALE
BROWN LIME
WHIRLPOOL SS.
QUEENSTON SHALE

**STRATIGRAPHIC NAMES USED
IN THIS REPORT**

	NORTHWESTERN PA.	SOUTH-CENTRAL, CENTRAL, AND EASTERN PA.
MIDDLE SILURIAN	CLINTON OR NIAGARA GP.	WILLS CREEK FM. BLOOMSBURG WILLIAMSPORT SS. MBR. FM.
	GUELPH-LOCKPORT DOL.	McKENZIE MBR.
	ROCHESTER SH.	ROCHESTER SH.
	IRONDEQUOIT DOL.	KEEPER SS.
LOWER SILURIAN	ROSE HILL FM.	ROSE HILL FM.
	REYNALDES DOL.	CREASTOWN IS. MBR.
	GRIMSBY SS.	CASSTANEA MBR.
	TONGUE	TUSCARORA FM.
MEDINA GR.	CABOT HEAD	
	MANITOULIN DOL. SH.	
	WHIRLPOOL SS.	
U. ORDOVICIAN	QUEENSTON SHALE	JUNIATA-TUSC. FM. JUNIATA FM.

SHAWGUNGE FM.
EASTERN PA.

Figure 32 Regional stratigraphic correlation of the Medina Group (from Plotrowski, 1981).

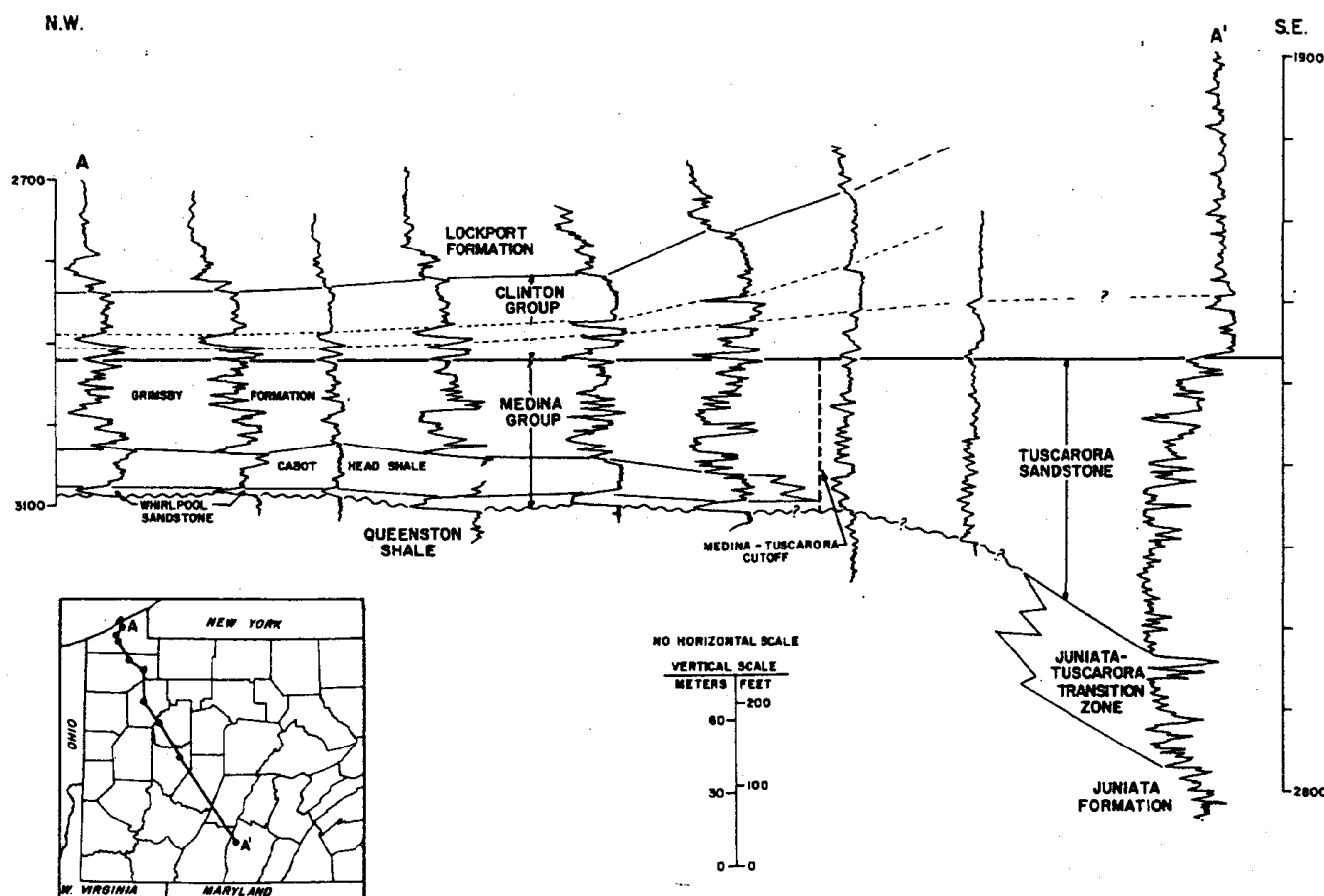


Figure 33 Regional subsurface cross section of the Medina Group and Tuscarora Formation in the subsurface of western Pennsylvania (modified from Piotrowski, 1981).

Pennsylvania Geological Survey in 1980. Recently completed studies of these cores (Laughrey, in press; Laughrey and Donahue, 1982; Laughrey, 1982) have documented the sedimentologic and diagenetic history of the Medina Group in northwestern Pennsylvania. The stratigraphic and sedimentologic aspects of these studies are summarized in the following section so that the users of this guidebook can compare the facies and sedimentary characteristics of the Tuscarora Formation, seen on this field conference, with those of the laterally equivalent stratigraphic units in the subsurface to the northwest.

Stratigraphic and Sedimentologic Overview

Lower Silurian strata of the Medina Group are all included in the Llandoverly Stage and probably represent a large portion of Llandoverly time (Berry and Boucot, 1970, p. 184). The regional stratigraphic relations among the Medina Group, in the subsurface of northwestern Pennsylvania, and its equivalents in central and northeastern Pennsylvania, western New York, Ohio, and Ontario are described in detail by Piotrowski (1981) and summarized in Figure 32. The Medina Group lies disconformably over red beds of the Upper Ordovician Queenston Formation and conformably underlies marine mudrocks and argillaceous dolostones of the Middle Silurian Clinton Group. Medina rocks consist of interbedded sandstones and mudrocks with minor amounts of carbonates. The group attains a maximum thickness of approximately 200 feet (60 meters) in central Warren, Forest, Clarion, Armstrong, Butler, and Beaver Counties and thins to the

northwest where it has an average thickness of 140 to 160 feet (42 to 48 meters) along the Lake Erie shoreline. The entire unit is less than 120 feet (37 meters) thick beneath the central part of Lake Erie.

On the basis of gamma-ray correlation we recognize four major stratigraphic units within the subsurface Medina Group (Figures 33 and 32). In descending order, these are: 1) the Grimsby Formation (interbedded sandstones, siltstones and shales; 2) the Cabot Head shale; 3) the Manitoulin Dolomite; and 4) the Whirlpool Sandstone. Figure 33 illustrates the regional stratigraphic relations of these units in the subsurface of northwestern Pennsylvania, and correlation with the Tuscarora Sandstone to the south and east. This cross-section, modified from Piotrowski (1981), shows that the Medina Group is characterized by a "broken sandstone" gamma-ray signature in northwestern Pennsylvania. The interval becomes less shaley to the east and southeast until it grades into the uppermost portions of the Tuscarora. The upper portion of the Grimsby Formation appears correlative with the shaley Castanea Member of the Tuscarora Formation (not distinguished in Figure 33); the lower portion of the Grimsby coalesces into the principal sandstone unit of the Tuscarora. The Cabot Head Shale and the Whirlpool Sandstone are truncated by an apparent unconformity to the southeast. Piotrowski (1981) defined the strike of this truncation, which occurs along the line of maximum Medina thickness, as the paleoshoreline during the time of Medina deposition. The Manitouline Dolomite, a minor unit in the Medina Group of Pennsylvania, is restricted to the Lake Erie region in the extreme northwest corner of the state.

Orientation of cross strata in the Medina Group shows well-defined north-westward and northeast-southwestward sediment transport directions (Martini, 1971). This is in accord with the results of Yeakel (1969) and Cotter (1982) who studied the laterally equivalent clastics to the southeast (Tuscarora Sandstone). Ziegler and others (1977), Johnson (1980), and Cotter (1982) place Pennsylvania approximately 25° to 30° south of the equator during the Early Silurian. This puts the region under the variable influence of wet south-westerly winter winds and drier, easterly summer winds (Ziegler and others, 1977). Cotter (1982) postulates that the Early Silurian climate of Pennsylvania was similar to that of the present day Mexican Pacific coast with an early winter rainy season and relatively arid conditions during the remainder of the year.

Lower Silurian clastics entered the Appalachian depositional basin during the last pulse of the Taconic orogeny (Cotter, 1982). Sands of moderately high quartz content shed from foreland fold-belt highlands directly into the adjacent foreland basin (Dickinson and Suczek, 1979). The highlands shielded the basin from magmatic arc- and suture belt-source rocks so that the Lower Silurian sands were initially derived from recycling of earlier sedimentary sequences (Martini, 1971) and possibly from positive areas on the craton (Knight, 1969). The sedimentary source cover was eventually stripped during the later part of Early Silurian time resulting in detrital contributions from the plutonic igneous rocks of the arc orogen (Folk, 1960).

Martini (1971) presented a detailed sedimentological analysis of the Medina Group based on outcrop studies along the Niagara Escarpment in western New York and southern Ontario. He demonstrated that the Medina owes its origin to deposition in a shelf-longshore bar-tidal flat-deltaic complex (see Martini, 1971, p. 1252, Figures 3 and 4). Laughrey (in press) defined descriptive facies of the Medina Group in the subsurface of northwestern Pennsylvania on the basis of petrological studies of whole-diameter cores. The observed facies sequence is remarkably compatible with Martini's model. For example, a core cut from the Athens gas field, in eastern Crawford County, Pennsylvania exhibits a vertical sequence which is almost identical to the Medina sections at Niagara Gorge in western New York state and at Niagara Glen in Ontario (Laughrey, in press). A core cut from a well in the Geneva Field of southeastern Crawford County shows a sequence of facies similar to the sections described by Martini (1971) west of Stoney Creek, Ontario (Laughrey, in press).

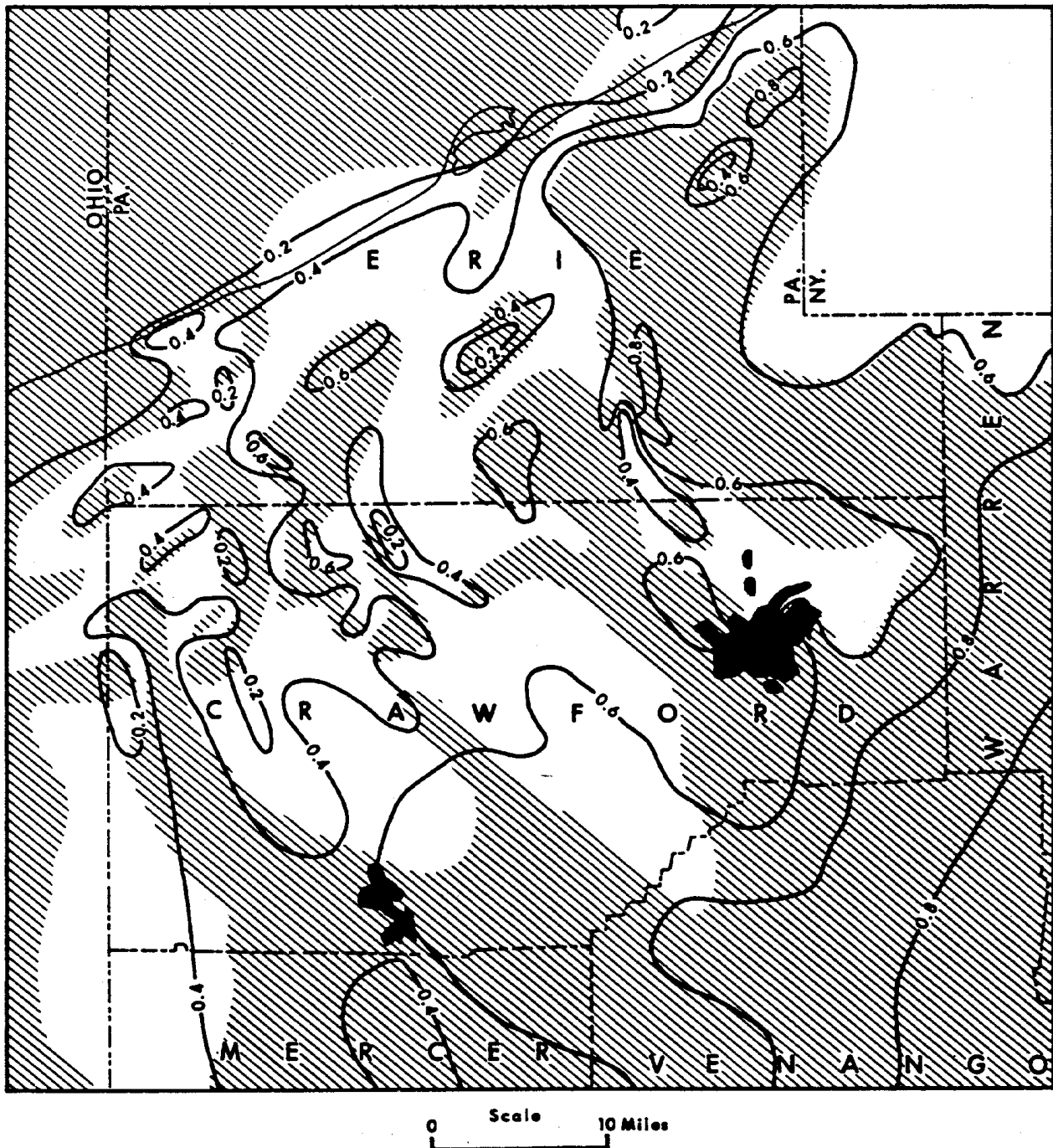


Figure 34 Subsurface distribution of Medina Group clastics in northwestern Pennsylvania. Stippled areas are regions underlain by 50% clean sandstone as measured on gamma-ray logs. Contours represent the sand/shale ratio (from work maps used by Piotrowski, 1981, and on file with the Pennsylvania Geological Survey, Pittsburgh office).

No single modern analogue is appropriate for comparison with the stratigraphic sequences observed in the Medina Group of northwestern Pennsylvania. A combination of some ancient and modern depositional models, however, provides several instructive parallels with the processes and environments that influenced the Medina depositional system. Figure 34 shows the regional distribution of Medina Group sandstones in a portion of northwestern Pennsylvania, based on geophysical log calculations of net sandstone and sand-shale ratios. Facies interpretations of the overall

distribution (Laughrey, in press) suggest that the Whirlpool Sandstone is present as a basal transgressive sandstone which was deposited on top of the older deltaic coastal-plain sediments of the Queenston Formation. Offshore and longshore bars of the Whirlpool migrated up the shoreface to the southeast along with the transgressing sea. A stabilized shoreline developed along the line of thickest Medina development from central Warren County to central Beaver County. Shelf muds of the lowermost Cabot Head Shale overlie sandy shelf sediments of the distal Whirlpool. Progradation of the shoreline resulted in the deposition of transitional silty sands and lower shoreface sands of the upper Cabot Head. These units are, in turn, overlain by middle and upper shoreface and nearshore sands of the lowermost Grimsby Formation. Varicolored red and green argillaceous sandstones of the uppermost Grimsby, which formed within a prograding coastal sand/mud complex, generally overlie these coastal sands. This entire vertical sequence, as just described, is similar to the vertical sequence of retrogradational and progradational facies described for the coast of Nayarit, Mexico by Curray and others (1969). A similar sequence occurs in the prograding sandy shoreline sequences that have been documented in the Cretaceous Gallup Sandstone of New Mexico (Harms and others, 1982). This sequence is applicable to Martini's (1971) interdistributary regions (p. 1252, Fig. 3) and to the light areas in Figure 34. Selected facies of this sequence are described in Tables 7, 8 and 9.

	FACIES G1	FACIES G2	FACIES G3
LITHOLOGY	Grayish red (5R4/2) to pale green (5G7/2), very fine- to fine-grained quartz wackes interbedded with very light gray (N8), silt-sized quartz arenites, hematitic mudstones, and dolomitized, hematitic, silty biosparite.	Grayish red (10R4/2) to light gray (N7), fine- to medium-grained subarkoses, sublitharenites, and quartz arenites interbedded with dark reddish brown (10R3/4) hematitic mudstones.	Very light gray (N8) to light gray (N7), fine-grained quartz arenites and sublitharenites interbedded with greenish-gray (5G6/1), very fine-grained quartz wackes and medium light gray (N6) mudstones. Some glauconite.
SANDSTONE TEXTURE	Poorly to moderately well sorted; variable grain size trends; positive skew; grains are subangular to subrounded; fabric is matrix-supported.	Moderately well- to very-well sorted; fining upward sequences; slightly positive skew; subrounded- to well-rounded grains; fabric is grain-supported and displays predominantly point and concavo-convex particle contacts; hematitic clay drapes are common at the top of fining upward sequences; foreset laminae commonly exhibit inverse grading.	Well sorted to very well sorted; fining upward sequences; slightly positive skew; rounded- to well-rounded grains; grain-supported fabric; predominantly concavo-convex, long, and sutured grain contacts.
SEDIMENTARY STRUCTURES	Medium to very strongly bioturbated; distinct mottling; lenticular, flaser, and wavy bedding; trough cross-stratification; small-scale ripple cross-lamination; mudcracks; micro-faulted parallel laminae.	Tabular cross-stratification; low-angle cross-stratification; trough cross-stratification; ripple cross-lamination is superimposed on some of the tabular cross-stratified sets; minor flaser and lenticular bedding; some mud cracks; scour surfaces overlain by abundant mud clasts are common.	Planar and tabular cross-stratification with mud clasts common as basal lags; low-angle cross-stratification with internal, intricately braided cross-laminae; climbing ripple cross-laminae with mud drapes; lenticular and flaser bedding.
FOSSILS AND TRACE FOSSILS	Brachiopods (<i>Lingula</i> sp.); Gastropods (unidentified); phosphatic shell fragments; <i>Arthropycus</i> ; abundant <i>Skolithos</i> ; <i>Monocraterion</i> ; possible <i>Rusophycus</i> ; possible <i>Diplocraterion</i> .	Some horizontal burrows are present in the thin, flaser and lenticular bedded intervals.	None
GEOMETRY	Widespread, uniformly thick (40-50 feet: 12-15 meters) sheet geometry.	Thick (30-45 feet; 9-13.5 meters), narrow sandstone bodies oriented perpendicular to the shoreline.	Twenty-five to 35 foot (7.5-10.5 meters) thick, linear sandstone bodies oriented parallel to depositional strike.
FACIES ASSOCIATIONS	Conformably underlies the Middle Silurian Clinton Group marine carbonate rocks and mudstones; may overlie Facies G2 or G3.	Underlies Facies G1 and overlies Facies G3.	Underlies Facies G1 or G2; overlies the Cabot Head Formation.
ENVIRONMENTS OF DEPOSITION	Coastal sand/mud flats; tidal plain; tidal creeks; coastal lagoon.	Deltaic; mixed fluvial and paralic setting; ephemeral braided fluvial channel; tidal plain; beach ridge.	Littoral marine; barrier inlet sand body developed through shore-parallel inlet migration.

Table 7. Summary of facies and sedimentary characteristics of the Grimsby Sandstone in northwestern PA

	FACIES CH1	FACIES CH2	FACIES CH3	FACIES CH4	FACIES CH5
LITHOLOGY	Light brownish-gray (5YR6/1) to medium dark gray (N4), argillaceous siltstone and interbedded mudstone.	Light gray (N7), very fine- to fine-grained subarkose and sublitharenite. Glauconitic.	Light gray (N7) very fine-grained subarkose with medium dark gray (N4) mudstone laminae spaced throughout the facies.	Interlaminated very fine-grained to coarse silt-sized arkosic wacke and mudstone. Light gray (N7) to medium dark gray (N4).	Medium gray (N5) to medium dark gray (N4), sandy and silty. illitic-chloritic mudstone. Non-fissile.
SANDSTONE TEXTURE	None	Moderately to moderately well sorted; coarsens upward with mud clasts concentrated at the top of the upward coarsening sequence; grains are subrounded to rounded; fabric is grain supported and concavo-convex contacts are the most common.	Moderately sorted; no apparent grain size trend; grains are subrounded; grain-supported fabric; sutured grain contacts.	Moderately sorted; graded sand and silt laminae pass up into mud grade material. Grains are subrounded; fabric is matrix-supported.	None
SEDIMENTARY STRUCTURES	Extensively burrowed to bioturbated; indistinct wavy and irregular laminations.	Intricately braided sets of cross-laminae; swaley sets of cross-laminae; near-horizontal fine laminae; indistinct low-angle cross-stratification.	Ripple bedding; small-scale oscillation-ripple cross-lamination is distinctly developed; mudstone laminae drape some ripple forms; thin, single flat laminae and low-angle cross-laminae also occur; convolute bedding.	Ripple lamination; flasers and lenticular laminae. Wavy and irregular bedding.	Indistinct horizontal laminations and bedding. Very strongly bioturbated.
FOSSILS AND TRACE FOSSILS	<u>Arthropycus</u> .	Minor burrows.	Abundant <u>Chondrites</u> .	Abundant <u>Chondrites</u> .	Very fossiliferous: gastropods; crinoids; corals; <u>Chondrites</u> .
GEOMETRY	Thin, elongate bed always associated with Facies CH2.	Narrow, elongate sandstone ribbons developed perpendicular to depositional strike.	Thin sheets and pods.	Extremely discontinuous pods and lenses.	Thick blanket deposit.
FACIES ASSOCIATIONS	Overlies facies CH2; underlies Grimsby Sandstone units.	Always occurs developed within the Cabot Head shaly lithologies. Underlies CH1 and overlies CH3. Upper contact is abrupt but conformable. Lower contact is gradational with Facies CH3.	Gradational upwards and downwards with Facies CH2 and CH4.	Gradational upward with Facies CH3; gradational downward with Facies CH5.	Underlies Facies CH4; overlies Whirlpool Sandstone.
ENVIRONMENTS OF DEPOSITION	Offshore marine: interpreted to have capped the bar units described in Facies CH2. Originally formed as ripple-laminated silt and clay and later reworked by burrowing organisms.	Shallow marine: sandstone originated as low-relief sand dune bed-form which developed in response to sustained bottom currents.	Shallow marine: rippled sand layers occasionally blanketed by mud; formed as subaqueous straight-crested ripple forms which developed in response to notably variable depositional energies; burrowers active during low current periods.	Shallow marine: formed as discontinuous patches of rippled sand on mud-dominated shelf.	Offshore marine: shelf mud accumulation.

Table 8. Summary of facies and sedimentary characteristics of the Cabot Head Shale in northwestern PA

	FACIES WP1	FACIES WP2
LITHOLOGY	Light gray (N7) very fine-grained quartz arenite interlaminated with medium gray (N5) mudstone. Glauconitic.	Light gray (N7), very fine-grained subarkoses and quartz arenites. Glauconitic.
SANDSTONE TEXTURE	Individual sandstone laminae are well sorted; sandstone and mudstone laminae alternate rhythmically; individual sandstone laminae average 1.0 cm in thickness and are themselves inversely graded; the number of mudstone laminae increase upward; sand grains are well rounded; fabric of individual sandstone laminae is grain supported and contacts are long to sutured.	Well sorted; grain size coarsens then fines upwards; positive skew; rounded- to well-rounded grains; grain-supported fabric; predominantly long and sutured grain contacts.
SEDIMENTARY STRUCTURES	Graded bedding; even laminations; individual sandstone laminae are parallel laminated and some have parting lineations developed along internal surfaces.	Planar lamination; low-angle cross-stratification; ripple cross-laminations; tabular cross-stratification; parting lineations; synaereal shrinkage cracks.
FOSSILS AND TRACE FOSSILS	None	None
GEOMETRY	Thin, widespread unit which is transitional between Facies WP2 and overlying Cabot Head Shale.	Ten- to 20-foot (3-6m) thick sheet sandstone.
FACIES ASSOCIATIONS	Conformably underlies Facies CH5 of the Cabot Head Formation; transitionally overlies Facies WP2.	Underlies Facies WP2; disconformably overlies the Queenston Formation.
ENVIRONMENTS OF DEPOSITION	Offshore marine; storm influenced deposition associated with the sublittoral sheet sand complex of Facies WP2.	Offshore marine; sublittoral sheet sand.

Table 9. *Summary of facies and sedimentary characteristics of the Whirlpool Sandstone in northwestern PA*

Narrow belts of bedded fluvial deposits which are developed normal to the shoreline intermittently interrupt the vertical sequence just described. In map view, these units are present as flattened, lobate extensions of sandstone (stippled area of Figure 34). Selected facies characteristics of these sandstones and associated sediments are described in Table 8. These sandstones cut down into underlying littoral and shoreface deposits during a period of relatively stable shoreline conditions, permitting the development of small deltas at river mouths. The deltaic units consist, in ascending order, of distributary mouth bar, channel, tidal flat, nearshore, and tidal plain deposits. This sequence resembles the upper portions of the modern day Klang River Delta of Malaysia (Coleman, 1976). A more suitable analogue may be found in the Gascoyne Delta of western Australia which was described by Johnson (1982). Here, the climate is semi-arid and the Gascoyne River flows intermittently into Shark Bay. The Gascoyne deltaic sequence forms a regressive terrigenous wedge which cuts into basal littoral deposits. The deltaic sequence itself contains channel bar, delta bay, and strandplain sheet sediments. The subaerial sequence of the Gascoyne Delta consists of a "narrow, axial belt of channel sands and levee silts flanked by extensive red-brown muds" (Johnson, 1982, p. 547). Laughrey and Donahue (1982) compared the fluvial Medina's remarkably straight channel orientation and dominance of trough and planar crossbeds, with hematitic clay drapes, to some of the facies characteristics of the Nubia Sandstone in southwest Egypt.

An abrupt transition from dolomite shales to fossiliferous and argillaceous dolostones typically marks the contact between the upper Medina and the overlying Clinton Group. Marine deposits of the Clinton Group formed by a rise in Upper Llandovery sea level and a shifting of the paleoshoreline to the north (Brett, 1982).

Conclusions

Interpretations of the subsurface Medina Group facies and depositional systems are compatible with the depositional history of the Tuscarora formation proposed by Cotter (1983). The Whirlpool Sandstone was deposited as a sublittoral sheet sand. The initial Early Silurian transgression to the southeast occurred rapidly enough for some of

the shoreface sands to escape erosion. More stabilized shelf conditions were established after Whirlpool deposition. The shelf in northwestern Pennsylvania was predominantly muddy, although sublittoral tidal- and/or storm-worked linear bars prograded across the ancient muddy shelf. The Whirlpool and the Cabot Head formations, respectively, are believed to be laterally equivalent to the lower paralic beach facies and western cross-laminated shelf sand wave facies of the Tuscarora Formation as described by Cotter (1983). The Grimsby Sandstone of northwestern Pennsylvania is largely equivalent to the Castanea Member of the Tuscarora. Various paralic facies occur within the Grimsby and represent regressive coastal deposits which underlie the coastal-protected deposits of Cotter's (1983) red, Skolithos-burrowed lithofacies in the Castanea. Our interpretations of the Medina Group, in the subsurface of northwestern Pennsylvania, depart from previous Medina models in three ways:

1. The Cabot Head shale is interpreted as an outer-shelf mud belt rather than a prodelta mud. This interpretation is supported by geometry, fossil content, trace fossils, and vertical position in the stratigraphic sequence.
2. Sandstones in the Cabot Head Shale are interpreted as offshore sand bars rather than as distributary channel sands. This interpretation is based on geometry, trace fossils, authigenic mineralogy, textural maturity, sedimentary structures, grain-size trend, and vertical assemblage.
3. The Grimsby Sandstone is interpreted as a mixed littoral, fluvial, and tidal plain deposit. Small deltaic deposits are described, which formed through rapid and ephemeral deposition rather than through continuous deposition in a large delta complex.

References Cited

- Berry, W. B. N. and A. J. Boucot, 1970, Correlation of the North American Silurian Rocks: Geol. Soc. Amer., Spec. Paper 102, 289 p.
- Brett, C. E., 1982, Stratigraphy and facies relationships of Silurian (Wenlockian) Rochester Shale: Layer-cake geology reinterpreted (abs.): AAPG Bull., v. 66, p. 1165.
- Coleman, J. M., 1976, Deltas: Processes of Deposition and Models for Exploration: Continuing Ed. Pub. Co., Inc., Champaign, IL, 102 p.
- Cotter, E., 1982, Tuscarora Formation of Pennsylvania: SEPM, Eastern Sect. Guidebook, 1982 Field Trip, 105 p.
- _____, 1983, Shelf, Paralic, and Fluvial Environments and Eustatic Sea-Level Fluctuations in the Origin of the Tuscarora Formation (Lower Silurian) of Central Pennsylvania: Jour. Sed. Pet., v. 53, no. 1, p. 25.
- Curray, J. R., F. J. Emmel and P. J. S. Crampton, 1969, Holocene history of a strandplain, lagoonal coast, Nayarit, Mexico: in A. A. Castaneres and F. B. Phleger, editors, Coastal Lagoons, a symposium; Univ. Nacional Aut6noma, Mexico, p. 63-100.
- Dickenson, W. R. and C. A. Suczek, 1979, Plate tectonics and sandstone compositions: AAPG Bull., v. 63, p. 2164-2182.
- Folk, R. L., 1960, Petrography and origin of the Tuscarora, Rose Hill, and Keefer formations, Lower and Middle Silurian of Eastern West Virginia: Jour. Sed. Pet., v. 30, p. 1-58.
- Harms, J. C., J. B. Southard and R. G. Walker, 1982, Structures and sequence in clastic rocks: SEPM Short Course Notes no. 9, 249 p.

Johnson, D. P., 1982, Sedimentary facies of an arid zone delta: Gascoyne Delta, western Australia: *Jour. Sed. Pet.*, v. 52, p. 547-565.

Kelley, D. R., 1966, The Kastle Medina gas field, Crawford County, in Oil and gas developments in Pennsylvania in 1965, Pennsylvania Geological Survey, 4th ser., Progress Report 172, p. 30-44.

Kelley, D. R., and W. G. McGlade, 1969, Medina and Oriskany production along the shore of Lake Erie, Pierce field, Erie County, Pennsylvania, Pennsylvania Geological Survey, 4th ser., Mineral Resource report 60, 38 p.

Knight, W. V., 1969, Historical and economic geology of Lower Silurian Clinton sandstone of northeastern Ohio: *AAPG Bull.*, v. 53, p. 1421-1452.

Laughrey, C. D., 1982, Diagenesis and secondary porosity in Medina reservoir sandstones, Athens and Geneva fields, Crawford County, Pennsylvania (abs.); *AAPG Bull.* v. 66/8, p. 1171.

_____, in press, Petrology and reservoir characteristics of the Lower Silurian Medina Group reservoir sandstones, Athens and Geneva fields, northwestern Pennsylvania: PA Geol. Survey, Min. Res. Rept.

_____ and J. Donahue, 1982, Diagenetic trends within the Tuscarora-Medina sequence in the northern Appalachians: *Proc. Appalachian Basin Indust. Assoc.*, Fall Mtg., Blacksburg, VA 13 p.

Martini, I. P., 1971, Regional analysis of sedimentology of Medina Formation (Silurian), Ontario and New York: *AAPG Bull.*, v. 55, p. 1249-1261.

Parks, J. M., R. A. Gallagher and E. Cotter, 1982, Tuscarora Sandstone (Silurian), Central Pennsylvania: Preliminary Quantitative Grain Shape Analyses of Cotter's (1982) Facies-Fluvial, Estuarine, Beach, and Marine(?) Shelf (abs.): *AAPG Bull.* v. 66, no. 8, p. 1173.

Pees, S. T., 1983, Model area describes northwestern Pennsylvania's Medina play: *Oil and Gas Journal*, May 23, 1983, p. 55.

Piotrowski, R., 1981, Geology and natural gas production of the Lower Silurian Medina Group and equivalent rock units in Pennsylvania: PA Geol. Survey, 4th ser., Min. Res. Rept. M82, 21 p.

Smith, N. D., 1970, The braided stream depositional environment: Comparison of the Platte River with some Silurian clastic rocks, north-central Appalachians, *Geological Society of America Bulletin*, v. 81, p. 2993-3013.

Smosna, R. and D. Patchen, 1978, Silurian Evolution of Central Appalachian Basin: *AAPG Bull.*, v. 62/11, p. 2308-2329.

Thompson, A. M. and W. D. Sevon, 1982, Excursion 19B: Comparative sedimentology of Paleozoic clastic wedges in the central Appalachians, U. S. A.: *Intl. Assoc. Sedimentologists*, 11th Intl. Congr. Sed., Hamilton, Ontario, 136 p.

Yeakel, L. S., Jr., 1962, Tuscarora, Juniata, and Bald Eagle paleocurrents and paleogeography in the Central Appalachians: *Geol. Soc. Amer. Bull.*, v. 73, p. 1515-1540.

Ziegler, A. M. and others, 1977, Silurian continental distributions, paleogeography, climatology, and biogeography: *Tectonophysics*, v. 40, p. 13-51.

**ROAD LOG AND STOP DESCRIPTION
FIRST DAY - FRIDAY, SEPTEMBER 30, 1983**

<u>Miles</u>	<u>Interval</u>	
0.0		Danville Interchange, Interstate 80 entrance to Sheraton Inn on secondary road East of PA 54. Drive west to PA 54.
0.2	0.2	Intersection PA 54, turn left (south).
0.8	0.6	Outcrop of Moyer Ridge Member of Bloomsburg Formation on left dipping 25° north.
0.9	0.1	Intersection PA 642 on right, continue ahead on PA 54.
1.2	0.3	Intersection PA 642 on left, continue ahead on PA 54.
1.4	0.2	Outcrop of Rose Hill Formation on left.
1.5	0.1	Outcrop of hematitic sandstone bed in Rose Hill Formation on left. Dip is 10° north.
1.8	0.3	Crossing axis of Montour Ridge anticline.
2.1	0.3	Large outcrop of Rose Hill Formation on left, dipping 15° south.
2.6	0.5	Junction with U.S. 11; turn right (south).
3.5	0.9	Bald Top Road on right, Rose Hill Formation with bedding dipping 20° south. Spaced cleavage dips 40° south. This small 20° angle between cleavage and bedding is characteristic of the south limb of the Montour Ridge Anticline in this region.
4.0	0.5	Two small creeks on right flow in gorges cut into uppermost Tuscarora Formation (Castanea Member). Additional Tuscarora exposures occur on the right for the next half mile.
5.0	0.5	Pull off to right at Stop I; vehicles will go ahead, turn around, and park .3 miles ahead at far end of exposure.

STOP I. DANVILLE

This fine exposure owes its presence to the incision of a northward-sweeping bend of the Susquehanna River into the south flank of Montour Ridge (Figs. 1, I-6). The succession exposed here ranges from the central part of the Middle Silurian Rose Hill Formation through to the upper part of the Upper Silurian Bloomsburg Formation. The order of consideration will be that Cotter will initially deal with the sedimentological interpretation of units from the upper Rose Hill through to the upper Mifflintown Formation. From that point, Nickelsen will focus on the structural complexities in the upper Mifflintown and the Bloomsburg Formations.

Please be cautions! Traffic is commonly heavy and moving very fast. Stay off the paved road surface.

SEDIMENTOLOGY

Of the ten informal Middle Silurian units (see earlier section of guidebook), this outcrop proceeds uninterruptedly from just below Unit 4 through Unit 10, and then through most of the Bloomsburg. If you have not had time to read the section of the guidebook on the Rose Hill, Keefer, and Mifflintown Formations, it will prove helpful to go over the summary "Genesis of the Middle Silurian Succession". This locality can be assigned a position on the lithofacies framework diagram (Fig. 7) slightly to the left of the vertical row of unit numbers. That means that we are in what was the transitional area of the shelf, between the marginal shelf sand facies and the central mud facies (Fig. 8). During times of lowered sea level, the marginal shelf sand facies encroached northwestward toward the basin axis, leading to deposition of higher-energy monolithic units (Units 4,6). At other times, the area (this locality) was the site of low-energy mud

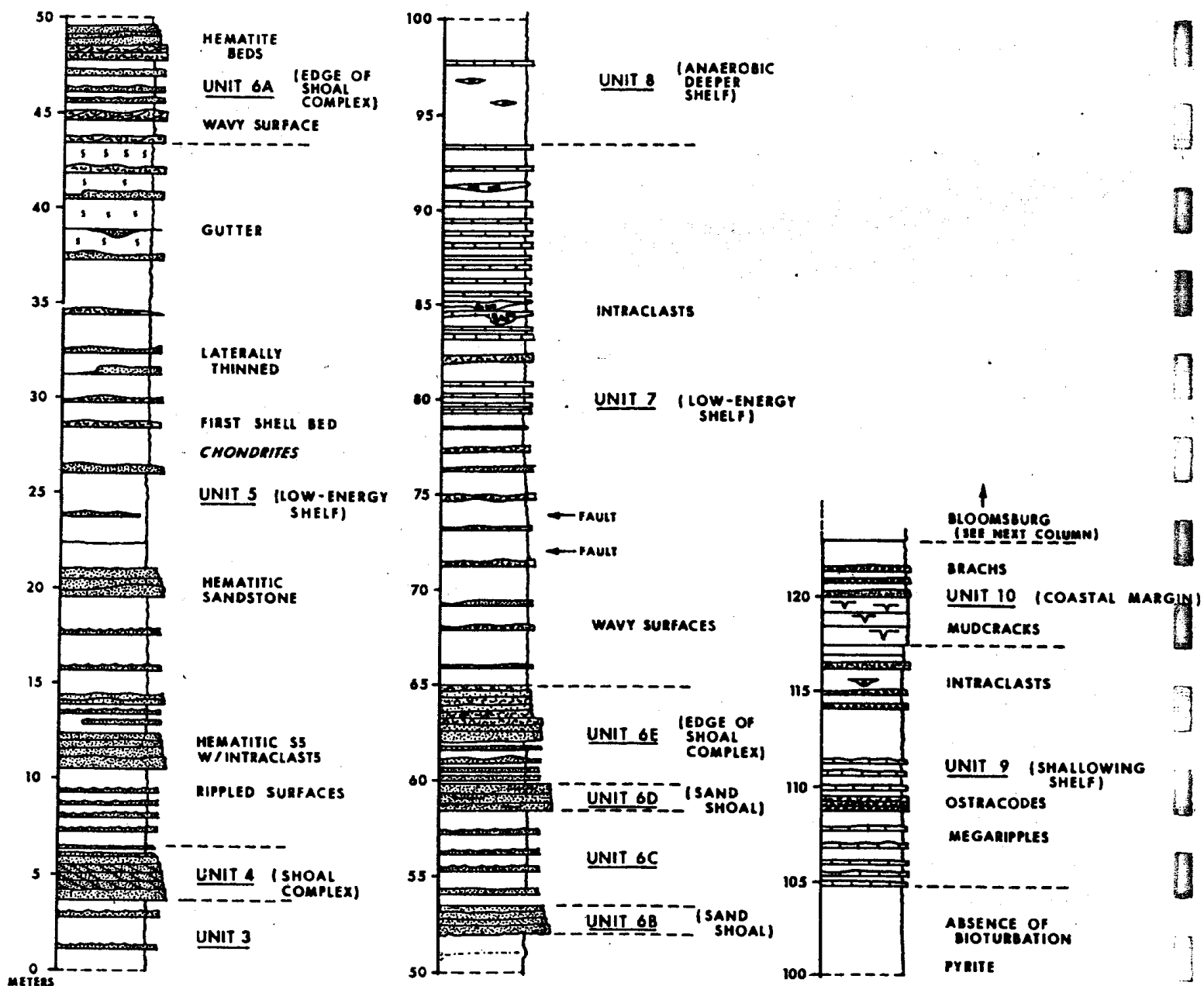


Figure I-1

Stratigraphic column, Middle Silurian units at Stop I, Danville, PA. White background is mudrock; symbols as usually understood; some features marked.

deposition, interrupted periodically by storm-generated influxes of sand and/or shell debris from the marginal shoals (Units 5,7,9). At a time of exceptionally higher sea level, the muds characteristic of the central mud facies were interrupted less frequently by storm deposits, and more monolithic black shale (Unit 8) accumulated.

The following outline of the principal features and conditions of origin of each of the informal units will permit you to guide yourself through this section. Signs placed on the outcrop at unit and subunit boundaries will orient you to stratigraphic position on the column of Figure I-1. You might disagree with the specific placement of some of these boundaries, yet most of them involve necessary arbitrary decisions at gradual and interfingering transitions.

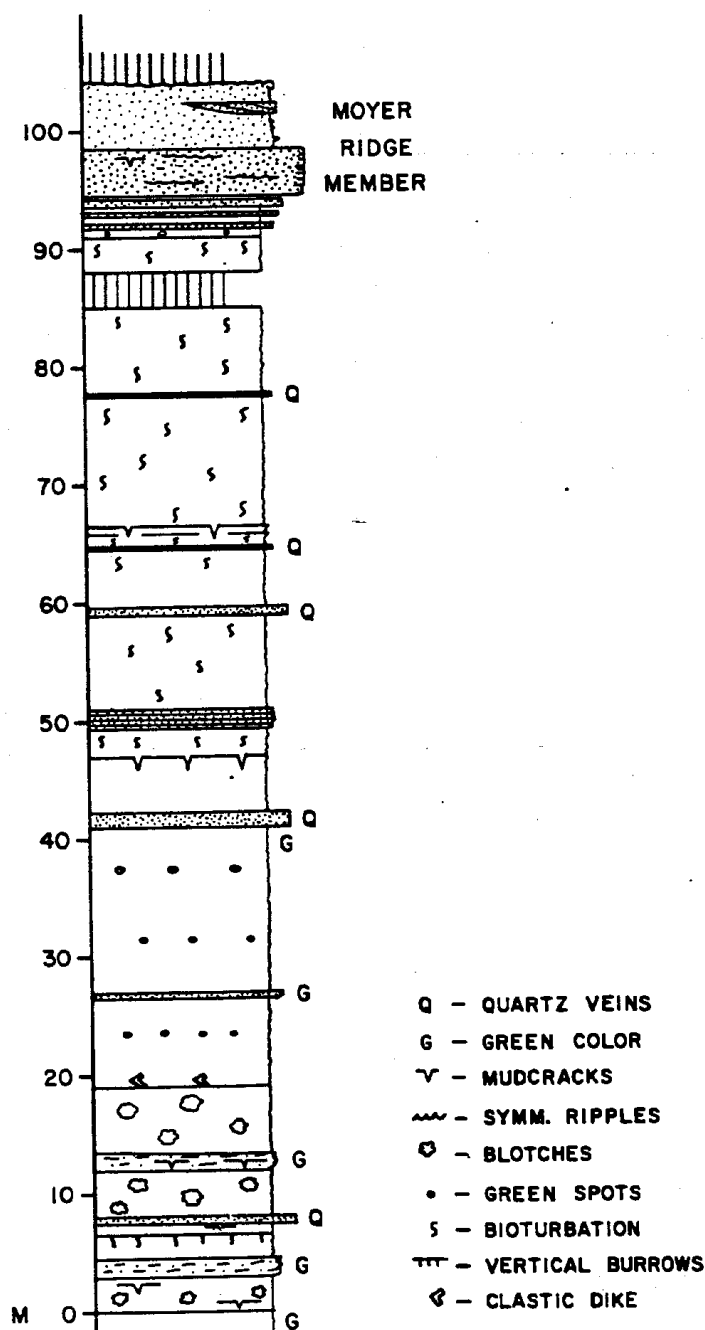



Figure I-2

Stratigraphic column, Bloomsburg Formation (Upper Silurian) at Stop I, Danville, PA.

Figure I-3

Features of storm beds in Middle Silurian sequence at Stop I, Danville, PA. Scale in A, B, and C is 15.2 cm long; in D each color bar is one cm.

- A. Interference ripples and horizontal biogenic structure (feeding tunnel?); lower half of Unit 5 (Upper shaly member, Rose Hill Formation).**
 - B. Straighter crests and longer wavelengths on symmetrical ripples on hematitic sandstone; base of Unit 5 (Upper shaly mbr., Rose Hill Fr.).**
 - C. Parallel laminated sandstone bed with rippled top intercalated within green fissile mudrock; lower part of Unit 5 at about 8 m (Fig. I-1).**
 - D. Sawed face transverse to individual storm bed; Unit 6C. Two laminasets; upper one has laminae parallel to internal discontinuity. Small white blebs are crinoid ossicles. Surface of bed weakly rippled and disrupted by large burrower.**
- 

The varieties of bed geometries and internal structures of the coarser-grained beds that are shown diagrammatically on the stratigraphic column (Fig. I-1) are organized by structural type on Figure 9. An idealized, composite storm bed (see discussion in earlier section of guidebook) based on the coarser-grained beds at this locality is shown as Figure 10 in that earlier discussion. Photographs of some of the features of this exposure are shown in Figures I-3, I-4.

MIDDLE SILURIAN UNITS, U.S. ROUTE 11, DANVILLE

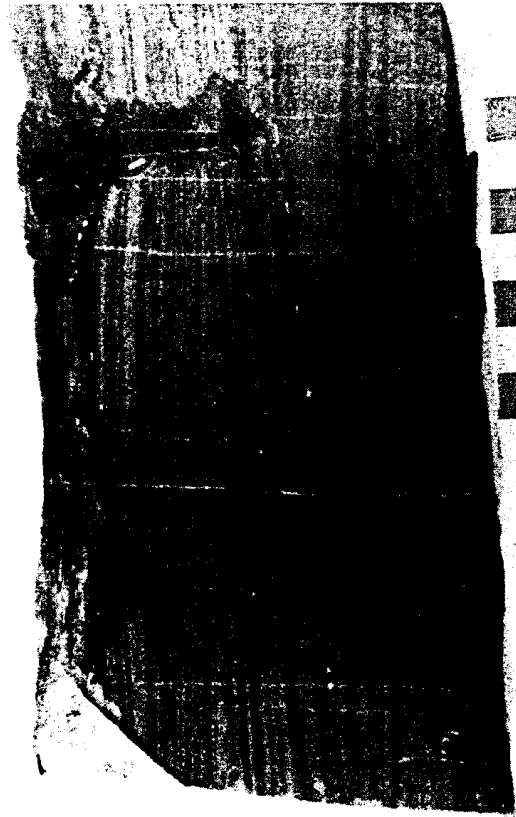
UNIT 4 (Center Member, Rose Hill Formation)

Features: Maroon-red hematitic sandstone; fine-to medium-grained; sorting poor to moderate; some quartz granules.
Mudrock intraclasts (both green and red) concentrated on bed boundaries; some internal mud drapes.
Interbedded fissile mudrock increases toward top.
Largely cross-laminated in tabular and lenticular beds; transport toward NW and N.
Symmetrical ripples on thinner sandstone beds in interbedded upper part.

Conditions of Origin: Megarippled shelf shoal complex.
Higher-energy traction transport of sand megaripples at a time of lowered sea level.
Agitation sufficient to accrete iron oxides to host grains.
Gradual reduction of energy levels as shelf became deeper; result of sea level rise and/or greater subsidence.



B



D



A



C

Figure I-4

Features of storm beds and rock cleavage in Middle Silurian sequence, Danville, PA. Scale in A, B, and C is 15.2 cm. In D, width of photo is 0.6 mm.

- A. Wavy-topped bioclastic limestone (skeletal grainstone) in upper part of Unit 5.
- B. Pronounced lateral thinning of sandstone bed; Unit 5 at 41 m (Fig. I-1).
- C. One half of gutter structure in Unit 5 at 39 m (Fig. I-1).
- D. Strongly cleaved McKenzie Limestone Member of Mifflintown Formation; bottom of Unit 9. The rock cleavage (E-W) is a spaced, pressure solution cleavage defined by flattened quartz and calcite grains and by dark, clay-carbon partings. Bedding (NW-SE) is marked by a deformed fossil. Partly crossed nicols. Field width 0.6 mm.

UNIT 5 (Most of upper shaly member, Rose Hill Formation)

Features: Mud-dominated and mixed heterolithic associations.

Mudrock is olive gray, mostly fissile; thin zones bioturbated, some reddish. Chondrites noted; few body fossils.

Coarser beds are sandstone (lower part) and sandstone and bioclastic limestone (upper part).

Two major styles of coarse-grained beds:

- 1) Rippled upper surfaces (Category A of Fig. 9); usually parallel base and top; variety of internal lamination, as shown in Fig. I-3.
- 2) Broadly arched (hummocky) upper surfaces (Category B of Fig. 9); bases flat; variety of internal lamination; more commonly bioclastic ls.

Additional styles of beds:

- 3) Channelforms - gutters (Fig. 9E); filled either with parallel lam. ss. (as at 38 m) or bioclastic ls. (as at 44.5 m).
- 4) Laterally thinned or terminated; examples at 12.3 m (above road), 34 m, 41 m (See Fig. 9F).

First bioclastic limestone is at 29 m.

First hematitized bioclastic limestone is at 35.5 m.

Contains zones of hematitic sandstone similar to that of Unit 4; these zones (as near 12 m and 20 m) judged too thin and separated to be grouped with Unit 4.

Conditions of Origin: Low-energy, slightly deeper marine shelf.

Placid, slow accumulation of mud in dysaerobic conditions below normal zone of wave agitation.

Periodic storm-generated, wind-driven currents flush storm beds from marginal shelf shoals toward deeper axial part of basin (Fig. 8).

Some marginal shoals were sandy, others had well-developed shelly fauna, others mixed.

Iron mineralization accomplished in oxidizing conditions of the marginal shoals; flushed to deeper water with the storm beds.

UNIT 6 (uppermost Rose Hill, Keefer, and lowermost Mifflintown Fms.)

These strata are grouped in Unit 6 in which there is evidence of persistent traction currents having caused lateral migration of larger, megaripple-like bed forms. Subunits of Unit 6 are defined largely on basis of compositional differences.



B



D




A



C

Figure I-5

Photomicrographs of varieties of hematite and chamosite from the same skeletal grainstone bed, Unit 6A, Allenwood, PA, along U.S. 11. A, B, and C are from same thin section, D from 10 cm higher in same bed. Narrow dimension of each photo equals 3.7 mm.

- A. Hematite coats crinoid ossicles; thin section Kf-4b.
 - B. Chamosite coats crinoid ossicles; Section Kf-4b.
 - C. Skeletal grain with meniscus-like coatings of chamosite (lighter bands) and hematite (darker bands); Section Kf-4b.
 - D. Secondary bladed hematite; Section Kf-4d.
- 

UNIT 6A Mixed heterolithic; mudrock with ss. and bioclastic ls.

Features: Mudrock; becomes gray within 1 m of base of subunit; biogenic reworking more common than below.

Coarser beds:

- 1) Cross-laminated bioclastic limestones; include compound and reactivated (Fig. 9C); composed largely of robust brachs and crinoids, some mudrock intraclasts.
- 2) Storm beds similar to those of Unit 5; both symmetrically rippled tops (Fig. 9) and arched hummocklike tops (Fig. 9); also laterally thinned, but less pronounced (Fig. 9); more burrowing down into tops of storm beds.

Hematite and chamosite common and abundant, particularly in bioclastic ls; patterns in individual beds complex; contains Danville Ore Bed.

Contains vertical patterns of both fining-upward and coarsening-upward sequences.

Conditions of Origin: Edge of megarippled shelf shoal complex.

Persistent and largely coast-parallel current caused lateral migration of shell debris megaripples.

Other times of storm bed accumulation, deriving sediment from the megarippled shoals.

Hematitization and chamositization accomplished in agitated conditions of the megarippled shoals.

UNIT 6B Monolithic quartz sandstone.

Features: Very fine-grained; carbonate-cemented; scattered small crinoid ossicles.

Base faulted (ball-and-pillow); interior structureless.

Above basal bed, increasing abundance of thin shales draped over wavy and rippled sandstone surfaces.

Some burrowing down into tops of sandstone beds, several thinner beds more extensively mottled.

Conditions of Origin: Margin of winnowed sand shoal.

Sand emplaced rapidly over muddy substrate, followed by gradual slight deepening and return to storm bed accumulation.



B



D



A



C

UNIT 6C Mixed heterolithic to mud-dominated heterolithic.

Features: Mudrock is medium gray and silty; about half fissile and half slightly burrowed.
Sandstones have sharp bases, wavy or interference rippled tops; internal laminae are horizontal and/or broadly arched (hummocky) (Fig. 9); varieties shown on Fig. I-3.
Beds commonly 1-2 cm, up to 6-8 cm; thinner beds more mottled, others have shafts into upper part only (Fig. I-3D).
Crinoid ossicles strewn along laminae.

Conditions of Origin: Lower-energy subtidal; below normal agitation level.
Periods of quiescence interrupted by influx of storm beds, probably from adjacent shelf sand shoals.

UNIT 6D Monolithic quartz sandstone.

Features: Quartz arenite; fine-grained, well-sorted, ankerite-cemented.
Blocky, laterally continuous beds with slight mud coatings at several laterally continuous partings; slow broad swales.
Appears massive, but has small-scale symmetrical ripple lamination at numerous levels; top surface shows complex interference ripple pattern.
Near top some broken skeletal material and small intraclasts in a 1 cm band.

Conditions of Origin: Symmetrically rippled sand shoal.
Nearly continuously in zone of wave agitation; sand winnowed and sorted.
Periodic penecontemporaneous broad scour events, possibly related to storms.

UNIT 6E Sand-dominated to mixed heterolithic associations.

Features: Basal part mostly thin-bedded sandstone with broadly arched and symmetrically rippled surfaces (Fig. 9A, B); laminae horizontal and broadly wavy (hummocky); horoz. biog. structures on surfaces.
Through unit, increasing proportion of mudrock and change in composition of coarser beds to bioclastic limestones; thinner-bedded toward unit top.
Some beds graded, with basal shell lags; other beds laterally pinch and swell (Fig. 9, Type B2) like starved hummocks.
Slight iron content in some bioclastic limestones.

Conditions of Origin: Edge of shelf shoal; below normal wave-agitation during fair weather. Rapid introduction of storm beds, at first from marginal sand shoals; subsequently from organic shoal, possibly related to margin of sand shoal (see Fig. 8).

UNIT 7 Mud-dominated heterolithic association (includes lithologies called Rochester and lower part of McKenzie -- parts of Mifflintown Formation).

Features: Medium gray, fissile mudrock; calcareous above 79 m.
Coarse beds in lower part (up to 79 m): bioclastic ls. and thin ss (some composite - Fig. 9, Type A6), bed tops wavy; interference patterns uncommon. (This part equivalent to Rochester)
Coarse beds in upper part (79 m-93 m: bioclastic ls., intraclastic ls., and micrite; some large *Favosites*; contorted and convoluted bed in center; toward top largely micrites. Some discontinuous intraclast beds. Upper bed surfaces less wavy than below.

Conditions of Origin: Slightly deeper shelf; lower energy.

Most of time, tranquil mud accumulation, little oxygen.

Periodic storm bed emplacement; some ripping up of clasts; some induced slumping.

Change of composition of both mudrock and coarse sediment above 79 m indicates final waning of Taconic source terrain and local, subtidal origin of much of the mud and all of the coarse sediment. Any shelf shoals now likely to be organic shell banks, bioherms, or oolite shoals.

UNIT 8 Monolithic black shale.

Features: Medium gray to black, fissile, pyritic shale.

Lower and upper part calcareous; one meter at center (99-100 m) noncalcareous.

Very thin beds of micrite and ostracod-rich skeletal wackestone, packstone, and grainstone.

Conditions of Origin: Anaerobic deeper shelf.

Tranquil mud deposition; few storm beds, transported in coarser sand-sized shell fragments from shallower water.

Water composition likely to have changed to brackish - absence of stenohaline organisms.

UNIT 9 Mud-dominated and mixed heterolithic carbonates.

Features: Calcareous mudrock, largely fissile, but with zones of small-scale burrowing (Chondrites).

Coarser-grained beds: nearly all are ostracod coquinas; some are structureless micrite; composite beds (Fig. 9, Type A6) with basal ostracod lags and micritic tops.

Internal lamination (where noted) is horiz., parallel; most show no structures.

Coarse bed top surfaces are both broadly wavy and symmetrically rippled (some interference).

Thin beds of intraformational conglomerate.

Several channelform gutters with shell debris.

In last few meters, several brachiopod-rich bioclastic limestones.

Conditions of Deposition: Shallowing deeper shelf.

Calcareous mud accumulates for long periods in low-energy setting.

Periodic rapid influxes of shallower-water sediment (mud, ostracod valves, brachiopods), with structural patterns identical to storm beds.

UNIT 10 Transitional heterolithic

Features: Lower part - transition to greenish mudrock (noncalcareous) with desiccation cracks (begin at 118 m) and to red Bloomsburg-like mudrock.

Middle part - medium-gray fissile, noncalcareous shale with thin, brachiopod-rich bioclastic limestones; shell beds similar to those at top of Unit 9.

Upper part - transition in composition and color to Bloomsburg Formation; mixed Chondrites - burrowed and desiccated mudrock.

Conditions of Origin: Low-energy coastal margin. Mud-dominant coast with little evidence of wave or tidal activity.

BLOOMSBURG FORMATION

The Bloomsburg Formation has received little sedimentological study since Hoskins (1961) demonstrated that the formation is not all featureless mudrock. Hoskins' conclusion (1961, p. 103-105) that the Bloomsburg was rapidly deposited in a brackish paralic zone along a prograding low-energy coast continues to be the dominant model for the environmental interpretation (see, e.g., Faill and Wells 1974, p. 49). Red muds were fed to this prograding coast by a network of sluggish streams (de Windt, 1973).

At Danville, the Bloomsburg can be considered in three parts, each approximately roughly a third of the formation thickness. General features are shown on the column of Figure I-2.

A. Bottom Third (to about 40 m)

Largely red mudrock, but with some green mudrock zones. Thin beds of green (and some red) sandstone and coarse siltstone are spaced through the mudrock; some are readily located because they have conspicuous quartz veins. Desiccation cracks are common. The "clastic dikes" found just below 20 m (see Structural Geology Station F, below) are fillings of such mud cracks. Long vertical burrows are present in some of the mudrocks.

Many of the detailed features of the mudrock are related to soil characteristics. Platy and blocky fractures indicate incipient ped generation, and there are various degrees of caliche nodule development (called "blotches" on the column of Fig. I-2). The curved, slickensided surfaces characteristic of many Bloomsburg exposures are poorly exhibited here (see Stop V, Watsontown). These characteristics show that sediment accumulation took place under conditions of alternate wet and dry seasons, with the dry season relatively pronounced (Buol and others, 1980, p. 232). Central Pennsylvania at this time was approaching the distinctly arid conditions shown by features of the Wills Creek and Tonoloway Formation above the Bloomsburg, so it is not surprising to find evidence of a pronounced dry season during Bloomsburg time.

B. Middle Third (from about 40 to about 85 m)

This red mudrock appears largely bioturbated and structureless. Green coloration is absent (in both mudrock and sandstones; also no green reduction spots). Desiccation cracks are much less common, and soil-generated features are difficult to find.

C. Upper Third (above about 85 m)

With the approach of the Moyer Ridge Sandstone Member, small, 1-2 mm diameter, green reduction spots can be found in sandstone (see Structural Geology Station I, below). The sandstone beds themselves are relatively structureless, aside from some symmetrical wave-generated ripples. The very short spacing (wave-length) of these ripples indicates that water depths were extremely shallow. This agrees with the appearance of desiccation cracks in associated beds.

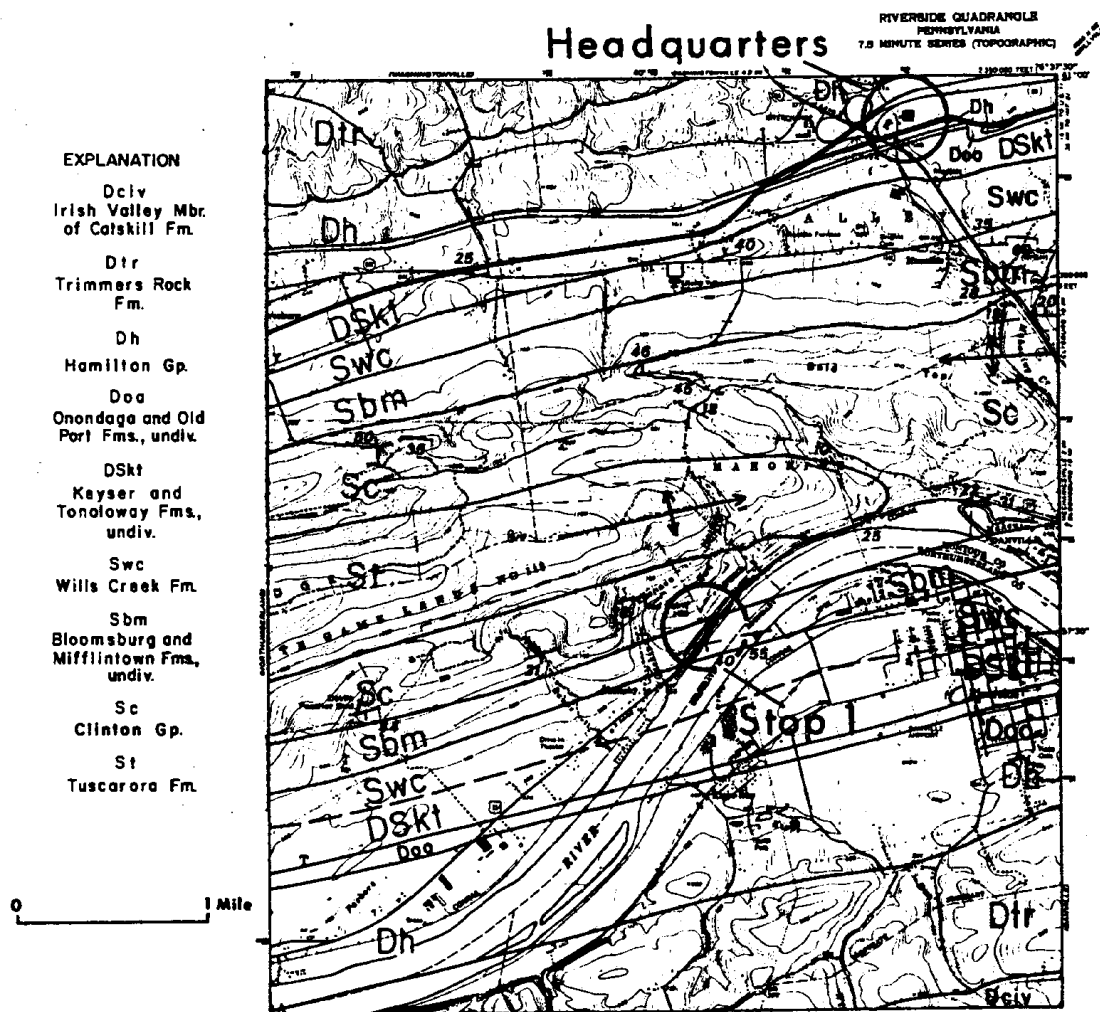


Figure I-6

Geologic map of Berwick Anticlinorium near Stop 1, modified from Berg and Dodge (1981).

STRUCTURAL GEOLOGY

This apparently simple structural setting of rock cleavage dipping more steeply than uniformly south-dipping bedding on a limb of the Berwick anticlinorium (Fig. I-6, 7) is a good introduction to some of the subtle structural complexities of the region. There is more here than a casual observer might observe. Perhaps a careful look will provide a solution to the questions that a number of perceptive geologists have carried with them from this outcrop.

1. What is unique about this outcrop?
 - A. The angle between bedding and cleavage ($10-20^\circ$) is smaller than elsewhere in the region except other outcrops on the south limb of the Berwick anticlinorium. This fact plus better cleavage than elsewhere suggests this is an environment of large finite strain, which doesn't extend across the anticline to the same rocks on the north limb.
 - B. Cleavage transects sandstone dikes which were mudcrack fillings formerly approximately perpendicular to bedding. The sandstone dikes are now rotated clockwise so they intersect bedding at $45-55^\circ$. Normally, throughout the rest

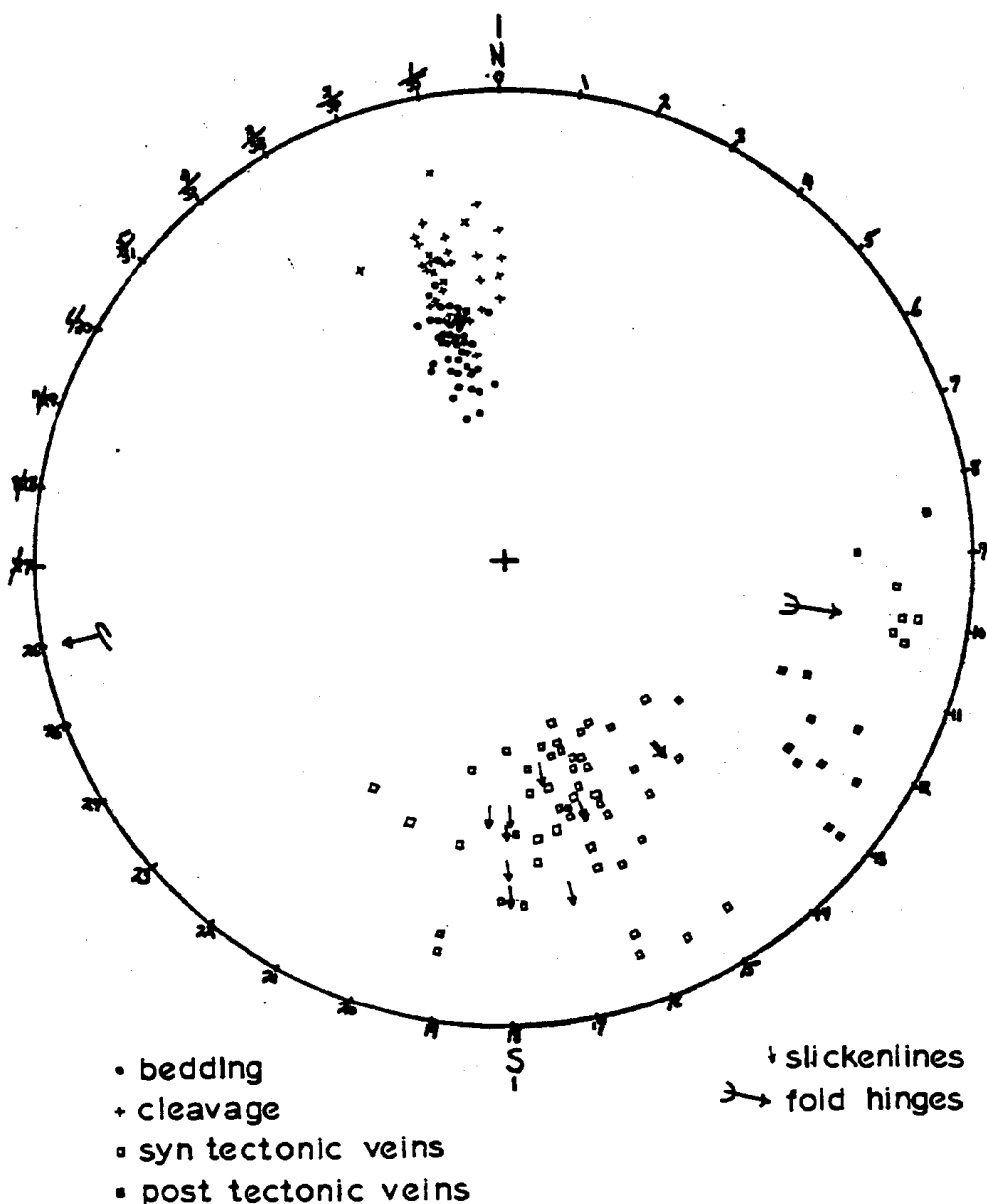


Figure I-7

Lower hemisphere, equal area stereographic projection of structural data at Stop I.

of the region where the bedding-cleavage angles are greater than 60° , cleavage parallels mudcrack fillings. At this locality mudcrack fillings have been folded (shortened) either: 1. during pre-tectonic sedimentary compaction or 2. during tectonic shortening perpendicular to cleavage.

- C. Reduction spots are either highly deformed $x:y:z = 1.4:1:47$ or only slightly flattened in an s-plane depending upon rock type or, perhaps, structural position.
- D. Calcite veins in the Mifflintown Formation and quartz veins in the Bloomsburg Formation were emplaced pre, syn, and post-tectonically with respect to flexural-slip folding and the formation of rock cleavage. Pre- or syn- tectonic veins have been rotated clockwise and counter-clockwise either by simple shear or pure shear pressure solution providing conflicting evidence of the geometry of progressive deformation that shaped the rock.

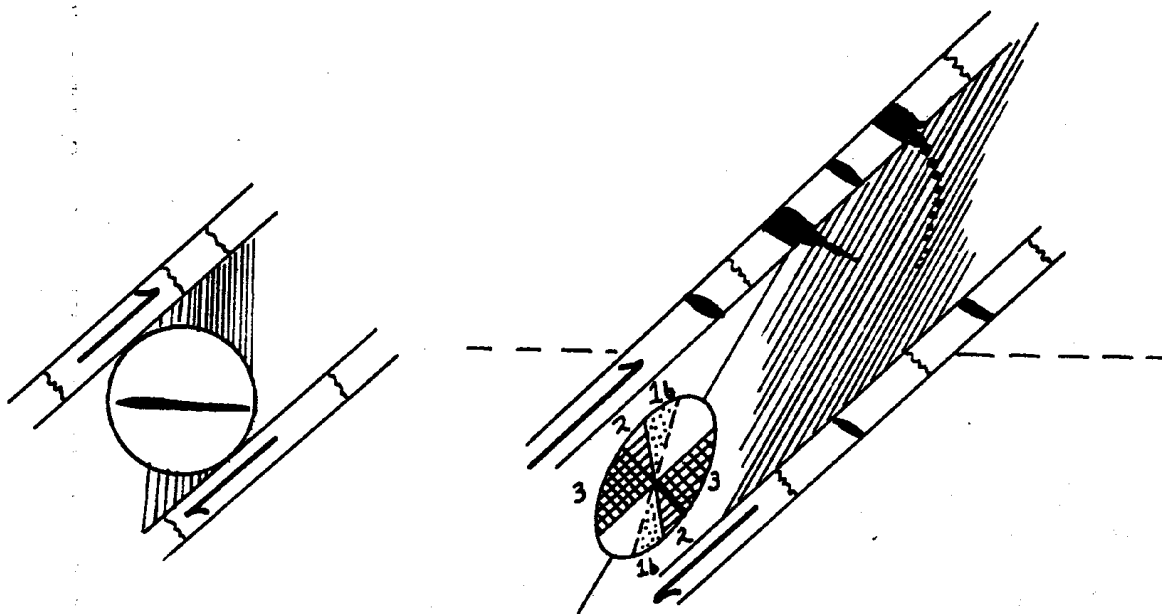


Figure I-8

Schematic drawing of rotated and extended veins at Stations B, C, and D resulting from progressive deformation, in this case a clockwise simple shear.

Description of Stations

Structural features to be observed here are: bedding, spaced cleavage, a reverse fault with associated drag folds, bedding plane slickenlines formed during flexural slip folding, several generations of joints filled with quartz or calcite veins, pre-cleavage veins rotated clockwise or counterclockwise, reduction spots, deformed and undeformed, undeformed mud crack polygons and burrows viewed on bedding planes, and rotated, folded, and transected (by cleavage) sandstone dikes. Stations A to I where these features may be observed have been marked on the outcrop and are described below:

Station A: Drag folds in both the hanging and foot wall of this small fault have two cleavages; 1. the more penetrative cleavage exposed elsewhere in the outcrop that intersects bedding at an angle of 20° and, 2. a more widely spaced (3-7 mm) fracture cleavage parallel to the axial surface of the drag folds.

Station B: Many of the calcite veins here strike $60-90^\circ$ and are gash veins concentrated in a horizontal shear zone along which the upper part of the outcrop has been thrust N or NW over the lower part (Fig. I-13). As the veins pass from brittle limestone to ductile shale beds they thin or change to multiple veins and show evidence of pressure solution and rotation. Progressive deformation by rotational simple shear has first caused shortening by pressure solution perpendicular to the veins in shale and then clockwise rotation and stretching as the veins passed from Zone 3 (compression) to Zones 2 and 1b (compression followed by extension) (Fig. I-8). Veins that don't show clockwise rotation either stayed within Zone 3 or were formed after the main period of flexural slip folding and cleavage formation. Several thick, strongly cleaved shale beds contain pressure solved remnants of gash veins that appear as though they may have rotated counterclockwise, suggesting non-rotational progressive deformation by pure shear in some beds (Fig. I-13).

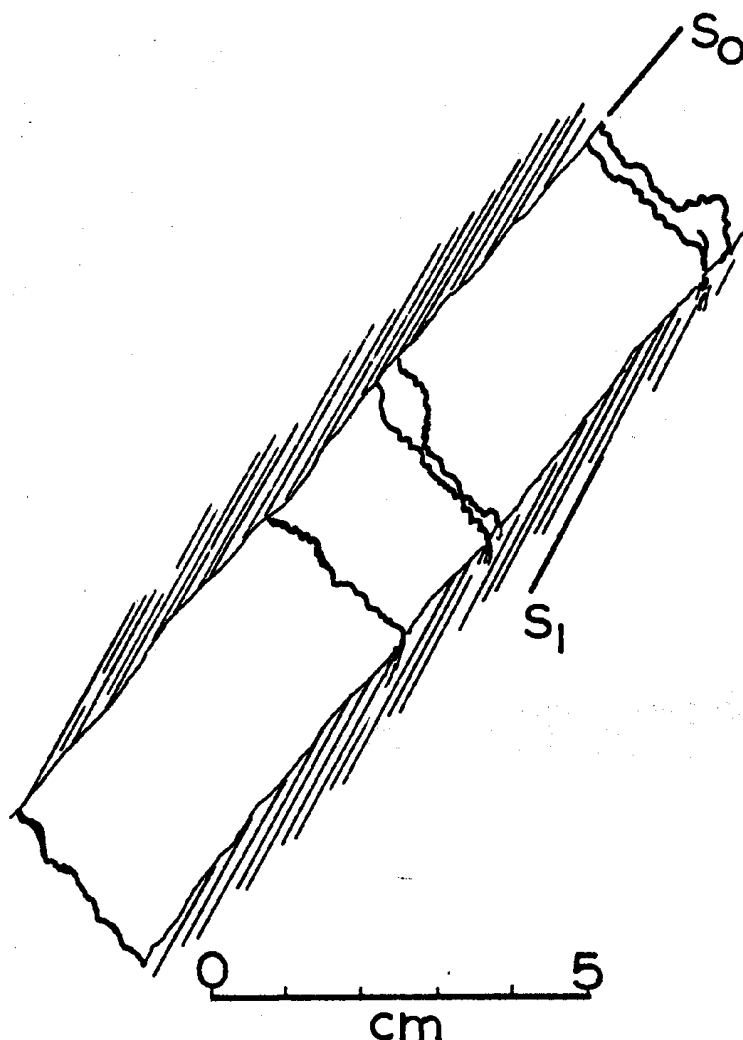


Figure I-9

Drawing of a hand specimen of interbedded fine-grained silty limestone and limy well-cleaved shale. Irregular, stylolitic, pressure solution cleavage in limestone is presumably a relic of layer parallel shortening in horizontal beds. (S_0) The strong refracted cleavage in limy shale (S_1) results from progressive simple shear during flexural slip folding.

Stations C and D: There are additional examples of veins that have been pressure solved and rotated clockwise during progressive simple shear. Figure I-9 drawn from a hand specimen collected here shows irregular pressure solution planes perpendicular to bedding in a limestone and the refracted cleavage in the limy shale bed intersecting bedding at only 10° (Fig. I-4D). This rock experienced layer parallel shortening before folding followed by the buckling, flexural-slip, jointing, and progressive simple shear that produced the pervasive cleavage in shales and the rotation of early calcite veins.

Station E: Two prominent sets of calcite veins can be structurally differentiated and placed in relative sequence. Calcite veins striking 65° at this station have been rotated at each shale layer by clockwise simple shear, indicating that they were emplaced before flexural-slip folding and development of cleavage were completed (Fig. I-10). During progressive rotational deformation the veins in shale passed from Zone 3 (compression) to Zone 2 or 1b (extension) with the result that they are

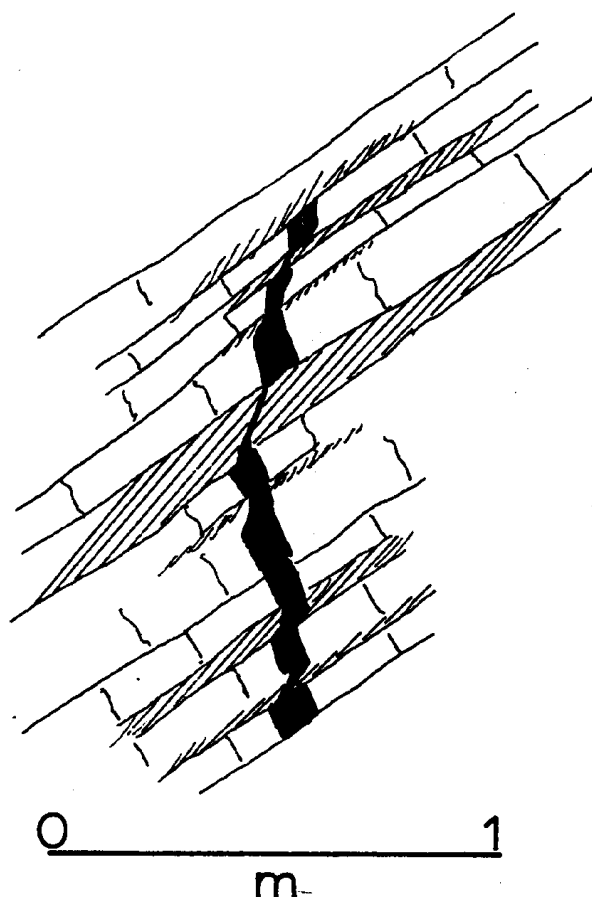


Figure I-10

Drawing of pre- or syn-tectonic calcite veins at Station E showing clockwise rotation at shale layers during cleavage formation in simple shear.

thinned, stretched, and slickenlined (Az. 142°). It is probably that veins in shale were not as thick initially as veins in limestone beds.

The other prominent set of calcite veins striking 30° is postfolding because it passes through all beds without deflection.

In one brittle limestone bed, 20 cm thick, the early 65° vein is joined by other early veins striking 10° and 300° to allow simultaneous extension in several directions, yielding incipient "chocolate table" boudinage. As would be expected here, bedding lies within Zone 1 (elongation) of the finite strain ellipse.

Conodonts collected at this locality have CAI $4\frac{1}{2}$ (A, Harris, personal communication, 1981) which suggests heating to the upper end of the range $190-300^{\circ}\text{C}$ (Epstein, et al, 1977). Both prefolding (Az. 65°) and post-folding (Az. 30°) calcite veins contain 2 phase aqueous fluid inclusions which permit estimates of their temperatures of filling. Our preliminary results for Temperature of Homogenization (T_H), Temperature of Freezing (T_F) and Temperature of Filling (T_{FF}) are:

Az 65° pre-folding vein

T_F -21° to -25.6°C , $\bar{x} = -24.6^{\circ}\text{C}$

T_H $+102.5^{\circ}\text{C}$ to $+130^{\circ}\text{C}$, $\bar{x} = +116^{\circ}\text{C}$

T_{FF} $+254^{\circ}\text{C}$ (with pressure correction)

Az 30° post-folding vein

$T_F -26.4^\circ$ to -28.7° C, $\bar{x} = -27.5^\circ$ C

$T_H +116^\circ$ C

$T_F + 304^\circ$ C (with pressure correction)¹

¹ Estimated thickness of overlying stratigraphic column at the time of the Alleghany Orogeny = 9.5 km consisting of 7 km of local, Anthracite Region, stratigraphy plus 2.5 km inferred Carboniferous and Permian (Hower and Davis, 1981). Pressure correction is assumed to be the mean of $P_c + P_p = 166$ mpascals calculated as $P_p / \text{depth} = 100$ bars/km and $P_c / \text{depth} = 250$ bars/km.

Thus, ambient temperatures during the Alleghany Orogeny derived from Conodont Color Alteration and Temperature of Homogenization measurements from syn and late tectonic veins are in good agreement. It should be pointed out, however, that incorrect estimates of stratigraphic thickness above this point (9.5 km) during the Alleghany Orogeny could result in inaccurate Temperature of Filling estimates (pressure correction accounts for 140° of the estimated Temperature of Filling). Pressure probably exceeded the mean of P_c and P_p used for this P correction and this should mean higher temperatures than those reported. On the other hand, the geothermal gradient calculated by dividing overburden thickness (9.5 km) into the two Temperatures of Filling (254° C and 304°) is 26.7° C and 32° C per km both very reasonable gradients for areas like the Appalachian Basin.

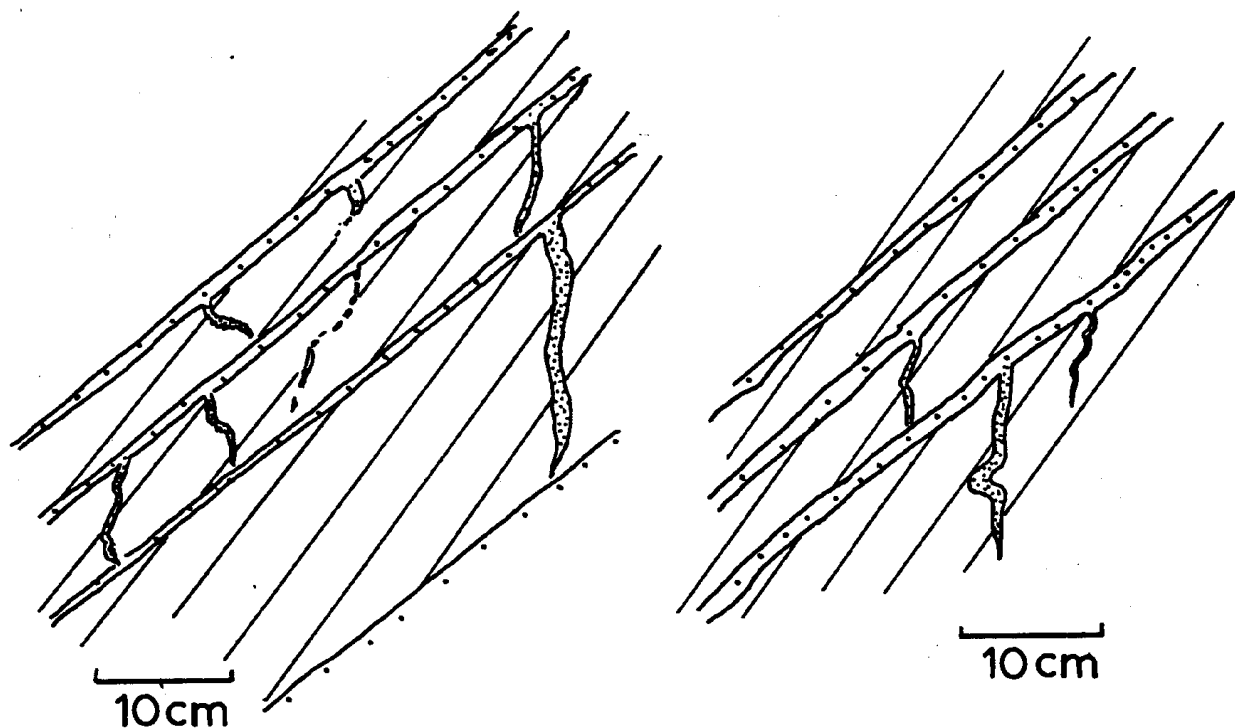


Figure I-11-A

Drawing of folded rotated and extended sandstone dikes transected by cleavage at Station E.

Station F: Sandstone dike mud crack fillings showing folding, rotation, and extension are transected by cleavage. They presumably were formed initially perpendicular to bedding. It is possible but not likely that these dikes were folded during pre-lithification and pre-tectonic sedimentary compaction. Because of the distribution

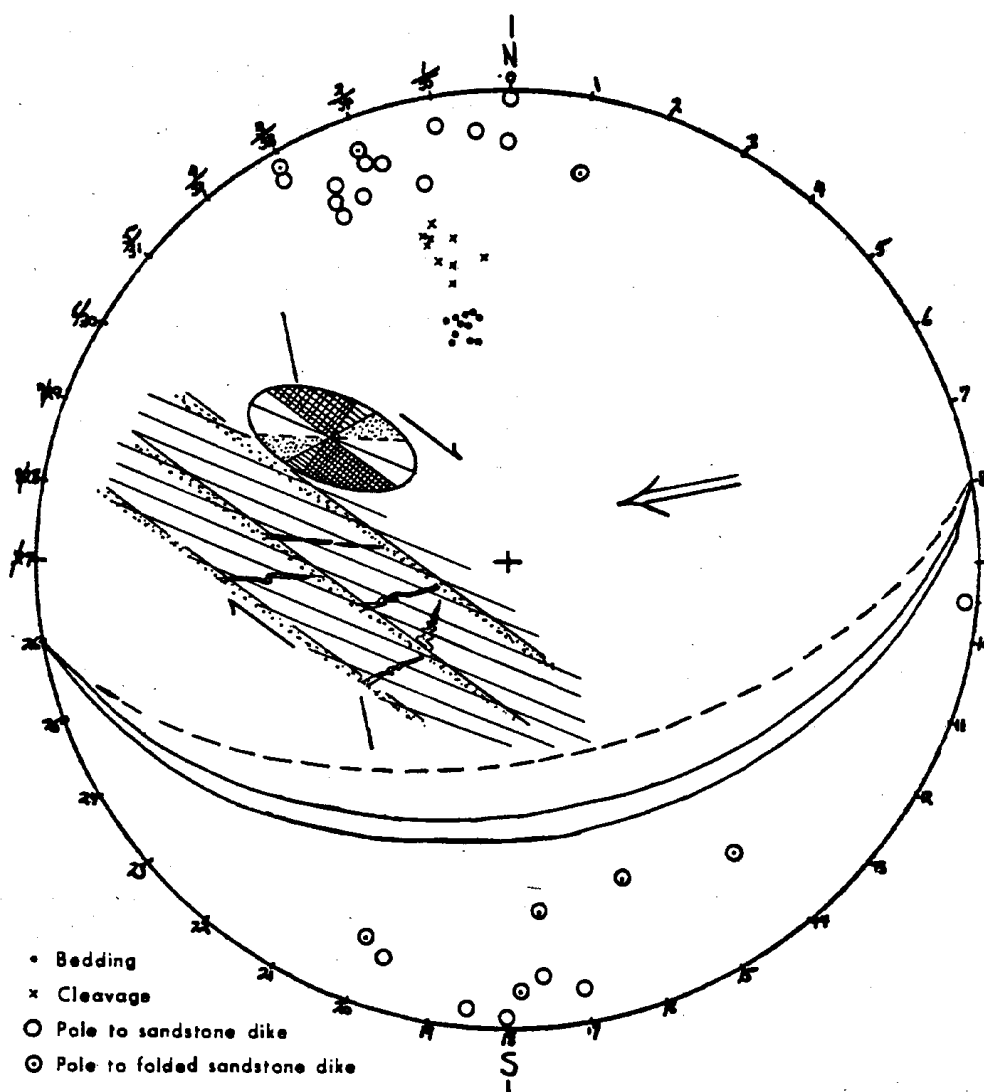


Figure I-11-B

Stereographic projection of bedding, cleavage and sandstone dikes (folded and unfolded) at Station E. Inset viewed parallel to arrow shows the progressive deformation leading to dike orientation and configurations (folded, extended).

of folded versus rotated-extended dikes shown in Figure I-11, we believe they were folded and then rotated clockwise and extended during progressive deformation by simple shear from Zone 3 to 2 or 1b as depicted in the inset sketch on the stereographic projection (Fig. I-11B).

Stations G to H: In this red mudstone, reduction spots have been deformed into triaxial ellipsoids $x > y > z$ - 1.4: 1: .47, based upon measurement of 13 three dimensional ellipsoids and 29 two dimensional sections. The x axis is oriented down the dip of the well-developed cleavage while z is perpendicular to cleavage. This station and another outcrop on Fishing Creek in Bloomsburg, PA, record the highest finite strain observed in the Bloomsburg reduction spots of the region. High strain is caused by localized simple shear due to flexural slip folding on the south limb of the Berwick Anticlinorium and must be related to the rock type between Stations G and H. Reduction spots at Station I in more sandy Bloomsburg Formation near the top of the section are only slightly deformed.

Station H: Two pre-cleavage quartz veins in this green shale have been (folded) rotated counterclockwise, and boudinaged (Fig. I-12). Unlike most of the rest of the outcrop, progressive deformation in this well-cleaved, highly-deformed green shale has lead to non-rotational pure shear or what has been called inhomogeneous bulk flattening (Bell, 1978). The quartz veins were folded in Zone 3 and then rotated and extended as they entered Zones 2 and 1b.

Station I: In the thick interval of sandy Bloomsburg Formation between Station H and Station I no definitive structures appear. At Station I many small (1 to 4 mm) reduction spots are oblate ellipsoids slightly flattened in the bedding and/or cleavage of a sandy mudstone. Sections of reduction spots in the prominent S plane are circles, the ratio of the short axis is .74. Reduction spots here are less deformed than those between Stations G and H, probably because of stiffer rock type, perhaps because of structural position.

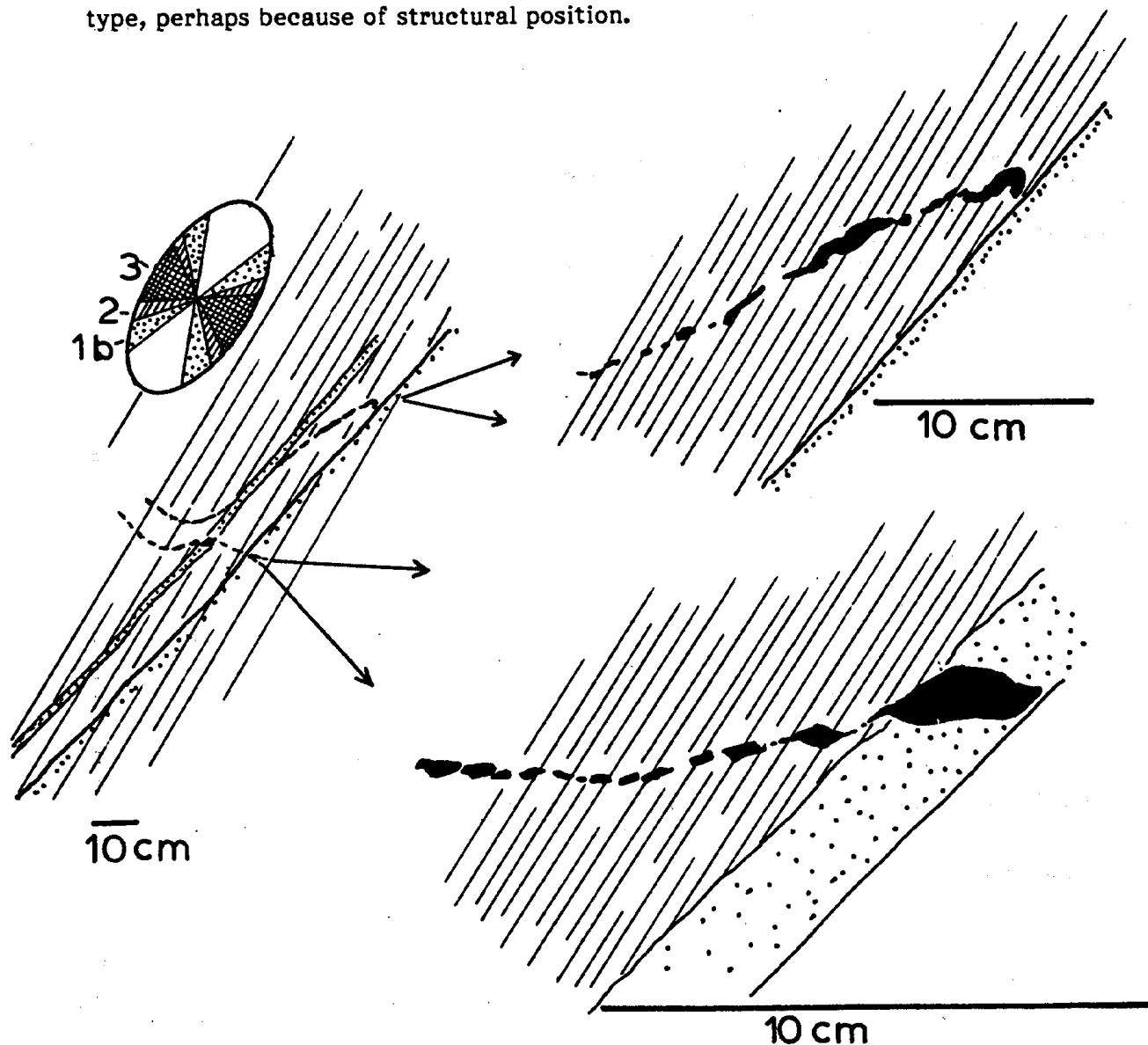


Figure I-12

Drawing of early quartz veins at Station H that were folded, rotated counterclockwise and extended during localized pure shear progressive deformation.

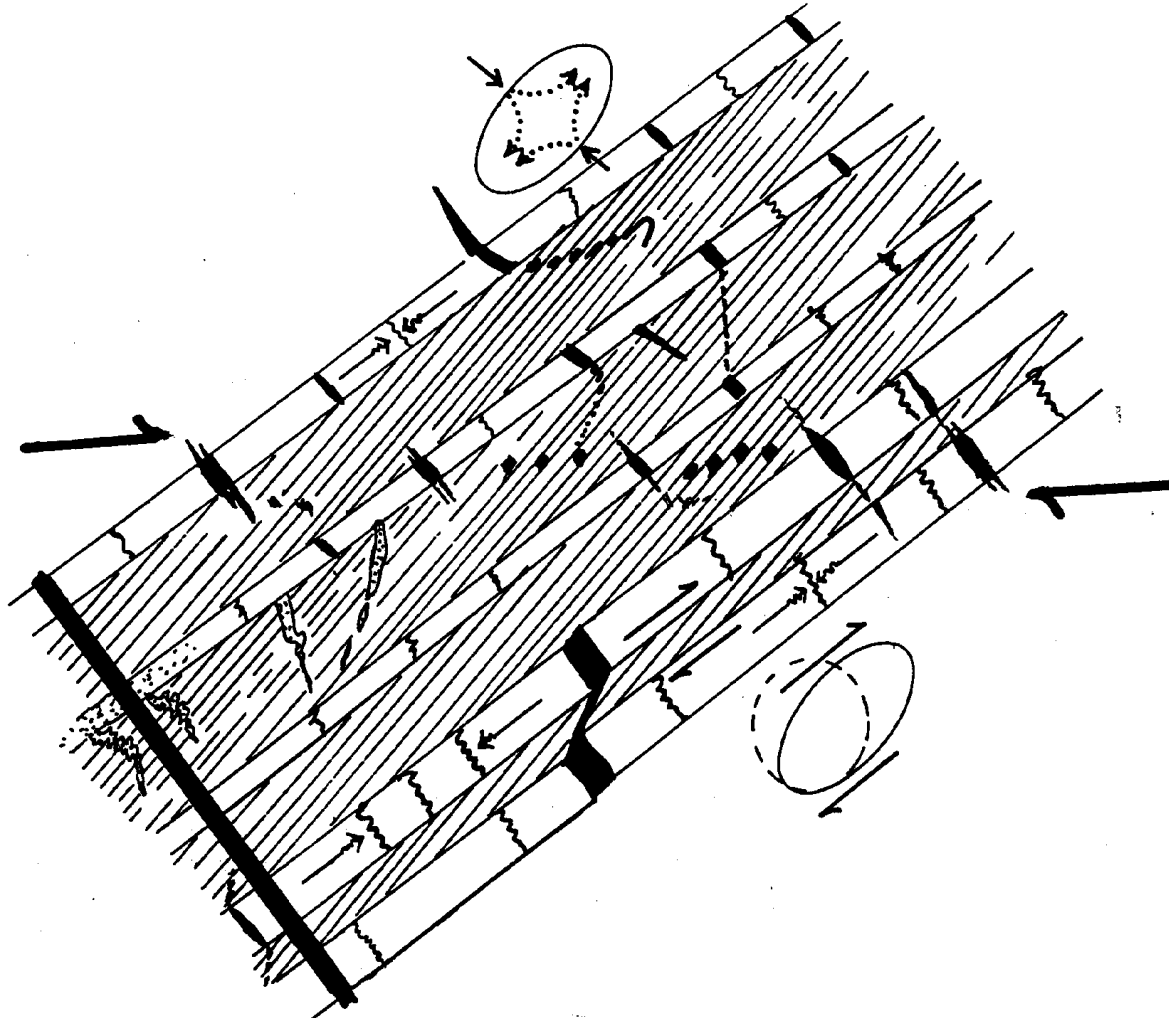


Figure I-13

Cartoon summarizing all of the structural features at Station 1.

STRUCTURAL SUMMARY

Figure I-13 is a cartoon summarizing all of the structural features of the outcrop. This outcrop is noteworthy in the region because it illustrates strong cleavage and relatively high strain resulting from localized progressive simple shear on one limb of the Berwick Anticlinorium. Some beds have deformed by progressive pure shear. Finite strain differences within the outcrop appear to be related to rock type but may result from stratigraphic position. Veins can be structurally dated as pre or syn-folding and post-folding but all formed in the temperature range 250-300° C as indicated by both Conodont Alteration Colors and Temperatures of Filling of fluid inclusions. The sequences of formation of structures was:

1. layer parallel shortening in horizontal beds recorded as spaced, stylolitic, pressure solution planes perpendicular to bedding in limestones (Fig. I-9);
2. buckling and flexural-slip folding leading to jointing in limestones and sandstones and clockwise rotational deformation and strong pressure solution cleavage in limy shales, intersecting bedding at 10-20° (Figure I-4d). Early quartz and calcite filled joints and sandstone dikes are deformed in either simple shear or pure shear progressive deformation to create folded, pressure solved, or boudinaged markers (Fig. I-8, 10, 11, 12);
3. horizontal, northwest-directed, incipient thrusting occurred in shear zones cutting across bedding prior to the completion of folding and cleavage (Fig. I-13); and
4. late, Az. 30°, post-folding veins cut all previous structures after folding and cleavage formation.

<u>Miles</u>	<u>Interval</u>	
5.3	0.3	Leave Stop 1; drive east on U.S. 11 (north).
7.9	2.6	Turn right on PA 54 (East); follow Mill St. through Danville.
8.3	0.4	Enter bridge spanning North Branch of Susquehanna River.
8.6	0.3	Enter Northumberland County at south end of bridge.
8.7	0.1	Cross railroad and turn left to continue on PA 54 (east).
9.1	0.4	Outcrop of Mahantango Formation on right; the location seaward of the Mahantango deltas determines the paucity of sandstone.
9.3	0.2	Shales associated with the thin nodular limestone zone of the Tully.
9.4	0.1	Begin half mile long exposure of shales leading into the Trimmers Rock sandstone/shale sequence. Route then continues across rolling farmland on soils above the Catskill Formation for about 5 miles, crossing Northumberland Syncline.
14.1	4.7	Descent through the Irish Valley Member of the Catskill Formation into the underlying Trimmers Rock Formation.
15.4	1.3	Trimmers Rock Formation exposed on the right as road descends toward town of Elysburg.
16.0	0.6	Enter Village of Elysburg.
16.3	0.3	Turn right onto Penn Avenue just beyond Airstream dealer.
17.8	1.5	As steel buildings of Kirsch Company come into sight on left, note physiography: driving down strike valley in Devonian shales; scarp slope to right (north) on Trimmers Rock Formation; low hills to left (south) are made by sandstones in the Mahantango Formation.
17.9	0.1	Turn left on road that leads to Paxinos.
18.1	0.2	Cross railroad; Jacob Church becomes evident on left.
18.3	0.2	Vehicles stop for passengers to disembark; vehicles will drive $\frac{1}{2}$ mile ahead to park on side of road to Shamrock, turn around to face east so group can reboard and head directly to Paxinos. Group walks half mile from part A to part B of Stop 2.

Stop II - Jacob Church - Shamrock

(Participants will debark at Jacob Church and walk .8 km ($\frac{1}{2}$ mile) south to Shamrock where buses will be waiting).

INTRODUCTION

This exposure is included in the field trip to illustrate strikingly different deformation mechanisms and structural features associated with several rock types in the Middle Devonian Mahantango Formation. Presumably the finite strain throughout the outcrop is similar, yet the physical expression of this strain in the several rock types is different. Structural features to be seen include: open folds with cleavage fans, several cleavage types associated with different lithologies, wedge (intrabed, thrust) faults, conjugate, strike slip pressure-solution slip surfaces, quartz-filled syntectonic veins, and a small scale example of thrust tectonics and the development of ramp anticlines.

STRATIGRAPHIC SETTING

The Mahantango Formation in central Pennsylvania generally includes the strata between the Marcellus Formation and the Tully Limestone. Together with the Marcellus, the Mahantango is equivalent to the Middle Devonian Hamilton Group (see review by Harper and Piotrowski, 1979).

The history of the Mahantango in central Pennsylvania involves a series of progradational episodes by a lobate deltaic depositional system analogous to the modern Rhone Delta (Kaiser, 1972). A succession of northwestward, multicyclic advances of this deltaic system from a source terrain in the vicinity of the York Highlands left a series of northwestward-thinning sandstone members intercalated within shale members (Kaiser, 1972; Faill and Wells, 1974). One of the most significant of these sandstone members of the Mahantango is the Montebello Sandstone.

Here, in the Selinsgrove Anticlinorium, we see the Montebello Sandstone at its most distal position. At Stop II-A (Jacob Church) all that remains is siltstone and very fine sandstone just before the member thins out completely between here and the church to the north. We shall proceed to Stop II-B (Shamrock) in the center of the anticlinorium, where a syncline exposes thicker beds of slightly coarser Montebello. A further 800 m to the south at Paxinos, along the south margin of the anticlinorium, the Montebello contains even thicker and coarser-grained sandstones (Locality 75 of Kaiser, 1972). This sequence of lithologic changes is related to the position of farthest advance of the Montebello deltaic system. The following comments attempt to place the strata of Stops II-A and II-B into the context of that deltaic system.

The Montebello at Stop II-A consists of bioturbated coarse siltstone and very fine sandstone. Deposit-feeders churned finer carbonaceous and argillaceous bands in with formerly cleaner sands and silts. The overall rate of sedimentation was sufficiently low so that bioturbation was complete before the substrate surface was raised a significant amount. In a deltaic system, such conditions obtain in distal parts of the prodelta environment, sufficiently far seaward of the delta front to avoid turbidite deposition of significance (Kaiser, 1972, p. 84).

At Stop II-B (Shamrock), we shall walk past interbedded shales and sandstones (showing less bioturbation than at II-A and exhibiting symmetrical ripples) to thicker beds (up to 2 m) of fine sandstones. Bed bases are sharp and flat; tops are flat to undulating, and some have symmetrical ripples. One can find horizontal and broadly wavy (hummocky?) laminae in some beds. These are features that are characteristic of the distal delta front and proximal prodelta.

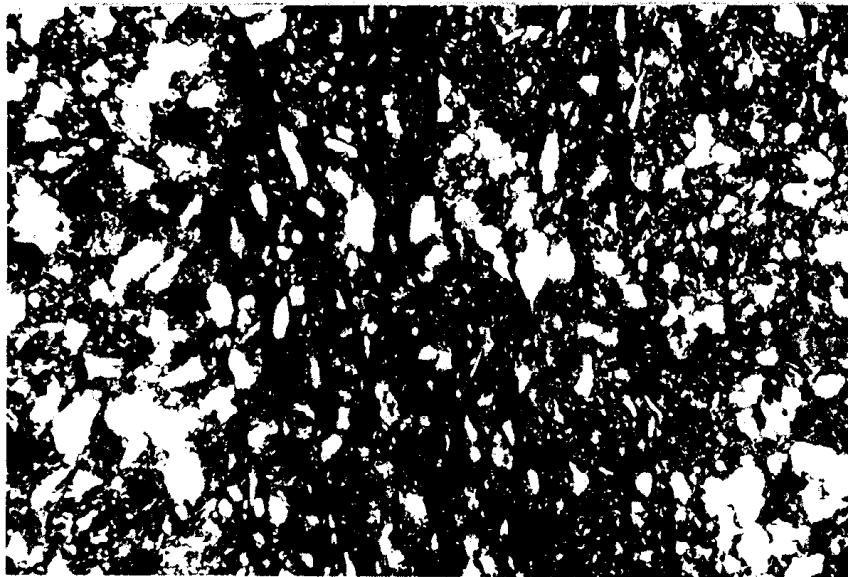
The still coarser and thicker sandstone at Paxinos (about 800 m farther south) has features that indicate deposition in the proximal delta front and distributary channel environments. We won't visit this Paxinos exposure, but at Stop IV (Selinsgrove Junction), about 20 km (13 mi) WSW of here we will examine a Montebello sequence very similar to



A

Figure II-1A

Polished and etched slab of bioturbated Mahantango Formation from Stop II-A. Dark cleavage zones are spaced .5 to 2 cm apart and commonly parallel to burrows. cm scale in lower left



B

Figure II-1B

Thin section of Mahantango Formation from Stop II-A showing a cleavage zone (A domain) in the center bordered on both sides by unclesaved rock (B domains). In the A domain quartz has been flattened by pressure solution and residual clay and carbon have collected. Clay carbon partings are .02 to .1 mm thick. Width of field 2 mm, crossed nicols

that at Paxinos. The coarser sands are above prodelta and distal front deposits, and they are associated with coquinas that were deposited on the delta platform.

The three Montebello exposures across the Selinsgrove Anticlinorium, therefore, represent the appropriate sequence of depositional environments at the position of the most distal advance of the deltaic depositional system: proximal delta front to delta front/prodelta transition to distal prodelta. This feathering out of the Montebello across the anticlinorium is well shown in the map pattern presented by Arndt and others (1973).

STRUCTURAL GEOLOGY

The argillaceous sandstone near Jacob Church and the quartz arenite near Shamrock have responded differently to stress. The argillaceous sandstone has open folds and prominent somewhat asymmetric cleavage fans verging north. This is a spaced cleavage, developed in cleavage zones .5 to 2 cm apart. As described in Nickelsen (1972, p. 109), and illustrated in Figure II-1A the dark, clay-rich cleavage zones parallel burrows which served both as conduits for water movement and lithologic contrasts which favored solution. Between cleavage zones are unstrained "B" domains where the original rock fabric is undisturbed. Within cleavage zones, or "A" domains, is a network of anastomosing clay-carbon partings < .1 mm thick containing the insoluble residue of massive pressure solution. "A" domains have phyllosilicates and quartz oriented parallel to the cleavage plane. Phyllosilicates have been oriented by rotation due to lack of support during dissolution and by growth in clay-carbon partings. Quartz has been corroded by pressure solution into disk-shaped grains lying in the cleavage (Fig. II-1B). Pressure solution-dissolution strain mechanisms have dominated the fabric development in this rock, which began prior to folding and continued throughout its structural history. Perhaps 10% of this rock has been removed in solution but the only obvious sink for this dissolved material is the quartz and calcite-filled transverse joints that make up the face of the outcrop. They are inadequate for the task.

The well-bedded quartz arenite near Shamrock at the south end of the exposure is more interesting because of the variety of structural features and the structural sequence that it documents. This outcrop was described by S. Davis (1981) as part of a senior thesis at Bucknell University. Her summary diagram of structure orientations (Davis, 1981, Fig. 23) (following rotation around the strike of bedding to bring bedding to horizontal and other structures to their pre-folding attitude) has been reproduced here as Figure II-3. Unlike the outcrop to the north at Jacob Church, two mechanisms of deformation are present, pressure solution and brittle shear failure on conjugate wedge faults. Pressure solution in these cleaner sandstones is not as pervasive and the pitted surfaces that are coated with insoluble residue are more irregular in strike and dip and spaced widely (5-10 cm). Most important, surfaces of dissolution are of two types:

1. Type A pressure solution planes have a mean strike of 78° ($S = 70^{\circ}$), approximately paralleling the trend of the Shade Mountain anticline, and are interlocking "pitted", stylolitic surfaces marked by residual accumulations of insoluble clay and carbon. No quartz fibers were observed on these surfaces, and they show no preferred orientation of irregularities.
2. Type B pressure solution planes occur in two orientations, 310° ($S = 80^{\circ}$) and 36° ($S = 80^{\circ}$) intersecting at an acute angle of 86° . The surfaces are grooved and ridged horizontally parallel to the intersection between the bed and the steeply dipping solution plane. Quartz fibers up to 2 mm long grow in grooves, oriented parallel to the grooves and ridges. The distribution of irregularities,

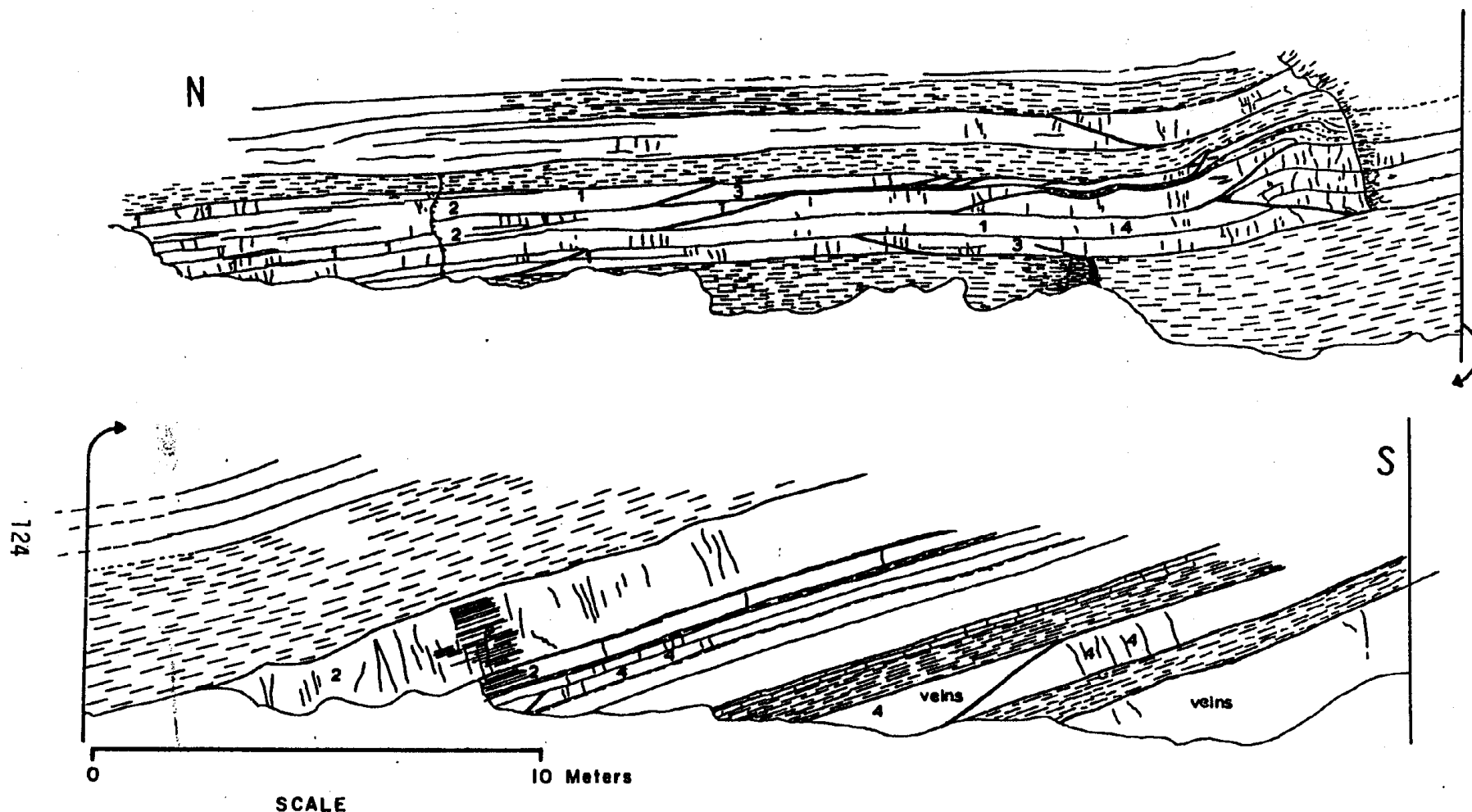


Figure II-2

Drawing of outcrop at Station II-B, near Shamrock. Tongues of Montebello sandstone show small scale thrusts (wedges), incipient fault duplexes, and flat-ramp-flat thrust complexes that have developed into a ramp anticline. Structures to be observed include:

1. *Right lateral pressure solution slip surfaces*
2. *Left lateral pressure solution slip surfaces*
3. *Right lateral Mohr Coulomb wrench faults*
4. *Spaced pressure solution cleavage*



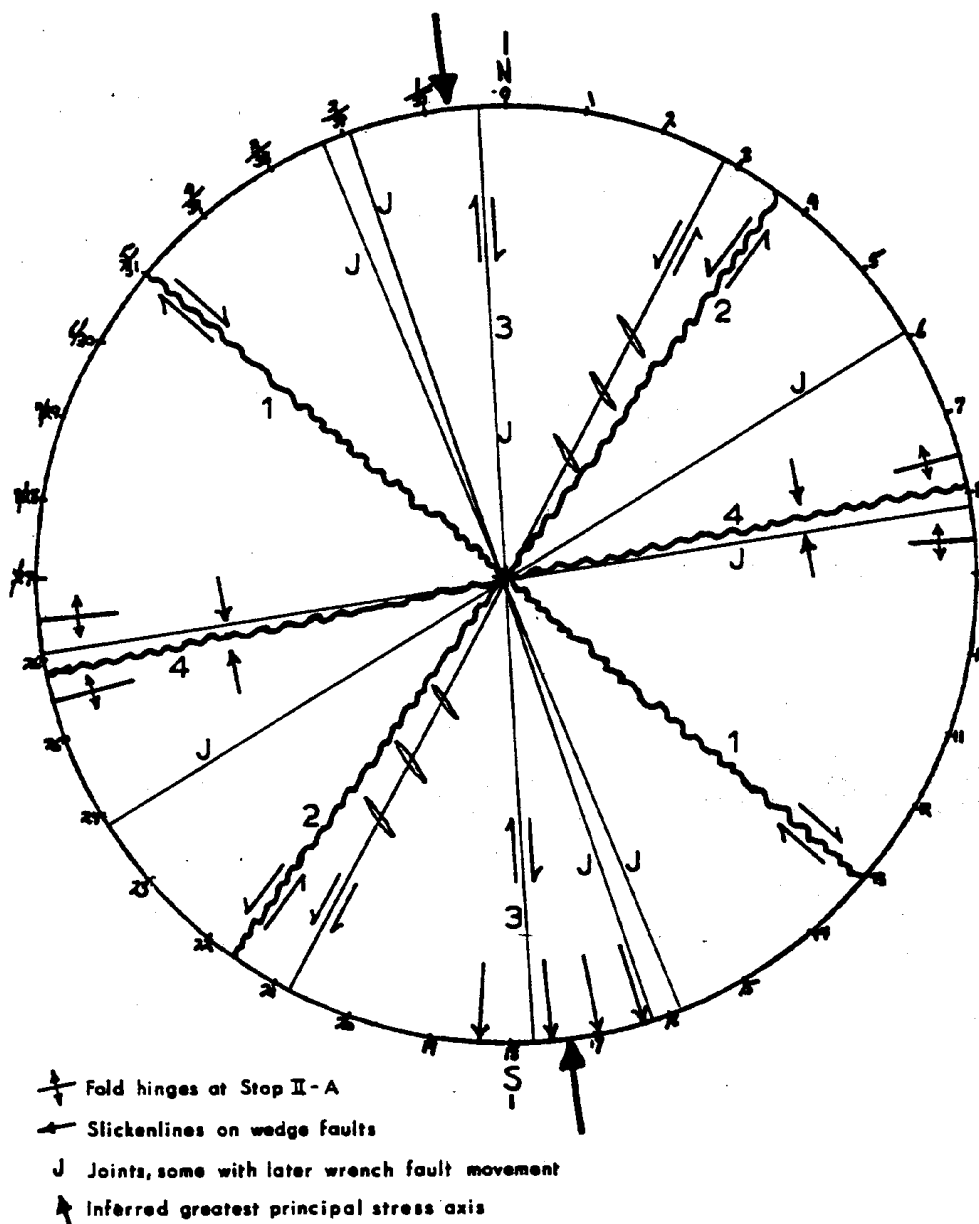


Figure II-3

Summary orientation diagram of rotated structures at Stop II.

1. Right lateral pressure solution slip surface
2. Left lateral pressure solution slip surface
3. Right lateral Mohr Coulomb wrench fault
4. Spaced pressure solution cleavage

steps, concentrated insoluble residues, and quartz fibers clearly demonstrate strike slip movement in a right-lateral sense on the 310° set and a left-lateral sense on the 36° set. The large dihedral angle between the conjugate surfaces and their distinctive architecture suggest that these Type B planes are pressure-solution slip surfaces as described by Marshak et al (1982) from the Apennine fold belt, Italy. Marshak et al (1982, p. 1019) have pointed out the theoretical problems with 90° dihedral angles between conjugate shear surfaces if the Mohr-Coulomb criterion applies. With standard values for the

angle of internal friction, normal dihedral angles in brittle rock and even unconsolidated sand are 60° or less (for example at Bear Valley, Stop 3, the mean dihedral angle is 33°). Hence, to explain these surfaces special conditions are necessary, perhaps a network of pre-existing fractures, or pressure-solution slip initiated along 45° planes of maximum shear stress prior to complete consolidation of the rock.

The left lateral Az 36° pressure solution slip planes are better developed, having larger surfaces and large, open gash veins that pervade parts of the outcrop displaying oriented quartz crystals. The Az 310° pressure solution slip surfaces are smaller, commonly restricted to one bed, and more irregular and pitted. Despite these differences the Az 36° and Az 310° pressure solution slip surfaces are thought to be conjugate. Their acute bisector strikes 173° which is also approximately perpendicular to the hinges of the two anticlines near Jacob Church. Thus, both the pressure solution slip surfaces and folds at this outcrop could have formed under the same greatest principal stress orientation of 173° . Other rarer faults of a vertical, wrench fault attitude strike approximately north-south and seem to follow preexisting quartz-filled joints and overprint the conjugate pressure solution slip surfaces.

Unlike the conjugate pressure solution slip surfaces in wrench fault positions, the small wedge faults throughout the outcrop appear more like normal shear fractures obeying Mohr-Coulomb criteria of brittle failure. The wedge faults are most commonly smooth, slickensided surfaces intersecting bedding at $10-20^\circ$. Some surfaces, however, show grooves, ridges and fibers that are similar to those on the pressure-solution slip surfaces in wrench fault positions. Movement on the wedge faults has provided an excellent small-scale example of flat-ramp-flat geometry, ramp anticlines, and a horizontally-floored anticline comprised of stacked imbricate fault wedges. This outcrop could serve as a small scale model for many of the first order Appalachian anticlines (Fig. II-2). Slickenlines on wedge faults are oriented between 162° and 184° paralleling the acute disector of the pressure solution-slip planes and the normal to fold axes. Thus, all structures in the outcrop could have formed under the same principal stress axis orientation.

Finally, the outcrop contains several good examples of syn-tectonic veins filled with obliquely oriented quartz crystals that precipitated while wrench faults were active. The quartz crystals contain healed fractures dotted with many secondary fluid inclusions, both aqueous two-phase inclusions and methane-rich inclusions. A reconnaissance study of three samples from different veins in the outcrop has revealed several populations of inclusions based upon T_F and T_H (Davis, 1981). The range in Temperatures of Homogenization for various fluid inclusions of the 3 samples was 107°C to 260°C , with a mean of 177.7°C . Our study of this outcrop is continuing and we hope this report might stimulate others to check our findings.

SUMMARY

In summary, this outcrop has shown the dependence of structural behaviour upon rock type. Presumably the finite strain and environmental parameters were similar but argillaceous sandstone behaved differently from the quartz arenite of the Montebello Member. Argillaceous sandstone has deformed by pressure solution along close-spaced planes commonly focused on sedimentary structures. The quartz arenite has deformed by pressure solution in widely-spaced, irregular, stylolitic planes and by pressure solution slip on planes of right lateral and left lateral slip that meet at dihedral angles of 90° . As deformation proceeded the pressure-solution slip mechanism gave way to brittle shear faults represented best by wedge faults cutting sharply through beds at angles of only $10-20^\circ$.

<u>Miles</u>	<u>Interval</u>	
18.8	0.5	From parking spot, turn right, continue toward Paxinos.
19.7	0.9	Stop sign at junction with Pa Route 487; turn right (west).
20.0	0.3	Stop sign at junction with PA Route 61; turn left (south).
20.1	0.1	Culm burner can be viewed to the left.
20.3	0.2	Trimmers Rock Formation exposed on the right for 0.2 mile.
21.4	1.1	Scattered poor outcrops of Irish Valley Member of Catskill Formation. Exposures on railroad track above road are type section, Irish Valley Member.
21.7	0.3	Redbeds are part of Sherman Creek Member of Catskill Formation.
22.1	0.4	View ahead to water gap where Shamokin Creek cuts through ridge made of Pocono Formation.
23.0	0.9	In gap, Pocono Formation exposed to left and above railroad to right.
23.2	0.2	Mauch Chunk Formation exposed on bank of Shamokin Creek (to right).
23.7	0.5	Large pile of culm visible ahead on side of Pottsville Formation ridge.
23.8	0.1	Small outcrop of Mauch Chunk Formation on right. Mangle Motors on left. New car anyone?
24.4	0.6	Basal part of Pottsville Formation crops out.
24.5	0.1	Glen Burn Mine on left.
24.6	0.1	PA Route 225 to right; continue ahead on PA Route 61.
24.9	0.3	Turn right onto PA Route 125 (South); drive down Market Street, Shamokin.
25.0	0.1	Cross Shamokin Creek; Anthracite Museum is up the road to left.
25.5	0.5	Bear right around grocery store to follow PA 125 down Bear Valley Avenue.
26.2	0.7	PA 125 (South) turns left near old mine entrance (Nov., 1934) from which acid mine drainage emerges; continue straight ahead on Bear Valley Avenue.
27.6	1.4	Pavement ends; disembark and follow rutted road at angle up to the right. To Stop 3, Bear Valley Strip Mine. Vehicles turn around and wait at this point.

Stop III - Bear Valley Strip Mine

INTRODUCTION

The Bear Valley Strip Mine, 30,000 m² of continuous outcrop, shows both cross sections and bedding plane exposures of two disharmonically folded Pennsylvanian cycles of sedimentation. We will observe a great variety of structural features (including 3rd order folds, rock cleavage, joints, and thrust, wrench and extensional faults), the sequence of structural stages of the Alleghany Orogeny, and sedimentary features such as plant fossils, coal, and ironstone concretions.

The regional setting of the Bear Valley Strip Mine is provided by the Geologic Map of the Southern Half of the Shamokin (15 minute) Quadrangle by Arndt, Wood and Schryver (1973). The mine is situated among several 2nd order folds on the south limb of the 1st order Shamokin Synclinorium, which is part of the Western Middle Anthracite Field. Wood, Trexler and Kehn (1969) and Wood and Bergin (1970) provide the best general descriptions of the geology of the Anthracite Region.

Figure III-1 shows structure stations A through G and sedimentary feature stations I and II. The coal and underlying sandstone of the Mammoth Bottom Split Coal Bed (#8) have been folded into two third (size) order anticlines and synclines. Most bedrock surfaces exposed in the mine show ironstone concretions at the top of the sandstone. The coal is visible only at Station II. At the east end of the mine a well-exposed disharmony can be seen between the folds in the underlying Mammoth Coal Zone at the bottom of the mine and the synclinal fold in the #9 cycle in the East wall (Fig. III-2). The fold disharmony is presumably related to different thicknesses of the dominant sandstone member in the structural lithic units above and below the mined coal, resulting in different wavelengths of folds.

STRUCTURAL GEOLOGY

Most of the structural stages of the Alleghany Orogeny present throughout the northern Valley and Ridge Province can be seen here, as will be demonstrated at Stations A through G, Figure III-1. Figure III-9 shows the relative age of the overlapping stages that have been depicted in the cartoon of Figure III-10. Briefly, Alleghany deformation proceeds from layer parallel shortening (Stages II, III, IV) to major folding (Stage V) to layer parallel extension (Nickelsen, 1979).

Station A - From the northwest corner the third order folds and fold disharmonies can be seen and the route of the walk to other localities described. The view of the southwest corner (Fig. III-4) shows overprinted Stage IV conjugate wrench fault systems and a Stage IV thrust. Note that the dihedral angle of conjugate wrench faults is approximately 35°. You are standing on the crest of the North Anticline, here a flat-topped, box fold. The floor of the coal swamp beneath you has impressions of large lycopsid trees and stigmara (roots).

Station B - One hundred meters east of Locality A along the North Anticline, Station B provides an excellent view of the north limb of the Whaleback Anticline showing Stage IV thrusts and conjugate wrench faults, Stage V folding, and Stage VI extension joints and faults (Fig. III-3). The North Anticline is different, chevron, shape at this locality. (See Fig. III-2).

Station C - This locality is in the southwest corner offers an opportunity to observe, close up, the Stage IV wrench and thrust faults shown in Figure III-4. Primary crenulation

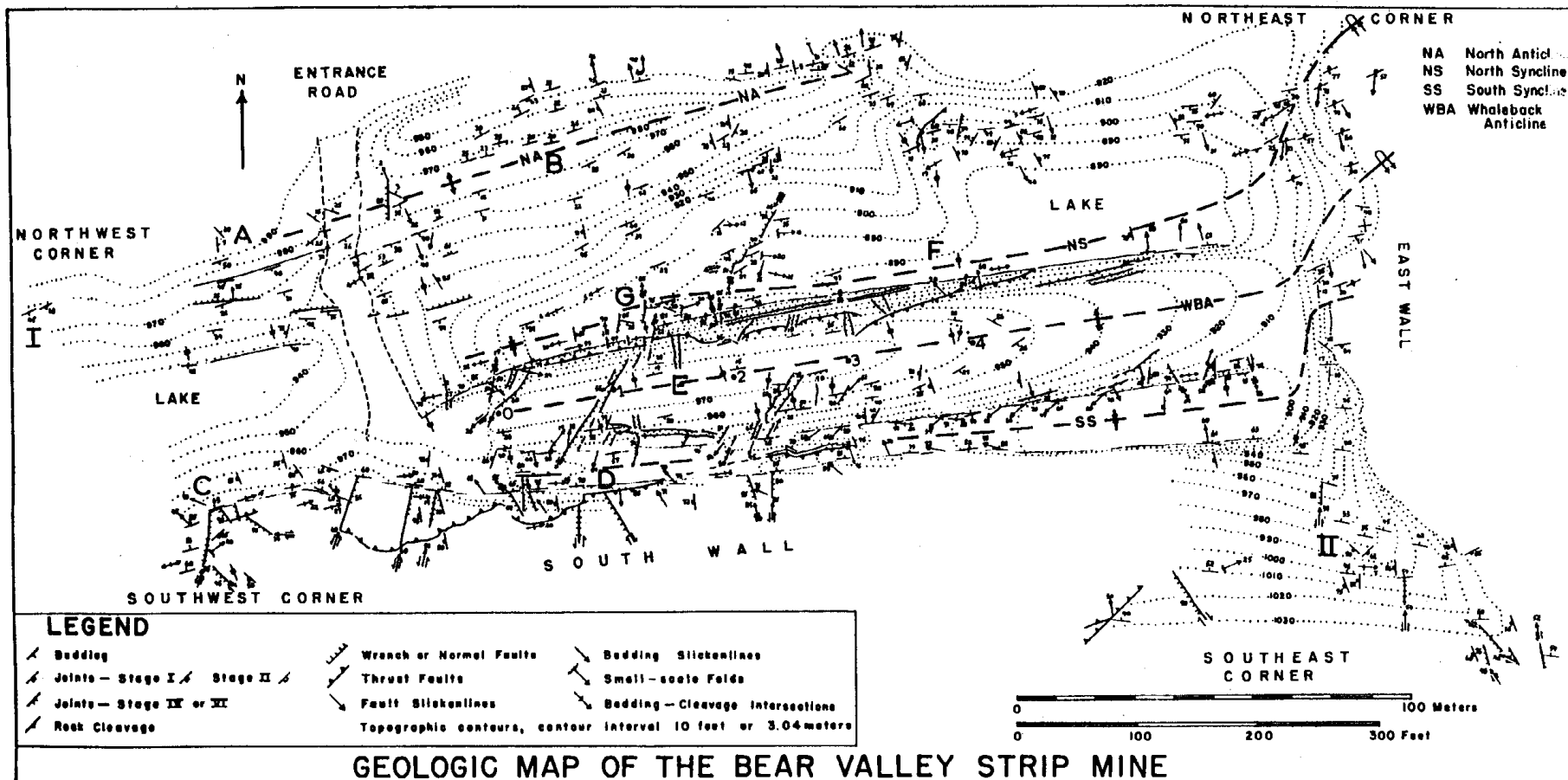
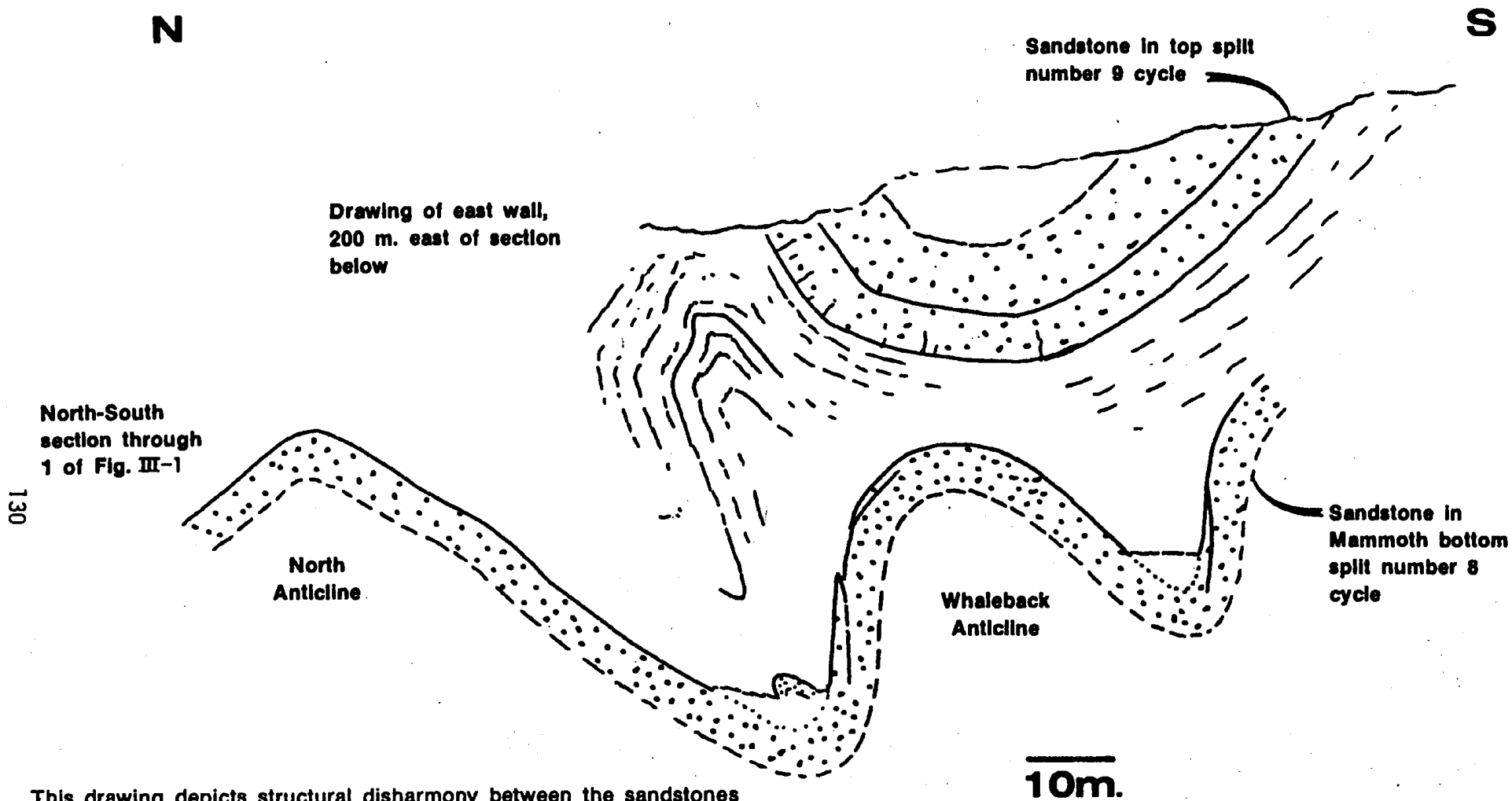


Figure III-1

Geologic map of the Bear Valley Strip Mine Stations A-G and I, II are shown



This drawing depicts structural disharmony between the sandstones in the number 8 and number 9 cycles of sedimentation. The Whaleback anticline decreases in amplitude and plunges east under the syncline in the number 9 cycle, which is exposed in the East Wall of the mine. Thus this composite section overemphasizes the disharmony between the two sandstones.

Figure III-2

Section of Bear Valley Strip Mine

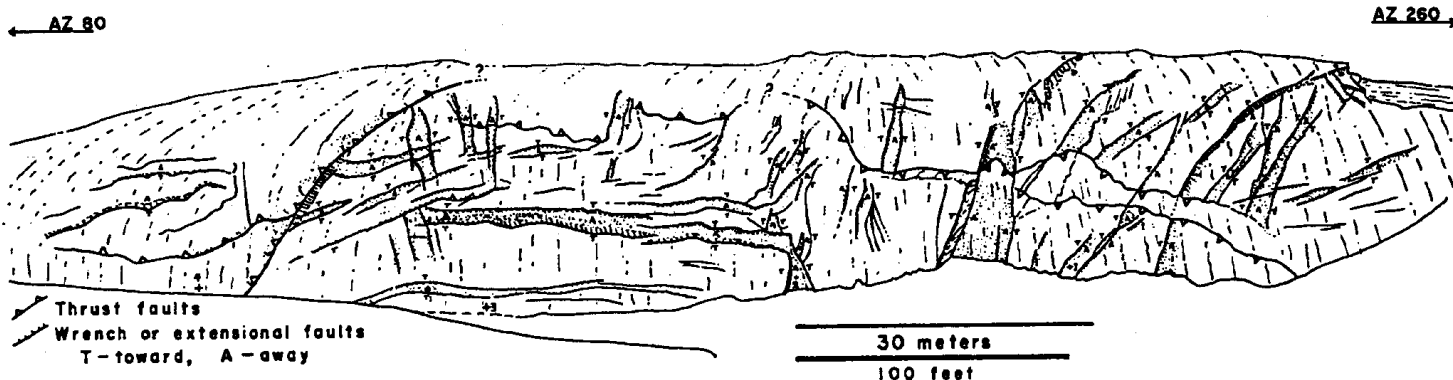


Figure III-3

Drawing of structures exposed on the north limb of the Whaleback Anticline. View from Station B

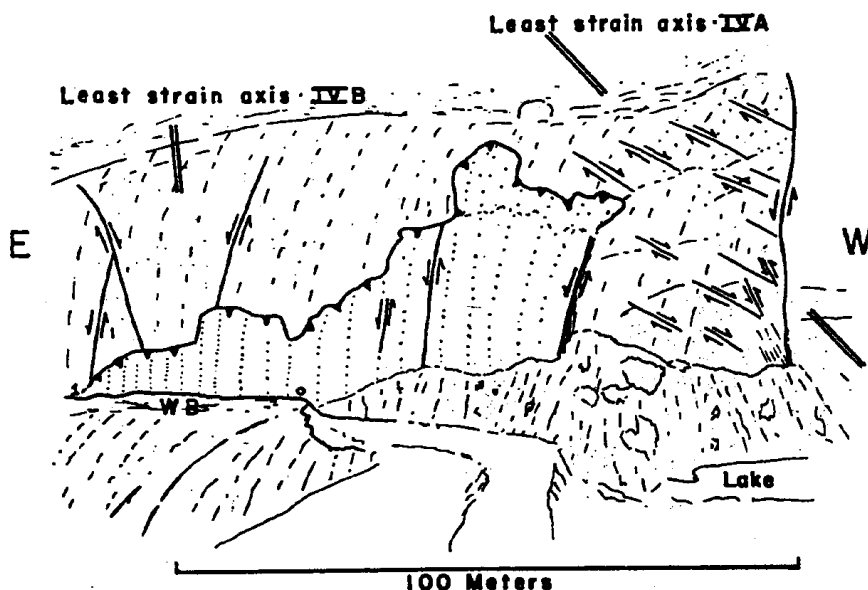


Figure III-4

Drawing of structures in the southwest corner, Bear Valley Strip Mine. Two overprinted conjugate wrench fault systems (IV A and IV B) and a thrust are shown. View from Stations A and C.

cleavage occurs in shales beneath the sandstone (Fig. III-11A). Large ironstone concretions can be recognized as the stiffest member of the sedimentary succession, showing only Stage II joints and surface slickenlines that demonstrate how other strata have shortened and flowed around them. The contact between concretions and their enclosing rock are shear planes or boundary zones (Currie et al, 1962) between different structural lithic units. Relative shear sense is in opposite directions on the two ends of the stiff structural lithic unit. These concretions illustrate that no constant direction of "transport" is essential in a thick pile of sedimentary rocks of different ductility which are undergoing differential layer-parallel shortening. The sequence of structural stages is established by offset of Stage II joints by Stage III pressure solution cleavage and by drag of Stage III cleavage-bedding intersections against Stage IV wrench faults. All of these structures formed by layer-parallel shortening in horizontal beds prior to folding (Fig. III-10).

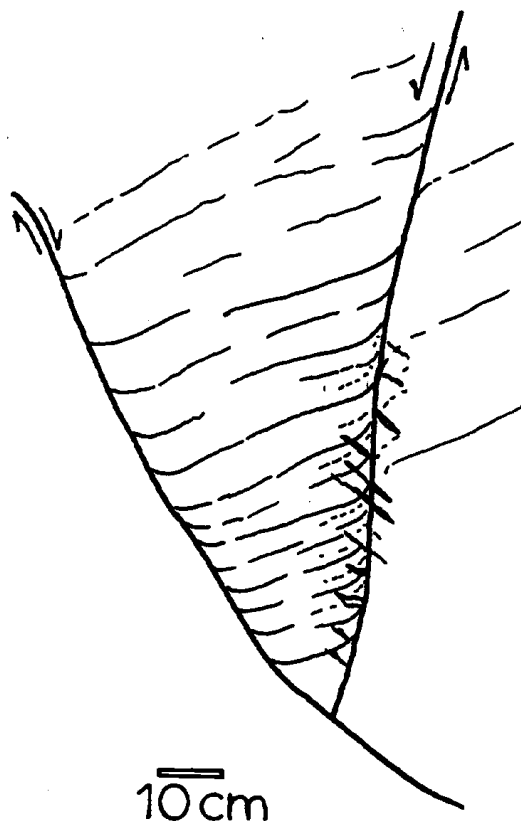


Figure III-5

Conjugate right lateral and left lateral wrench faults (Stage IV) distort bedding-cleavage intersections (Stage III). En echelon gash veins along the left lateral fault cut bedding-cleavage intersections. Station D.

Station D - Conjugate Stage IV wrench faults, drag of cleavage-bedding intersections against Stage IV wrench faults (Fig. III-5), thrust faults, wrench faults overlapping Stage V folding, and Stage VI extensional grabens can all be seen at this locality, situated in the South Syncline.

Station E - A walk along the crest of the Whaleback Anticline provides the best view of the fold disharmony to the east (Fig. III-2) as well as views of Stage II joints, the inter-relationships of Stage IV wrench and thrust faults and Stage VI strike joints on the wall to the south. The sandstone beneath you has deformed by both intergranular grain adjustments including pressure solution at grain contacts and changes in packing, and by intragranular crystal-plastic deformation mechanisms manifested by quartz deformation lamellae. Deformation lamellae are concentrated in deformation bands extending into grains from stress concentrations at contacts between grains. Large detrital micas caught between quartz grains deforming by intergranular and intragranular processes have been kinked (Figure II-11C and D). We believe intracrystalline deformation has played a previously under-estimated role in the deformation of sandstones of the Valley and Ridge Province. Onasch (1983, Fig. 5, p. 80) has come to a similar conclusion. Spaced cleavage from quartz-rich siltstone in the East Wall is illustrated in Figure III-11B. This fabric has resulted from pressure solution, rotation and grain-boundary sliding, crenulation of micas oriented perpendicular to cleavage, and new growth of illite.

Station F - Station F provides close up views of thrust faults and extensional grabens on the north limb of the Whaleback Anticline (Figure III-3). Evidence for the relative age of Stage IV thrust faults and Stage V folding can be seen here and is summarized in Figure III-7A. We know thrust faulting preceded folding because flexural slip associated with folding has reversed the slip sense on thrust faults causing a pull back of the tip of the thrust and an uncovering of the thrust surface. Thrust faults and their slickenlines consistently trend counterclockwise of the third order folds of Stage V (Figure III-7B).

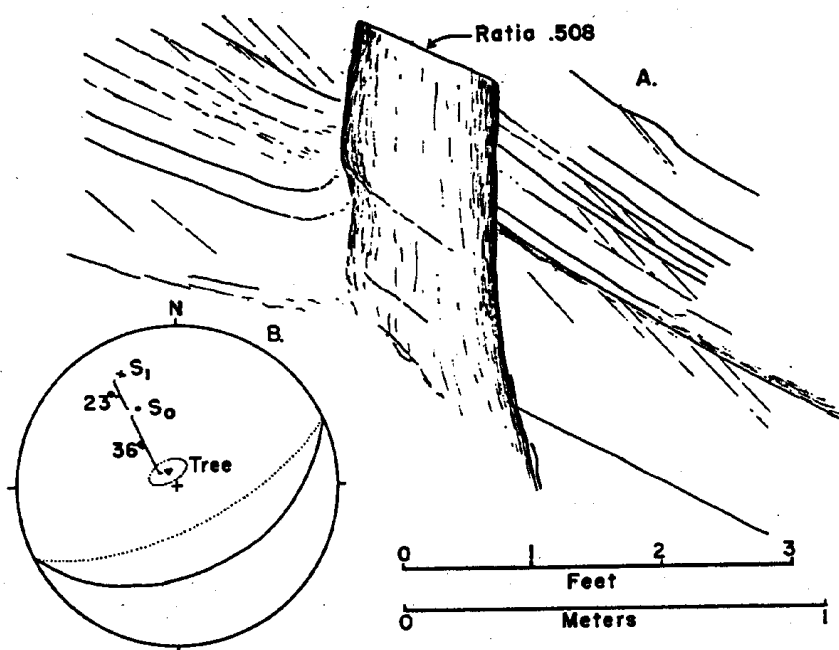


Figure III-6A *Drawing of an upright, deformed lycosid tree trunk, bedding and cleavage. Station I.*

Figure III-6B *Equal area projection showing angular relations between bedding, cleavage, and the elliptical axis of the tree trunk.*

Station G - Wrench faults on the north limb of the Whaleback Anticline at several spots show time overlap with Stage V folding and eventual utilization of earlier faults by movements associated with Stage IV layer-parallel extension. Figure III-8 shows curving slickenlines on a wrench fault surface that demonstrate concurrent folding and faulting. The fault was initiated under compression as a wrench fault cutting beds dipping 40° but has ended movement as an extensional fault, contributing to extension parallel to the hinge of the Whaleback Anticline.

SEDIMENTARY FEATURES

Locality I - This spot shows a rare, upright, Carboniferous tree, $\frac{1}{2}$ meter in diameter and projecting more than a meter upward into overlying bedded shales and siltstones. The tree trunk has been rotated counterclockwise and deformed to an elliptical cross section by flexural-slip simple shear during folding and by pure shear flattening, during formation of rock cleavage (Figure IV-6). Simple shear and pure shear cannot be isolated and possibly all progressive deformation was by simple shear.

Locality II - This locality in the southeast corner of the mine is the only place where the Mammoth Bottom Split Coal Bed #8 is visible and available for sampling. Nearby, on the large sandstone bedding surfaces, are 25-foot long impressions of lycosid tree trunks.

COAL RANK AND TEMPERATURES OF LOW-GRADE METAMORPHISM

Estimates of ambient temperatures during coalification and Alleghanian deformation in this region are available from coal rank, appearance of pyrophyllite, Conodont Alteration Colors and fluid-inclusion-homogenization temperatures.

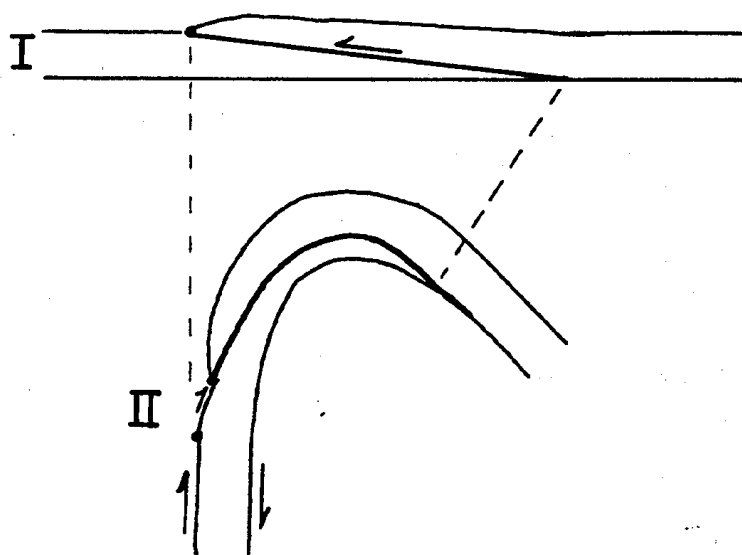


Figure III-7A

Drawing showing how thrust faulting followed by flexural slip folding causes pull back of the hanging wall to expose a fault surface. Station F.

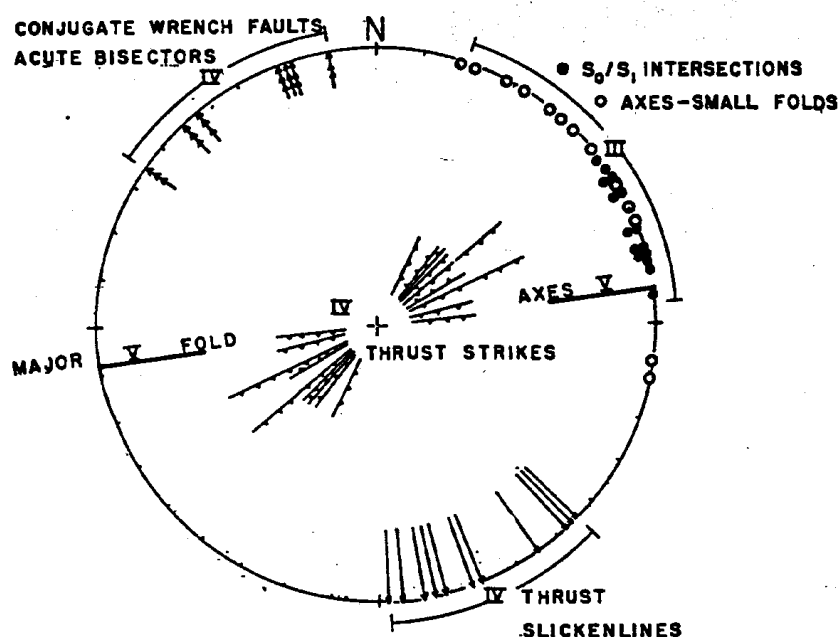


Figure III-7B

Equal area projection showing angular relations of structures in the Bear Valley Strip Mine after rotation with bedding to pre-folding attitude.

Data on coal rank, from fixed carbon and vitrinite-reflectance measurements in the local area are given in Table III-1.

Coal in this part of the Western Middle Anthracite Syncline is on the borderline between semi-anthracite and anthracite based upon fixed carbon percent and maximum vitrinite reflectance (R_{max}). The Lykens Valley #2 Coal that has slightly higher maximum reflectance and fixed carbon values (Table III-1) is approximately

Table III-1. Coal rank measurements near Bear Valley Strip Mine

Sample #	Seam	Locality	Fixed Carbon %	R _{max}	R _{min}	R _{mean}
PSOC 83	Mammoth 8 1/2	Carbon Run Colliery	87.4	2.679	1.799	2.329
84	Mammoth 8	SW of Shamokin	88.9	2.716	1.633	2.279
85	Mammoth 8	" "	92.3	2.623	1.848	2.316
PSOC 627	Lykens Valley	N. Mountain Mine NW of Shamokin	89.5	3.040	2.120	2.675
628	Lykens Valley		90.1	3.038	2.369	2.776
629	Lykens Valley	" "	89.0	2.956	2.189	2.654
630	Lykens Valley	" "	92.2	2.863	1.877	2.465

(Data from Pennsylvania State University Coal Data Base, Coal Research Section, University Park, PA 16802 - Personnel communication, Jeff Levine, April 1981)

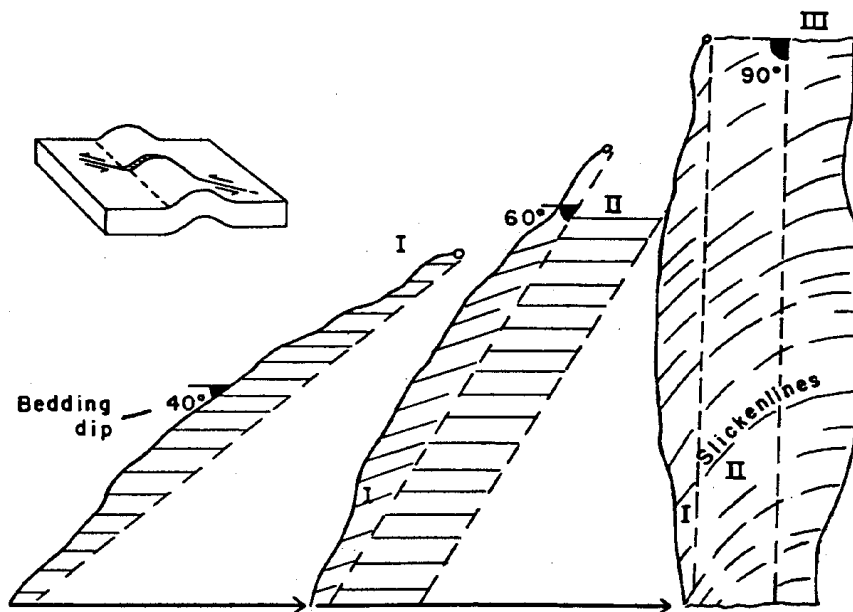


Figure III-8

Interpretation of curved slickenlines on a transverse fault exposed at Station G. Folding to 40° north dip preceded wrench faulting but subsequent to that the fold and fault evolved together.

RELATIVE AGE - STAGES

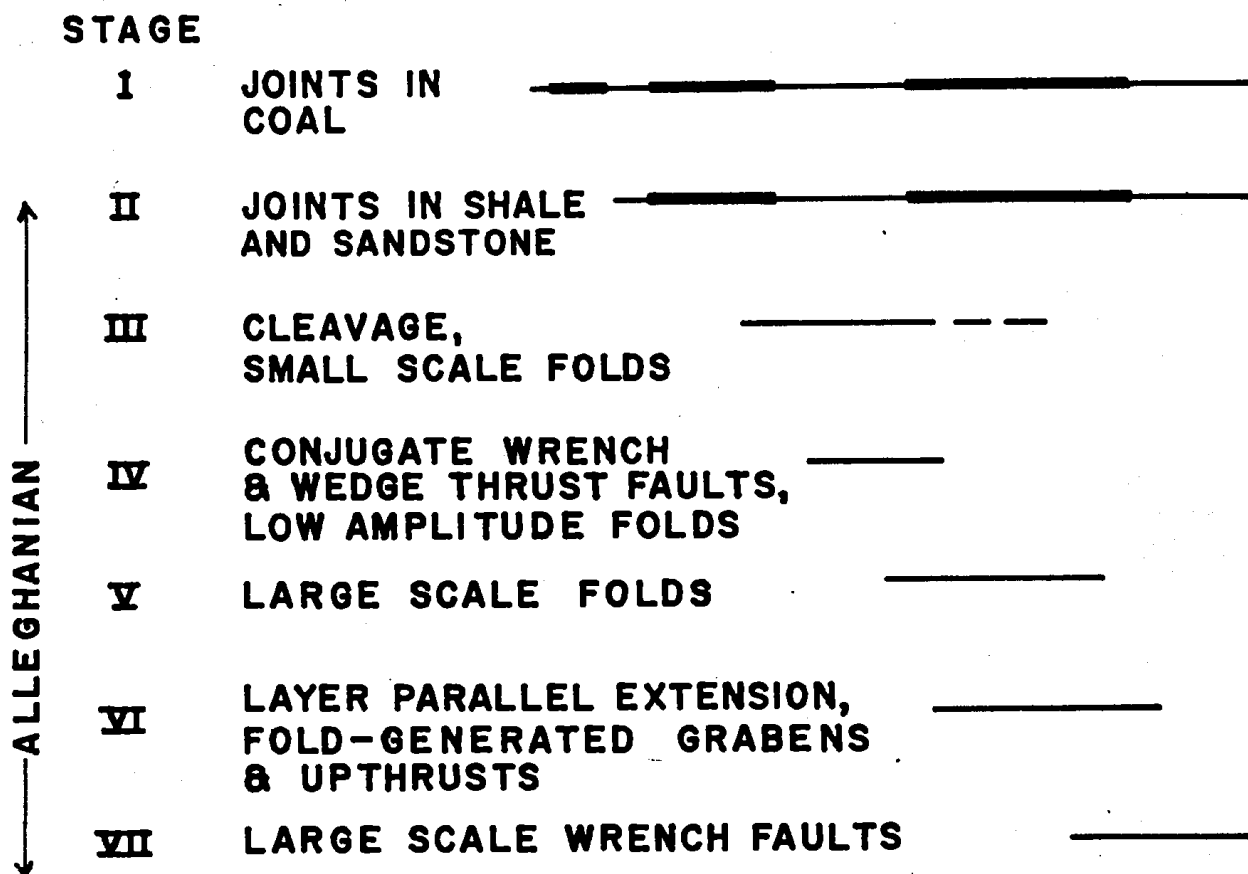


Figure III-9

Table showing relative ages of structural stages I-VII.

700 feet below the Mammoth #8 coal bed. (The vitrinite reflectance values recorded in the vicinity of Bear Valley suggest temperatures of approximately 185° C during coalification and the Alleghany Orogeny (Levine, this volume).

Three other indications of the temperatures of these anthracites and semi-anthracites during their burial history are available in the region. Pyrophyllite ($\text{Al}_2\text{Si}_4\text{O}_{10}(\text{OH})_2$) of metamorphic origin has been reported in underclays of the Western Middle Anthracite Syncline at Ashland and Shenandoah 12 miles east of Shamokin by Hosterman, Wood and Bergin (1970, . C92), and as replacements of plant fossils farther east (Myer et al., 1977). Hosterman and others have estimated that the reaction to produce pyrophyllite from illite and quartz occurs at temperatures between 250° and 450° C and pressures between 2 and 9 kb (p. C96). Harris, Harris, and Epstein (1970) have demonstrated that the Anthracite Region is an unusually hot geographic portion of the Valley and Ridge Province, with temperatures as indicated by the Conodont Alteration Index (CAI), decreasing from this region both northwestward across strike and southwestward along strike. No limestones bearing conodonts have been sampled close to Shamokin. But in Lower Devonian outcrops 10 to 15 miles southwest, west, and northwest of Shamokin, Harris, Harris and Epstein have recorded CAI values of 4 of 4½, suggesting that temperatures of 190 to 300° C affected these rocks. Fluid inclusions in quartz that fills joints at Bear Valley have been studied by N. Orkan and B. Voight of Pennsylvania State University (personal communication, 1983). We have incorporated their results in

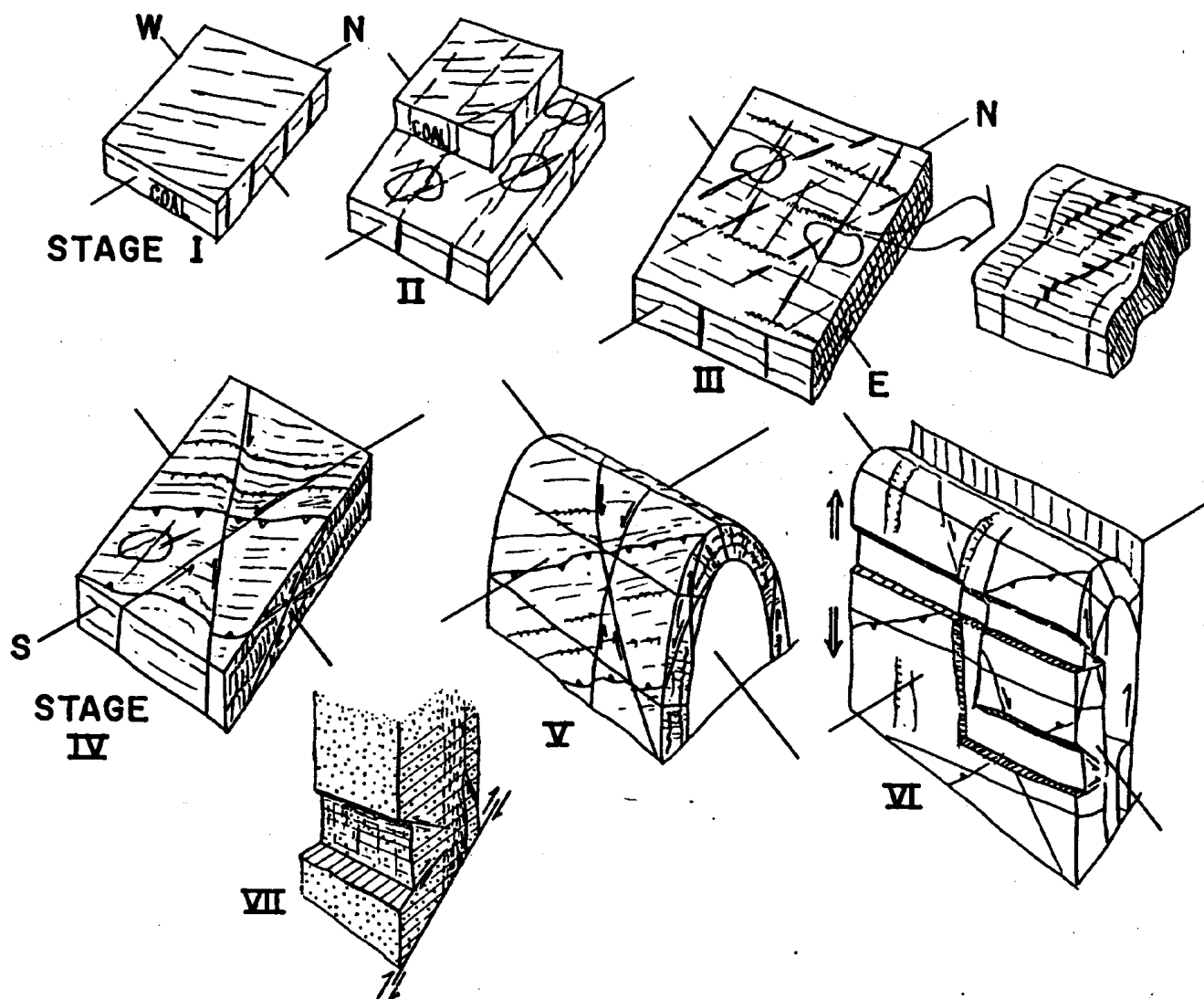


Figure III-10

Cartoon schematically showing the sequential development of structures in the Bear Valley Strip Mine through stages I-VI.

this account. Inclusions at Bear Valley contain variable amounts of CH_4 which invalidate their interpretation as simple H_2O - NaCl systems. CH_4 -rich and H_2O -rich inclusion pairs in individual samples can be used to estimate paleotemperature, T , and fluid pressure, P , as was done by Mullis, (1979) in the Swiss Alps. At Bear Valley Strip Mine the freezing temperature of CO_2 in CH_4 - CO_2 inclusions established inclusion composition at 85 mole % CH_4 , 15 mole % CO_2 and allowed P to be determined from the Temperature of Homogenization (T_H) of CH_4 . P was determined to be 1150 bars. The homogenization temperature of adjacent aqueous inclusions was 205°C and this is inferred to be the filling temperature of the inclusions. According to Orkan and Voight, "taking lithostatic pressure as the maximum limit to P implies a minimum overburden of 5 km and maximum paleogeothermal gradient of 37°C/km ".

In summary, information from a number of sources indicates that the Carboniferous rocks near Shamokin experienced ambient temperatures between 185 and 205°C during coalification and Alleghanian deformation. Paleotemperatures to the east were probably higher as indicated by Hosterman et al (1970), Myer et al (1977), and Levine

(this volume). With normal geothermal gradients of 30° C/km this implies 6 to 8 km of stratigraphic section above the Bear Valley Strip Mine during the Alleghany Orogeny. Orkan and Voight have measured P in CH₄-rich fluid inclusions and estimated a stratigraphic column 5 km thick above the Bear Valley Mine which suggests a paleogeothermal gradient of approximately 40° C/km. Clearly we have insufficient data at this time to decide whether ambient temperatures of coalification and Alleghanian deformation resulted from a thick sedimentary cover or an abnormal geothermal gradient.

SEDIMENTOLOGY

The Llewellyn Formation here was deposited in the lower alluvial plain and/or the upper deltaic plain. Thick cross-laminated sandstone units above scour surfaces are channel deposits, and the thinly interbedded shales and sandstones formed in various parts of the overbank/backswamp region. Only a crude cyclicity is exhibited here.

Scattered about on the major surface exposed through most of the mine are conspicuous, rusting ironstone (siderite) concretions. Most are spaced randomly; a few line up along Carboniferous trees. Typically, their shape in plan is irregularly circular to oval, and they are flattened in the plane of bedding. The concretions occur at the interface between the medium-grained channel sandstone and the overlying Carboniferous mudrock and coal. Because the median plane of the concretions was commonly above the sandstone surface, many of them have fallen from the surface when the mudrock and coal was removed. Although many concretions have septarian centers and are generally extensively weathered, one can in places make out ghosts of original lamination passing from the sandstone through the concretions.

The main core of each concretion is nearly all siderite, as intergrown spherulites and a small proportion of euhedra. Nearly all the original sandstone grains have been replaced. In some cases, laminae of coarser quartz can be found to pass from the host sandstone into the concretion; these commonly show only partial replacement by siderite. Toward concretion margins the siderite spherulites are more separated, leaving between them unreplaced quartz and/or clays. Small euhedra of pyrite have also been found in the marginal zone.

Figure III-11

Photo micrographs, cleavage and deformation mechanisms, Bear Valley Strip Mine.

Figure III-11 A

Primary crenulation cleavage in shale near Station C. Bedding NW - SE, cleavage N - S. Crossed nicols, width of field .25 mm

Figure III-11B

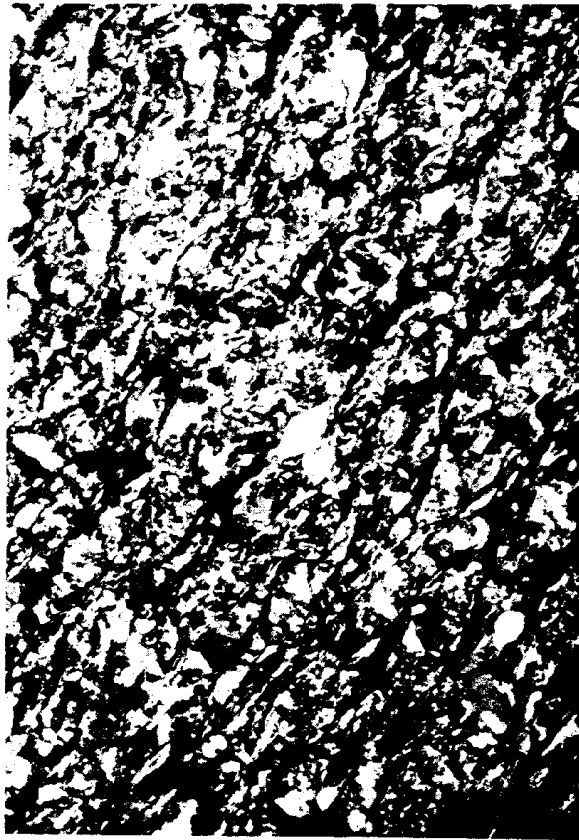
Spaced cleavage from quartz-rich siltstone in northeast corner. Anastomosing, cleavage planes (NW-SE), are clay-carbon partings with parallel phyllosilicates. Quartz is oriented parallel to cleavage (due to pressure-solution) or parallel to bedding (NE -SW). Crossed nicols, width of field .75 mm

Figure III-11C

Quartz wacke from crest of Whaleback Anticline. Intragranular deformation shown by quartz deformation lamellae in bands emanating from grain contacts. Crossed nicols, width of field .6 mm

Figure III-11D

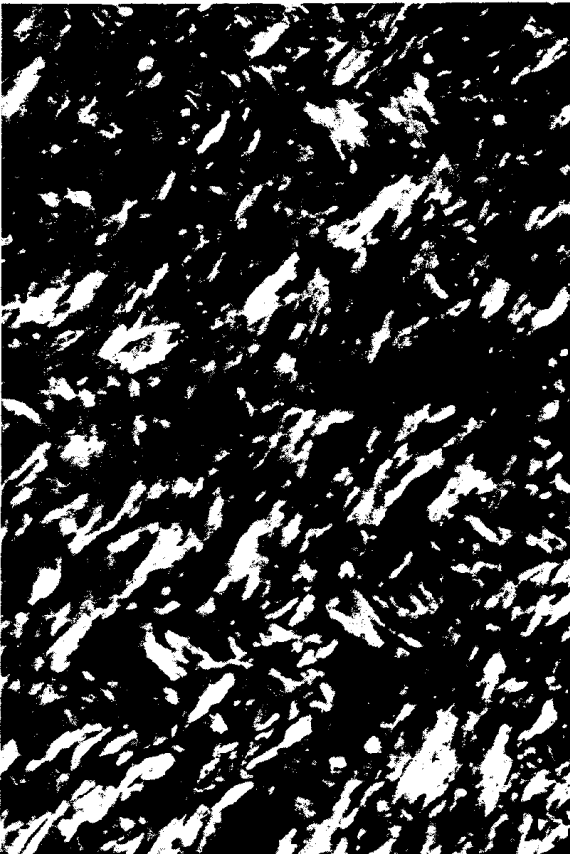
Detrital mica in quartz wacke of C. Packing changes, grain boundary sliding and intragranular deformation in the quartz framework have created local stress concentrations that have folded the mica. Crossed nicols. width of field .25 mm.



B



D



A



C

Two of the elements in the explanation of the genesis of such siderite concentrations are the source of the iron and the source of carbon dioxide. It appears likely that dissolved iron in Carboniferous river water became trapped as pore water, possibly in association with kaolinitic clays (Carroll, 1958; Matsumoto and Iijima, 1981). In the diagenetic reducing conditions, the various iron oxides and hydroxides were converted to soluble ferrous iron, and carbon dioxide was generated principally by fermentation of organic matter (Matsumoto and Iijima, 1981, p. 253). During compaction, the pore water could migrate until it reached a permeability barrier, such as this sandstone-mudrock interface, where siderite precipitated and replaced primary materials (Raiswell and White, 1978; Matsumoto and Iijima, 1981).

It is commonly suggested that such concretions form very early in diagenesis, probably at burial depths less than 100 m (Matsumoto and Iijima, 1981, p. 246). The high degree of differential compaction of the basal mudrock around the stiff concretions suggests that these Llewellyn concretions also formed quite early. Their growth would proceed until the available supply of iron was depleted.

SUMMARY

The Bear Valley Strip Mine is the best exposure in the northern Valley and Ridge Province for demonstrating the sequence and overlap of stages of the Alleghany Orogeny. Stage I is pre or early Alleghany jointing in coals, best seen in the Appalachian Plateau to the northwest (Nickelsen and Hough, 1967). Stage II is transverse extensional jointing in sandstones and ironstones which is overprinted by layer parallel shortening involving Stage III crenulation and pressure solution cleavage and Stage IV conjugate wrench and wedge (thrust) faulting. All previous structures were rotated by Stage V folding which initiated layer parallel extension leading to Stage VI extensional faults (strike and transverse "grabens"), extensional joints parallel to fold hinges and upthrusts growing out of folds. Stage VII wrench faults that cut all previous structures cannot be seen at Bear Valley. During the orogeny, strain mechanisms changed from extensional rupture manifested by Stage I and II joints to pressure solution, intergranular grain to grain adjustments, crenulation of sedimentary fabrics, recrystallization, and intragranular crystal-plastic mechanisms during Stage II and V, to shear fracturing and renewed extensional rupture during Stage IV, VI, and VII.

We have reported recent measurements that may indicate the environmental parameters that directed the strain mechanism and sequence of deformation. Evidence from conodonts, coal and fluid inclusions indicate that local ambient temperatures during the Alleghany Orogeny ranged from 185 to 205° and that pressures exceeded 1 kb, corresponding to overlying stratigraphic thicknesses of 5 to perhaps 6 or 8 km.

LUNCH

<u>Miles</u>	<u>Interval</u>	
27.6		Return east on Bear Valley Avenue.
29.2	1.6	Stop sign at junction with PA Route 125; turn right to PA 125 (south).
30.1	0.9	Entering Village of Burnside.
31.4	1.3	Turn right (west) before leaving crestal region of ridge.
31.5	0.1	Pottsville Conglomerate. Sharp Mountain Member exposed on right for 0.3 mile; physiography for next 5 miles will show Pottsville Conglomerate as ridge to right (north), Pocono Formation as ridge to left (south) and strike valley in the Mauch Chunk Formation.
32.4	0.9	Stop sign; turn right on road to Trevorton.
37.2	4.8	Begin gradual ascent of Pottsville Conglomerate ridge.
38.0	0.8	Beginning of outcrops of Pottsville Conglomerate; on right for about 0.3 mile, dipping steeply north.
38.3	0.3	Crest of ridge; as road descends, note microwave tower in distance to the west, that marks the western terminus of this anthracite synclorium (i.e., Western Middle Field).
38.7	0.4	Land on both sides of road has been stripped, backfilled, and reforested.
39.2	0.5	Outcrops of Llewellyn Formation visible.
39.4	0.2	View ahead and above to coal stripping operation. Reading Anthracite shovel visible from here in 1982.
39.9	0.5	Through water gap in Pottsville Conglomerate.
40.4	0.5	Stop sign at junction with PA Route 225; turn right (east).
40.8	0.4	At about point opposite Line Mountain Middle School, turn left (north on PA Route 890).
41.0	0.2	Road bends left and ascends Pocono ridge.
41.8	0.8	Begin 0.2 mile of Pocono Formation outcrops.
42.0	0.2	Summit of road; begin descent.
42.1	0.1	Additional Pocono outcrop on left. View to the north is across rolling Catskill farmland to Tuscarora anticlinal ridges in the far distance. Prominent cliff is Shikellamy Lookout at confluence of the West and North Branches of the Susquehanna River.

<u>Miles</u>	<u>Interval</u>	
44.3	2.2	Outcrop of Catskill Formation on right.
45.0	0.7	Trimmers Rock Formation on right.
45.2	0.2	Entering Village of Augustaville; continue ahead on PA 890.
46.7	1.5	Mahantango Formation makes small hill; outcrops visible next to road.
47.2	0.5	Road intersection; turn left (west) in front of white stone memorial.
51.1	3.9	Stop sign at junction with PA Route 147; turn left (south). Outcrop of Marcellus Shale on right.
51.7	0.6	Road curves around anticlinal nose (plunging left) on Keyser/Old Port Formations. Valley to the left is in Marcellus Shale and Mahantango is in hills beyond that.
53.5	1.8	Poor outcrop of Marcellus to left.
54.5	1.0	Borrow pits in Marcellus Shale and roadcut of Selinsgrove Limestone on left.
54.6	0.1	Junction of graded road on left. Passengers disembark and vehicles turn around and park on graded road facing west.

Stop IV Selinsgrove Junction

INTRODUCTION

At this stop we will see cleavage duplexes and a tip line in Marcellus Formation, strain discontinuities and strain gradients related to rock type and thrusting, cleavage halos, and a stratigraphic section of the Onondaga (Selinsgrove) Limestone, Marcellus Formation, including Purcell Member and Tioga Ash Bed with its associated gamma ray peak, and Mahantango Formation, including one coarsening upward, prograding delta cycle.

This locality has a number of excellent exposures of structural features in the Onondaga Limestone, Marcellus Shale, and Mahantango Formation on both limbs of the Selinsgrove Junction Second Order Anticline. We will first visit a long railroad cut (Stations A, B, C and D) through the south limb of the anticline where the Onondaga, Marcellus and Mahantango Formations are almost continuously exposed, and then visit two small quarries along Route 147 in the Marcellus on the north limb (Stations E and F).

The most significant structural features are thin (1 - 2m) and thick (60 m), bed-parallel zones of rock cleavage and intense strain (layer-parallel shortening - LPS

- >30%) interbedded with relatively unstrained (LPS - <5%), unclesved rock. The upper and lower contacts of the cleaved zones are abrupt strain discontinuities at thrust faults marked by slickensided surfaces, slickenlines, and cataclastically broken and milled quartz that was originally precipitated synorogenically in gash veins and faultstep pressure shadows. Each bed-parallel zone of intense strain consists of a spaced cleavage that is grossly perpendicular to bedding but in detail dragged against the roof and floor thrusts to produce a sigmoidal pattern. Although the roof and floor thrusts are zones of concentrated shear, the geometric relation between shear planes, foliation planes and undeformed rock outside the rock is not that of previously described shear zones (Ramsay and Graham, 1970, Ramsay and Allison, 1979, Ramsay, 1980) or ductile deformation zones (Mitra, 1979). Rather, they are cleavage duplexes, which are bed-parallel zones of intense strain expressed as rock cleavage bounded by floor and roof thrusts. Those cleavage duplexes have developed along the border of relatively undeformed overlying and underlying thrust sheets. Fault duplexes have previously been illustrated (Dahlstrom, 1970, fig. 22) as imbricated packets of stiff and ductile beds confined between floor and roof thrusts and successively accreted in the direction of transport by thrust faulting of the foot wall, as illustrated in the sequential diagram (Figure IV-12) adapted from Boyer and Elliott, (1982, fig. 19).

Figure IV-13 is an analogous interpretation of how these cleavage duplexes may have formed sequentially in ductile shale sections by the following steps:

1. Propagation of a thrust fault tip line (Boyer and Elliott, 1982, fig. 2, 11) into a shale section, with development of LPS and spaced cleavage. In thin section, this spaced cleavage is a primary crenulation cleavage (i.e., crenulation of detrital, bed-parallel phyllosilicates with concentrated pressure solution on the limbs of crenulations, as indicated by clay-carbon partings (residual concentrations of carbon and phyllosilicates oriented parallel to S_1)). (Figure IV-9)
2. Spaced cleavage is associated with 30% LPS and thickening at the tip line as well as propagation of the floor thrust under this cleavage in the direction of transport.
3. 1 and 2 are repeated several times and thrust faults then ramp through the cleaved zone from the floor thrust to the contact with the overlying unclesved rock. As this continues, the cleavage becomes enclosed between floor and roof thrusts.
4. As 1, 2 and 3 repeat, the cleavage duplex is formed with floor thrust, and roof thrust bounding sigmoidal cleavage. Cleavage is initiated by LPS perpendicular to bedding (pure shear) but is later dragged into a sigmoidal pattern by simple shear against the roof and floor thrusts. It is likely that LPS and creation of rock cleavage reduces shale ductility, promoting propagation of the duplex.

Our structural geology objectives are to demonstrate the evidence for the above interpretation. In addition, we will show aspects of the stratigraphy, particularly gross lithologic characteristics as they are related to structure, and the Tioga Ash Bed and its associated mineralogy and gamma ray peak.

General Geologic relations are shown on the Geologic Map (Figure IV-1) Geologic sections (Figure IV-2) and the composite structure section (Figure IV-3). Detailed stratigraphic sections with structural features shown are present in Figure IV-4.

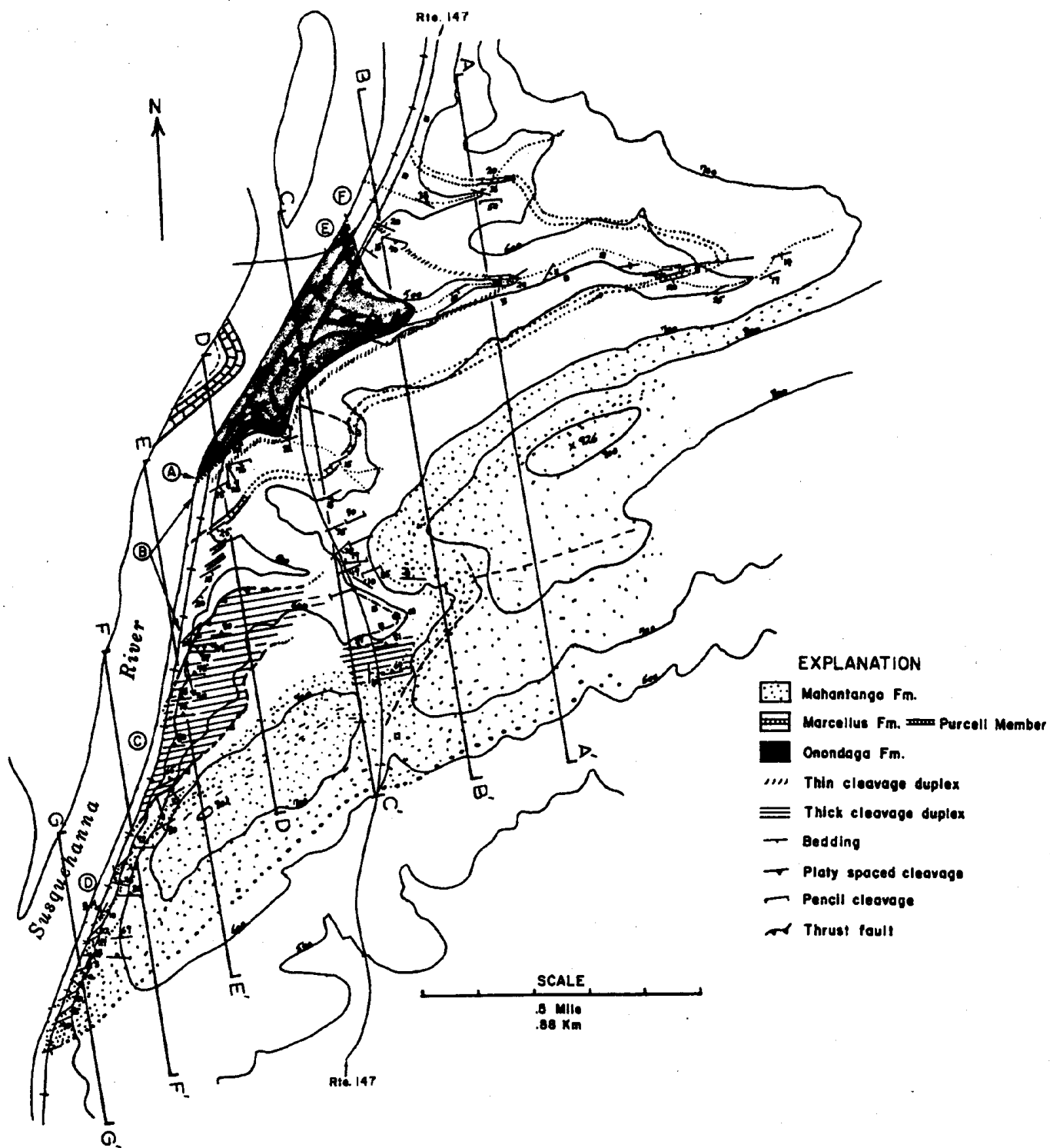


Figure IV-1

Geologic Map of the Selinsgrove Junction Area

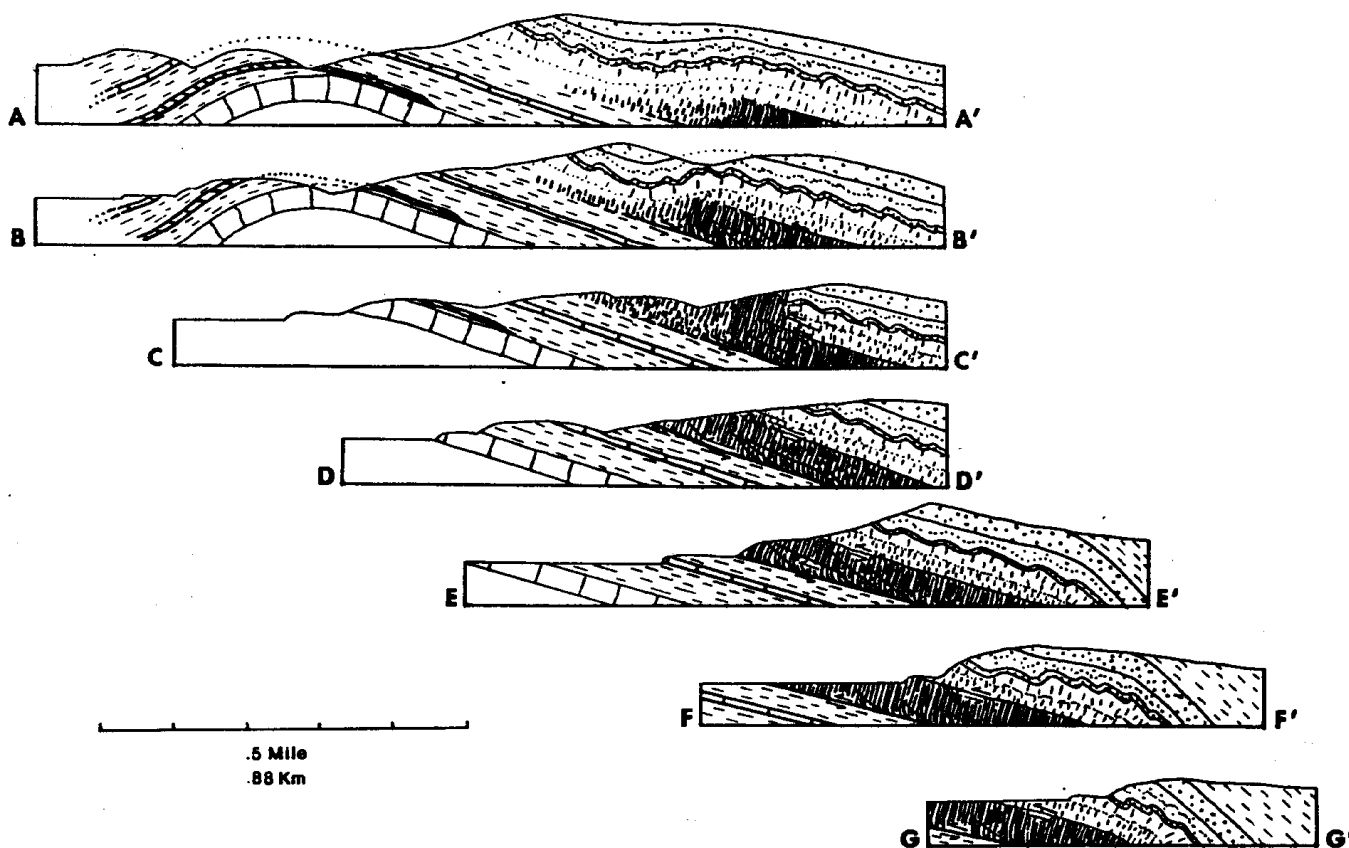


Figure IV-2

Geologic sections A, B, C, D, E, F, G of the Selinsgrove Junction Area

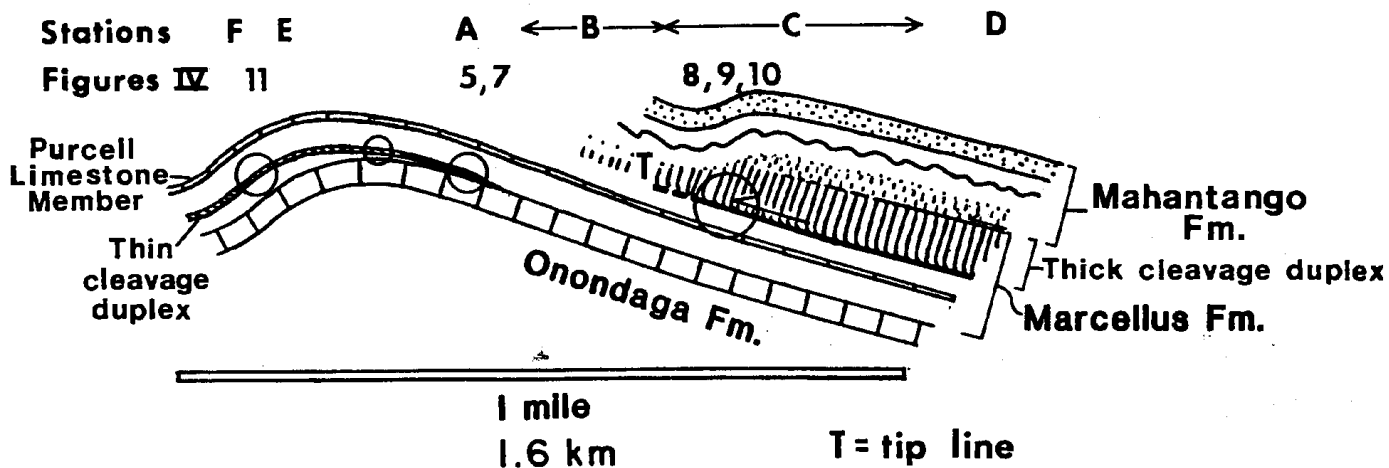


Figure IV-3

Composite geologic section of Stop IV showing main structural features, stations A-F to be visited, and locations of figures 5, 7, 8, 9, 10, 11

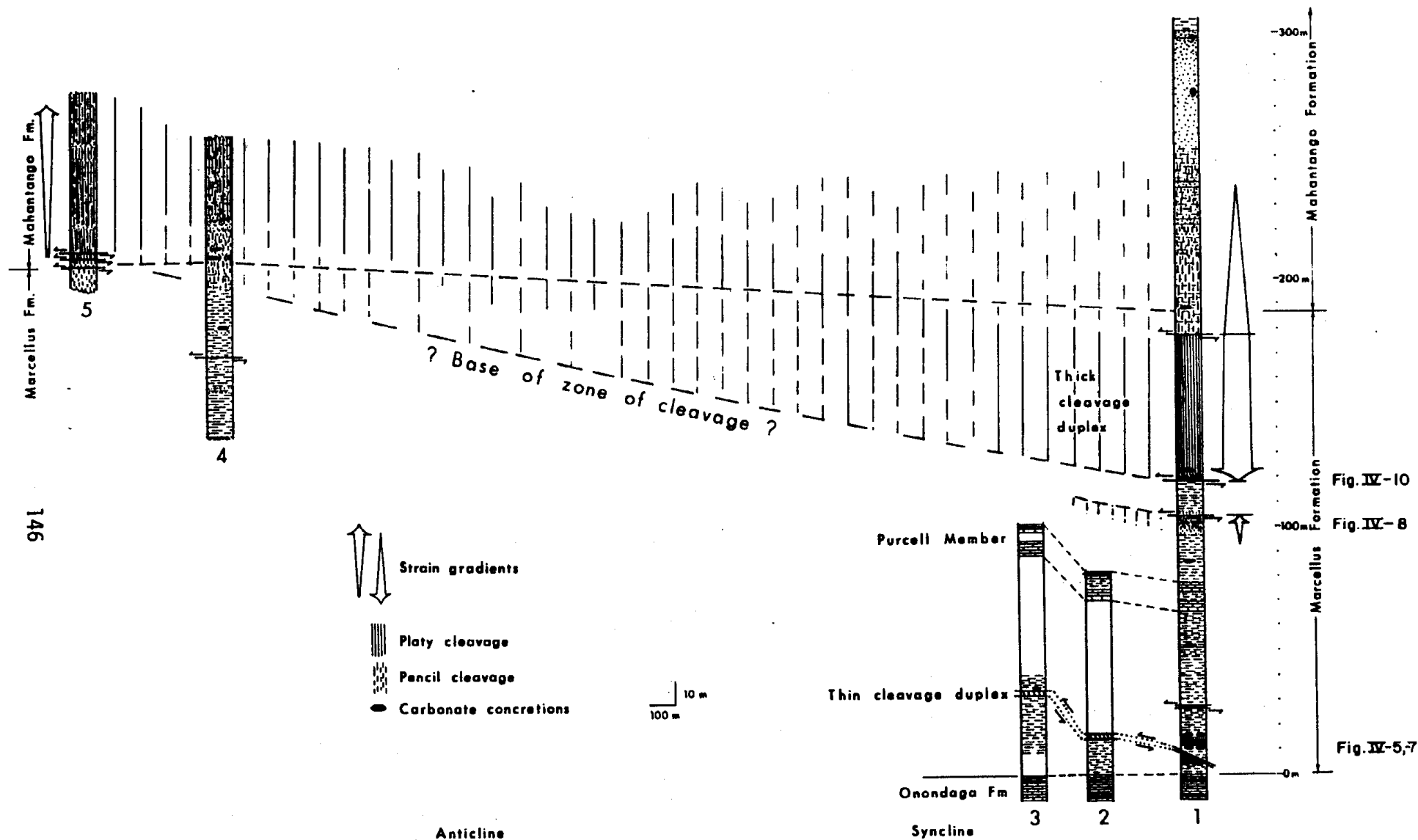


Figure IV-4

Composite stratigraphic sections showing structural features and correlation of stratigraphy and structures

1. South limb of Selinsgrove Junction second order anticline (SJSOA)
2. Crest of SJSOA
3. North limb of SJSOA
4. Route 147 road intersection at $76^{\circ}48'30''$, $40^{\circ}50'08''$
5. Route 147 .4 km south of the bridge over Shamokin Creek

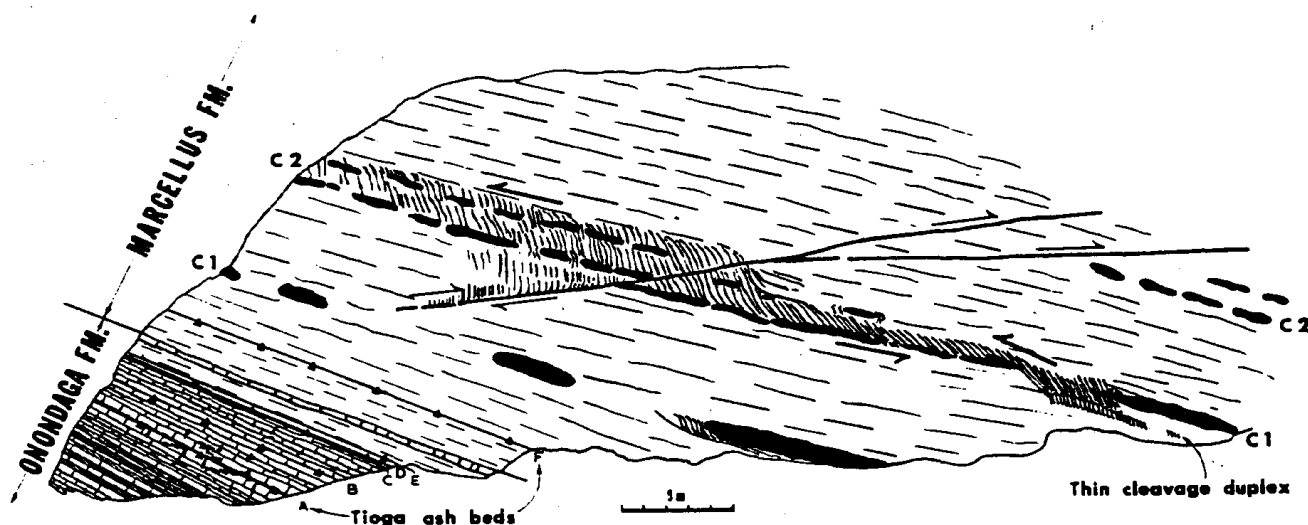


Figure IV-5

Drawing of outcrop of Onondaga Limestone-Tioga Ash Bed - Marcellus Formation and the thin cleavage duplex at Station IV-A

Station A

The thin cleavage duplex is exposed in the lower Marcellus Formation on both limbs of the anticline, climbing section above the Onondaga Limestone from 5 m on the south limb, to 15 m on the crest, to 33 m on the north limb. On the south limb (illustrated in Figure IV-5) the following features can be seen.

1. LPS in Onondaga Limestone expressed as spaced pressure solution cleavage, and intra-bed wedge faulting (zones of en echelon gash veins).
2. Cleavage refraction from limestone (90°) to shale beds (20°). Angles are bedding-cleavage angles.
3. The thin cleavage duplex in the Marcellus Shale tracking a carbon-rich shale zone between two layers of carbonate concretions that show cleavage halos. Cleavage halos form at the end of relatively stiff carbonate concretions that do not deform during LPS of surrounding shale. Above and below the concretions at the contact with shale are slickensided surfaces that serve as boundary zones between the different strains in the shale and the concretions.
4. The thin cleavage duplex is cut and displaced by a small back thrust illustrated in Figure IV-5. The well-exposed thin cleavage duplex serves as a small scale model of the thicker cleavage duplex that is found higher in the section. Bed parallel detachment or decollement zones show an affinity for carbon-rich shales such as this zone in the Marcellus Formation. Other examples in the Appalachians are the Antes Shale in the Ordovician above the "Trenton" Limestones (Pierce, 1966, pp. 45-52), certain parts of the Chattanooga Shale of southern Virginia (Kepferle, Pryor and Potter, 1981, p. 10), the Millsboro shale, W.VA (Wheeler, 1978), and Pennsylvanian coal measure coals and shales in southwestern Virginia and in the Cumberland Plateau of Tennessee (Harris and Milici, 1977, plate 3 and 8).
5. The Tioga Ash Bed and its associated gamma radiation peak in the carbon-rich shales at the contact between the Onondaga and Marcellus. The Tioga Ash

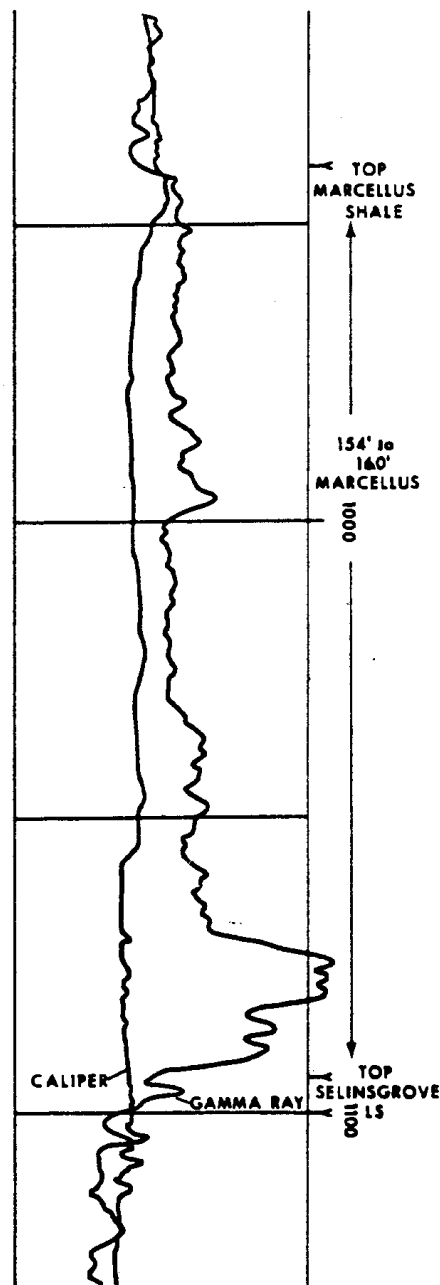


Figure IV-6

*Gamma ray log from Wilhour well, Stonington, PA near Stop II.
Log show parts of Onondaga, Marcellus and Mahantango section*

Bed is represented as 6 distinct, buff-colored, blocky, .5 to 20 cm, mineralized beds below the carbon-rich shale between carbonate concretion zones Ca 1 and Ca 2 where the largest peak of gamma radiation is found (see accompanying article by R. Smith and J. Way). This gamma radiation peak is recognized in well logs throughout the Appalachian basin, appearing similar to the log from the Wilhour well at Stonington, PA near Stop II (Figure IV-6). Although the Marcellus Formation is marked by generally higher gamma radiation than overlying and underlying units, there is only one obvious peak, located near the base of the section, which is important here because it can be used to prove that the partially exposed thin cleavage duplexes on the crest and north limb of the anticline are at the same stratigraphic horizon. Also, in the tectonically thickened Marcellus Formation south along the RR tracks, no other radiation peak has been found, thus indicating that the base of the Marcellus is not repeated by thrusting.

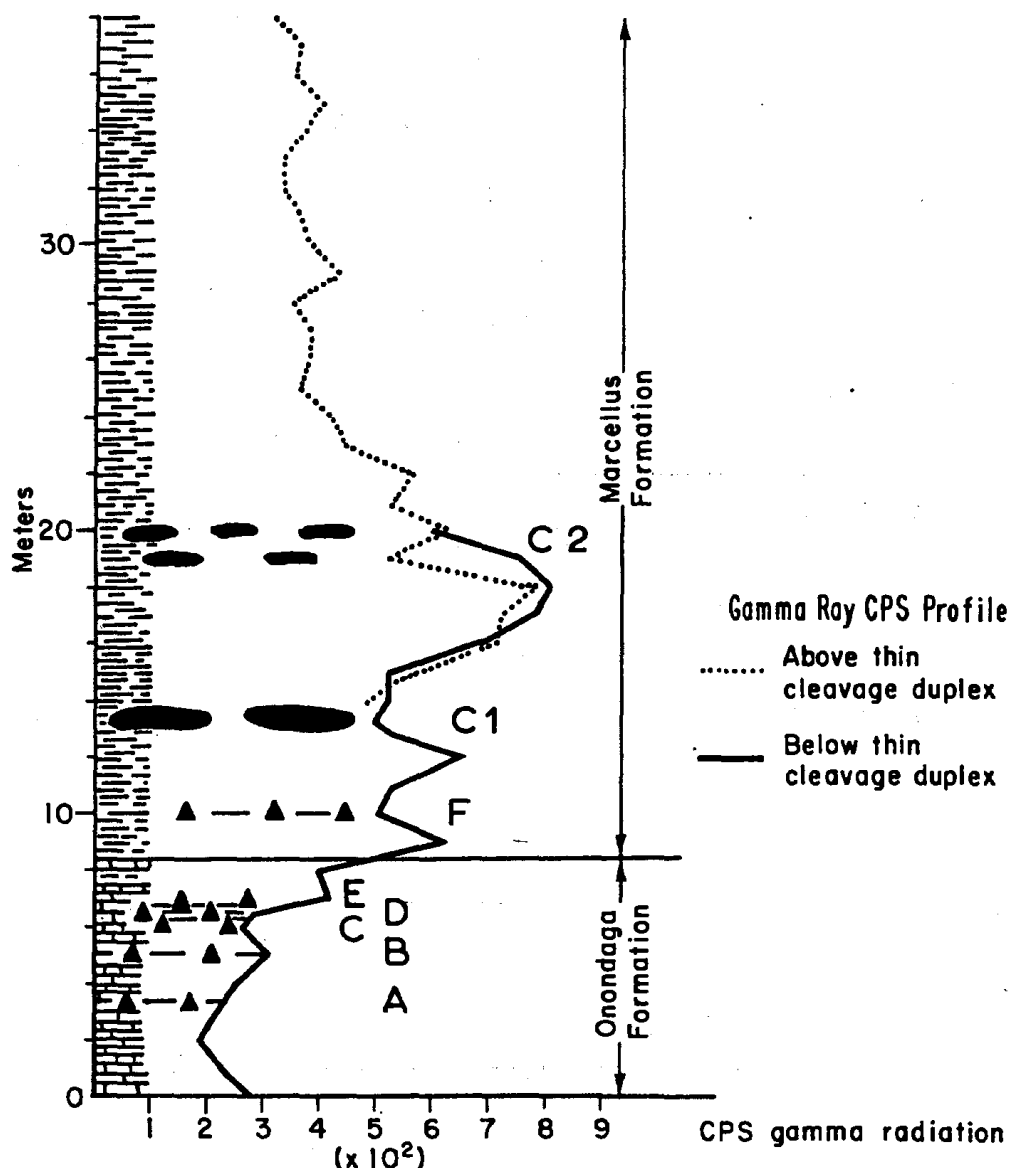


Figure IV-7 Gamma ray log at Station IV-A, compare to outcrop drawing, figure IV-5

Station B

Walk south along the RR track observing nearly continuous exposures of Marcellus Shale with no cleavage or thrusting (see Figure IV-4). At 45 meters above the base of the Marcellus a solitary carbonate concretion shows no cleavage halo, thus indicating no layer parallel shortening in this part of the section. At 60 to 70 meters above the base is the Purcell limestone member, which when cut and then etched with HCL, shows thin clay-carbon partings indicating pressure solution and minor layer-parallel shortening. Generally, Station B which comprises 100 meters of Marcellus shale including the Purcell limestone member does not show evidence of pervasive cleavage, cleavage halos, thrusting or other indicators of strain. It stands in contrast to Stations A and C where there is abundant evidence of layer-parallel shortening and thrusting.

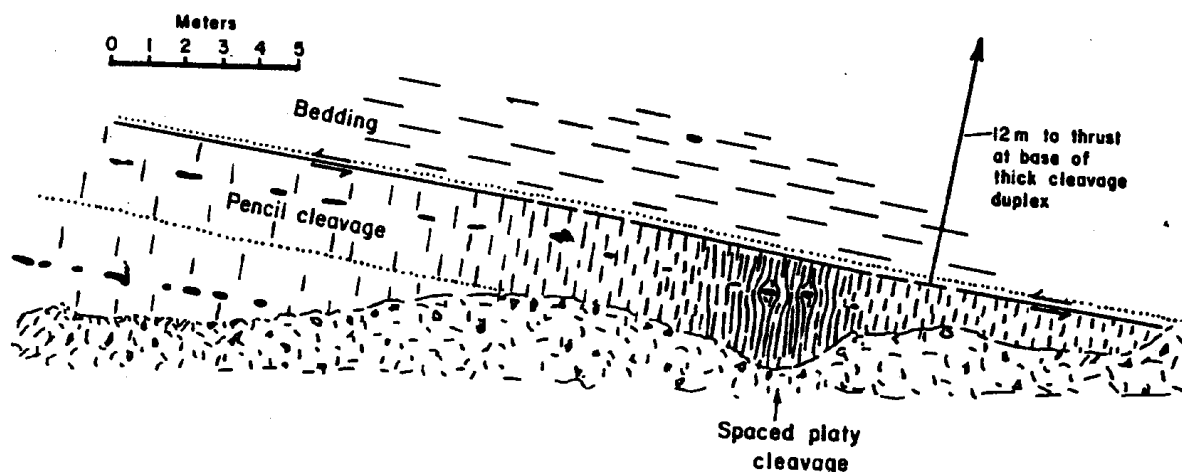


Figure IV-8

Drawing of Marcellus Formation 12 meters below the base of the thick cleavage duplex showing cleavage halos, the pyrite-silt marker beds, gradation from platy spaced cleavage to pencil cleavage, and a minor thrust serving as top boundary of a strain gradient. Station IV-C.

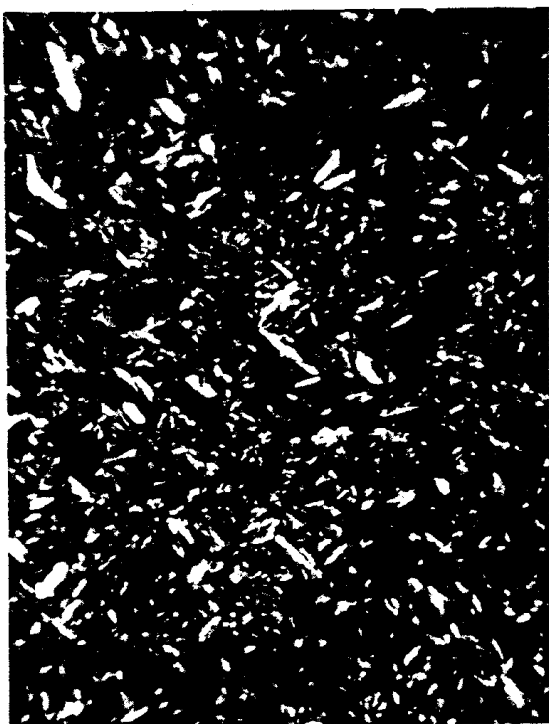
Station C

Here a number of deformation features may be seen, including the thick (60 m) cleavage duplex, highly cleaved Marcellus Shale within the duplex, the basal thrust that brings cleaved Marcellus over bedded Marcellus (Figure IV-10), simple shear at the base of the thick cleavage duplex that drags cleavage against the thrust, imbricate thrusts rising off the basal thrust and forming kinks or reorientations of cleavage, cleavage halos around carbonate concretions, (Figure IV-8, 9), strain gradients revealed by changes from pencil cleavage to platy, spaced cleavage, and, finally, the roof thrust of the thick cleavage duplex where platy spaced cleavage changes upward to pencil cleavage. Primary crenulation cleavage exposed in the thick cleavage duplex is associated with 33% LPS (Figure IV-9A).

Figure IV-9

Photographs of crenulation cleavage and cleavage halos, Marcellus Formation

- A. *Crenulation cleavage in thick cleavage duplex, Station C Bedding E-W, cleavage N-S. 33% layer parallel shortening of crenulated phyllosilicates in B domains. Crossed nicols, width of field .6 mm*
- B. *Same field as A photographed in plane light to show N-S clay-carbon partings, A domains, parallel to cleavage*
- C. *Cleavage halo at ends of carbonate concentration in uncleaved shale. Locality: Section 4, Figure IV-4, 10 cm ruler for scale*
- D. *Cleavage halo around carbonate concretion in strongly cleaved shale with greater than 30% LPS. Locality: Figure IV-8. Coin = 2.2 cm for scale*



A



B



C



D

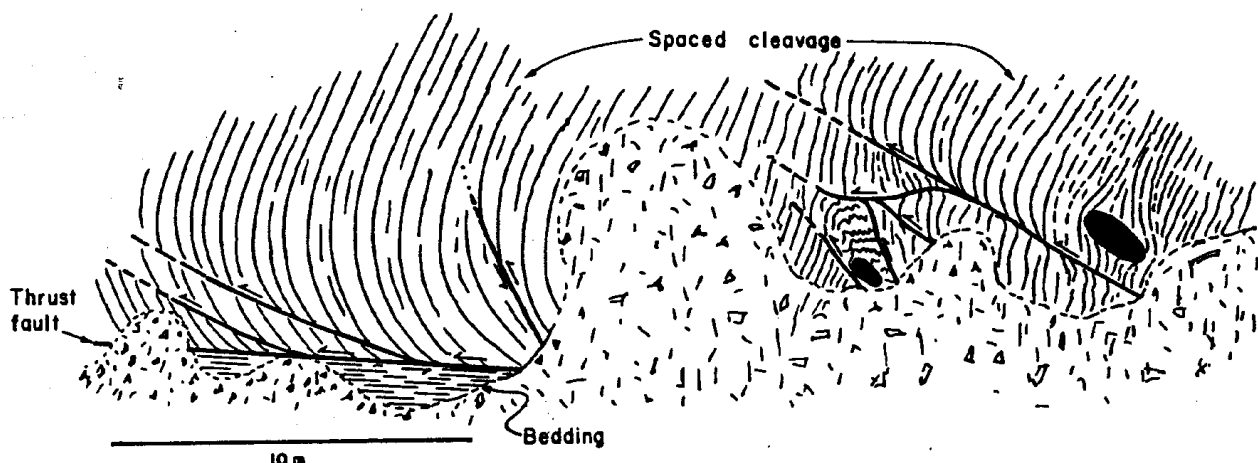


Figure IV-10

Drawing of structural features above and below the basal thrust of the thick cleavage duplex at Station IV-C. Note:

1. *Bedding, no cleavage below the thrust*
2. *Counter clockwise rotation (drag) of cleavage in duplex against basal thrust*
3. *Imbricate thrusts rising off the basal thrust which cut and kink the platy spaced cleavage*

Station D

Farther south along the RR the Mahantango Formation contains a coarsening upward, prograding cycle that culminates in the 40 meter thick, massive, Montebello Sandstone, exposed on both sides of the track. Before reaching this massive sandstone, interbedded sandstone and shale north of the signal tower show rock cleavage, fourth order folding, and wedging; all structures that accommodate LPS. It is not known whether LPS by these mechanisms is equal to the shortening due to cleavage in the underlying Marcellus, but our interpretation on Figures IV-2 and IV-3 shows LPS in different parts of the section to be equal.

The traverse south along the RR track stops at the Montebello sandstone. Three features are noteworthy: 1. the abrupt change to shale above the Montebello Sandstone that initiates the next coarsening upward Mahantango cycle; 2. brachiopod death assemblages concentrated near the top of the Montebello; and 3. a pre-folding wrench fault surface with slickenlines only 15° from the fault-bedding intersection, exposed on the west (river) side of the RR track. This fault is another manifestation of the LPS prior to major folding.

Field trip participants should now turn around, return to the road at the buses and then walk north to two quarries in the Marcellus Shale on the north limb of the Selinsgrove Junction second order anticline.

Station E

Marcellus Shale in the first quarry to the north is uncleaved, dipping north above the Onondaga Limestone. No evidence of LPS exists in this quarry.

Station F

In the second quarry to the north the thin cleavage duplex dips north, paralleling bedding, through the middle of the quarry. The sigmoidal cleavage (Figure IV-11) abruptly terminates against the floor and roof thrusts at striking strain discontinuities. This cleavage is a spaced cleavage appearing microscopically as a primary crenulation cleavage with clay carbon partings on limbs and/or fold hinges (Figure IV-9A, B). No cleavage or other evidence of LPS is evident in overlying or underlying shale. This cleavage duplex is 33 meters above the Onondaga Limestone here on the north limb but the gamma radiation peak found within 10 meters of the top of the Onondaga Limestone on the south limb is also detected here. This is interpreted as repetition of section by thrusting along the cleavage duplex. The dip and sigmoidal asymmetry of the thin cleavage duplex indicate that the thrusting probably preceded major folding.

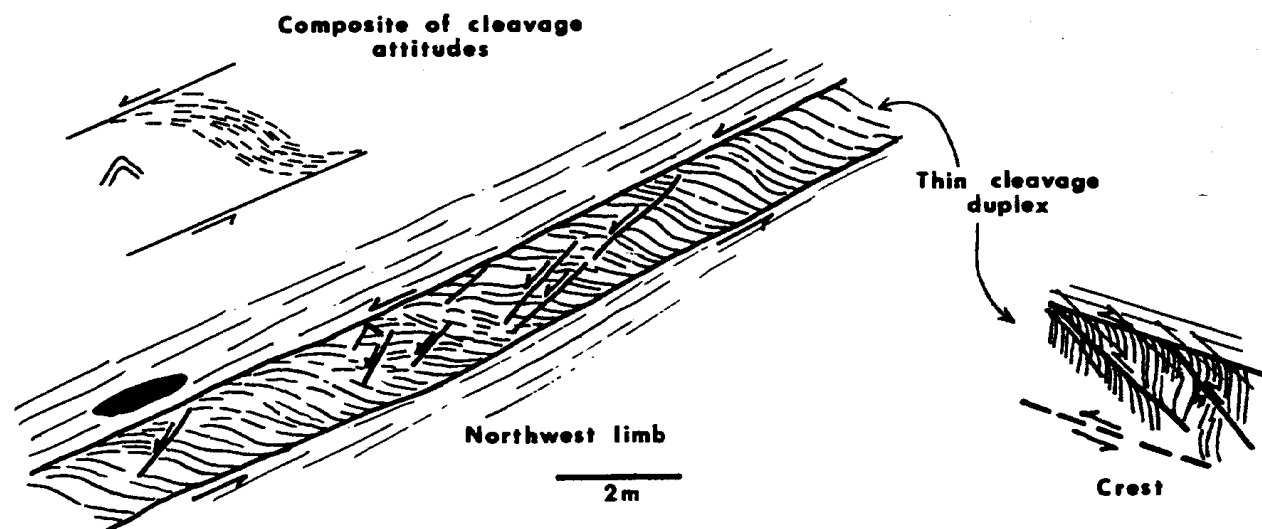


Figure IV-11

Drawing of the thin cleavage duplex as seen at the crest and north limb of SJSOA. The composite shows attitudes of all measured cleavage planes within the duplex plotted in correct relative position from top to bottom. Station IV-F.

SUMMARY

You have seen:

1. Strain concentrations related to both the tip line of thrust faults propagating through dominantly shaley sections and the contrasting ductilities of carbonate concretions and enclosing shale (cleavage halos).
2. Abrupt strain discontinuities where strongly cleaved rock is separated from uncleaved rock by a thrust fault or a slickensided boundary zone.

3. Gradual strain gradients where sedimentary, bed-parallel shale fabric is overprinted by cleavage of gradually increasing dominance. The observed progression is:

shale → pencil cleavage normal to bedding, bedding still preserved → platy spaced cleavage, normal to bedding, bedding obliterated

Pencil cleavage in areas of the Valley and Ridge of SW Virginia is associated with >5 to <24% LPS (Reks and Gray, 1982) which agrees with our observations.

4. Spaced pressure solution cleavage in limestone. Cleavage planes are either irregular stylolitic or planar, but both types are marked by concentrations of insoluble residues called clay-carbon partings (Nickelsen, 1972).
5. Spaced primary crenulation cleavage in highly strained shale (LPS >30%). Bed parallel phyllosilicates are crenulated on wavelengths of .02 to .06 mm and limbs or crests of crenulations have undergone pressure solution, and accumulation of clay-carbon partings. LPS estimates for platy cleavage is based upon measuring crenulations in "B" domains. "A" domains where pressure solution is dominant have probably been shortened more.

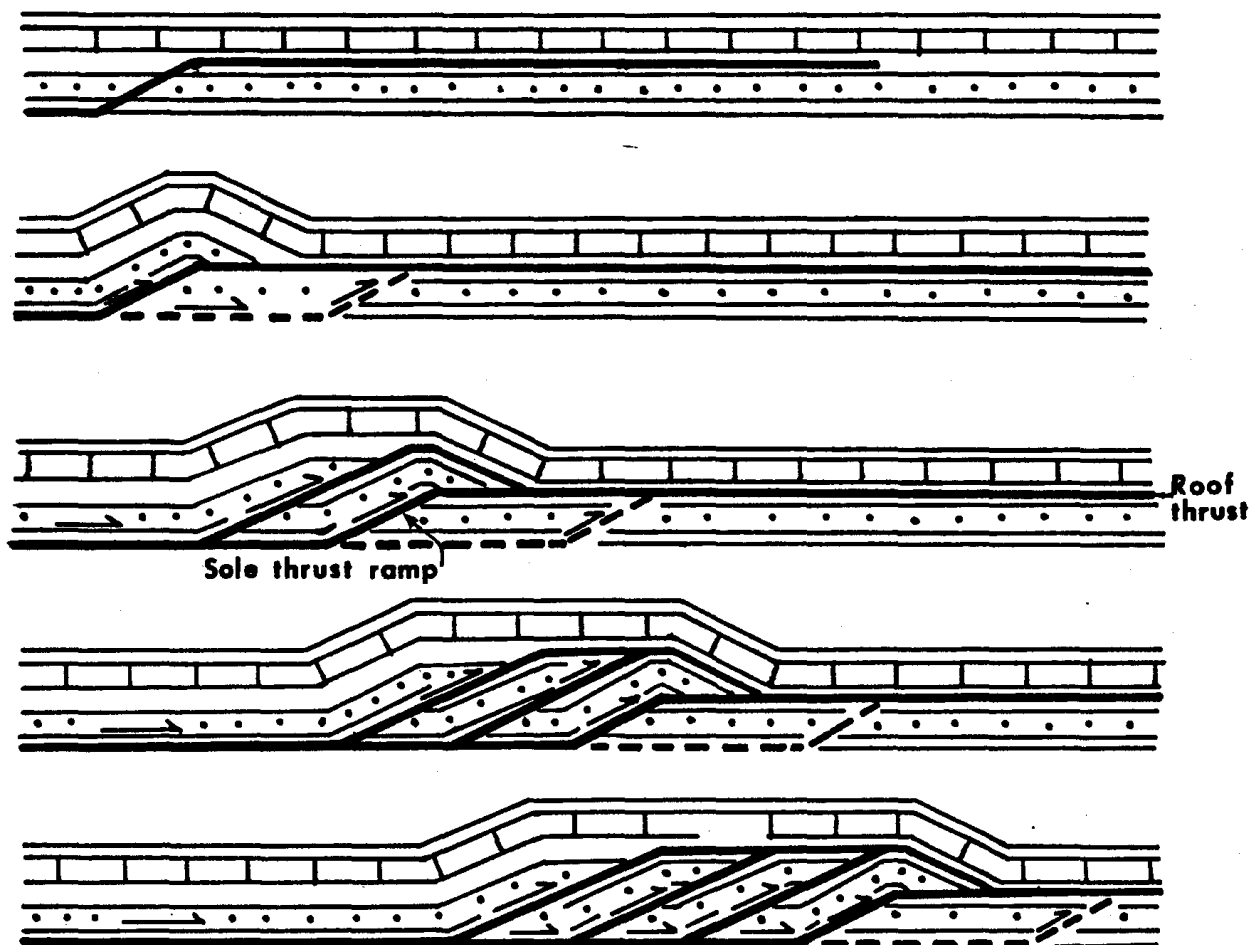


Figure IV-12

Drawing of duplex propagation after Boyer and Elliott (1982)

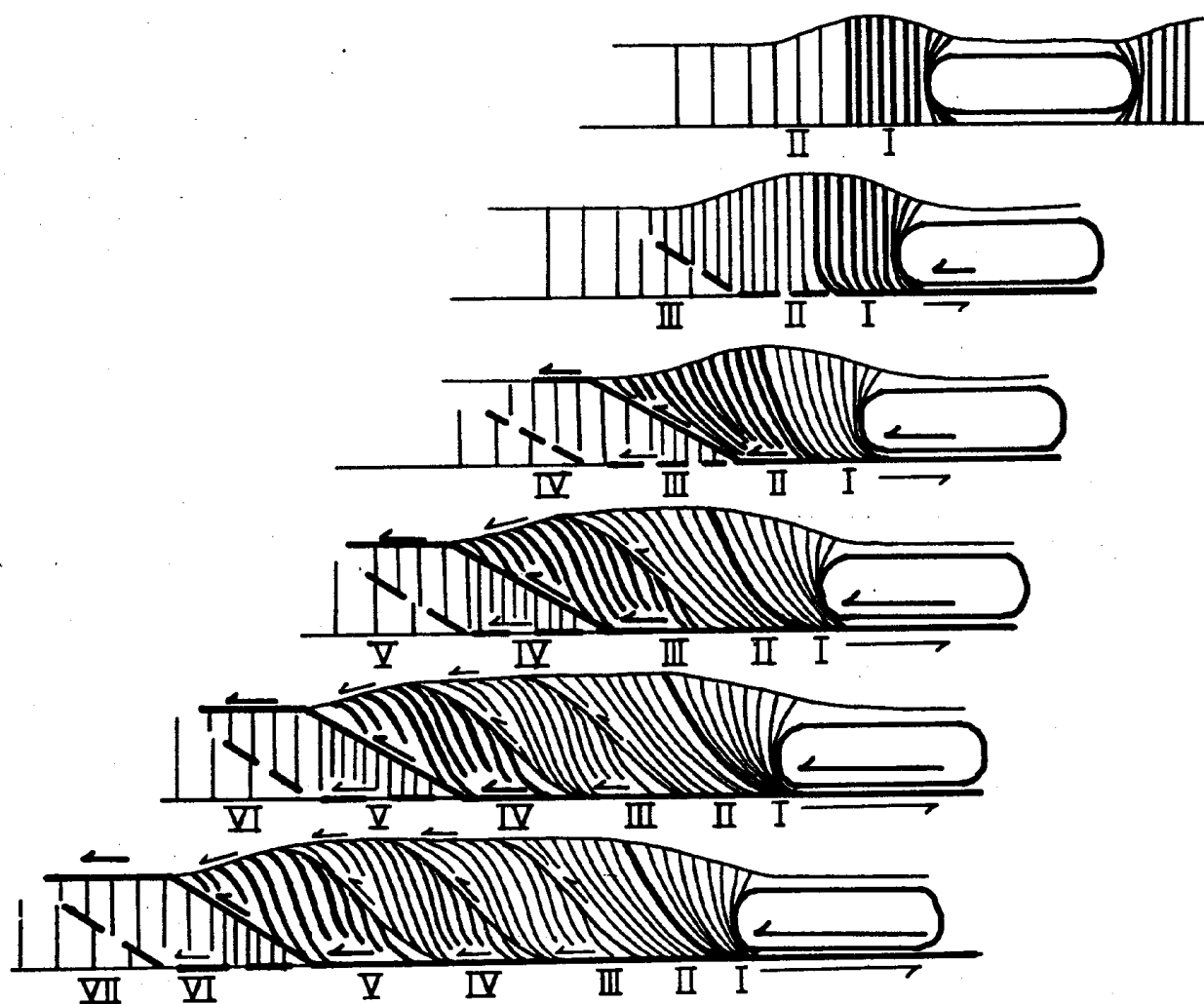


Figure IV-13

Drawing of inferred sequence of propagation of the cleavage duplex in the Marcellus Formation

6. Intrabed thrust faults or wedges (Cloos, 1961) which accommodate layer parallel shortening in stiff rocks such as the Selinsgrove (Onondaga) Limestone and Mahantango Formation Sandstones.
7. Stratigraphic relations of the Onondaga, Marcellus and Mahantango Formations, and the Tioga Ash bed and its overlying gamma radiation peak.
8. Rock cleavage changing orientation and asymptotically approaching the abrupt strain discontinuity that bounds it.
9. Imbricate thrusts and kink bands that rise off the basal thrust and cut or distort rock cleavage.
10. Quartz precipitated in gash veins or fault step pressure shadows along the floor thrust of the thick cleavage duplex. This quartz contains CO₂ - CH₄ fluid inclusions that permit estimation of ambient pressure and temperature during thrusting.

These features have been interpreted in the following way:

1. Abrupt strain discontinuities bounded above and below by thrust faults have been called cleavage duplexes and their method of incremental propagation has been suggested. Strain concentrations related to both the tip line of thrust faults and stiff rock types enclosed in ductile rocks have been recognized, but it would be difficult to differentiate the two types of strain concentration in a poorly exposed area. Perhaps the two types are transitional. Rock type related strain concentrations in a horizontal sedimentary sequence undergoing uniform LPS may actually initiate thrusting at points where stiff, unyielding, strata abut ductile strata. Small scale examples are cleavage halos around concretions, but regional facies changes from predominantly shale to sandstone may provide large scale examples. Both the Mahantango and Marcellus Formations have sand facies to the southeast that may promote stress concentrations in the area of the field trip, leading to thrusting or formation of rock cleavage. In this view, stress concentrations that are analogous to crystallographic line defects (dislocations) may initiate at stiff inhomogenities or facies boundaries and propagate through the section as cleavage duplexes.
2. Layer-parallel shortening precedes thrusting and folding and is manifested in different rock types by: spaced pressure solution cleavage (argillaceous sandstone or limestone), spaced primary crenulation cleavage with domainal pressure solution (shale), and wedging (non-argillaceous limestone and sandstone). Crenulations in a few clear examples have produced 30% layer parallel shortening but the strain associated with well-developed platy cleavage is probably greater.
3. The superposition of the cleaved Marcellus found in the thick cleavage duplex upon uncleaved Marcellus Formation means that the cleavage developed earlier, to the southeast, probably by pure shear perpendicular to bedding, and was brought to its present position by thrusting. At the floor thrust of the thick cleavage duplex the pre-existing cleavage was dragged by simple shear so that it asymptotically approaches the plane of the floor thrust. As this cleavage was thrust and sheared it was also cut by imbricate thrusts and kink bands rising off the floor thrust.
4. The thin cleavage duplex is stratigraphically associated with the Onondaga Limestone-Marcellus Shale contact, Tioga Ash Bed, and the black carbonaceous shales with their gamma radiation peak. This duplex can be correlated across the crest of a second order fold by its associated gamma radiation peak. The constant vergence of cleavage within the duplex on southeast limb, crest and northwest limb of the fold suggests that it formed before folding as a fault zone climbing section toward the northwest in the direction of transport. It is probably no accident that this carbonaceous shale with the associated formerly bentonitic composition served as the detachment horizon for thrusting.

<u>Miles</u>	<u>Interval</u>	
54.6	0	Re-enter PA 147 and turn right (north)
58.2	3.6	Road intersection on right. Large exposure of Marcellus Shale grading up to Mahantango Formation. Bedding fissility at road corner changes northward and up section to pencil cleavage. Refer to Section 4, Fig. IV-4 which was measured from here to 58.3.
58.3	0.1	Begin 0.4 mile synclinal outcrop of Mahantango Formation with excellent spaced cleavage.
58.6	0.3	Mahantango Formation, dipping south, with bedding plane thrust faults separating zones of different cleavage aspect - pencil or spaced, Section 5, fig. IV-4.
58.8	0.2	Outcrop of Mahantango Formation sandstones dipping north; south end of bridge crossing Shamokin Creek.
59.0	0.2	Entering Sunbury; bear right to continue on PA 147.
59.9	0.9	Turn left to follow PA 147.
60.0	0.1	Turn right to follow PA 147 (north). Flood wall on left separates town from Susquehanna River; across river is a fine exposure of Trimmers Rock Formation.
60.3	0.3	Continue ahead on PA 147 as PA 61 turns right.
60.4	1.0	Pass replica of Fort August (right).
60.8	0.4	Turn left to cross Susquehanna River branch on steel bridge.
61.3	0.5	Cross second steel bridge.
61.6	0.3	Junction with U.S. Route 11; turn right (east) toward Danville, passing through town of Northumberland.
62.3	0.7	Leaving Northumberland.
65.0	2.7	Gravel quarry on right producing gravel from a Pleistocene terrace.
65.5	0.5	Outcrop on left of Mahantango Formation dipping south.
66.3	0.8	Two Pleistocene valley-train terraces of the North Branch of the Susquehanna River are well exposed.
68.1	1.8	Wickes Lumber on the right.
69.9	1.8	Stop 1 on the left.
72.5	2.6	Junction PA 54, turn left (north) on Rt. 54.
75.0	2.5	Turn right to Sheraton Inn.
75.2	0.2	Entrance to Sheraton Inn. End Day 1.

2ND DAY - SATURDAY, OCTOBER 1, 1983

<u>Miles</u>	<u>Interval</u>	
0.0		Depart from entrance to Sheraton Inn on secondary road east of PA 54. Drive west to PA 54.
0.2	0.2	Turn right (north) on PA 54.
0.4	0.2	Turn right into entrance ramp for Interstate 80 West.
2.1	1.7	Outcrops of shaly Mahantango Formation both sides of I-80.
5.1	3.0	Entrance to rest area on right.
7.3	2.2	Crossing Chillisquaque Creek; view ahead to dip slope of Keyser-Old Port ridge.
8.9	1.6	Crest of low ridge is outcrop belt of south-dipping Keyser and Old Port Formations. Hills ahead are Wills Creek Formation.
12.7	3.8	Exit right for PA 147 northbound.
13.1	0.4	Exit right from PA 147 at Watsontown-McEwensville exit.
13.3	0.2	At end of exit ramp turn left (west) toward Watsontown.
14.5	1.2	Junction PA 405, turn right (north) on PA 405. The Susquehanna River, West Branch is on your left.
15.7	1.2	Entrance to Watsontown Brick plant on right. Turn right toward office.
15.8	0.1	Office, Watsontown Brick plant.

Stop V - Watsontown Brick Company Quarries

(Stations A, B, C, and D will be visited to demonstrate sedimentary and deformation features. Buses will deposit participants at Station A and be reboarded at Station D.)

INTRODUCTION

These quarries are the best exposures in the region to demonstrate the correlation that exists between rock type, sedimentary structures, and tectonic structures within the Bloomsburg Formation. Here, progressive deformation which is more characteristic of the Bloomsburg Formation of this region can be observed.

PALEONTOLOGY

by

Donald M. Hoskins

The Bloomsburg Formation in this area contains a fauna generally characterized by large numbers of specimens of a few species of microscopic ostracods (Hoskins, 1961). These are usually found concentrated in thin zones interbedded in the mass of red mudstone that makes up the bulk of the Bloomsburg above and below the Moyer Ridge Member. The Moyer Ridge Member is a zone of about 10 meters of siltstone and sandstone and, in this quarry, forms the south wall at Station A.

Most remarkable at this locality is the occurrence of fragments and complete and nearly complete head shields of cyathaspid fish. These occur near the top of the Moyer Ridge in a zone about 1 cm-thick and localized in an area about 10 meters in length.

Complete head shields recovered from Station A measure 30-32 cm in length and appear to be the Genus Vernonaspidis. Vernonaspidis has been found in many localities in late Silurian rocks in North America (Denison, 1964).

Prior to this discovery of cyathaspid fish head shields, complete shields had been known from the Bloomsburg only in outcrops near Delaware Water Gap (Beerbower and Hait, 1959).

The normal occurrences of cyathaspid fish fossils in the Bloomsburg are microscopic and broken pieces of larger scales and shields. These and scales of thelodont fishes have been reported from the ostracod zones in the Bloomsburg by Giffin (1979) and Hoskins (1961).

The occurrence of complete cyathaspid head shields and broken fragments at Station A represents a fortuitous preservation of a mass of fish "bone" most likely flushed into the sedimentary basin from a near-shore environment. The mass of broken plates, with only a few complete shields, indicates considerable current reworking as the material was rapidly transported to its present location.

REFERENCES CITED

- Beerbower, James R., and M.H. Hait, Jr., 1959, Silurian fish in northeastern Pennsylvania and northern New Jersey, Pa. Acad. of Science, v. 33, p. 198
- Denison, Robert H., 1964, The Cyathaspididae, a family of Silurian and Devonian jawless vertebrates, Fieldiana, v. 13, n. 5
- Giffin, Emily B., 1979, Silurian vertebrates from Pennsylvania, Jour. Paleontology, v. 53, n. 2, p. 438
- Hoskins, D.M., 1961, Stratigraphy and paleontology of the Bloomsburg Formation of Pennsylvania and adjacent states, Pa. Geol. Survey, 4th ser., Bul. G 36

STRUCTURAL GEOLOGY

The Bloomsburg Formation contains a variety of sedimentary structures that both influence the development of structural features and record the finite strain. Sedimentary structures of particular interest are-

1. organic burrows, normally perpendicular to beds;
2. mud-crack polygons, with associated sandstone dikes extending several feet down into the underlying strata;
3. reduction spots,
4. blocky, fragmental textures in mudstones interpreted to be peds with clay skins resulting from Silurian soil-forming processes;
5. saucer-shaped, slickensided surfaces interpreted to be shear surfaces created in unconsolidated soil or sediment by expansion and contraction.

Organic burrows are best developed in the Moyer Ridge sandy member (Figure V-6), but may be found throughout the Bloomsburg here and elsewhere (Geiser, 1974). Rock cleavage commonly parallels and is best developed at burrows where diffusion and pressure solution were enhanced by through-bed flowage of fluids (Nickelsen, 1972, p. 109).

Mud-crack polygons are large, two-dimensional strain markers recording finite strain in the bedding plane (yz) that approximately equal the finite strain of yz planes in reduction spots. Sandstone dikes marking the edge of mud-crack polygons may be folded and rotated around a vertical axis toward the rock-cleavage (xy) plane during progressive deformation by pure shear. Edges of mud-crack polygons that nearly parallel cleavage become planes of concentrated diffusion and pressure solution, with resulting thick residual accumulations of insoluble residue. Late in the sequence of Alleghany deformation when vertical extension by brittle shear and extension fracturing was occurring (Stage VI), sandstone dikes and sand-filled burrows were broken by horizontal joints that dilated and became filled with quartz and calcite. In a sample of 5 dikes at Station D, illustrated in Figure V-6, a mean of 15% vertical extension was measured (range 12.6-17%).

Reduction spots in shale and mudstone may be compacted perpendicular to bedding and later tectonically shortened (layer-parallel shortening) but in sandstones, at the same locality, they commonly are spheroidal, thus strongly suggesting that suitable reduction spots in shales and mudstones were also originally spherical. Where green beds or green irregular patches elongated in bedding occur, the reduction spots are commonly not originally spherical. Strained reduction spots were not measured in such areas.

Clay-skin coated peds are of interest because they provide perpendicular-to-bedding clay films which are commonly tracked by later rock cleavage. Little or no pressure solution is necessary to create strong preferred orientation of clay minerals in rock cleavage that happens to follow the clay film in peds.

Saucer-shaped slickensided surfaces (SSS surfaces) are currently being studied by M. B. Gray, Bucknell '84, who has provided the following information. In undeformed Bloomsburg Formation at Muncy, PA, where 20% vertical compaction is recorded by flattened reduction spots, these surfaces intersect bedding at less than 40°, and in 3 dimensions are symmetrical, saucer-shaped domes or basins with radiating slickenlines

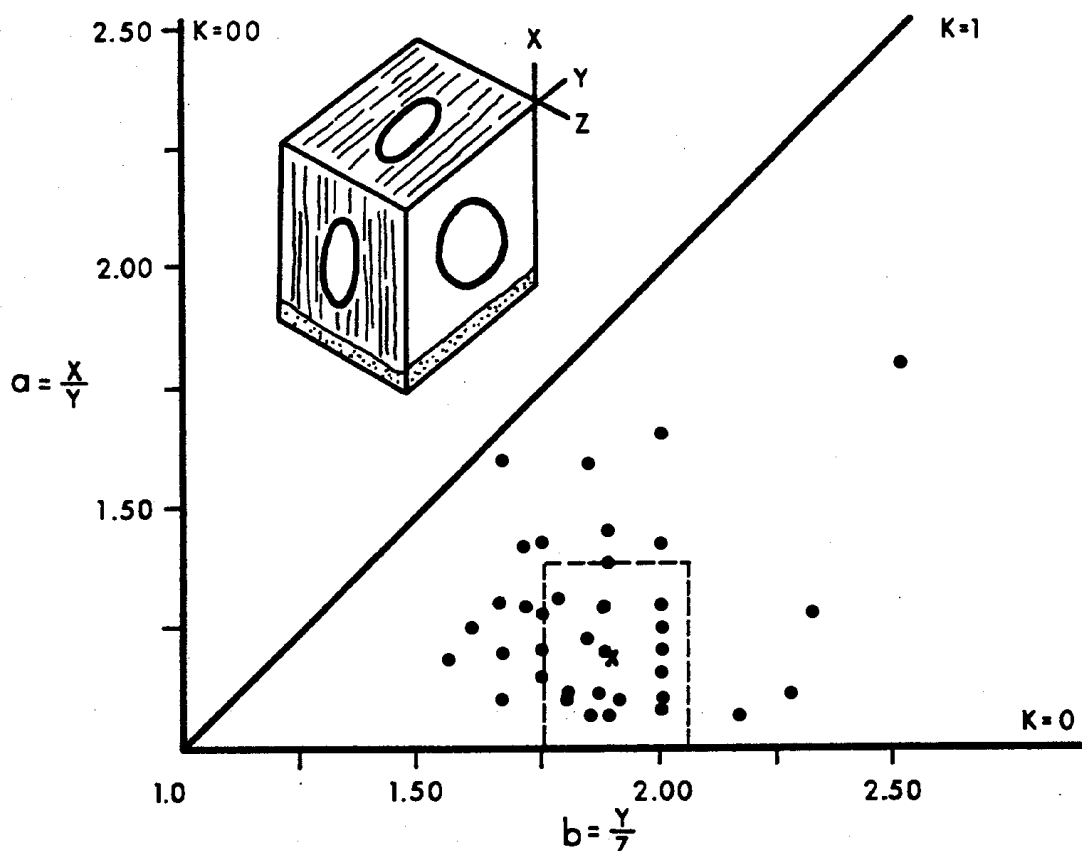


Figure V-1

Flinn diagram to show shape of 54 reduction spots. (Knowles, 1978, Fig. 12)

(Figure V-3A, B). They are thought to be surfaces of shear failure formed prior to consolidation in muds or soils undergoing expansion and contraction. Similar surfaces are reported from modern vertisols, which are montmorillonite-rich soils subjected to seasonal wetting and drying (E. Ciolkosz, personal communication, 1983; Foth and Schafer, 1980, p. 85-90, Fig. 4-2). With layer-parallel shortening as at Stop V, the surfaces have become spoon-shaped with slickenlines clustering closer to the axis of the spoon, which is also the rock-cleavage direction (Figure V-3C, D, V-4). We currently believe the slickenlines have been rotated around the perpendicular-to-bedding (\bar{x}) toward the trace of cleavage and are thus crude strain markers. Preservation of these surfaces through 50% layer-parallel shortening is remarkable, yet they appear to have persisted as discrete surfaces within rock undergoing ductile deformation. SSS surfaces of appropriate orientation have been followed by fiber-filled wedge faults during the last stages of deformation.

Unlike Stop I, where progressive simple shear was the dominant influence on cleavage attitude and finite strain, the Bloomsburg Formation at Stop V appears to have deformed in a progressive pure shear that has been recorded in both ductile and brittle structures. The dominant S-plane in most Bloomsburg outcrops is spaced cleavage, initiated perpendicular to bedding in horizontal layers, and rotated with bedding to other attitudes. An especially abrupt fault contact between two differently oriented bedding-cleavage domains is visible at Station D (Figure V-6).

Reduction spots flattened in the cleavage and slightly elongated down the dip of cleavage record the finite strain and volume loss associated with cleavage formation.

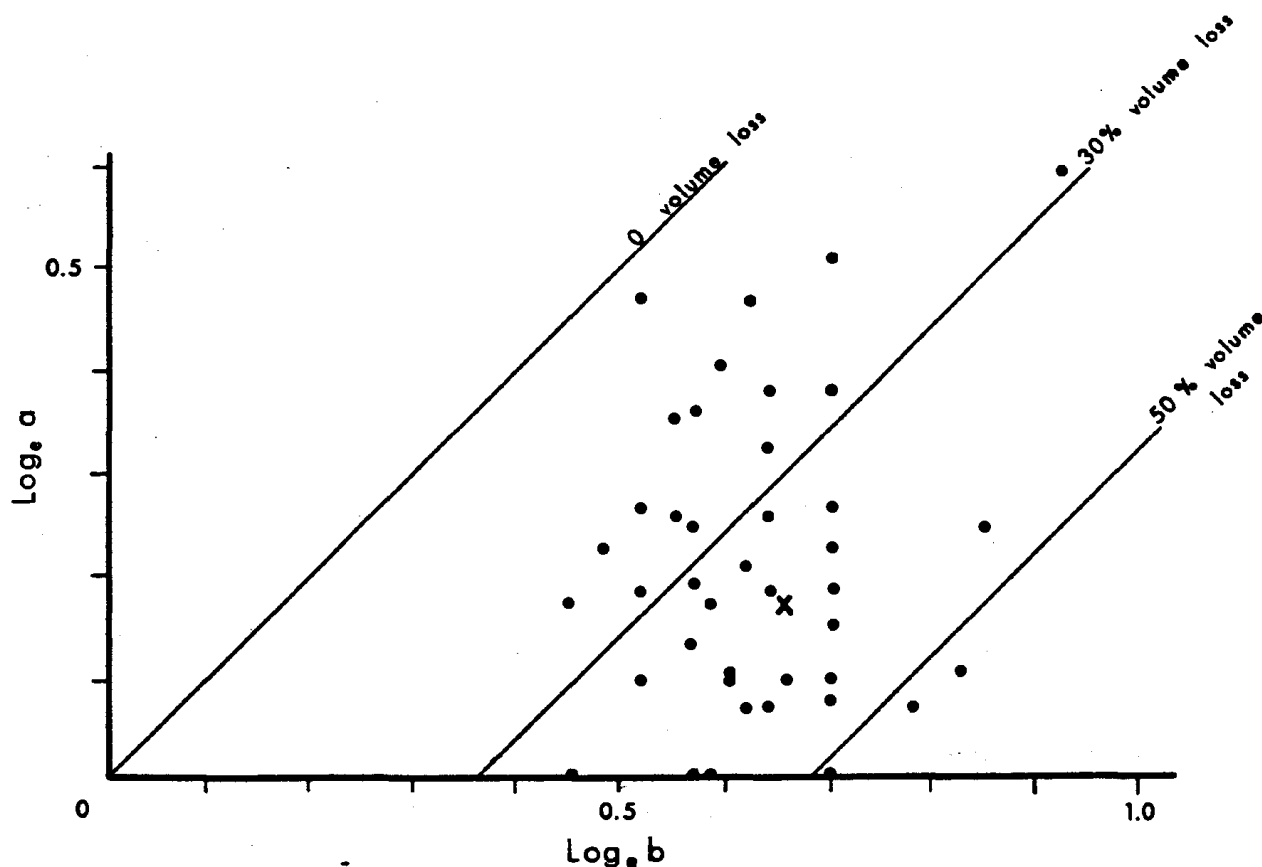


Figure V-2 Flinn diagram (natural log a vs. b) to show possible volume loss, same 54 reduction spots. (Knowles, 1978, Fig. 13)

The x axis is parallel to cleavage dip (and burrows), y parallels cleavage strike and z is perpendicular to the xy cleavage plane. Knowles (1978) measured 54 three-dimensional reduction spots at 4 localities with the following results:

Locality	N	mean $x:y:z$ ratio
Watson town Brick	20	1.19:1.00:0.53
Quarry S. of Watson town	15	1.16:1.00:0.52
Turbot Ave., Milton	12	1.17:1.00:0.55
RR S. of Brick Quarry	7	1.29:1.00:0.53

Knowles plotted the reduction spots on a Flinn diagram ($a = \frac{x}{y}$ vs. $b = \frac{x}{z}$) (Figure V-1) which shows that all ellipsoids lie in the field between flattening ($k=0$) and plane strain ($k=1$). Both volume loss due to pressure solution and volume-constant ductile flow have contributed to the shape of these deformed reduction spots. Tectonic strain is not thought to have contributed significantly to elongation in y because calcite and quartz over-growth and late extensional veins related to reduction spots all depict extension in x , down the dip of cleavage. Thus, the deformation is assumed to have been a plane strain.

Volume loss perpendicular to z can be estimated on a logarithmic Flinn plot ($\log_e a$ vs. $\log_e b$) (Figure V-2) which shows that the shape of most reduction spots at these localities can be explained by volume loss, perpendicular to cleavage, ranging between 5 and 55%. Thirty mud cracks from Stop V, Station C, have a mean long:short (yz) ratio in bedding of 0.55 (Knowles, 1978). Thick insoluble-residue accumulations on spaced cleavage that parallels the edge of mud-crack polygons demonstrate that there has been considerable volume loss due to pressure solution.

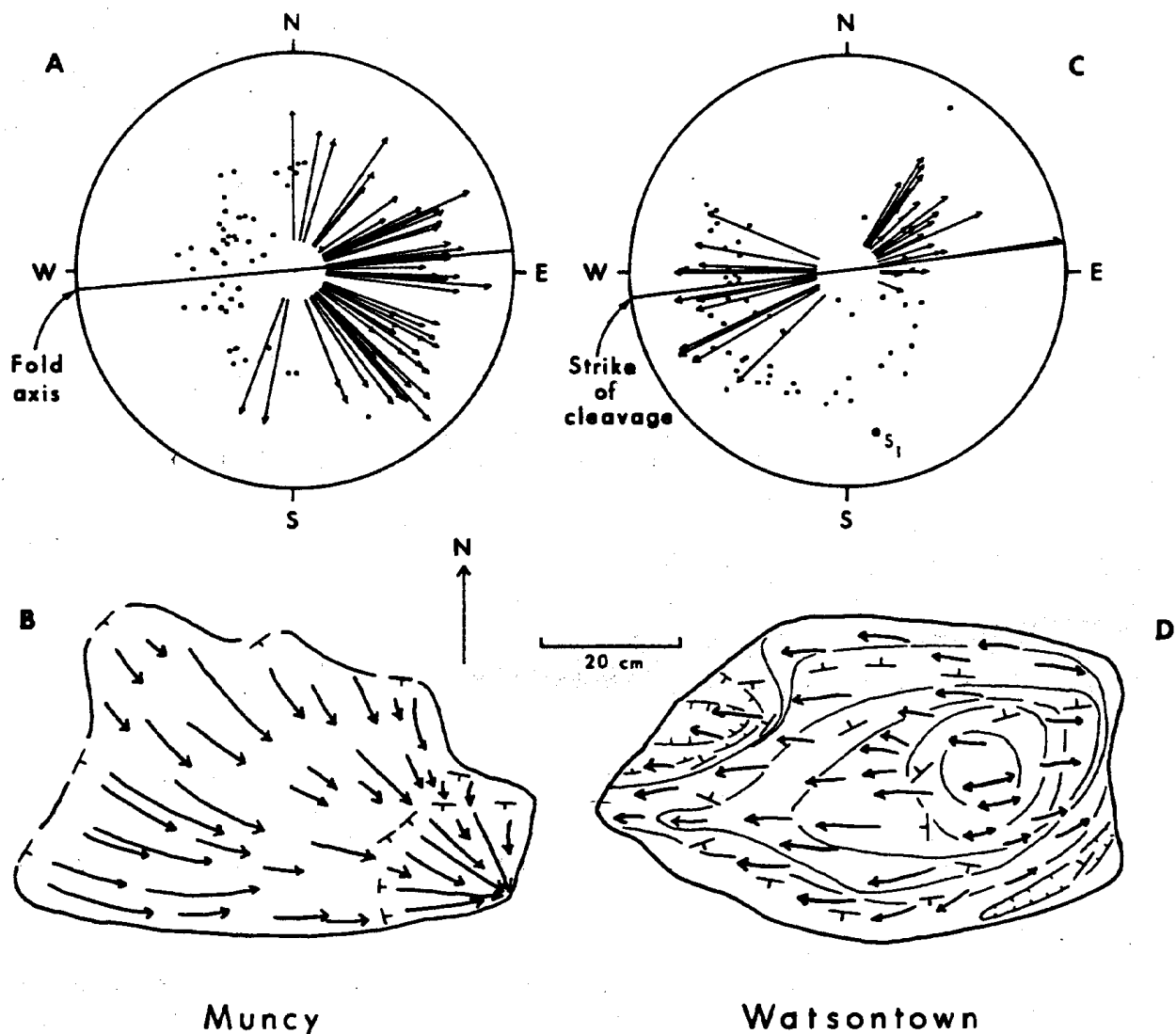


Figure V-3

Saucer-shaped slickensided surfaces

- A. Lower hemisphere stereographic projection of poles to surfaces and slickenlines on surfaces. Not tectonically deformed, but compacted 20% perpendicular to bedding. Muncy, PA
- B. Map of a portion of a SSS surface. Muncy, PA
- C. Stereographic projection of spoon-shaped slickensided surface showing poles to surface and slickenlines on surface. Slickenlines are grouped near the axis of the spoon, parallel to the strike of cleavage. Surfaces tectonically deformed during cleavage formation, Watsonstown Brick Quarry
- D. Map of portion of spoon-shaped slickensided surface at Watsonstown Brick Quarry.

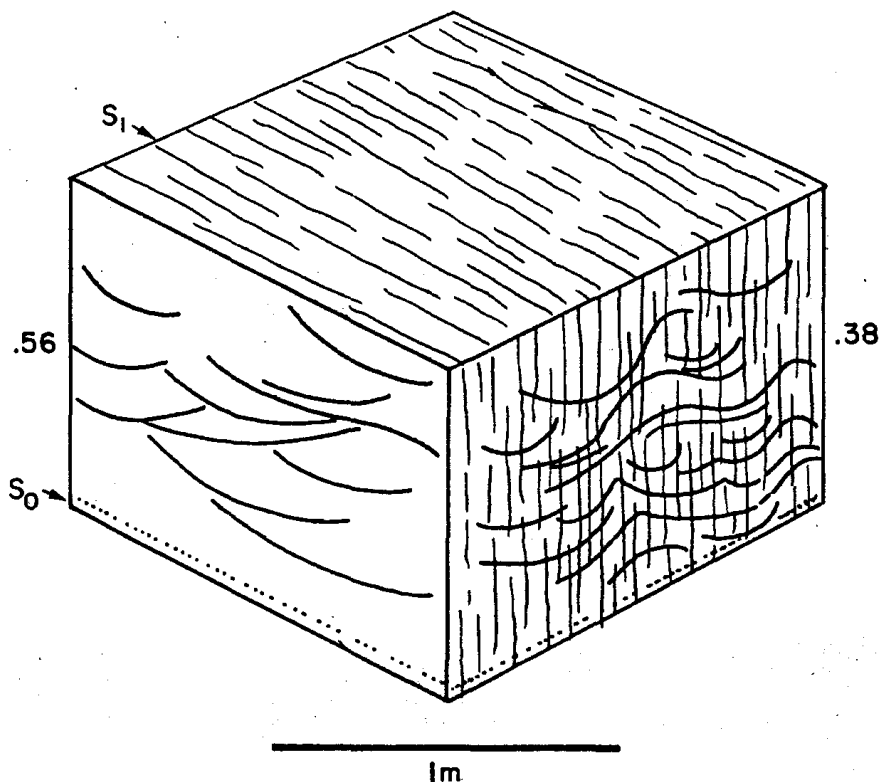


Figure V-4

Schematic three dimensional sketch of SSS surfaces viewed perpendicular and parallel to cleavage (S). Surfaces are arcs of circles of different mean diameter when viewed in different planes. Diameters are: .38 m perpendicular to S_1 .56 m parallel to S_1

Following the ductile deformation of reduction spots and mud-crack polygons that had also created spoon-shaped slickensided surfaces, brittle rupture mechanisms become more important. Sandstone dikes were extended 15% in a vertical direction and spoon-shaped slickensided surfaces of appropriate shear orientation were followed by wedge faults (Figure V-5). The wedge faults opened vertically while also showing right- and left-lateral slip, creating spaces to be filled incrementally with calcite fibers. The growth-fiber vectors of displacement all lie in the xz plane corresponding to the direction of layer-parallel shortening as indicated by cleavage and the minimum strain axis (z) of reduction spots (Figure V-5). The displacement vector of the fibers does not parallel the orientation of slickenlines on the SSS surfaces thus suggesting that the two structures are independent. The slickenlines cluster along the strike of cleavage as shown in Figure V-3C, whereas the fibers on the wedge faults that track SSS surfaces are perpendicular to the cleavage trace. The structures described above may be seen at:

Station A - Located at the east end of the main quarry, fossil-(fish bone) coated bedding planes, burrows, rock cleavage, deformed-reduction spots, and fiber-filled conjugate wedge faults following SSS surfaces may be seen in loose blocks or the working face. Note reduction spots which are essentially pancake-shaped in the cleavage plane (xy) with slight elongation in the x direction parallel to organic burrows (Figure V-1). The rock is either the Moyer Ridge Sandstone Member making up the dip slope to the south or the uppermost Bloomsburg mudstone between the Moyer Ridge Member and the overlying Wills Creek Formation.

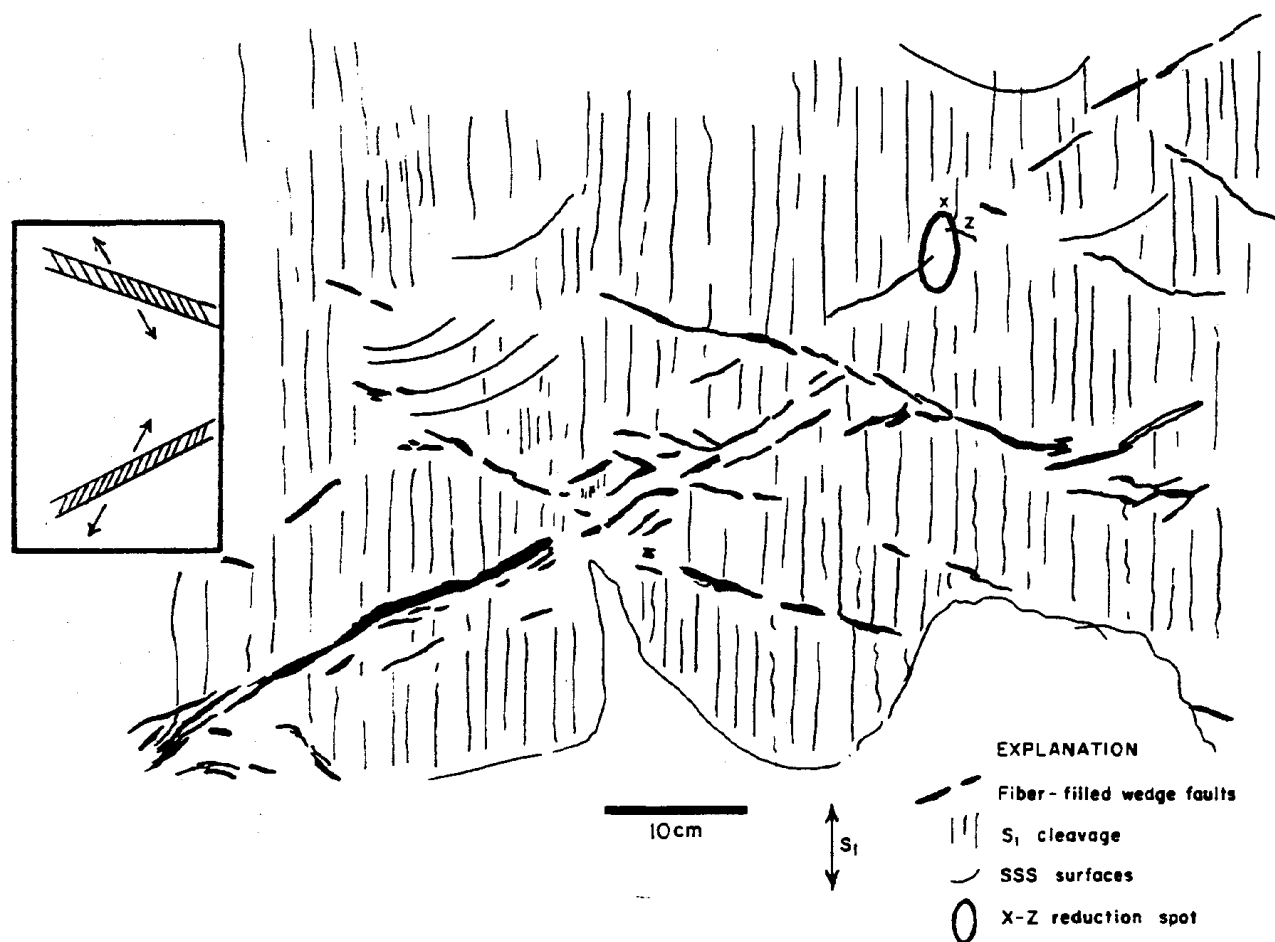


Figure V-5

Drawing of xz plane showing deformed reduction spot (ratio .46) and fiber-filled conjugate wedge faults cutting cleavage but following SSS surfaces.

Station B - On an upper level to the east of Station A, there are good examples of spoon-spaced slickensided surfaces, rock cleavage parallel to organic burrows, and fiber-filled wedge faults of small displacement (Figure V-3C, D; V-5). Fiber orientations indicate incremental antitaxial growth and shear displacements of several millimeters. Although we believe the SSS surfaces have been deformed by ductile flow during creation of cleavage, there is no obvious cleavage trace on the SSS surface.

Station C - North of Station A are loose blocks showing deformed mud-crack polygons and insoluble residue accumulations in spaced cleavage planes formed by massive pressure solution along the borders of mud cracks. The ratio of long:short (yz) dimensions of the mud cracks is: 0.55 and this is essentially equal to the yz ratios in deformed reduction spots at Station A. Throughout the region a common feature of well-developed, spaced cleavage planes that have formed by concentrated pressure solution is the fiber-filled calcite veins that parallel the spaced cleavage planes at this station. They are thought to form as later buckle folding creates new space along the margins of cleavage-bounded blocks (Bajak, 1981).

Station D - Station D is a ten-minute walk west to the Railroad tracks south of the brick plant. You will walk along the base of the dip slope of the Moyer Ridge Member. At the Railroad, the outcrop in the Moyer Ridge Member contains cleavage parallel to abundant organic burrows, and vertically extended sandstone dikes or fiber-filled wedge faults (Figure V-6). The only structures unrelated to pre-existing sedimentary features are the

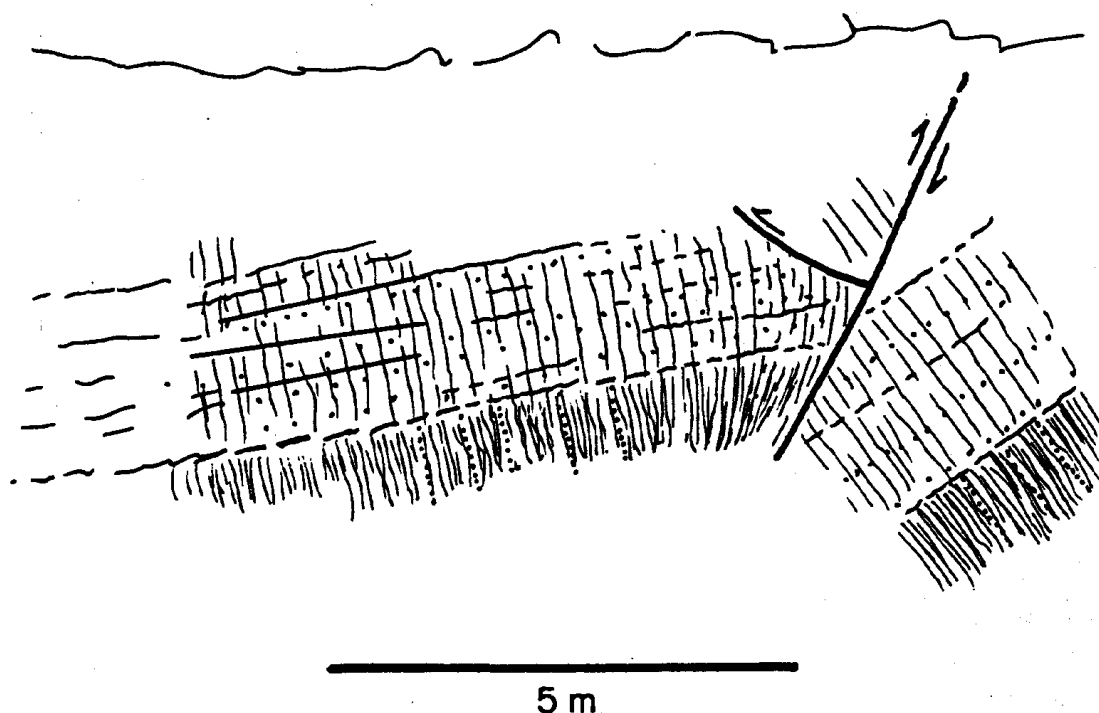


Figure V-6

Drawing of outcrop of Moyer Ridge Member to show abrupt, fault-related change in attitude of bedding and cleavage. Cleavage parallels sandstone dikes and burrows

wedge joints occurring in two conjugate shear orientations bisected by bedding but showing no evidence of slip. The main reason for visiting this outcrop is to demonstrate the small thrust fault at the abrupt contact between two bedding-cleavage domains. Simple shear adjacent to the fault has reoriented some cleavage, but most strain in both domains was accomplished by pre-folding and pre-faulting pure shear that continued through both ductile cleavage genesis and brittle extension of sandstone dikes and fiber-filled wedge faults. This is the essential difference between the deformation of the Bloomsburg Formation here and at Stop I.

In summary, these outcrops have demonstrated non-rotational progressive deformation by pure shear resulting in shortening and volume loss perpendicular to cleavage and extension down the dip of cleavage. We believe the y axis in mud-crack polygons and reduction spots has remained constant and that the deformation has been a plane strain. Ductile Stage III cleavage formation was coaxial with later, brittle, vertical extension by Stage IV wedge faulting and Stage VI extension jointing. Though primary sedimentary structures have played a dominant role in directing the orientation and style of deformation in different rock types there is no evidence that any of the structures originated prior to sedimentary diagenesis and lithification.

Ductile strain mechanisms included pressure solution-diffusion aided by appropriately oriented sedimentary structures, as well as volume-constant flow mechanisms probably including intergranular grain-boundary sliding and packing changes and intragranular crystal-plastic gliding (quartz deformation lamellae).

<u>Miles</u>	<u>Interval</u>	
15.8		Return to PA 405.
15.9	0.1	Junction PA 405; turn right (north).
16.5	0.6	Junction PA 44 on right; continue north on PA 405-44 into Watsontown.
16.7	0.2	Traffic light, center of Watsontown.
18.7	2.0	Turn left (west) off PA 405, following PA 44 in Village of Dewart.
21.1	0.4	Crossing West Branch, Susquehanna River, 12-ton weight limit.
21.6	0.5	Junction U.S. 15 in town of Allenwood. Turn left (south) on U.S. 15.
22.3	0.7	Folded McKenzie Limestone Member studied by Groshong (1975). Strain gradually decreases down section into Rose Hill Formation. No red hematitic sandstones, such as were seen at STOP I, are present in this section.
22.9	0.6	Royer's Trailer Court on right side of U.S. 15; buses park facing south.

Stop VI. South White Deer Ridge

SEDIMENTOLOGY

One's initial impression of such a quartz arenite unit stratigraphically below such a great thickness of Rose Hill Shale is that it must be the top of the Tuscarora Formation. However, the occurrence of brachiopods and ostracods (including Zygosella sp., D. Hoskins, personal communication) near the base of the exposed sequence (lower part of Unit B), and the lack of characteristics typical of the upper part of the Tuscarora (Castanea Member), demonstrate that the quartz arenite is developed in the lower Rose Hill Shale.

Following the transgression of the Rose Hill Sea over the coastal sand/mud flats of the Castanea Member of the Tuscarora, central Pennsylvania was generally the site of low-energy shelf conditions. However, you will note in the early part of this guidebook that the southeastern margin of the depositional basin was relatively consistently the site of higher-energy megaripped sand shoals (see Figures 7, 8). This is one place at which such a marginal sand shoal was developed at the time of transgression of the initial Rose Hill Sea. Because the coast at this time was so placid, little sand was derived by shoreface processes from the coastal sediment prism, and the generation of these lower Rose Hill sand shoals was such an uncommon event.

The principal sedimentologic features of the section exposed here are listed on the stratigraphic column (Figure VI-1), which also shows the subdivision of the section into five informal units. My judgment of the depositional setting of each of these units is presented below:

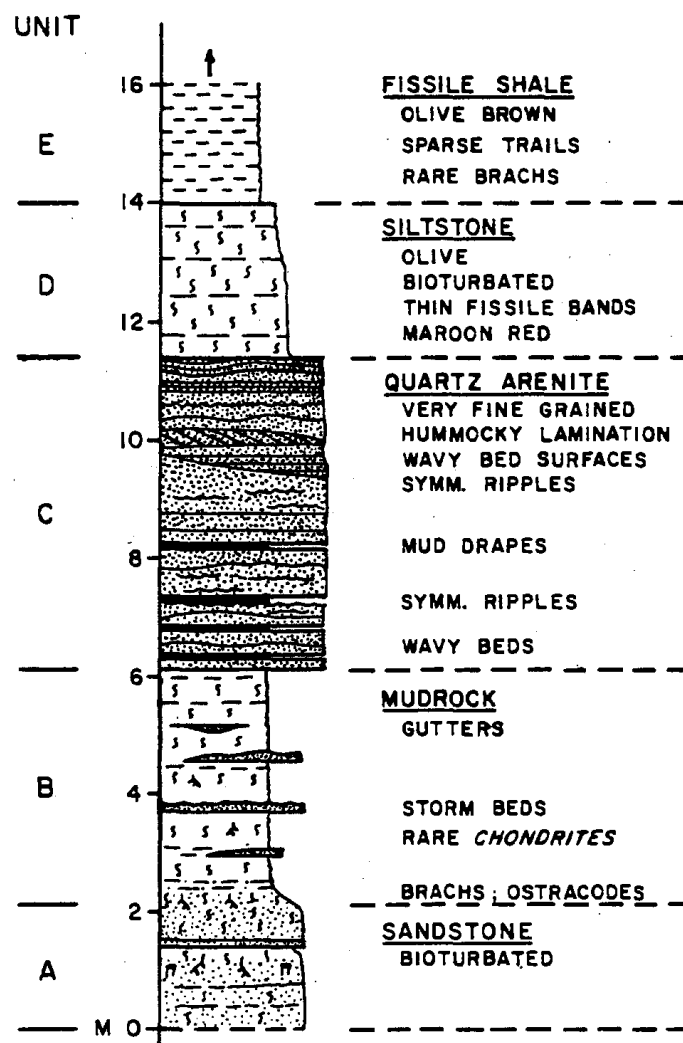


Figure VI-1

Columnar section, sandstone/shale units in lower Rose Hill Formation, South White Deer Ridge near Allenwood

Unit A. Distal shoreface. This interpretation is made more difficult by the lack of exposed strata below. It is not clear how far below Unit A is the top of the Castanea Member (red, *Skolithos*-burrowed lithofacies) of the Tuscarora, but the resistant topographic surface plunging to the east here as South White Deer Anticline suggests that there is little Rose Hill below this point. Favoring a distal shoreface interpretation are the storm-bed nature of the two more resistant beds ("parallel-to-burrowed" sequences), and the mixing of the vertical biogenic shafts (filter feeders?) with the more irregular structures of deposit feeders.

Unit B. Low-energy, shallow-marine shelf. Most of the time the sea floor was below the level of wave and current agitation, but infrequent storm events emplace thin sandstones with flat bases, flat internal lamination, and symmetrically rippled tops. The generation of such storm beds was discussed in the earlier consideration of Middle Silurian depositional history and the material dealing with Stop I (Danville).

Unit C. Offshore bar; megarippled sand shoal. A series of features indicate this origin. The unit has a flat, nonscoured base. The sandstone beds are commonly lenticular and have undulating tops. Symmetrical ripples occur on many surfaces (see in particular the

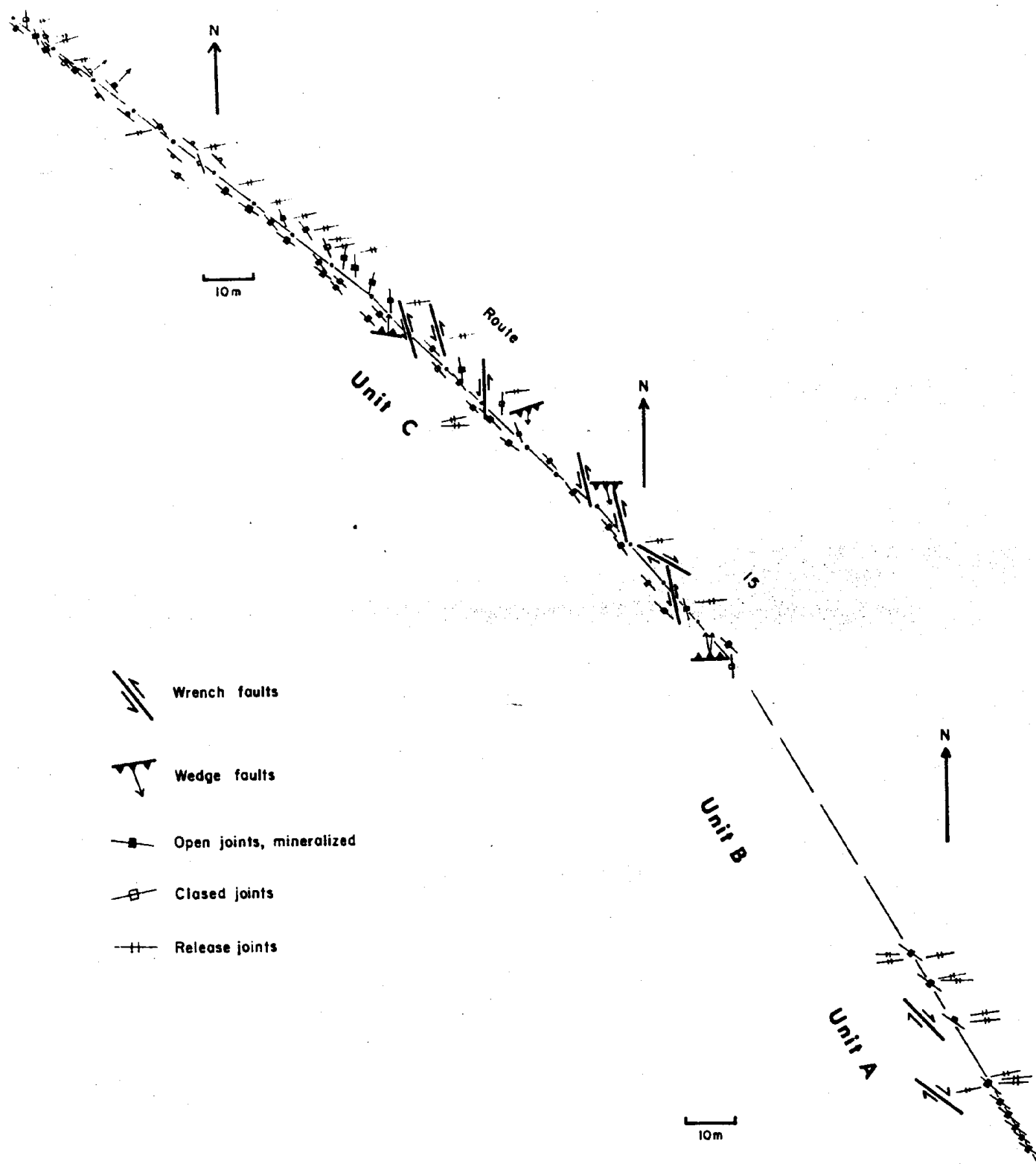


Figure VI-2

Map of Joints and Faults in Units A and C

strata between 9 and 9.5 m and between 10 and 11 m). Mudrock is not present in laterally discontinuous thin lenses, but rather the thin mudrock beds are of relatively constant thicknesses and are draped conformably over the wavy, undulating tops of sandstones.

Unit D. Abandoned bar; transition to deeper shelf. The siltstone toward the base is red and slightly hematized, a reflection of situations that occur higher in the Rose Hill (Clinton-type ore beds). There is an upward increase in the proportion of interbeds of fissile mudrock, indicating a gradual diminishing of the amount of infauna, probably because of a deepening into the dysaerobic zone as subsidence and transgression continued at the time of diminished sediment supply.

Unit E. Low-energy, shallow-marine shelf. Dysaerobic to anaerobic conditions inhibited infaunal burrowers. It is difficult to be specific about the reasons for the scarcity of storm beds of sandstone, for it could have been some combination of depth, distance from shore and/or shoals, unavailability of sand, and the relative infrequency of storms.

STRUCTURAL GEOLOGY

This outcrop is an unusual surface exposure of a zone of fracture porosity similar to the producing zone of gas wells in the Tuscarora Formation at the eastern edge of the Appalachian Plateau, 50 miles to the west. Wescott (1982) has described the porosity types in the Tuscarora Sandstone of the Appalachian Basin. We plan to illustrate the progressive development and relative structural age of the zone of fracture porosity exposed here (Figure VI-2).

Fracture porosity at Stop VI exists as open extension joints, partially filled with oriented quartz crystals which "prop" the fracture open. Most fractures are hydraulic joints opened by crack-seal mechanisms (Ramsay, 1980) with syntectonic incremental growth of quartz parallel to local strain paths. There is no evidence here of prior complete fillings of vugs by other mineral matter that has since been removed by surface weathering, although oxidation of sulfide and carbonate minerals within the fractures has stained many joint surfaces. Similar vugs encountered in gas wells of the Appalachian Plateau have remained propped open (Wescott, 1982, Figure 10) since the Alleghany Orogeny even though buried deeper than 10,000' beneath the surface.

Structural features that contribute to the history of fracture porosity at this stop include several sets of regional extension joints, conjugate wrench faults and wedge faults, the South White Deer Anticline, and release joints paralleling the anticline (Figure VI-2).

The earliest structures are quartz-filled, regional extension joints of sets A(325°), B(310°) and E(0°) recognized on the Appalachian Plateau by Nickelsen and Hough (1967) and found also in the Valley and Ridge Province by Groshong (1956), Boyer (1972), Faill (1979), and Ricci (1979).

They have been overprinted by a conjugate system of right-lateral and left-lateral wrench faults that show a wide range in orientation, perhaps because they are tracking pre-existing joints, or because they include overprinted conjugate systems of different orientations such as seen at Bear Valley, Stop III. Eric Miller, Bucknell 1984, has measured 41 left-lateral wrench faults (range in strike 332° to 20°) and 9 right-lateral wrench faults (range in strike 288° to 320°) at this outcrop. The mean strike of left-lateral faults is 355°, the mean strike of right-lateral faults is 303°, the acute dihedral angle between mean strikes is 52° and the bearing of the acute bisector of the dihedral angle is 329°. Since this acute bisector is the most likely orientation of the greatest principal-stress axis (σ_1) responsible for wrench faulting, it is interesting to note that it is 25° counterclockwise from the perpendicular to the axial trace of the South White Deer Anticline (Figure VI-2). Wrench faulting appears to have closely followed extensional jointing in the structural sequence because some wrench faults follow and deform the pre-

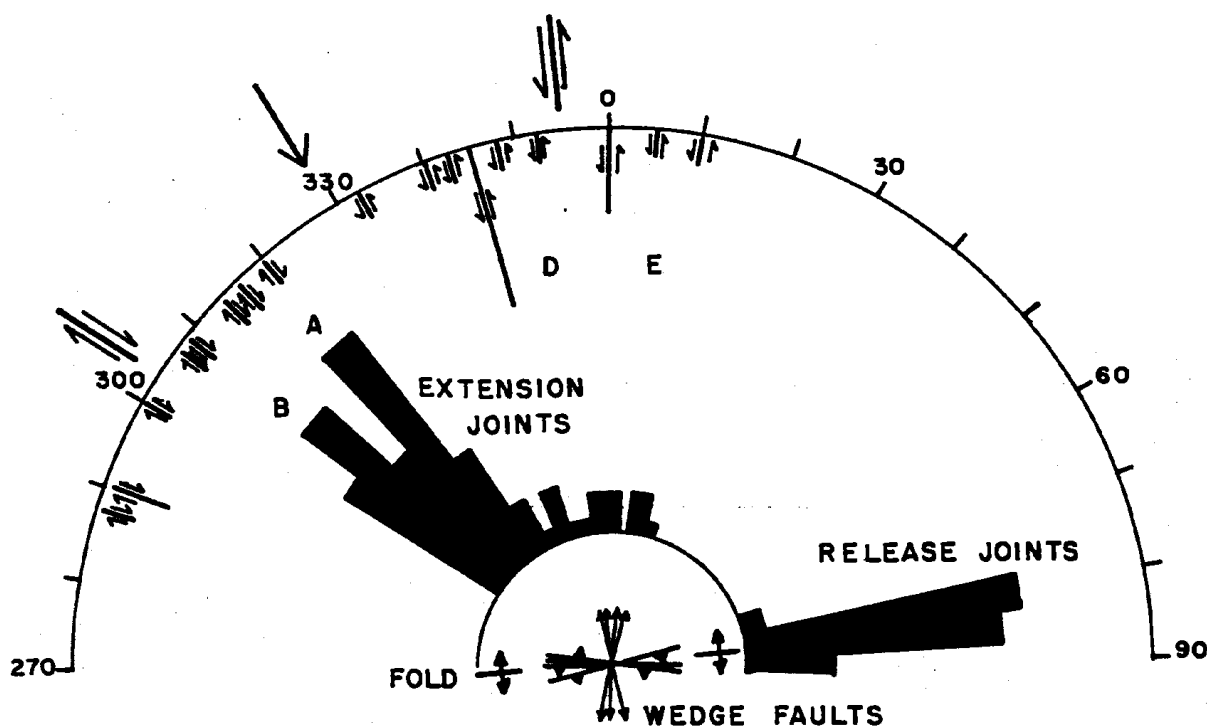


Figure VI-3

Circular histogram summarizing orientations of Joints (extension and release), wrench faults (right lateral and left lateral), wedge faults and their slickenlines, and the South White Deer anticlinal axis.

The acute bisector of conjugate wrench faults strikes 329°

existing quartz fillings of extensional joints and because gash veins generated by simple shear along wrench faults, in places, parallel regional extension joint sets. Figure VI-3, illustrating small-scale relationships between an early extension joint, a left-lateral wrench fault and its gash veins, and late release joints may serve as an example of structural relationships you can observe in the field. Microscopically, it can be seen that the crack-seal mechanism has resulted in repeated cracking and new quartz growth emanating from seed grains in the country rock or from earlier, intersecting joints (Figure VI-4). The quartz in veins is intersected by healed fracture planes filled with countless secondary fluid inclusions that have yielded a range of Temperatures of Homogenization (Lilly, 1982). Primary inclusions are also available in euhedral quartz crystals penetrating the open vugs. Temperatures of Homogenization (T_h) range from 121°C in some primary inclusions to 194°C in secondary inclusions. Figure VI-5 is a copy of Figure 11 of Lilly (1982) showing Temperature of Homogenization (T_h) vs. Temperature of Freezing (T_f) for inclusions judged to be primary, pseudosecondary, or secondary in veins of different orientation and slightly different structural age (304°) (310°) (315°) (340°) and (346°).

Since some methane inclusions are present it is possible that no pressure correction is necessary and that Temperatures of Homogenization are approximately equal to Temperatures of Filling. The nearest conodont CAI values range from 3½ to 4 (A. Harris, personal communication, 1981), suggesting heating temperatures of 150 to 250°C, only slightly higher than Lilly's determinations.

Wedge faults dip either north or south and have slickenlines grouped around a north-south orientation which is approximately perpendicular to the South White Deer Anticline. The greatest principal stress axis inferred for wedge faults is thus parallel to a normal to the South White Deer Anticline, and rotated 25° clockwise from the σ_1

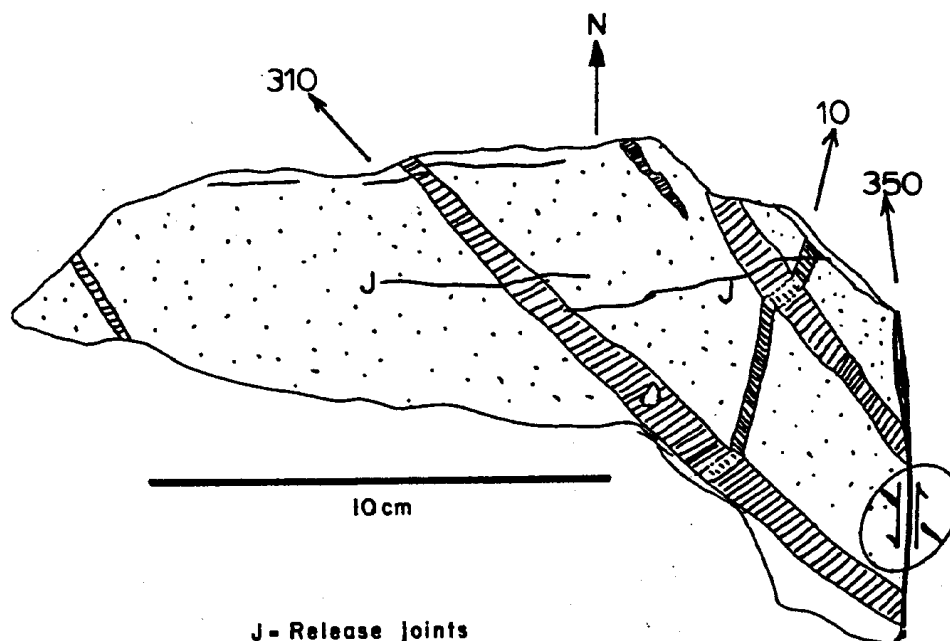


Figure VI-4

J - Release joints
Drawing of hand specimen showing sequential formation of the cumulative fracture pattern. Stage II extension joints (10°) are overprinted by gash veins formed by left lateral wrench faulting, perhaps following pre-existing joints. Stage VI release joints overprint all other structures.

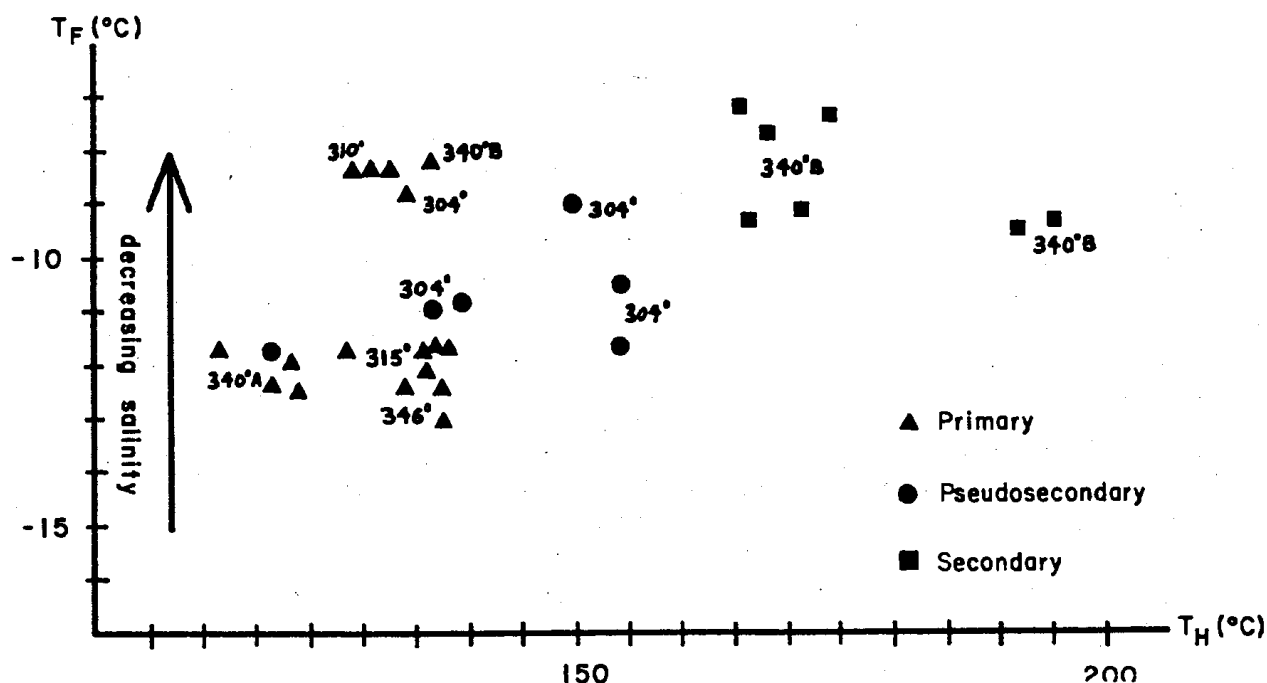


Figure VI-5

Plot of T_H vs. T_F for aqueous fluid inclusions from veins oriented 304° , 310° , 315° , 340° , and 346° (Lilly, 1982)

orientation of the presumably earlier wrench faults. All structures have been folded by the South White Deer Anticline and overprinted by closed, unmineralized strike joints (80°) of "release" origin. (Be sure to observe how release joints cut all previous structures - joints, quartz veins, slickensides and slickenlines.) Some evidence such as the offset of wedge-fault slickensided surfaces and slickenlines by extensional joints of 315° orientation suggests that extensional jointing and conjugate wrench and wedge faulting all

occurred at about the same time. However, we have interpreted the dominant evidence to indicate the following sequence:

1. Stage II regional extension jointing of several different orientations and times (Engelder and Geiser, 1980)
2. Stage IV wrench faulting overprinting and overlapping in time some of the extensional jointing
3. Stage IV wedge faulting post-dating a 25° clockwise rotation of stress axes
4. Stage V folding
5. Stage VI release jointing

This structural sequence may have important implications in the search for subsurface fracture porosity. The important porosity at this outcrop results from pre-folding, extensional jointing and wrench faulting. Open joints are commonly gash veins adjacent to wrench faults that intersect fold axes at 30° to 90° . Throughout the region where these wrench faults occur in steeply-dipping folded beds (Stop III and Stop VII), their slickenlines parallel the fault-bedding intersection, thus suggesting origin before folding. Due to the low bedding dip, evidence here of pre-folding wrench faulting is equivocal. Zones of fracture porosity, such as this one, would be expected to trend northwest across the strike of later anticlines and merely be overprinted by the later anticlines. Systematic drilling of anticlinal crests may occasionally intersect transverse zones of fracture porosity such as this one but will mostly find Stage VI release joints which in this outcrop do not contribute significantly to porosity. Stage VI release joints may connect pre-existing zones of vuggy porosity or may be more open where bedding dips are steeper. Thus, at some localities, they may contribute significantly to fracture porosity (Berger and Wheeler, 1979). However, we believe that zones of closely-spaced, transverse, regional, Stage II extension joints and gash veins associated with Stage IV wrench-fault zones offer the best potential for subsurface fracture porosity.

The structural features described above may be seen best in the stiff stratigraphic units - Unit A, at the south end of the outcrop, and Unit C (Figure VI-2).

Unit A - Open, quartz-filled, extension joints of regional set B (310°) may be seen, overprinted by release joints (85°) parallel to the fold axis. Most of the right-lateral wrench faults measured at this outcrop occur here above the road level in Unit C.

Unit C - The south third of the road outcrop of Unit C has several reentrants where the following structural features may be seen:

1. left-lateral wrench faults with slickenlines, quartz fibers, and oriented quartz crystals in vugs, all approximately parallel to the inferred slip direction of the fault.
2. gash veins with oriented quartz crystals demonstrating syntectonic incremental growth oblique to vein walls. Fluid inclusions in these oriented quartz crystals and fibers were trapped during Stage IV of the Alleghany Orogeny and should indicate ambient temperatures.
3. various, quartz-filled, regional joint sets.
4. wedge faults dipping both north and south. Their presence here on the anticlinal crest strongly suggests that they were formed prior to Stage V folding because beds in this position should not experience bedding-plane slip during flexural-slip folding. Of course, it could be argued that "pinning" has occurred at some place on a fold limb, which could result in simple shear across the crest of the anticline.

<u>Miles</u>	<u>Interval</u>	
22.9	0	After reboarding, continue south on U.S. 15.
25.7	2.8	Exit right to Interstate 80 West, continue West on I-80.
27.8	2.1	View north (right) shows the gradual eastward plunge of the anticline making up South White Deer Ridge (site of Stop V); this highway heads west up a synclinal valley between two anticlinal ridges.
36.5	8.7	Drive past Mile Run exit; continue ahead on Interstate 80.
41.8	5.3	Ramp exiting toward rest area; Enter rest area for lunch stop.

LUNCH

41.8	-	Continue west on Interstate 80.
43.2	1.4	Exit 28 (Carroll); continue ahead on I-80.
44.7	1.5	Begin extensive road cut on right. From uppermost Reedsville (<u>Orthorhynacula</u> zone), through entire Bald Eagle, and into lower Juniata Formation.
45.1	0.4	Redbeds on both sides of highway (Juniata Formation) continue for about ten miles.
50.1	5.0	Loganton exit; stay on I-80.
53.9	3.8	Extensive outcrop of Juniata both sides.
54.5	0.6	View ahead to the "Big Cut" in the Bald Eagle and lowest Juniata Formations.
55.3	0.8	Emerge into Nittany Valley, floored by Cambro-Ordovician strata, mostly carbonates.
57.6	2.3	Exit right at Exit 26 toward Lock Haven; at stop sign at base of exit ramp, turn right (north).
58.2	0.6	View ahead to water gap where Fishing Creek is incised in ridges of the Bald Eagle and Tuscarora.
60.6	2.4	Pass outcrop of Salona Formation (left of road).
60.8	0.2	Go under bridge; continue north on PA Route 220 North.
61.8	1.0	Park far onto right hand shoulder, near blue information sign.

Stop VII, Mill Hall

SEDIMENTOLOGY

Complete exposures of the Tuscarora Formation are rare, but to have a section such as this with so much shale is truly extraordinary. Such a complete section is an important check on interpretations assembled as a composite of scattered partial sequences. Fortunately, the history of Tuscarora deposition here is quite consistent with the interpretation based on the less-complete exposures of the region.

The earlier chapter of this guidebook dealing with the Tuscarora, and the two other publications (Cotter, 1982, 1983), review the depositional history of the Tuscarora. Important components of that history include an initial transgression related to glacioeustatic sea-level rise with a sourceward translation of a high-energy beach system over the alluviated coastal plain. Then followed a period of relative stability of sea level, when central Pennsylvania was part of the marine shelf, and sandwave complexes (megarippled sand shoals) migrated across the area. And finally, Tuscarora history came to an end with a couplet of sea-level changes. With lowered sea level a coastal sand/mud flat prograded basinward, and during the following rise, the Rose Hill sea resubmerged the region.

This is the story demonstrated by the extraordinary Mill Hill section. This locality is so distal, the major record here is of coastal and shelf origin. In fact, it is difficult to demonstrate that any part of this section is of terrestrial, non-marine origin. One way to consider this exposure is that if you had ever wondered what the Tuscarora would be like in the subsurface under the Appalachian Plateau, you now have an opportunity to view it. Ask an Amoco geologist about the close correspondence between this Tuscarora section and the one in their producing well in the Devil's Elbow Field northwest of Bellefonte.

I have divided this Mill Hall section into seven informal units, designated A through G in the text and on the columnar section (Figure VII-1). Each of these units is described and discussed below so that you might guide yourself through the sequence. Don't overlook the structural geologic features keyed to these same units (see following material for this stop).

Let me call to your attention a number of variations from the Tuscarora seen farther south in the outcrop belt of central Pennsylvania. The transgressive, high-energy beach system is here preserved as inlet deposits (Unit C) of a barrier beach that was separated from the channeled coastal margin (Unit A) by a shallower lagoon (Unit B). The shallow marine shelf (Units D,E,F) was muddier, and the slightly less mature sand of the megarippled sand shoals was separated by areas of mud substrate. The resulting interbedded mudrock makes it easier to see the diagnostic geometry of the shelf sandstone beds. And the relatively thick red, *Skolithos*-burrowed lithofacies has exposed its lower and upper contacts and the details of its channel sandstone and marine shale intercalations.

Unit A: Channeled Coastal Margin

The basal 30 meters of the Tuscarora (Figure VII-1) consists of fine- and medium-grained, matrix-rich sublitharenite and lithic wacke (Figure VII-2B) with thin interbeds of dark olive-green, fissile shale. Shale intraclasts are commonly concentrated above broadly concave-upward scour surfaces and below thin- to medium-scale cross lamination. Nearly all cross laminae show that sediment transport was to the northwest,

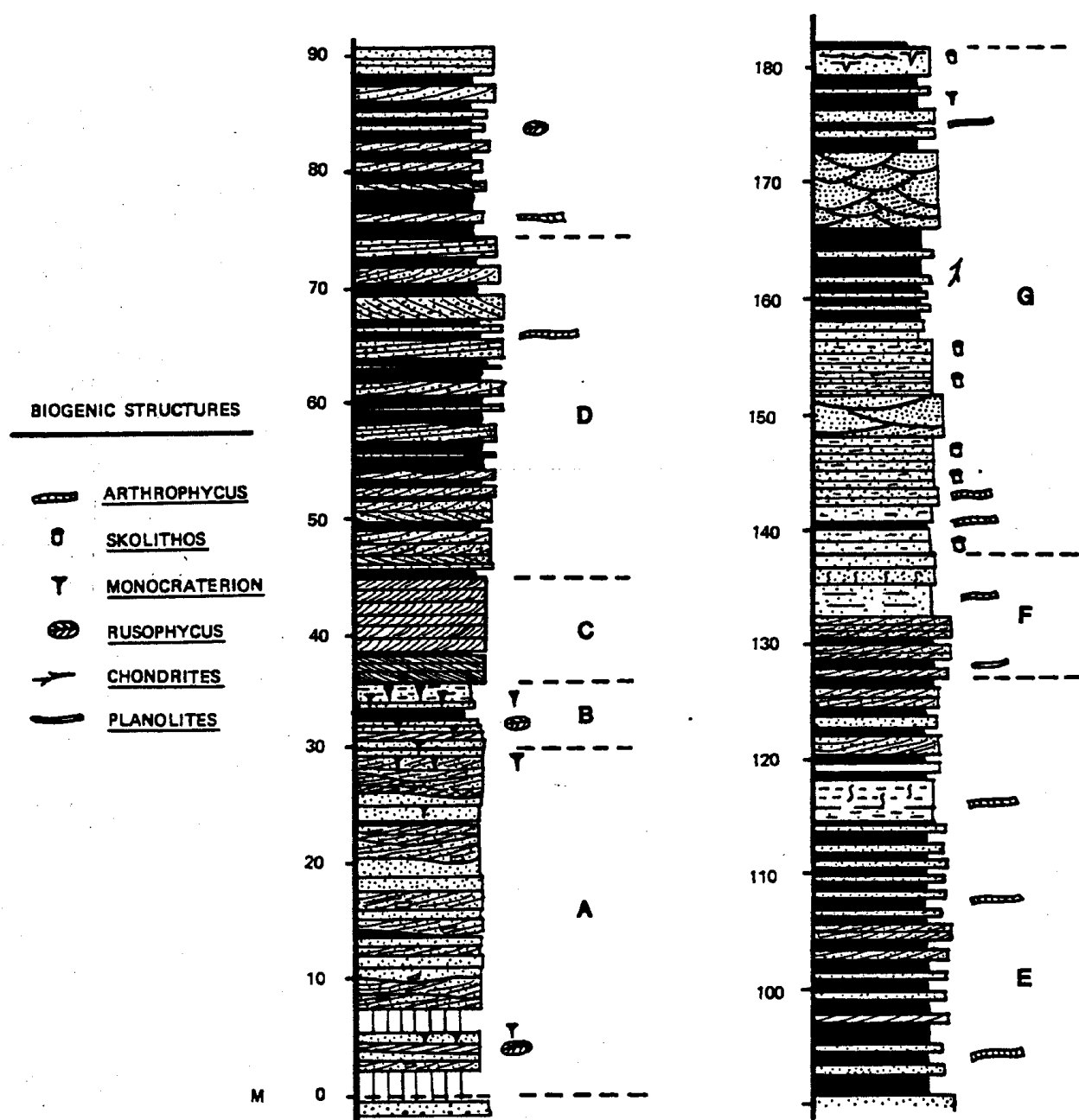


Fig. VII-1

Stratigraphic column of the Tuscarora Formation at Mill Hall. Shows division of the formation into seven informal units (A-G)

but several have been found that indicate southeastward transport. Within the unit there are general upward trends: a decrease in the proportion of shale, an increase in the thickness of cross-stratified sets, a subtle increase in sandstone grain size, and an increase in the abundance of biogenic structures. The most common biogenic structure is Monocraterion (shown for Unit B in Figure VII-2A). Rusophycus (Figure VII-2A) was found in beds about four meters above the base.

Deposition is interpreted to have occurred in a channelled coastal-margin setting. Many of the features are consistent with a fluvial origin, however, a marine influence is indicated by the presence of Rusophycus and Monocraterion and by the uncommon landward-directed cross laminae. Thus, this coastal margin might have been affected by eustarine flow. Some of the vertical trends suggest deltaic outbuilding, but a few simple delta sequences cannot easily explain the characteristics of Unit B above.

Unit B: Coastal Lagoon

In the next six meters, dark fissile silt-shale contains a number of thin beds of very fine and fine-grained lithic wacke (Figure VII-2D). Some sandstone beds wedge out laterally. Relatively thicker sandstone beds contain bipolar (herringbone) cross lamination. Very thin sandstone beds are very fine grained and current-ripple laminated, with common mud drapes. The vertical shafts of Monocraterion are profuse in several sandstone beds (Figure VII-2C). Two Rusophycus on a loose block below probably come from this unit.

The depositional setting of this unit was normally low-energy and relatively anoxic. This led to accumulation of organic-rich dark shales. Periodically, higher energy currents that at times reversed direction introduced sand that could serve as host to filter-feeding organisms until mud blanketed the substrate again. The setting is interpreted to have been a back-barrier lagoon, based on the described features and also on the complimentary diagnosis of the overlying Unit C as a barrier-beach sequence. Lagoonal deposits typically are bioturbated and contain brackish-water fossils, yet the lack of these in this unit is consistent with the general absence of fossils and extensive bioturbation in the entire Tuscarora.

Unit C: Barrier-Beach Inlets

The nearly white color of this unit stands in striking contrast to the dark-gray shales that are immediately below (Figure VII-3A). Most of Unit C is mature to supermature quartz arenite in which the grains are greater than 99 percent quartz, medium-grained, moderately to well-sorted, and subround to round (Figure VII-3B). This is significantly more mature than the lithic wackes of underlying units or the sublitharenites of overlying units. Beds are of medium thickness and have generally even and parallel surfaces; internal structures are small- and medium-scale trough and planar cross lamination. In the lower third of the unit sediment transport was directed toward the southeast (sourceward), and in the upper two-thirds transport was consistently toward the northwest (seaward). Several thin beds of black shale are intercalated within the white quartz arenites of this unit.

Several lines of evidence point to the origin of Unit C in barrier-beach inlets. Beach deposits are known to have a greater compositional and textural maturity (Folk, 1960; Mack, 1978). The stratigraphic position of Unit C between Unit B (interpreted as lagoonal) and Unit D (interpreted as of shelf origin) indicates that it is a coastal deposit. In addition, the particular assemblage of sedimentary structures is indicative of inlets through a barrier beach.

For some time it has been realized that the depositional record of a barrier island will consist in large part of inlet deposits (Hoyt and Henry, 1967; Moslow and Heron, 1978; Hayes, 1980). Features of inlet deposits have been reviewed by Hayes and Kana (1976), Elliott (1978), Friedman and Sanders (1978), Reinson (1979), and Hayes (1980).

In this barrier-beach-inlet context, scouring at the base of the inlet placed the mature quartz arenite of Unit C in sharp contact with the lagoonal shales of Unit B (Reinson, 1979, p. 66). The basal part of Unit C records flood-oriented inlet flow toward the southeast, and the upper part records ebb-oriented toward the northwest (see Hayes and Kana, 1976; Reinson, 1979, Figure 17). Intercalated shale accumulated in slack-water periods (Greer, 1975) as reported by Elliott, 1978, p. 171-172). The absence of lags of shell or gravel in Unit C results from the lack of body fossils in the entire Tuscarora

Fig. VII-2

Features of Tuscarora Formation at Mill Hall. In this and the next two figures, photos are grouped in vertical pairs keyed to the informal units.

- A. Rusophycus on base of sandstone bed from Unit A, 4m above contact with Juniata Formation.
- B. Photomicrograph of sandstone from Unit A; narrow dimension is 3.7 mm.
- C. Monocraterion penetrating thin sandstone interbed from Unit B.
- D. Photomicrograph of matrix-rich sandstone interbed from Unit B. Note that grain size is finer than that of sandstones in Units A and C. Narrow dimension is 0.92 mm.

Formation depositional system and from the restricted range of grain size in this distal barrier-beach complex. As transgression proceeded, higher parts of the beach system were contemporaneously decapitated by shoreface and shelf processes (Swift, 1976b, p. 321-2; Moslow and Heron, 1978; Stahl and other, 1974; Kraft and John, 1979).

Unit D: Shelf Sand-Wave Complexes

In this sandstone-dominated heterolithic unit, light-brown sandstone in approximately one-meter-thick zones alternates with zones less than a meter thick of shales and subordinate thin sandstones (Figure VII-3C). Shale is much less common toward the base of the unit. Most of the sandstone is poorly to moderately sorted, subangular to subround, and medium to coarse grained (Figure VII-3D). This is coarser than sandstones above or below Unit D. Granule-sized grains are present in some beds, including some of the thin sandstones in the shale-dominated zones, but there are no basal lags and no grading. There is, therefore, no correlation between grain size and bed thickness. The sandstones are sublitharenites, containing between 5 and 10 percent lithic grains and chert (Figure VII-3D).

There is a generally similar geometry to both thick and thin sandstones. Basal surfaces are distinctly flat and upper surfaces are broadly wavy (Figure VII-3C). All sandstone beds have sharp contacts at both base and top. Within thicker sandstones there are internal bed partings inclined at low to medium angles in the direction of sediment transport (Figure VII-3C). Between these partings are thin to medium, trough and planar cross lamination. Direction of sediment transport was principally to the northwest, but several zones of larger-scale cross lamination record transport to the southeast. In the more sandstone-dominated lower part of Unit D, a few meters above the white sandstone of Unit C, there is a larger-scale, bipolar (herringbone) cross-laminated sandstone. Some wavy upper surfaces have an asymmetry in which the steeper side faces the principal sediment-transport direction (northwest) and has approximately the same inclination as the major internal partings (Figure VII-3C). Arthropycus and other infaunal, deposit-feeder structures occur on the soles of a number of sandstone beds, particularly those intercalated within shale.

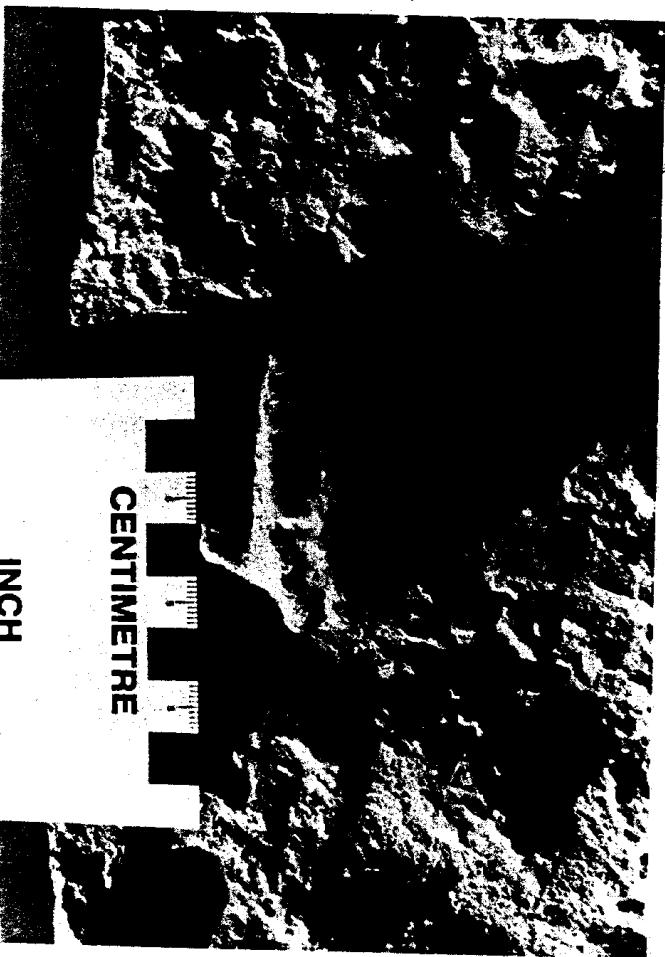
These strata are interpreted as shelf deposits. Migration of complex, megarippled, sand shoals transported medium- and coarser-grained sand to a part of the shelf seaward of the shore-face. Mud formed the substrate between the sand shoals and over which the shoals migrated. The source of the sand is undetermined, but the principal direction of sand-wave migration was seaward, although periodically landward migration



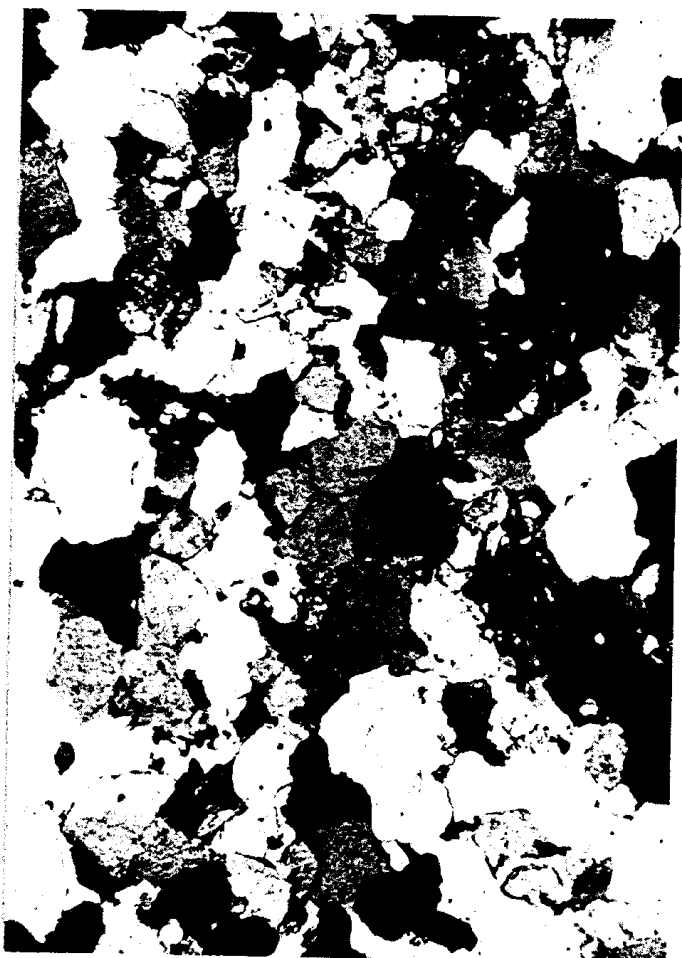
C



D



A



B

Fig. VII-3

Features of Tuscarora Formation at Mill Hall (STOP VII).

- A. Unit B (center), overlain by white quartz arenite of Unit C.
- B. Photomicrograph of white quartz arenite (Unit C), interpreted as a beach inlet deposit. Narrow dimension is 3.7 mm.
- C. Unit D - shelf sand wave complexes with flat bases and wavy tops. Staff against outcrop is 1.5 m long and is placed about 61 m above Juniata contact (see Fig. VII-1).
- D. Photomicrograph of sublitharenite from sandstone units shown in Fig. VII-3C above. Narrow dimension is 3.7 mm.

occurred. The superposition of Unit D on the barrier-inlet deposits of Unit C suggests that the sand shoals were in the inner part of the shelf and in connection with the shoreface. Thus, the migrating sand-wave complexes were similar to modern "shoreface-connected sand ridges" (Swift and others, 1978). However, the compositional and textural differences between Units C and D require that the shelf sand-wave complexes were not simply detached from the top of the shoreface as transgression continued. A more complex genetic relationship appears to be required.

Unit E: Slightly Deeper Shelf

With roughly equivalent proportions of sandstone and shale, this unit has a mixed heterolithic character. Sandstones continue to be poorly to moderately sorted sublitharenites. Grain sizes are more varied than in Unit D. Most beds are medium grained, but others are fine grained and still others are coarse and very coarse grained. Most sandstone beds have flat bases and broadly arched tops. Lateral continuity is great, but a number of sandstone beds wedge out laterally. Thicker sandstone beds are cross laminated. Some thinner beds have small-scale cross lamination or current-ripple lamination. Biogenic structures are more common than in Unit D below. Arthropycus and a variety of other deposit-feeder structures are on numerous bed soles. Arthropod marks, including one Rusophycus have been found. And a number of examples of possible Lockeia are present.

Deposition of this unit took place in marine-shelf conditions of lower overall energy than during deposition of Unit C. Mud accumulation persisted longer between the introductions of thinner, finer-grained, sand-wave complexes. The most direct explanation for this is that Unit E accumulated farther on the shelf and probably in deeper water than the conditions in which Unit D formed. However, patterns of sand-shoal buildup on shelves are not necessarily this direct, and other, more complex, explanations are possible.

Unit F: Inner-Shelf, Sand-Wave Complexes

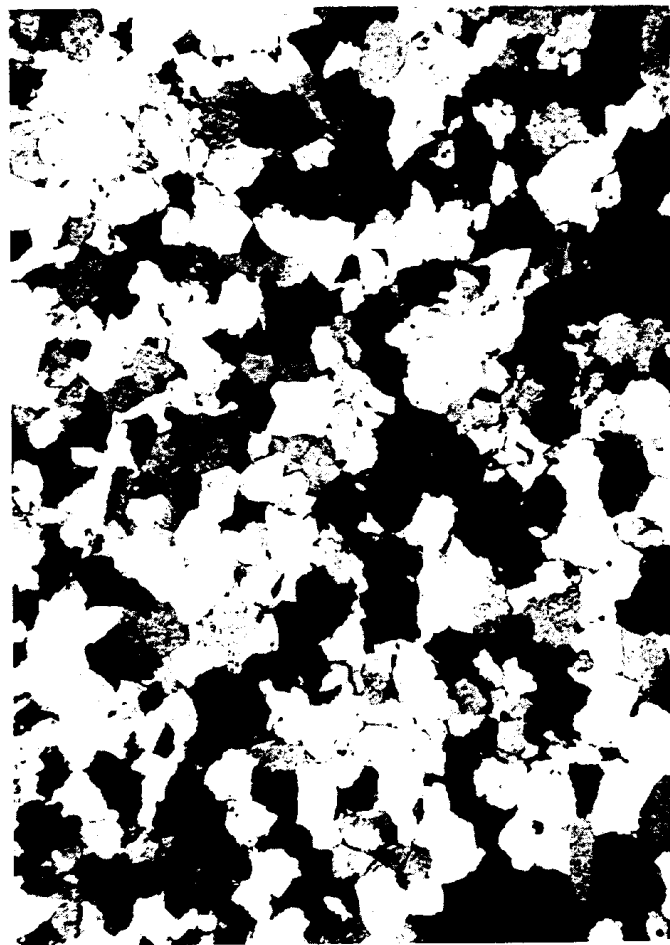
This unit returns to the sandstone-dominated heterolithic pattern of Unit D, except that the sandstones are thinner, the grain sizes are smaller, and there are no landward-directed cross laminae. The abundance and thickness of sandstone beds increase gradually toward the top of the unit. Arthropycus is common on sandstone bed soles. Some sandstone beds toward the top of the unit are more thoroughly bioturbated. (Figure VII-4A shows the upper part of Unit F.)



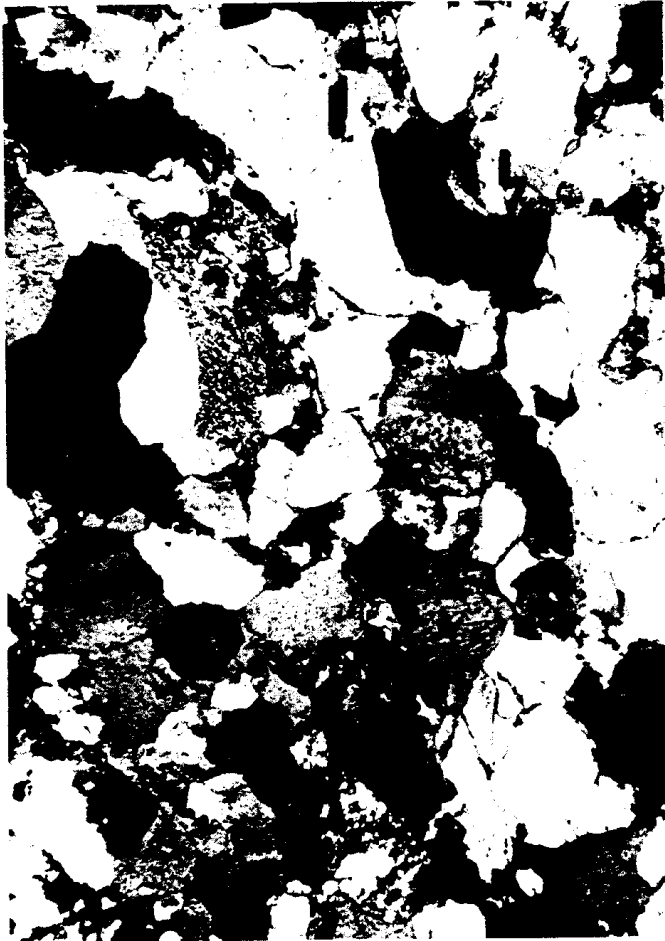
A



C




B



D

Fig. VII-4

Features of Tuscarora Formation at Mill Hall (STOP VII).

- A. Units F (right half of section) and lower part of G. Diplocraterion occurs in apparently structureless bioturbated unit in center of photo.
 - B. Two burrowing styles of Arthropycus on base of red sandstone from lower, transitional part of Unit G. Specimen came from blocks to lower left in this photo.
 - C. Center of photo has tan, fine-grained, cross-laminated channel sandstone within red, Skolithos-burrowed lithofacies (Unit G at 150 m on Fig. VII-1).
 - D. Photomicrograph of sandstone shown in Fig. VII-4C (above). Narrow dimension of photo is 0.92 mm.
- 

Processes of sedimentation were similar to those that operated during accumulation of Unit D, yet the reduced scale of features implies that these processes were of somewhat lower intensity. Sand-wave complexes migrated across the inner part of a normally muddy shelf.

Unit G: Coastal Sand/Mud Flats

The uppermost 43 meters (Unit G) consist of the red, Skolithos-burrowed lithofacies. This is the Castanea Member of the Tuscarora, named by Swartz (1934) after the village of Castanea, about 4 miles (6 km) east of this stop. The base of Unit G was placed at the base of the first maroon-red, Skolithos-burrowed sandstone, and the unit extends to the fossiliferous green shales of the Rose Hill Formation. The red sandstone is very fine to fine-grained and matrix-rich. Most of the Skolithos are short, stubby, vertical cylinders, but extended slender forms also occur. Most of the red sandstones are structureless because of the extensive biogenic activity. In some beds, there are remnants of current-ripple lamination and/or fine sand streaks. In the lower transitional part of Unit G, the red sandstone alternates with drab gray and brownish sandstones; in this part, Arthropycus (Figure VII-4C) appears on the soles of both red and nonred sandstones that are Skolithos-burrowed. Diplocraterion can be found in a drab bioturbated bed. Thus, these lower sandstones record the activity of both filter feeders and deposit feeders.

Within Unit G, there are two broadly channelform zones (centered at 150 and 168m) of light-brown, fine-grained, sublitharenitic sandstone (Figures VII-1, 4B, 4D). These contain trough cross lamination that indicates northwestward sediment transport. The scale of the troughs appears to decrease upward in the zone. Also within Unit G are zones of drab mudstone, intensely burrowed by small-scale Chondrites. Within a meter of the Rose Hill Shale near the top of Unit G, well-developed desiccation marks occur in beds that are also burrowed by Skolithos.

The conditions of deposition of Unit G were associated with coastal sand/mud flats. The broad, extensive flats were profusely riddled by the burrows of the filter feeders that made Skolithos with a variety of forms. Seaward-flowing channels drained the flats. A number of instances of long-term inundation of the coastal flats caused deposition of the Chondrites-burrowed shale. The history of Unit G was terminated by the submergence that introduced the Rose Hill Sea to the region.



A



B



C



D

STRUCTURAL GEOLOGY

Although bedding is nearly vertical, this outcrop is northwest of the region of high mesoscopic strain in the Valley and Ridge Province. The well-exposed, small-scale structures of Stops I to V are less obvious here, yet studying some of these structures in this setting where they are incipient and not overprinted by intense later deformation may illustrate their early development.

The regional setting for both Stop VII and VIII is shown by Figure VII-5, a generalized section drawn 12 miles to the northeast by Faill and Wells (1977, Figure 1). Stops VII and VIII are on the northwest limb of the Nittany Anticlinorium generally assumed to be the ramp anticline formed as the basal decollement climbed section from the Cambrian Waynesboro Formation to the Middle Silurian "Salina" underlying the Appalachian Plateau to the northwest. The view to the northwest from Stop VII toward the Alleghany Topographic Front shows the Silurian through Mississippian section with dips gradually decreasing up to the horizontal Pocono Sandstone at the lip of the Plateau. Figure VII-5 shows more second- and third- order folding in the foothills of the Appalachian Plateau than has been recognized in this area.

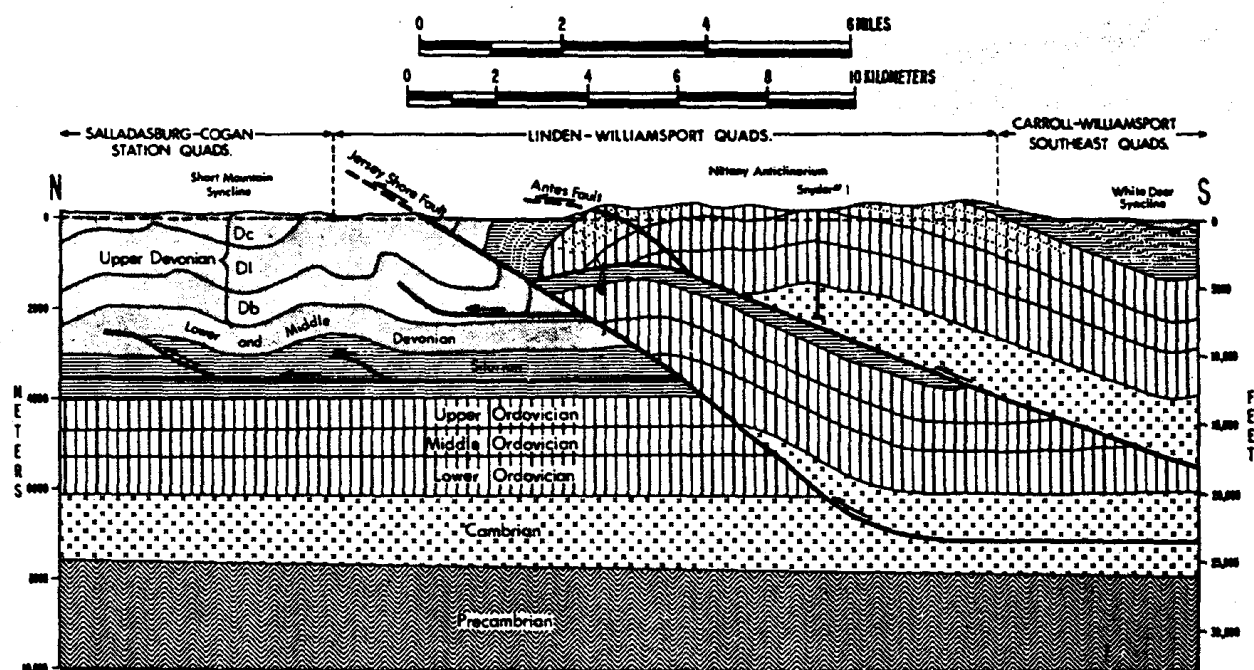


Figure 1. Generalized cross section of the Paleozoic rocks and Alleghanian structures in the Linden-Williamsport and adjacent quadrangles. The major structure at the surface, the Nittany anticlinorium, lies over a complex of thrust faults which mark the northwest limit of major transport on the decollements underlying the Valley and Ridge province. The Jersey Shore fault is the largest surface expression of these faults.

Fig. VII-5

Generalized structure section of the northwest limb of the Nittany Anticlinorium and the Alleghany Front (Faill and Wells, 1977, Fig. 1).

At the base of this outcrop is a horizontal kink boundary between two different attitudes of bedding, the upper part dipping 65° northwest, the base dipping 80° southwest (overturned). Mesoscopic structures can be divided into those which developed as a consequence of clockwise simple shear during flexural-slip folding and

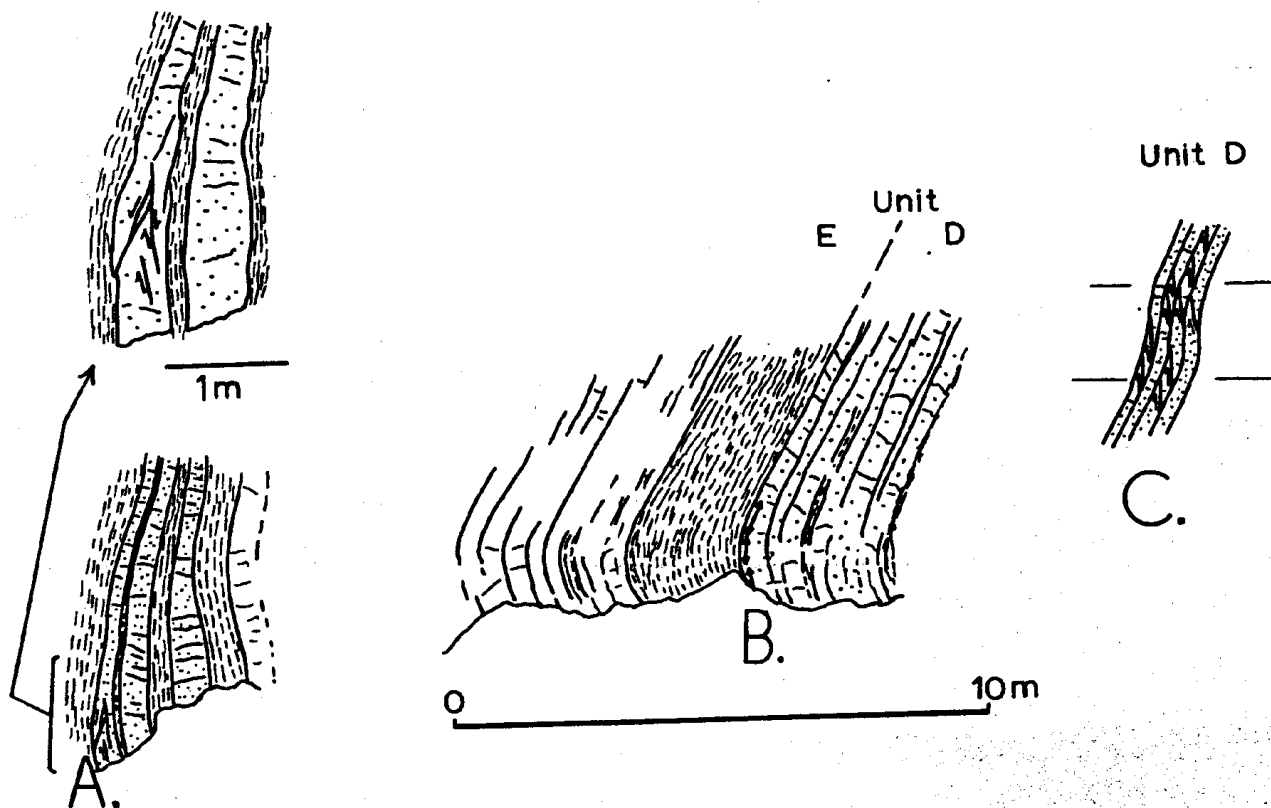


Fig. VII-6

Drawing of structural details at 3 localities in the Tuscarora Formation

- A. *Bed thickening caused by pre-folding wedge faulting.*
- B. *Folded slickenlines on a pre-folding wrench fault surface.*
- C. *Wedge faults related to a late kink band.*

these formed earlier by Stage IV layer-parallel shortening prior to folding. Within stratigraphic Unit E of the Tuscarora Formation is a clockwise parasitic fold that is compatible with the simple shear sense during Stage V on this limb of a fold.

Farther down section, also in Unit E, is a complex of both up- and down-dip-directed wedge faults that were formed during Stage IV, pre-folding, layer-parallel shortening. They are believed to be early because they are directed both ways and not compatible with the expected clockwise simple shear on this limb of a fold. Note that the complex of wedge faults is located on the hinge between the two major bedding attitudes and that 25% thickening of one sandstone bed occurred at this point during the Stage IV layer-parallel shortening (Figure VII-6A).

At the top of stratigraphic Unit D is another relic of Stage IV layer-parallel shortening, in this case by wrench faulting (Figure VII-6B). Here, a right-lateral, wrench-fault surface shows slickenlines at a constant angle of only 15° to the bedding-fault intersection, both above and below the horizontal kink boundary that divides the whole outcrop into an upper, northwest-dipping domain and a lower, southeast-dipping domain. These slickenlines were folded through an angle of 35° around the kink boundary while the enveloping bedding of the major fold limb was being rotated to an approximately vertical attitude. Both of these rather obscure structures in this low-strain environment repeat the evidence for the Alleghanian structural sequence that was illustrated at Bear

Valley Strip Mine that is, layer-parallel shortening in stiff beds prior to folding leads to conjugate Stage IV wedge and wrench faulting. These structures may be rotated to other attitudes by Stage V folding.

Finally, in stratigraphic Unit C there is a horizontal kink band showing a counterclockwise rotation of bedding through an angle of 15° . This has created a number of small, up-dip-oriented wedges in several beds. The wedges are restricted to the small area of the horizontal kink band. Hence they are here as a consequence of the formation of the kink band, probably during Stage V folding. They are pointed out to illustrate the difference in style, orientation, and frequency between pre-folding (LPS) Stage IV wedges and Stage V wedges that have formed as a consequence of folding.

In summary, due to mild deformation, it is possible to differentiate prefolding Stage IV structures from similar structures formed as a consequence of Stage V folding. Also, this is a last look at Valley and Ridge structures before they disappear under the cover of the Appalachian Plateau. It is reassuring to find less-deformed elements of the same structural sequence that was recognized in more deformed areas to the southeast. These observations support the notion that the time sequence of structural stages conforms to the geographic distribution of structures that are representative of the various stages (Nickelsen, 1980). Structures of earliest stages extend farthest northwest and are overprinted successively to the southeast by younger stages. At Stops VII and VIII we are on the north-western boundary of Stage V high-amplitude folding and Stage VI layer-parallel extension. Stage IV wrench and wedge faulting probably extends northwest of here for some unknown distance. We know that Stage III deformation of fossils and incipient cleavage formation extends 150 km northwest into the Appalachian Plateau as documented by Nickelsen (1966), Engelder and Engelder (1977), Engelder (1979).

<u>Miles</u>	<u>Interval</u>	
61.8	-	Return to vehicles; continue north on PA 220.
62.5	0.7	Underpass at Mill Hall exit; continue ahead on U.S. 220.
64.8	2.3	Ramp at exit to Castanea; stay on U.S. 220 North.
66.8	2.0	On far side of bridge over Susquehanna, park on road berm as far as possible for Stop VIII.

Stop VIII. Castanea

SEDIMENTOLOGY

The rippled and megaripped bed surfaces arrayed here occur in the McKenzie Limestone Member of the Mifflintown Formation. They represent about 12 meters at the top of informal Unit 9 (see earlier consideration of the genesis of Middle Silurian units and the material for Stop I - Danville), up to the first red mudrock, which begins the transition (Unit 10) into the Bloomsburg Formation.

Description of Lithologies

This part of the McKenzie (Unit 9) is a mud-dominated heterolithic association, consisting of interbedded skeletal grainstones (about 20%) and calcareous mudrock (about 80%). The mudrock is for the most part fissile to platy, calcareous, illitic shale. There are very uncommon thin laminae of coarse silt, and some zones of finely disseminated pyrite. Body fossils are sparse, and include small delicate brachiopods and large orthocerids.

The grainstones form the beds with the rippled and megaripped surfaces. Most of these beds are impressively thin (Figure VIII-2A) with some having no material in parts of troughs ("starved megariipples"). Most of the grainstones are ostracod biosparites, but more diverse assemblages, including brachiopods, gastropods, and favosited corals, also occur. On some surfaces there are segregations by taxonomy, and brachiopods are more concentrated in one area and ostracods in others. Intraclast beds occur toward the eastern part of the outcrop (Figure VIII-1). The clasts are up to 50 cm long and are generally subhorizontal, although a number of smaller ones are more steeply inclined. Although the clasts are mud-draped, it is clear that their composition can vary in the same bed, but that the compositions are typical of the grainstones in the section.

Most common of the well-developed biogenic structures is Chondrites, found as ramifying, three-dimensional tunnel networks in both grainstones and mudrock. There are also some Planolites-like horizontal shafts, some of which have a slight concave-upward bend. One probable Bifungites was also found.

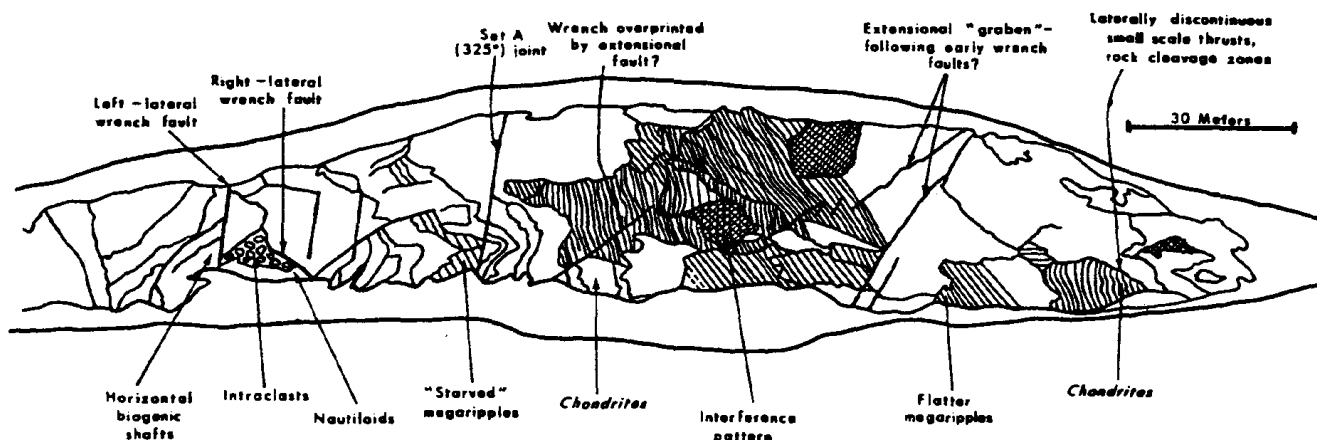



Fig. VIII-1

Sketch map of surface of outcrop of Mifflintown Formation, McKenzie Member, at Castanea. Made from photographs, so proportions and orientations might not be true. From Sacks (1981).

Fig. VIII-2

Features of rippled and megarippled surfaces, Castanea. Upper part of McKenzie Limestone Member of Mifflintown Formation; informal Unit 9. Photos taken by R. Sacks.

- A. *Two different dimensions of ripples. Approx. 10 cm wavelength on finer limestone bed, and broader wavelength on overlying grainstone. Note the thinness of this latter grainstone.*
 - B. *Broad wavelength ripples on bioclastic limestone (skeletal grainstone). Crests are rectilinear, low-amplitude, and relatively flat.*
 - C. *Large expanse of two varieties of ripple: (1) broad wavelength, sinuous, rounded crests, (2) smaller wavelength, interference pattern. Staff is 1.5 m long.*
 - D. *Closer view of broad, sinuous, rounded ripples similar to those in Fig. VIII-2C.*
- 

Description of Ripples and Megaripples

Most of the grainstone beds have flat bases and rippled tops (Figures 9, VII-2). Wavelengths range from 5 to 70 cm. Some ripples have rectilinear crests (Figure VIII-2B) but many others are sinuous and parallel (Figures VIII-2C,D). In profile, many ripples are symmetrical, with rounded crests, but others are asymmetrical or have flat crests (Figure III-2B). Over broad expanses of the same surfaces, and on many different surfaces, megaripples have a relatively consistent orientation and geometry. This can be seen in the photos of Figures VIII-2 and in the sketch map of the outcrop surface prepared by Sacks (1981). Most of the crests strike NW-SE (110° to 150°) (restored to horizontal), with only two sets striking NE - SW (65° - 75°).

Interpretation of Ripples and Megaripples

In his senior thesis at Bucknell University, Sacks (1981) attempted to use these ripples and megaripples to estimate water depth at the time of deposition. He used a variety of approaches, including those of Tanner (1966, 1971), Harms (1969), Baker (1970), Komar (1974), and Allen (1979). Aside from agreeing that the environment was wave-agitated, these analyses produced results that were not only unreasonable but contradictory. Ripples with shorter wavelengths were more consistent in suggesting that water depths were less than 12 meters, but these ripples are interbedded with megaripples (Figure VIII-2) that indicated depths near 50 meters.

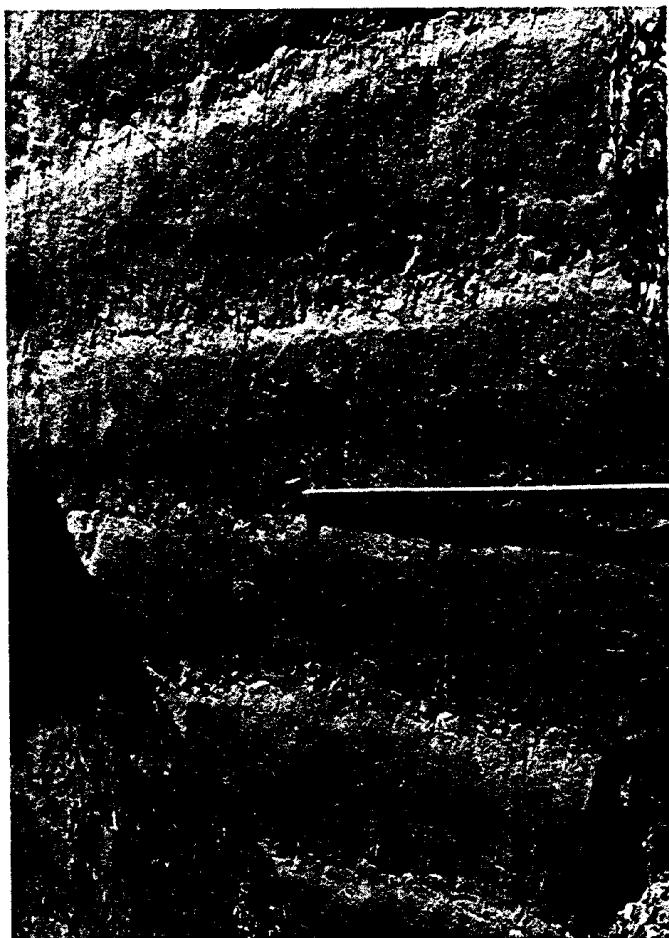
A possible resolution of this contradiction lies in the recognition that there are two genetic families of wave ripples. For orbital ripples (see Allen, 1981, for discussion and for synonyms), the generating shear stresses are somewhat lower and the wavelength is a function of the orbital diameter of the waves. Thus, it is possible to use the ripple spacing relative to the sediment grain size to obtain appropriate combinations of the formative wave conditions and water depth (see approach in Allen, 1981, and in Hunter and Clifton, 1982). The ripples here at Castanea that have wavelengths near 10 cm could be of this type, and then the depth estimates of less than 12 meters might be valid.



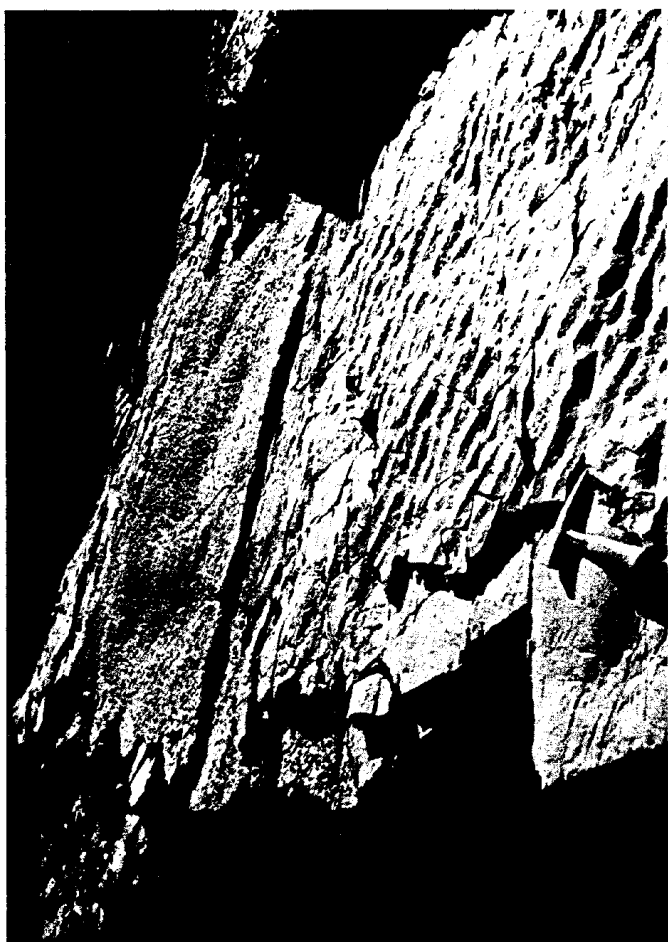
D



C



B



A

The other family of wave ripples is called anorbital (other names in Allen, 1981; see Hunter and Clifton, 1982). These are generated at somewhat higher oscillatory shear stresses, and their spacing is now dependent only on the grain size and independent of orbital diameter (Clifton, 1976). You will note at this outcrop that there is a general correlation between megaripple wavelength and grain size. That makes the larger megaripples inappropriate for most approaches to the estimation of water depth.

Discussion - Depositional Environment

During formation of the McKenzie Limestone Member (Unit 9), terrigenous muds began to flood over the southeastern flank of the Appalachian Basin as a sign of the advancing "Bloomsburg Delta" (Hoskins, 1961; Patchen and Smosna, 1975). The muddy basin axis was slightly to the west of its Keefer/Rochester position, and it was made up of a number of interconnected smaller segments, flanked by carbonate platforms (Patchen and Smosna, 1975). On the marginal carbonate shelf northwest of the axis, coral/stromatoporoid bioherms were possibly associated with paleotopographic highs on the underlying Keefer Formation (Crowley, 1973; Smosna and Patchen, 1978, 1980).

Here at Castanea we are viewing the record of the distal, carbonate part of the southeastern marginal platform. Terrigenous muds were beginning to accumulate, but had not yet ended carbonate deposition. Bioherm development is much less common southeast of the basin axis, but there is one such McKenzie bioherm about 700 meters west of this location (R. Cuffey, personal communication).

Into this distal, placid, increasingly muddy part of the southeastern shelf, coarse skeletal debris was flushed by the action of storms, generating grainstone beds with the flat bases and wavy tops we have seen to be so characteristic of "storm beds." The megaripple morphology on the surfaces of the grainstones are of the type likely to be formed by storms (Clifton, 1976; Hunter and Clifton, 1982, p. 141). Estimates of the water depths at which these beds were deposited are inconclusive, but from analysis of the smaller, orbital ripples, it appears likely that depths were less than 12 meters (Sacks, 1981).

The photographs of Figure VIII-2 illustrate the variety of ripples that occur at this exposure. Figure VIII-1 is a diagram of the surface prepared by Sacks (1981) using photographs of the outcrop. There is inevitably some distortion with this method, and the angular relations and proportions are not true. The amount of outcrop deterioration since 1981 means that not everything on the diagram is still there - even the graffiti must be renewed periodically. On the whole the diagram is reasonably accurate. We have added some directions to specific items to assist you in guiding yourselves.

STRUCTURAL GEOLOGY

This outcrop is a good companion for STOP VII because it demonstrates the effect of mild deformation upon different rock types (limestone and shale) and because it provides a different view of structures (bedding-plane exposures). Bedding dips 45° northwest and is unfolded on a small scale. Pressure-solution or crenulation cleavage, which is restricted to zones of high strain near small thrust or wrench faults, dips southeast perpendicular to bedding. All small-scale structures were possibly formed in response to layer-parallel shortening and later tilted to their present attitude during Stage V folding. The poorly exposed Bloomsburg Formation stratigraphically above the Mifflintown Formation exposure has yielded a few pieces of float with reduction spots that are flattened in bedding (oblate ellipsoids with short axis perpendicular to bedding). Structural data from this outcrop have been rotated with bedding to their pre-folding attitude (Figure VIII-3).

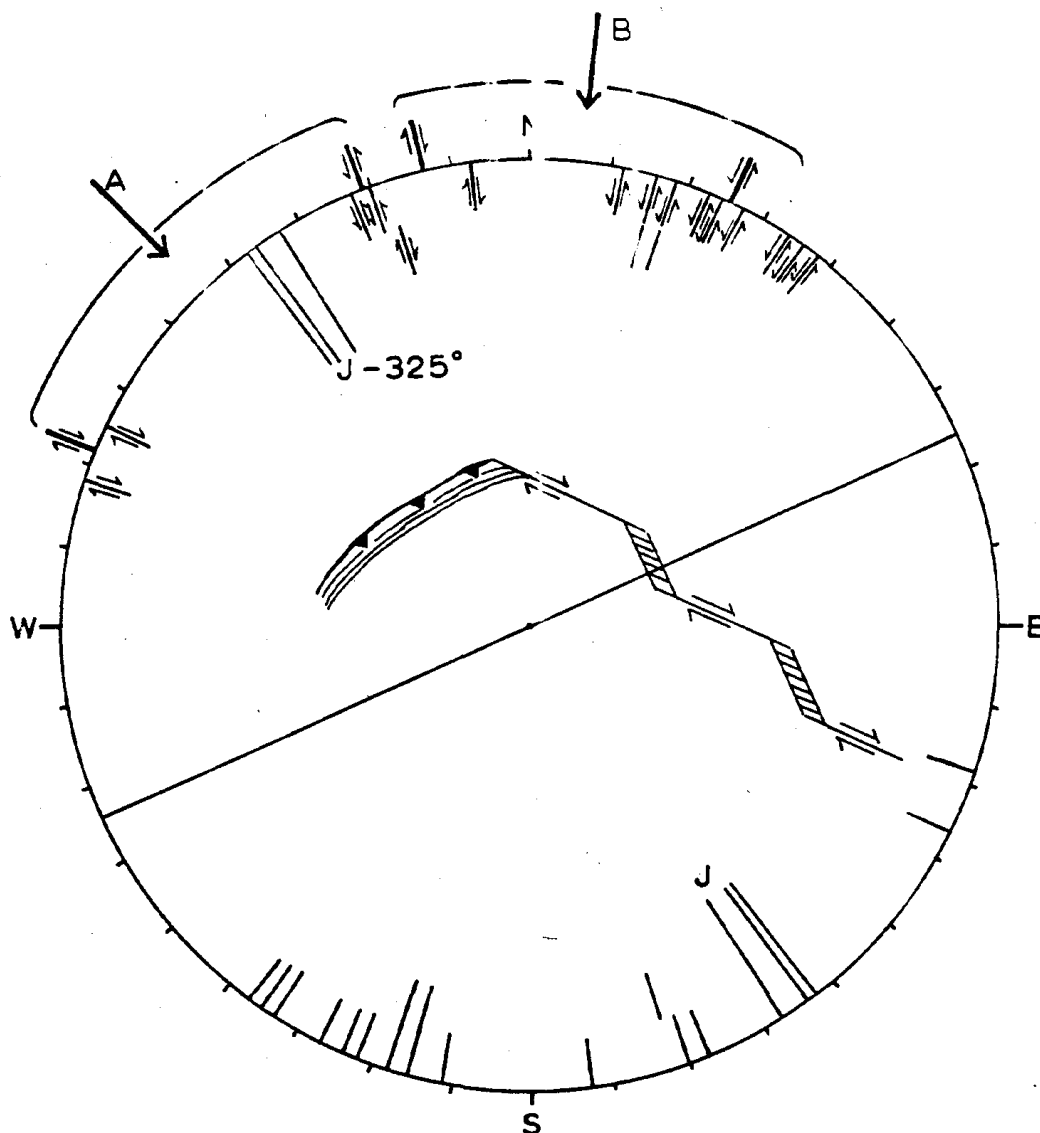


Fig. VIII-3 Lower hemisphere stereographic projection of rotated wrench faults and joints to show possible conjugate systems and their acute bisectors, A and B.

The outcrop has a confusing array of faults that may be interpreted in several ways. One interpretation is that the faults are all Stage IV wrench faults developed in two separate conjugate systems with very different orientations of σ_1 . Figure VIII-3 shows this interpretation with the acute bisectors of the two conjugate systems labeled A (315°) and B (6°). Neither of these systems is symmetrical with the dip of bedding or related to the orientation of the prominent joints trending 324° . The other interpretation accepts the A conjugate wrench-fault system but makes the large northeast-striking faults toward the southwest end of the exposure extensional faults with central down-dropped blocks, presumably of Stage VI relative age. Slip perpendicular to bedding is obvious in a few places but the debate hinges on whether these faults had pre-folding, strike-slip movement which was much later overprinted by the slip perpendicular to bedding. Look for the gash veins along these faults as you try to discern how they have moved. While studying the wrench faults note that they bound small domains of high strain marked by microfolds and pressure-solution cleavage in back of small frontal thrusts. Deformational features are not obvious, in keeping with the northwesterly geographic position of this outcrop, and it is difficult to read the structural fabric. The outcrop is perhaps more typical of the level of strain associated with the Appalachian

Plateau. For example, there are a few systematic regional joints trending 325° (Set A) that are similar in frequency and size to joints encountered on the Appalachian Plateau. The A set is the dominant joint in a domain on the Appalachian Plateau that extends 80 miles southwest along strike and 60 miles northwest from this station (Nickelsen and Hough, 1967).

<u>Miles</u>	<u>Interval</u>	
66.8	-	Reboard vehicles; continue ahead on U.S. 220 North to return to headquarters motel at Danville via Williamsport.
69.6	2.8	McElhattan/Woolrich exit; continue ahead.
72.3	2.7	Good view of Bald Eagle Mountain (Tuscarora Formation) to the right. We are driving along the Alleghany Front.
74.1	1.8	Pine Creek/Rt. 44 exit; continue on U.S. 220 to Williamsport.
90.3	16.2	In Williamsport, bear right to descend exit ramp at sign that indicates U.S. Rt. 15 to Lewisburg.
90.9	0.6	After a left and right turn at bottom of exit ramp and a half mile on straight road, turn left to follow U.S. 15 to Lewisburg. After this left turn, road circles around 180° to ascend bridge over Susquehanna.
92.0	1.1	Bend left 90° to follow U.S. 15 South.
94.0	2.0	Outcrop of Castanea Member of Tuscarora Formation to the right of the road.
94.8	0.8	Fine outcrop of the basal part of Tuscarora Formation on bench above steel retaining wall at this curve. Exhibits basal, horizontally laminated lithofacies.
103.2	8.4	Entering village of Allenwood.
105.5	2.3	Pass lower Rose Hill sandstone unit of Stop VI.
108.0	2.5	Interstate 80 intersection; go under bridge and circle up entrance ramp to head East on I-80; headquarters motel at Danville Exit is about 15 miles ahead.
123.0	15.0	Sheraton Danville Motel at Danville Exit. End of Day 2 and field trip.